The role of thioredoxins in acclimation to light

Dissertation
der Fakultät für Biologie
der Ludwig-Maximilians-Universität München

Vorgelegt von
Dejan Dziubek
aus Greifswald

München, Mai 2022

Erstgutachter:	Prof. Dr. Peter Geigenberger
Zweitgutachter:	Prof. Dr. Wolfgang Frank
Tag der Abgabe:	30. Mai 2022
Tag der mündlichen Prüfung:	6. Oktober 2022

ZUSAMMENFASSUNG

Die Umwandlung von Lichtenergie in chemische Energie durch Photosynthese stellt einen der wichtigsten Prozesse auf unserem Planeten dar. Wechselnde Lichtverhältnisse führen zu einer ungleichen Beanspruchung der Photosysteme in Pflanzen und nehmen Einfluss auf alle folgenden Prozesse in den Chloroplasten. Standortgebundene Landpflanzen sind oftmals in der Lage, sich an diese Veränderungen anzupassen. Dabei spielt die Proteinfamilie der Thioredoxine (TRX) eine wichtige Rolle. Thioredoxine sind plastidäre Oxidoreduktasen, die Energie in Form von Elektronen zwischen den plastidären Licht- und Kohlenstoffreaktionen vermitteln. Oxidierte TRX werden über eine Kaskade, beginnend bei Photosystem I (PSI), über Ferredoxin (Fd) und letztlich von Ferredoxin-Thioredoxin-Reduktase (FTR) reduziert, und daher als FTR System zusammengefasst. Daneben gibt es das Ferredoxin-NADPH-abhängige System (FNR), dessen Vertreter das NAPDH-abhängige Thioredoxin C (NTRC) darstellt, welches eine NADPH sensible Domäne und ein TRX vereint. Studien deuten darauf hin, dass sich diese beiden Systeme wechselseitig beeinflussen und so ihre Aktivität modulieren. Die Aktivität dieser Redoxmodulatoren ist durch die Thiol-Modifizierung von Cysteinen charakterisiert. Diese sehr schnell ablaufende Modulation im Sekunden- bis Minutenbereich ist maßgebend für die Stabilität und Funktion von Zielproteinen. Bekannte Aufgaben der TRX sind an erster Stelle die lichtabhängige Reduktion, und damit die Aktivierung von Calvin-Benson-Zyklus (CBC) Enzymen nach längerer Dunkelheit, die Aufrechterhaltung der Redoxhomöostase und des antioxidativen Systems, sowie der plastidären Genexpression.

Da wenig über die Rolle des FTR und FNR Systems in der Regulierung von längerfristigen Antworten auf sich verändernde Lichtbedingungen bekannt ist, wurde in vorliegender Arbeit nun mit Hochdurchsatzmethoden und dem Ansatz der reversen Genetik untersucht, welchen Einfluss die Thioredoxine *f*1, *m*1, *m*2 und NTRC auf Photosynthese, den zentralen Stoffwechsel, den CBC und auf das Proteom haben, sobald der Pflanze unterschiedliche Lichtenergie und Belichtungszeiten zur Verfügung stehen. Hier konnte gezeigt werden, dass die Zellantwort, auf Ebene der Photosynthese und des Stoffwechsels, auf kurzfristige Änderungen zwischen moderatem und stärkerem Licht im Bereich von Minuten bis Stunden eher wenig vom TRX/NTRC System abhängt. Bei schnelleren Wechseln zwischen Niedrig- und Starklicht im Bereich von Minuten, ist die photosynthetische Anpassung in *ntrc* Mutanten, die aus Kontrollbedingungen kamen, blockiert, während Wildtyppflanzen sich zunehmend

über Tage an diese Bedingung akklimatisieren konnten. Daraus lässt sich eine wichtige Rolle von NTRC in der Anpassung an rasch wechselndes, sogenanntes fluktuierendes Licht, welches natürlichen Bedingungen am nächsten kommt, ableiten. Bei weiterer, längerfristiger Akklimatisierung an Starklicht, Niedriglicht und fluktuierendes Licht, im Bereich von Tagen mit höherer durchschnittlicher Lichtintensität, zeigten sich größtenteils Überlappungen zwischen Wildtyp und den TRX Mutanten, wobei die meisten Änderungen im Starklicht sichtbar wurden. Im Wildtyp wurden hier der Zentralstoffwechsel, der CBC und Proteine zur Stressantwort angekurbelt, während Translationsprozesse heruntergefahren wurden. Die Störung der NTRC Expression beeinträchtige wie zuvor gesehen die Quanteneffizienz von Photosystem II, insbesondere in fluktuierendem Licht, aber auch in Starklicht. Durch den Vergleich mit allen weiteren Bedingungen fiel auf, dass der *ntrc* Mutante jegliche dynamische Anpassung und Stimulierung auf Ebene des Stoffwechsels und Proteoms, vor allem im Starklicht, fehlte. Es scheint schlüssig, dass NTRC für die langfristige Umgestaltung von zellulären Prozessen wichtig ist, die sich nicht nur auf den Chloroplasten beschränken und Teile des Translationsapparats steuern. Die Experimente unterstreichen unterdies die bekannten Rollen von TRX *f*1 und NTRC in der Regulierung des CBC unter Kontrollbedingungen und bei Übergängen zwischen Dunkelheit und Licht und haben dabei eine mögliche *in vivo* Rolle von den TRX *m*1 und *m*2 im CBC und der Photosynthese unter Niedriglicht aufgedeckt.

Zusammengenommen deuten die Daten darauf hin, dass es – trotz des sehr kurzlebigen Mechanismus von Redoxreaktionen – einen langfristigen Effekt gibt, der die Pflanze dazu befähigt, sich, besonders mit Hilfe von NTRC, auf wechselnde Lichtintensitäten einzustellen, um Photosynthese und Wachstum zu optimieren.

SUMMARY

The photosynthetic conversion of light energy into chemical energy represents one of the most important processes on our planet. Changing light conditions lead to uneven stress on the photosystems in plants and influence all subsequent processes in the chloroplasts. Sessile land plants are able to adapt to these changes. The protein family of thioredoxins (TRXs) plays an important role in these processes. Thioredoxins are plastid oxidoreductases that mediate energy in the form of electrons between plastidial light and carbon reactions. Oxidized TRXs are reduced on a cascade via photosystem I (PSI), ferredoxin (Fd) and eventually by ferredoxin-thioredoxin reductase (FTR), and therefore grouped together as the FTR system. In addition, there is the ferredoxin-NADPH-dependent system (FNR), whose representative is NAPDH-dependent thioredoxin C (NTRC), which combines an NADPH sensitive domain and a TRX. Studies suggest that these two systems interact to modulate their activity. The activity of these redox modulators is characterized by thiol modification of cysteines. This very fast modulation in the seconds to minutes range is crucial for the stability and function of target proteins. Known roles of TRX include, first and foremost, light-dependent reduction, and thus activation of Calvin-Benson cycle (CBC) enzymes after prolonged darkness, maintenance of redox homeostasis and the antioxidant system, and plastid gene expression.

Since little is known about the role of the FTR and FNR systems in regulating longer-term responses to changing light conditions, the present work has now used high-throughput methods and the reverse genetics approach to investigate the influence of the TRXs *f*1, *m*1, *m*2, and NTRC on photosynthesis, central metabolism, the CBC and on the proteome once different light energy and exposure times are available to the plant. Here it was shown that the cell response, at the level of photosynthesis and metabolism, to short-term changes between moderate and higher light in the range of minutes to hours depends rather little on the TRX/NTRC system. For more rapid changes between low and high light on the order of minutes, photosynthetic adaptation in *ntrc* mutants originating from control conditions is blocked, while wild type plants were increasingly able to acclimatize to this condition over days.

This suggests an important role for NTRC in adaptation to rapidly changing, so-called fluctuating light, which is closest to natural conditions. Further, longer-term acclimation to high light, low light, and fluctuating light, in the range of days with higher average light intensity, showed mostly overlap between wild type and the TRX

mutants, with most changes visible in high light. In the wild type, central metabolism, CBC, and stress response proteins were boosted here, whereas translational processes were down-regulated. Disruption of NTRC expression impaired the quantum efficiency of photosystem II as seen previously, especially in fluctuating light, but also in high light. By comparison with all other conditions, it was noticeable that the *ntrc* mutant lacked any dynamic adaptation and stimulation at the level of metabolism and proteome, especially in high light. It seems conclusive that NTRC is important for long-term re-modeling of cellular processes, that are not restricted to the chloroplast and control parts of the translational apparatus. Furthermore, the experiments highlight the known roles of TRX *f*1 and NTRC in the regulation of the CBC under control conditions and during transitions between darkness and light, and in the process, they have uncovered a possible *in vivo* role for TRXs *m*1 and *m*2 in regulating the CBC and photosynthesis under low light.

In summary, the presented findings suggest that, despite the very short-lived mechanism of redox reactions, there is a long-term effect that enables the plant to adapt to changing light intensities, especially with the help of NTRC, to optimize photosynthesis and growth.

TABLE OF CONTENTS

LIST OF FIGURES

LIST OF TABLES

ABBREVIATIONS

2-PG	2-phophoglyoclate
2-OG	2-oxo-glutarate
Abs	absorption
ADP	adenosine diphosphate
AMP	adenosine monophosphate
ANOVA	analysis of variance
ATP	adenosine triphosphate
BSA	Bovine serum albumin
d	days
ddH_2O	double distilled water
DEE	diethyl ether
ETC	electron transport chain
ETR	electron transport rate
F	fluorescence yield
FC	Fold change
FL	fluctuating light
FHL/ FL HL	high light phase of FL
FLL/ FL LL	low light phase of FL
Fm, Fm'	maximal fluorescence yield (from dark- and light-adapted plants, respectively)
Fo, Fo'	fraction of open PSII reaction centers (from dark- and light-adapted plants, respectively)
Fv	variable fluorescence
FW	fresh weight
Fd	Ferredoxin
FDR	false discovery rate
g	gravitational force; gram
h	hours
HL	high light
Hz	Hertz
KD	knock-down
KO	knock-out
LHC	light harvesting complex

liq. N2	liquid nitrogen
L	Liter
LED	Light emitting diode
LL	low light
MES	2-(N-morpholino)ethanesulfonic acid
min	minutes
Mg	magnesium
ML	medium light
NAD(P)(H)	Nicotinamide adenine dinucleotide (phosphate)(reduced)
o/n	over night
p	*p* value
PAGE	Polyacrylamide gel electrophoresis
PAM	pulse amplitude modulation
PAR	light intensity in µmol photons m^{-2} s^{-1} (photosynthetic active radiation)
PCA	principal component analysis
qT	state transition
r	Pearson correlation coefficient
ROS	reactive oxygen species
rpm	rounds per minute
s	seconds
SDS	Sodium dodecyl sulfate
TBS(T)	Tris buffered Saline (Tween 20)
TCA	Trichloroacetic acid; Tricarboxylic acid
TRX / *trx*	Thioredoxin protein / mutant
ΦII	Quantum efficiency of Photosystem II

1 Introduction

1.1 Photosynthesis in higher land plants

The autotrophic lifestyle of a sessile plant requires the capability to adequately adapted to and optimally utilize changing abiotic factors like light in order to grow, mature, flourish and reproduce. Oxygenic photosynthesis is executed in chloroplasts to generate chemical carriers of energy like ATP from light energy to eventually produce photo-assimilates like amino acids and sugars to meet the standards of a stable metabolism. Thus, the chloroplast plays a key role in various acclimation responses, acting on cellular level, both as a sensor of environmental change and a target of acclimation responses (Kleine et al., 2021).

1.1.1 Photosynthetic electron transport

Photosynthesis in plants involves many energy converting processes like nitrate- and sulfate assimilation and is not limited to carbon fixation. Light quanta are captured by thylakoid membrane bound light reactions centers of multi-protein complex photosystem II (PSII) and green pigment chlorophyll, which then transfers electrons in a consecutive excited state via a sophisticated serial transport system over photosystem I (PSI) onto Ferredoxin (Fd) (**Figure 1.1.1**). On the stromal site, reduced Fd acts as electron donor to assimilate sulfur and ammonium or to generate the reduction equivalent NADPH from electron acceptor $NADP^+$. Due to their maximal absorption at 680 nm and 700 nm, PSII and PSI are also called P680 and P700, respectively. Re-oxidization of P680 back to ground state involves the water-splitting complex of PSII, which produces oxygen and protons, latter ones contributing to the establishment of a transmembrane proton gradient used for the production of the pivotal energy source ATP. Light-harvesting complexes (LHCs) are substantially involved in energy absorption and transfer and are associated with chlorophyll *a* in the reaction centers of the photosystems. The cytochrome b_6f-complex is an intermediary oxidoreductase between PSII and PSI and further functions as a proton pump. Integral to this is the mobile electron carrier Plastochinon (PQ); the sum of intra-membrane PQ is considered as PQ-pool and reduced PQ (PQH_2) is important for an acclimatory response to changes in light quality (Puthiyaveetil, 2011). Apart from the above-mentioned linear electron transport from water to NAPDH, there exists a (pseudo-)cyclic electron transport around PSI, which re-transfers energy onto oxygen and thus only yields in ATP

production. This cyclic electron transport is active, when the NADPH/NADP$^+$ ratio is elevated (Kadereit et al., 2021).

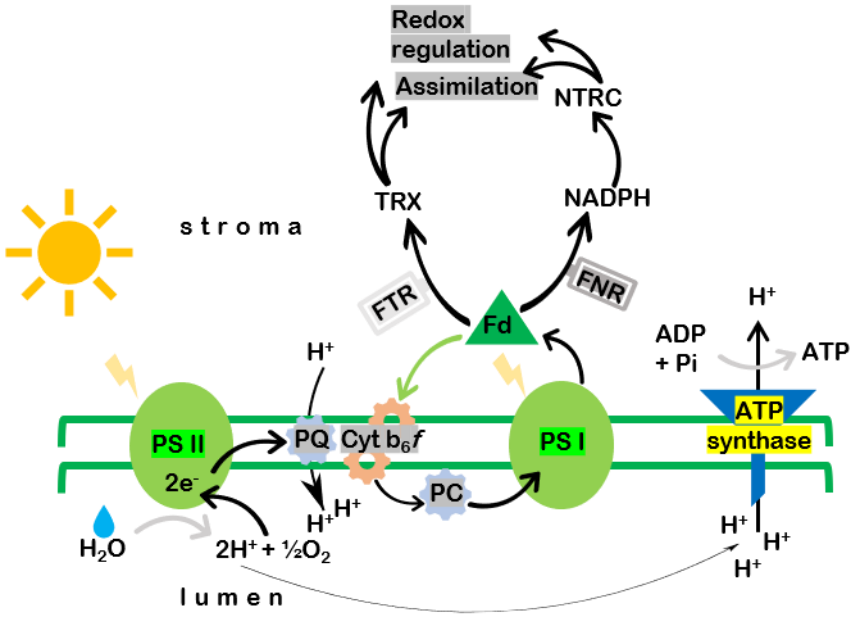

Figure 1.1.1. Overview of photosynthetic electron transport pathways in the chloroplast.
Light captured at photosystem II (PSII) leads to water splitting and generation of electrons, which are transferred over a cascade involving Plastoquinone (PQ), cytochrome b_6f and Plastocyanin (PC) onto photosystem I (PSI), and protons, which are used for ATP synthesis. Linear electron flow (LEF) involves energy transfer from PSI to stromal site Ferredoxin (Fd) and further distribution to Ferredoxin-Thioredoxin-Reductase (FTR) and thioredoxin (Trx) or Ferredoxin-NADP$^+$-Reductase (FNR) and NADPH-dependent thioredoxin reductase C (NTRC), which both act on multiple assimilatory and redox regulation processes. Cyclic electron flow (CET, green arrow) around PSI shuttles energy back from Fd to cytochrome b_6f and PQ.

1.1.2 Measurement of photosynthetic electron transfer

Chlorophyll *a* fluorescence measurements of dark-adapted leaves serve as physiological indicator of photosynthetic performance and stress in plants and is qualitatively correlated with changes in CO_2 assimilation (Baker, 2008). The model, in which photochemistry competes with the processes of fluorescence and heat loss for excitation energy in the pigment antenna of PSII, is used to estimate PSII photochemistry from fluorescence quenching, that results from both photochemical and non-photochemical processes (Butler, 1978; Baker, 2008).

Non-photochemical quenching (NPQ) is a natural protective mechanism to dissipate excess light energy as heat, but estimation of NPQ relaxation can also be used as a measure for stress. A major contributor to this protection is the high energy state quenching (qE), which responses to a change in thylakoid lumen pH (Holt et al., 2004). Besides, plants can manage energy dissipation via state transition (qT) involving

energy transfer from one photosystem to the other; both qE and qT are acting on short time scales. NPQ relaxation can also occur under longer-term periods, which is termed photoinhibiton (qI) and mostly involves high light (HL) conditions and damage on the reaction centers and LHCs of PSII (Maxwell & Johnson, 2000; Baker, 2008).
The term qL comprises all "open" PSII reaction centers and is widely used to estimate the oxidation state of PQ. PQ itself acts as an integrator of chloroplast redox states and subsequent gene expression to adjust the stoichiometry of photosynthetic complexes in response to changes in light quality (Dietzel & Pfannschmidt, 2008).
A pulse amplitude modulation (PAM) fluorometer is used to quantify chlorophyll *a* fluorescence (Schreiber, 1986; Murchie & Lawson, 2013) and to estimate the above mentioned parameters.

1.1.3 Carbon fixation in leaves

In the stroma, hexose is assimilated from ambient CO_2 and water and later used for the synthesis of starch and sucrose for energy storage. NAPDH and ATP from the light reactions provide 4 electrons to reduce one single carbon molecule in the chloroplast stroma. 6 mole CO_2, 12 mole NAPDH and 18 mole ATP are consumed to release one mole carbohydrate (C_6). This conversion of CO_2 to sugar is catalyzed by many enzymes operating in series within a circle, which was named after its first discoverers "Calvin-Benson-Bassham-Cycle" (CBC) (Bassham et al., 1954; Sharkey, 2019). The CBC is divided in three parts: the fixation stage, the reduction stage and the regenerative stage. Ribulose-1,5-bisphosphate (RuBP; C_5) is carboxylated by Ribulose-1,5-bisphosphate carboxylase-oxygenase (RuBisCO) in the very first step. CO_2 is incorporated into RuBP, which is then converted via unstable intermediates into two molecules 3-phosphoglycerate (3-PGA; C_3). Under low ambient CO_2, RuBisCO catalyzes the oxygenation of RuBP, yielding in 3-PGA and 2-phosphoglycolate (2-PG; C_2), therefore potentially reducing photosynthesis due to a depressed 3-PGA conversion. However, 2-PG metabolism passes multiple cell compartments and can be ultimately carboxylated and re-introduced into the CBC. In the next phase, 3-PGA is reduced to dihydroxyacetone phosphate (C_3) and glyceraldehyde-3-phosphate (C_3), which are in equilibrium. NADPH-dependent glyceraldehyde 3-phosphate dehydrogenase (GAPDH) is an important light-activated enzyme in this step. Other than hexose, triose-phosphate (TP; C_3) is the main photo-assimilate, that can be exported – together with 3-PGA – from the chloroplast to the cytosol. Three full circles are needed for the net-synthesis of one triose. Therefore, TP is the key for the subsequent synthesis of carbohydrates and the regeneration of CO_2 acceptor molecule RuBP, which comprises

the final stage of the CBC. Here, ribulose-5-phosphate-1-kinase, fructose-1,6-bisphosphate-1-phosphatase and sedoheptulose-1,7-bisphosphate-1-phosphatase, which are also light-activated via the Ferredoxin-Thioredoxin-system, are to mention particularly (Schopfer & Brennicke, 2010; Kadereit et al., 2021).

1.1.4 Plastidial end-product synthesis

CO_2-fixation and -reduction yield TP in the chloroplast. TP is exported to the cytosol, where the main transport sugar sucrose is produced. Besides sucrose, starch constitutes the biggest condensed and abundant form of oligosaccharides in the plant. In the chloroplasts, daylight is used to generate transitory starch, which can be mobilized at nighttime again and be converted into sucrose as a mobile compound to supply other plant parts. Longer-term storage in non-photosynthetic tissues involves specialized plastids called amyloplasts (Zeeman et al., 2010). When needed, transitory starch is cleaved into maltose and can be re-introduced into chloroplast metabolism as glucose-1-phosphate (G1P). Starch biosynthesis is coupled to the CBC via fructose-6-phosphate (F6P), which gets converted into glucose-6-phosphate (G6P) and G1P and further to ADP-Glucose (ADPG) under energy consumption. Starch synthases, branching enzymes and debranching enzymes are important for the final production of the starch granule (Streb & Zeeman, 2012). In this context, younger, developing tissues (sink) are not able to produce enough assimilates for their metabolism and are dependent on the supply and the import of assimilates from older, more developed leaf tissues (source) (Schopfer & Brennicke, 2010; Kadereit et al., 2021).

1.2 The redox system in chloroplasts

In simplest terms, oxidation-reduction (redox) processes are chemical reactions, in which electrons (e^-) are transferred from one reactant to another, but they can also involve combined hydrogen (proton) transfer. However, “reduction equivalents” usually include e^- and/or hydrogen. In photosynthesis, carbon in its highest oxidation state (CO_2) gets reduced to sugar $[CH_2O]_n$, which yields in energy release when consumed and re-oxidized to CO_2 (Schopfer & Brennicke, 2010). Therefore, redox reactions are critical for the balance between the chloroplast light - and carbon reactions, being interconnected by photo-reduced energy carriers (Fd, NADPH, TRX). Imbalances can lead to harmful reactive oxygen species (ROS) at PSI (Asada, 1999; Apel & Hirt, 2004). Hence, abiotic factors stimulating the light reactions are crucial determinants for photosynthetic efficiency.

1.2.1 Post-translational modification

Post-translational modifications (PTM) of cysteine residues play a prominent role in the regulation of cell metabolism and function of chloroplast enzymes (Lindahl et al., 2011; Michelet et al., 2013). Although cysteine residues occur less frequently, they are highly susceptible to dynamic modification (Wiedemann et al., 2020). Inter- and intramolecular disulfide bonds in proteins, that can undergo reversible redox regulation, are crucial for function and structure. These modifications are facilitated by enzymes like disulfide isomerases or thioredoxins.

1.2.2 Introduction to Thioredoxins and NTRC

The linear electron flow is addressed and depicted in **Figure 1.1.1**, which further indicates energy fluxes downstream of Fd. Two well-studied (Michelet et al., 2013; Geigenberger & Fernie, 2014) and interacting (Thormählen et al., 2015; Ojeda et al., 2017) regimes, the Ferredoxin-Thioredoxin-Reductase system (FTR) and Ferredoxin-NADP+-Reductase system (FNR), are the energy acceptors and distributors for subsequent redox regulatory processes in the chloroplast stroma, linking redox regulation to light. Other than the FTR, the FNR relies on the creation of NADPH, which is not only used for CO_2 fixation but also constitutes a reducing power for one of the key redox regulators in the chloroplast, the NADPH-dependent thioredoxin reductase C (NTRC; AT2G41680). NTRC is the plastid-localized isoform of the NTR protein family (Serrato et al., 2004), is introduced as an alternative system defending against oxidative damage, especially under low light conditions, via the oxidative pentose phosphate way (Pérez-Ruiz et al., 2006) and exhibits both a reductase and thioredoxin activity with redox-active cysteines (Bernal-Bayard et al., 2012). Reduced NTRC can modify redox-sensitive cysteine residues in target proteins, thereby altering their activity, even in the absence of light-driven electron flow. Aside from NTRC, TRX*f*1 and *m*-type Thioredoxins (TRX), being part of the FTR system, are one of the best-studied thiol-modifying enzymes (Michelet et al., 2013; Geigenberger et al., 2017) (**Figure 1.2.1**). TRXs can be found in all kingdoms of life, first being identified in *E.coli* as a hydrogen donor (Laurent et al., 1964; Lemaire et al., 2007), but they seem to be particularly overrepresented in plants (Lindahl et al., 2011). In *Arabidopsis* they are embedded in a family of small (approximately 12 kDa) oxidoreductases with a conserved redox-active site with the sequence WC(G/P)PC (Bob B. Buchanan & Luan, 2005) and 10 plastidial isoforms (2 TRX*f*, 4 TRX*m*, 1 TRX*x*, 2 TRX*y*, 1 TRX*z*) (Michelet et al., 2013). The investigation of redox regulation strongly implies the search for redox

active targets; Montrichard et al. (2009) and Geigenberger & Fernie (2014) provide lists of potential and confirmed targets of TRX and/or NTRC.

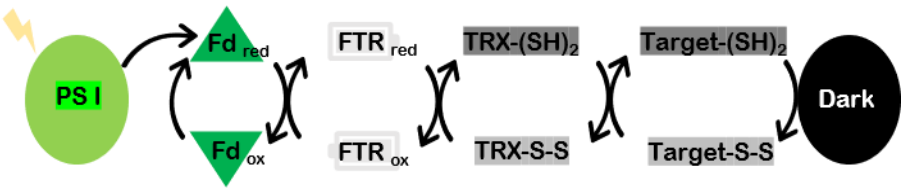

Figure 1.2.1. The ferredoxin/thioredoxin system and mode of action of reversible thiol-disulfide-based protein modification.
Fd, ferredoxin; FTR, ferredoxin thioredoxin reductase; PSI, photosystem I; ox, oxidized; red, reduced; SH_2, reduced thiol; S-S, oxidized disulfide (adapted from Michelet et al., 2013).

1.2.3 Regulation of light reactions

Regarding light reactions harbored in the thylakoid membrane, an early detected, direct redox-regulated factor is the CF_1-ATP synthase (Mills et al., 1980; Schwarz et al., 1997; Bob B. Buchanan, 2016; Carrillo et al., 2016). TRX*m*4 functions in down-regulation of NDH complex during CEF (Courteille et al., 2013), TRX*m*1, TRX*m*2 and TRX*m*4 function in biogenesis of PSII (Wang et al., 2013). Further, the demands of the CBC on reducing equivalents might dictate electron flow at the level of cyt b_6f complex (Eberhard et al., 2008), underscoring the importance of coordinating light and carbon reactions via redox mediation. Another study showed that slow NPQ relaxation is responsible for impaired short-term CO_2 fixation under changing light conditions (Kromdijk & Long, 2016), involving redox-sensitive xanthophyll cycle enzymes (Jahns et al., 2009; Hall et al., 2010; Naranjo et al., 2016). A stroma-thylakoid connection is postulated where Serine/threonine-protein kinase STN7, required for photosynthetic state transition (Bellafiore et al., 2005; Bonardi et al., 2005), is modulated via TRX (Rintamäki et al., 2000; Puthiyaveetil, 2011; Puthiyaveetil et al., 2012; Rochaix, 2013; Karamoko et al., 2013); evidence is supported by *in vitro* studies, also promoting a trans-thylakoid energy transfer proceeding from TRX*m*, thereby regulating targets on the lumen site (Motohashi & Hisabori, 2006, 2010; Hertle et al., 2013; Wunder, et al., 2013; Shapiguzov et al., 2016); however, the exact mechanisms remain to be resolved until now.

1.2.4 Regulation of stromal processes

The more prominent and well-investigated part of thiol-redox regulation relates to the light-activation of the CBC (Collin et al., 2003; Marri et al., 2009; Thormählen et al., 2013; Yoshida et al., 2015; Buchanan, 2016); under darkness, TRXs become oxidized

and as a consequence the CBC turns inactive. The chloroplastic isoform of Fructose-1,6-bisphosphatase (FBPase), compared to the cytosolic form, undergoes a light-dependent activation upon disulfide reduction via TRX*f* (Buchanan et al., 1967; Buchanan et al., 1971; Buchanan, 2016), which was shown to be highly specific (Collin et al., 2003; Yoshida et al., 2015). Therefore, regulating FBPase is also important for starch synthesis using F6P from the CBC. Additionally, TRX*f* is also a strong activator of ADP-glucose pyrophosphorylase (AGPase) (Thormählen et al., 2013), a major hub of starch biosynthesis (Neuhaus & Stitt, 1990; Geigenberger et al., 2005; Geigenberger & Fernie, 2014). Thioredoxin-regulated ß-amylase and α-glucan, water dikinase (Mikkelsen et al., 2005; Sparla et al., 2006) turned out to be of equal importance for plant fitness. Not solely redox- but allosteric regulation by 3-PGA stimulates the activity too and is part of a multilevel regulation regarding AGPase (Geigenberger, 2011). TRX*m* is the most versatile and most abundant group of isoforms of plastidic TRXs and plays a conjoint role with *f*-type TRX in activation of CBC enzymes as well as of NADP-dependent malate-dehydrogenase (NADP-MDH) – the so called "malate valve" –, that carries reducing power from the chloroplast to other cell compartments (Collin et al., 2003; Belin et al., 2015; Okegawa & Motohashi, 2015; Yoshida et al., 2015). Further, TRXs and NTRC are responsible for chlorophyll synthesis (Ikegami et al., 2007; Richter et al., 2013), leading to a pale phenotype in the *ntrc* mutant (Serrato et al., 2004; Pérez-Ruiz et al., 2006). A broad spectrum of overlapping functions within the TRX system and between TRX and NTRC could be observed, where NTRC is further attributed a significant role in starch metabolism (Michalska et al., 2009) and the antioxidant system by reducing 2-Cys peroxiredoxin, which acts on oxidative deactivation of chloroplast enzymes in the dark (Pérez-Ruiz et al., 2006; Ojeda et al., 2018).

1.3 Dissecting environmental influence on plant physiology

1.3.1 Light as key factor for plant fitness

Photosynthesis and CO_2 fixation are limited by environmental factors (light, temperature, water, etc.), that can turn into stress factors when their availability and quality is suboptimal or absent. Sessile plants have to deal with and adapt to these stressors to ensure growth and development. Strategies to cope with stress include tolerance, repelling/avoidance or reverting; the investigation of plant responses and acclimation strategies to changing environments is of special interest, because they determine the cultivation boundaries of crop plants (Kadereit et al., 2021). Environmental signals run down a cascade of perception and transduction to eventually

result into a molecular response (Pfannschmidt et al., 2001). Therein, redox processes controlled by TRXs or processes scavenging harmful ROS play a far-reaching role. In terms of light as external factor, low light intensities do not exhaust the full capacity of the photosynthetic apparatus to generate photo-assimilates (i.e. energy); excess light quanta saturate photosynthesis quite swiftly, so a substantial surplus of non-useable energy has to be quenched in order to prevent the inevitable formation of ROS, that harbor the potential to disintegrate cellular structures like DNA or lipid bi-layers (Kadereit et al., 2021). However, high excitation pressure can also be induced by lower light intensities, when the dark reactions are severely impeded (Pfalz et al., 2012). An apparent marker for light-dependent responses is the transformation of chlorophyll in the leaves. A lot of components of the photosynthetic apparatus are encoded in both the chloroplast and the nucleus; therefore it is almost certain that a concerted crosstalk between compartments is occurring, thus enabling complex acclimation processes (Walters, 2005). As mentioned earlier, the chloroplast redox state and the redox state of PQ in particular have the potential to coordinate expression of photosynthetic genes (Wagner et al., 2008; Bräutigam et al., 2009) and act as a novel integrator of environmental stimuli compared to cytosolic and nuclear phytochromes for instance (Eberhard et al., 2008). A key strategy of responding to light on the long run is called long-term response (LTR), acting on hours and days, and initially defined for changes in light quality, describing the stoichiometric adjustments of photosystem subunits in favor of the rate-limiting photosystem (Wagner et al., 2008). Compared to that, this thesis is thought to complement the plethora of studies on environmental stimuli by the factor *light intensity*, as suggested (Bräutigam et al., 2009). Beyond that, researchers are now becoming more and more aware of the fact that not only seasonal or daily but also shorter events, on the scale of minutes or seconds, like rushing clouds or mutually shading leaves in canopy levels, affect the light quality and quantity the plants perceive. Consequently, plants need to possess molecular adaptive processes to handle their fast-changing environments. In the course of this study, this natural phenomenon was carried into the lab to extensively study plant physiology under fluctuating light (FL) conditions, consisting of rapid alterations between higher and lower light intensities, and to compare the output with conventional growth conditions in constant light regimes.

1.3.2 Scope of -omics

Omics technologies are a broad emerging field aiming to study, identify and characterize complex biological systems and processes or (groups of) small molecules as

biomarkers for predicting or monitoring the current or future physiological state, respectively (Wanichthanarak et al., 2015). These technologies simultaneously collect and quantify large composites of molecules to describe an organism or respective tissue in its entirety and thereby go beyond the analysis of single parts of the system (Glinski & Weckwerth, 2006). This is particularly useful when designed as high-throughput method to draw global metabolomic or proteomic profiles. These studies are often exploratory fashioned and contrary, in the best case complementary, to classical knowledge-based studies (Glinski & Weckwerth, 2006). In the following, the impact of single and combined disciplines in the *omics* field, that are going to be used in this work, will be introduced.

A functional metabolism is a central characteristic for the definition of life and is the prime level of acclimation to a new steady state when facing stress conditions. Metabolic state and plasticity, supported by PTM and enzyme activation, represents the actual phenotype as a prompt response to the environment on the point, compared to gene expression or the proteome; however, signals from gene expression are amplified at the site of metabolites and feedback-regulated in the other direction (Hollywood et al., 2006). Metabolomics is mostly used to study substance fluxes or networks. Thereby, correlations and co-regulations among metabolites (and preferably other variables) are desired to describe the system, that is more than the sum of linear metabolic pathways (Glinski & Weckwerth, 2006). As outlined, it is hoped that metabolic profiles can describe the current and immediate phenotypes adequately, reveal re-adjustments in fluxes upon imbalances and therefore elucidate the prime levels of acclimation.

The proteome defines the entire number of proteins in a single cell or organism at a given state. Proteins come with a wide range of PTMs and other modifications rendering the field of proteomics rather complex and profound, compared to other disciplines. The widely used bottom-up proteomics, also called *shotgun* proteomics, separates and identifies a huge number of peptides in a mixture of digested proteins in a two-step procedure (Domon & Aebersold, 2010). However, it is useless without aligning this output with downstream analytical tools to be translated back into biology (Tyanova & Cox, 2018). A standard procedure of post-proteomic analysis includes data cleansing and processing, brief exploration by correlation or PCA for instance, statistics and finally functional analysis (Tyanova & Cox, 2018).

In conclusion, a combination of high-throughput *omics* approaches are expected to explore environmental influences on plant physiology on a global level and to build

predictive summaries of how plants adapt to environmental changes (Carrera et al., 2018).

1.4 Background and objectives of this work

1.4.1 Background

The identification and characterization of factors (proteins) involved in photosynthesis has come a long way in the past decades. Today the (redox-)regulatory interplay and hierarchy between these factors gain of importance and the chloroplast as central hub for acclimation processes moves more into scientific focus (Armbruster et al., 2011; Michelet et al., 2013; Geigenberger & Fernie, 2014; Thormählen et al., 2015; Flügge et al., 2016; Rühle & Leister, 2016; Leister, 2019; Cejudo et al., 2019; Kleine et al., 2021). In this work, a disruption of known genes (mutagenesis) was used to extensively investigate the effects on the phenotype, photosynthesis, metabolome and proteome on the model organism *Arabidopsis thaliana* (reverse genetics). A lot of information about the *in vivo* characteristics of chloroplast thiol-redox regulators is still missing. Thus, disruption of the genes *TRXF1* (Thormählen et al., 2013), *NTRC* (Pérez-Ruiz et al., 2006) and *TRXM1/TRXM2* (Thormählen et al., 2017) via T-DNA insertions (O'Malley & Ecker, 2010) should reveal the function of the corresponding proteins in WT plants under certain environmental stresses *in vivo*. The role of TRXs in photosynthesis under control conditions has been elucidated in the previous chapters, resulting in WT-like growth phenotypes in redox-deficient mutants *trxf1* and *trxm1m2* (Okegawa & Motohashi, 2015; Yoshida et al., 2015; Thormählen et al., 2015, 2017) but leading to a pale and dwarf phenotype in *ntrc* (Serrato et al., 2004; Pérez-Ruiz et al., 2006).

1.4.2 Objectives

In this thesis, different light regimes, photoperiods and intensities were applied on young and adult, but non-flowering, plants under controlled environments to further elaborate the single (TRX*f*1; NTRC) or combined (TRX*m*1*m*2) effects of thiol-redox regulators on growth, photosynthesis, metabolism and the proteome. In detail, following questions should be answered:

i) What are the *in vivo* roles of TRXs and NTRC in response to short-term changes in light intensity? How do TRXs and NTRC affect photosynthesis, photosynthetic state transition and metabolism in response to short-term HL (de-)acclimation?

ii) What is the time frame of photosynthetic acclimation to fluctuating light (FL) in WT? How do thiol-modifying TRXs and NTRC influence the progressive acclimation to FL?

iii) What are the *in vivo* roles of TRXs and NTRC in acclimation to long-term changes in light intensity? How do TRXs and NTRC influence growth and regulate photosynthesis, metabolism and the proteome in response to long-term changing light regimes?

Regarding the double-silencing of *TRXM1* and *TRXM2*, the respective *in vivo* roles compared to higher-order knockout mutants, displaying visible phenotypic changes, should be further clarified (Wang et al., 2013; Okegawa & Motohashi, 2015; Thormählen et al., 2017).

2 Material and Methods

2.1 Material

2.1.1 Instruments

Table 2.1.1. List of instruments.

Instrument	Model	Vendor
Blotting system	Mini-PROTEAN	Bio-Rad, USA
Centrifuge	5417R	Eppendorf, Germany
Cryo-mill	MM400	Retsch, Germany
ECL reader	Fusion Fx7	Vilber Lourmat, Germany
Photometer	FilterMax F5	Molecular Device, USA
Vacuum concentration	concentrator plus	Eppendorf, Germany

2.1.2 Programs, online tools and databases

Table 2.1.2. List of programs, tools and databases used in this thesis

Program	Source
agriGO	http://bioinfo.cau.edu.cn/agriGO
agriGO v2	http://systemsbiology.cau.edu.cn/agriGOv2
ImageJ v.1.52a	https://imagej.nih.gov/ij
MapMan v3.5.1	https://mapman.gabipd.org/de
MaxQuant v1.6.10.43	https://www.maxquant.org/
Mendeley 1.19.8	https://www.mendeley.com/guides/desktop
MetaboAnalyst v4.0 & v5.0	https://www.metaboanalyst.ca/
MS Office	https://www.office.com
Perseus v1.6.10.43	https://maxquant.net/perseus
Prism GraphPad v9.2.0	https://www.graphpad.com/
R v1.4.1106	https://www.r-project.org
REVIGO	http://revigo.irb.hr/
stringDB v11.5	https://string-db.org
SUBA4	https://suba.live/
TAIR	https://www.arabidopsis.org
Thalemine	https://bar.utoronto.ca/thalemine/begin.do
UniProt	https://www.uniprot.org
Venny v2.1	https://bioinfogp.cnb.csic.es/tools/venny/index.html

Table 2.1.3. List of R packages used in this thesis.

Package	Reference
calibrate	Graffelman & van Eeuwijk, 2005
circlize	Gu et al., 2014
cluster	Maechler et al., 2021
colortools	Sanchez, 2013
ComplexHeatmap	Gu et al., 2016
corrplot	Wei & Simko, 2021
corrr	Kuhn et al., 2020
devtools	Wickham et al., 2021
emmeans	Lenth, 2022
factoextra	Kassambara & Mundt, 2020
FactoMineR	Lê et al., 2008
ggextra	Attali & Baker, 2019
ggplot2	Wickham, 2016
ggthemes	Arnold, 2021
Hmisc	Harrell Jr, 2021
magrittr	Bache & Wickham, 2022
multcomp	Hothorn et al., 2008
naniar	Tierney et al., 2021
RcmdrMisc	Fox, 2022
RColorBrewer	Neuwirth, 2014
scales	Wickham & Seidel, 2020
tidyverse	Wickham et al., 2019
visdat	Tierney, 2017
yarrr	Phillips, 2017

2.2 Methods

2.2.1 Plant based methods

2.2.1.1 Plant material and growth

All seeds of the species *Arabidopsis thaliana* (Brassicaceae) used were genetically tested for homozygosity (data not shown). Seeds were from AG Geigenberger's stock (**Table 2.2.1**). Lines were generated in the Columbia-0 (Col-0) genetic background, which also served as the wild type (WT) control.

Table 2.2.1. Description of T-DNA lines.

Line	Protein	AGI	Reference	Germplasm
trxf1	TRX*f*1	AT3G02730	Thormählen et al., 2013	SALK_128365
trxm1m2	TRX*m*1 TRX*m*2	AT1G03680 AT4G03520	Thormählen et al., 2017	WiscDsLox375F05 SALK_123570.51.10.x
ntrc	NTRC	AT2G41680	Pérez-Ruiz et al., 2006	SALK_012208

Arabidopsis thaliana seeds were stratified for 48 h at 4°C in the dark, to disrupt seed dormancy. Afterwards, seeds were sown out on soil (Stender Vermehrungssubstrat A210; Stender AG, Schermbeck, Germany), put in the growth chambers (**Table 2.2.2**) and covered under a breathable cover until sprouting. The trays were moved occasionally to avoid positioning effects. Plants were fertilized on a weekly basis with 0.2 % Wuxal Super (MANNA, Wilhelm Haug GmbH & Co. KG, Ammerbuch-Pfäffingen, Germany).

Table 2.2.2. List of growth chambers and light sources.
ML, medium light; HL, high light; LL, low light; FL, fluctuating light; n.d., not defined. Spectra are displayed in **Supplement Figure 5.5.1.**

Chamber (Institute)	Light source	Diurnal rhythm (day/night)	Temperature (day/night)	Light intensity (µmol photons m^{-2} s^{-1})
LED-Percival (München)	LED	16/8 h	22/16 °C	80 (ML) 450 (HL)
LED-chamber (München)	LED	12/12 h	22/16 °C	125 (ML) 500 (1 min), 50 (5 min) (FL)
LED-chamber (Golm)	LED	12/12 h	20/16 °C	250 (ML) 900 (HL) 90 (LL) 900 (1 min), 90 (4 min) (FL)
Compartment chamber (München)	Mercury lamp	16/8 h	n.d. (cooling with fan)	900 (HL)

2.2.1.2 Determination of growth rate

The exponential growth of leaf areas of soil grown plants was documented every 2 days, starting 3 weeks after sowing, using Image PAM (Walz, Germany) and the following formula: growth = $A \times e^{\lambda \times t}$. A = initial state, e = Euler's number, λ = growth constant, t = time.

2.2.1.3 Harvesting of plant material

For analysis of metabolic processes in the leaf, the leaf rosette was generally separated from the hypocotyl under light without shading and immediately snap-frozen on liquid nitrogen (liq. N_2). Under cooling, the material was pulverized at 30 Hz (MM400, Retsch, Germany) and then aliquoted.

2.2.1.4 Chlorophyll fluorescence measurement

Measurements of chlorophyll *a* fluorescence were carried out using a pulse-amplitude modulation (Imaging PAM, Walz, Germany). Minimal fluorescence yield (Fo) of dark-adapted (30 min) plants was measured before illumination with a short saturating pulse (2700 µmol quanta m^{-2} s^{-1}) to determine maximum quantum efficiency of PSII (Fv/Fm=(Fm-Fo)/Fm). During measurement short pulses of saturating light were applied to measure maximal fluorescence yield (Fm'), ground (Fo') and steady state (Fs') fluorescence in order to calculate PSII quantum yield (Φ II = (Fm'-Fs')/Fm'), non-photochemical quenching (NPQ = (Fm-Fm')/Fm') and reduced PQ (1-qL = ((Fm' – Fs') × Fo')/((Fm' – Fo') × Fs')).

For electron transport rate (ETR) determination, chlorophyll absorption in dark-adapted leaves was measured, followed by actinic light illumination in the following series: 10 min 35 µmol photons m^{-2} s^{-1}, 10 min 56 µmol photons m^{-2} s^{-1}, 5 min 100 µmol photons m^{-2} s^{-1}, 5 min 230 µmol photons m^{-2} s^{-1}, 5 min 462 µmol photons m^{-2} s^{-1}.

2.2.2 Protein based methods

2.2.2.1 Protein determination

Protein determination was done by Dr. Stephanie Arrivault (MPI-MP, Golm) using desiccated pellets from LC-MS/MS extraction (cf. chapter 2.2.3.3). Dried pellets were re-suspended in 400 µL 0.1 M NaOH, heated for 30min and quantified according to Bradford (Bradford, 1976) with BSA as standard.

2.2.2.2 SDS-PAGE with following Immunoblotting

Extraction

20 (±2) mg of frozen leaf powder was extracted with 1mL of 16% (w/v) trichloroacetic acid (TCA) in diethyl ether pre-cooled to -80°C, mixed 3 times by vortexing every 20 minutes with in-between and subsequent overnight storage at -20°C. The following morning, the protein pellet was collected by centrifugation (13.000 rpm for 5 min at 4°C; Centrifuge 5417R, Eppendorf, Germany) and the TCA supernatant was carefully removed by pipetting. The pellet was washed by adding 1mL of 100% acetone stored at -20°C and inverting the tube 4 times by hand while working on ice. The pellet was collected once more by centrifugation, the supernatant removed and 1mL of fresh acetone added until the sample had been washed at least 3 times. The dried pellet was re-suspended in 200µL of sample buffer (10% [w/v] glycerol, 244mM Tris/HCl pH 8.5, 2% [w/v] SDS, 0.33mM Coomassie G-250, with or without freshly added 100mM DTT) with two Ø 4mm steel balls added and gently vortexed at room temperature (RT) for 10 min. Afterwards, the steel balls were removed, and the samples were heated to 42°C at 800 rpm horizontal shaking for 5 min. The insoluble material was collected by centrifugation at 14.000 rpm for 1 min at RT. The supernatant was used for subsequent gel electrophoresis.

Electrophoresis

For separation of proteins regarding size and phosphorylation state, a Phos-tag (Wako Chemicals GmbH, Neuss, Germany) was included in gel electrophoresis. A Zn^{2}+-Phos-Tag-PAGE based on a combination of Kinoshita et al., 2009, Kinoshita & Kinoshita-Kikuta, 2011, Longoni et al., 2015 and the manufacturer's instructions was used. The gel was cast in 1.5mm BioRad Mini-PROTEAN plates (Bio-Rad Laboratories, Inc., Hercules, USA) and was made up of three layers. Three volumes of the bottom layer resolving gel solution (357mM Bis-Tris-HCl pH 6.8, 10% [w/v] acrylamide/bis-acrylamide 37.5:1, 0.025% [w/v] ammonium persulfate [APS], 0.053% [v/v] N, N, N′, N′-tetramethylethylendiamine [TEMED]) were poured into the plates and topped with a layer of 70% (v/v) isopropanol and left to polymerize for approximately 30 min. The isopropanol was drained off and one volume of the top layer resolving gel solution containing the Phos-Tag (357mM Bis-Tris-HCl pH 6.8, 9% [w/v] acrylamide/bis-acrylamide 37.5:1, 80µM Phos-Tag, 160µM $ZnCl_2$, 0.025% APS, 0.053% TEMED) was poured on top and covered with isopropanol until it polymerized. Afterwards, the stacking gel (357mM Bis-Tris-HCl pH 6.8, 5% [w/v] acrylamide/bis-acrylamide 37.5:1, 0.025% APS, 0.053% TEMED) was cast with a 10-well comb inserted and the gel was wrapped in wet paper and left overnight at 4°C in the dark before being used. 5 µL of

sample supernatant (0.5 mg FW) was loaded. The gels were inserted into a BioRad Mini-PROTEAN Tetra Cell tank filled with freshly prepared running buffer (50mM Tris, 50mM 3-(N-morpholino) propanesulfonic acid [MOPS], 0.001% [w/v] SDS, freshly added 5mM $NaHSO_3$). The gels were run at constant 120V for 1h. After the separation was completed, the gels were rinsed in ddH_2O and equilibrated in transfer buffer (25mM Bicine, 25mM Bis-Tris, 1mM EDTA, 10% [v/v] MeOH, freshly added 5mM $NaHSO_3$) for 20 min. Proteins were transferred on a PVDF membrane at constant 100V and cooling for 65 min using a wet blot system. After transfer, membranes were briefly washed in ddH_2O and blocked with 5% (w/v) bovine serum albumin (BSA) in 10mL tris-buffered saline plus Tween 20 (TBST; 20mM Tris-HCl pH 7.4, 150mM NaCl, 0.1% [v/v] Tween 20) for 90 min under agitation. After blocking, membranes were incubated overnight at 4°C while agitated with freshly prepared primary antibody solution (polyclonal rabbit anti-LHCB2, AS01 003, Agrisera, Vännas, Sweden; 2% (w/v) BSA in 5mL TBST at a dilution of 1:5000). The following morning, the membranes were washed 4 times in TBST for 10 min. The membranes were incubated for 1h at RT while agitated with freshly prepared secondary antibody solution (polyclonal goat anti-rabbit, HRP-conjugated, AS09 602, Agrisera, Vännas, Sweden; 2% (w/v) BSA in 10mL TBST at a dilution of 1:20000). Finally, the membranes were washed 3 times in TBST and 1 time in TBS.

ECL readings

For chemiluminescent detection the membranes were analyzed using the Pierce™ ECL Western Blotting Substrate (ThermoFisher Scientific, Waltham, USA) and Fusion Fx7 reader (Vilber Lourmat Deutschland GmbH, Eberhardzell, Germany) with corresponding software. Quantification was done using ImageJ v.1.52a.

2.2.2.3 Proteomics

Mass spectrometric identification and quantification of peptides was performed at the MPI-MP in Potsdam/Golm by Dr. Alex Graf and Beata Siemiątkowska. In brief, measurements were performed on a Q Exactive Plus combined with HF mass spectrometer coupled with a nLC1000 nano-HPLC (both Thermofisher). Quantitative analysis was performed with MaxQuant v1.6.10.43 (Cox & Mann, 2008). The output was matched against the Arabidopsis proteome (UP000006548, April 2019) and initially edited with Perseus v1.6.10.43, where missing values were imputed with the default method (LNBio, 2014; Tyanova & Cox, 2018), to make use of downstream methods that require a complete data set.

2.2.3 Metabolite based methods

2.2.3.1 Quantitative detection of starch

The extraction and determination of starch was done according to Hendriks et al., 2003.

Extraction

20 mg of pulverized plant material was re-suspended in 250 µL (80% v/v) ethanol, vortexed and incubated for 30 minutes at 90°C. After centrifugation (10 min, full speed, RT) the supernatant was transferred into a new tube. The pellet was extracted once more with 80% ethanol and finally with 50% ethanol. All supernatants were pooled and frozen until further use.

Starch degradation

The pellet was first dried in a vacuum concentrator (concentrator plus, Eppendorf, Germany) for 30 minutes at 30°C (V-AL), re-suspended in 400 mL 0.1 M NaOH and incubated at 95°C for 1 hour while shaking. The solution was neutralized with adequate amount of 0.5 M HCl/acetate buffer (0.5 M HCl, 0.1 M acetate-NaOH pH 4.9). Then 40 µL supernatant were mixed with 110 µL starch degradation mix (50 mM acetate-NaOH pH 4.9, 2.8 U mL^{-1} amyloglucosidase, 4 U mL^{-1} α-amylase) and incubated o/n at 37°C.

Determination

The next day the sample was centrifuged for 5 min (full speed, RT) and 50 µL were mixed with 160 µL determination mix (100 mM HEPES /KOH pH 7, 3 mM $MgCl_2$, 3 mM ATP, 1.4 mM NADP, 3.4 U mL^{-1} glucose-6-phosphate dehydrogenase). After the reaction stabilized 0.45 U hexokinase was added an NADPH generation was measured. The amount of NADPH generated equals the amount of starch. The optical density (OD) was recorded using a photometer (FilterMax F5, Molecular Device, USA) at 340 nm (µmol NADPH = $\Delta OD / (2{,}85 \times \varepsilon)$; ε[1] (NAPDH) = 6.22).

2.2.3.2 GC-TOF-MS

Extraction and analysis of central metabolites by gas chromatography coupled with mass spectrometry was performed using the same equipment set up and exact same protocol as described in Lisec et al. (2006). Briefly, frozen ground material was homogenized in 300 µL of methanol at 70°C for 15 min and 200 µL of chloroform followed by 300 µL of water were added. The polar fraction was dried under vacuum, and the residue was derivatized for 120 min at 37°C (in 40 µL of 20 mg mL^{-1} methoxyamine-hydrochloride in pyridine) followed by a 30 min treatment at 37°C with

[1] Extinction coefficient according to the Beer-Lambert law.

70 µL of MSTFA (*N*-Methyl-*N*-trimethylsilyl-trifluoracetamid). An autosampler Gerstel Multi-Purpose system (Gerstel GmbH & Co.KG, Mülheim an der Ruhr, Germany) was used to inject the samples to a chromatograph coupled to a time-of-flight mass spectrometer (GC-TOF-MS) system (Leco Pegasus HT TOF-MS, LECO Corporation, St. Joseph, MI, USA). Helium was used as carrier gas at a constant flow rate of 2 mLs^{-1} and gas chromatography was performed on a 30 m DB-35 column. The injection temperature was 230°C and the transfer line and ion source were set to 250°C. The initial temperature of the oven (85°C) increased at a rate of 15°$Cmin^{-1}$ up to a final temperature of 360°C. After a solvent delay of 180 s, mass spectra were recorded at 20 scans s^{-1} with m/z 70-600 scanning range. Chromatograms and mass spectra were evaluated by using Chroma TOF 4.5 (Leco) and TagFinder 4.2 software. Analysis was performed by Dr. Saleh Alseekh (at the MPI-MP in Potsdam/Golm).

2.2.3.3 LC-MS/MS

Metabolites were measured after methanol/chloroform extraction from 15 mg pulverized fresh weight aliquots using an established reverse phase liquid chromatography coupled with tandem mass spectrometry (LC-MS/MS) platform (Arrivault et al., 2009). Stable Isotopic Labelled Internal Standards (SIL-IS) were added to rule out matrix effects for a subset of metabolites (Arrivault et al., 2015). Analysis was performed by Dr. Stephanie Arrivault (at the MPI-MP in Potsdam/Golm).

2.2.4 Ribosome profiling and RNA footprint

"Ribosome profiling" and "RNA footprint" analyses were conducted by Dr. Reimo Zoschke and colleagues (at the MPI-MP in Potsdam/Golm) according to Trösch et al., 2018.

2.2.5 Statistics

Assuming a normal distribution, a one-factorial or a two-factorial ANOVA was performed as standard test for parametric data to analyze differences among means (*post hoc* Tukey test). A repeated-measures t-test (reference WT or WT-ML) with a *post hoc* Benjamini-Hochberg correction served to evaluate proteomics. Statistical testing was done in R, using basic functions and the "stats", "emmeans" and "multcomp" packages.

3 RESULTS

In this thesis the effects of deficiencies in stromal thioredoxins TRX*f*1, TRX*m*1, TRX*m*2 and NTRC on cellular metabolism and photosynthesis during acclimation in different light intensities was elucidated. The investigation was accompanied by Chl *a* fluorescence measurements, small and large profiling *omics* experiments, exploring metabolic and proteomic adjustments. First, short-term responses (minutes to hours) to elevated light intensities on photosynthesis and metabolism were investigated by disrupting thiol-redox regulators TRX*f*1, TRX*m*1*m*2 or NTRC, which connect light- and carbon reactions in the chloroplast. Then, it was attempted to determine the time frame of photosynthetic acclimation processes to FL in the mutants' background. Finally, the attention was turned to the study of long-term acclimation responses (hours to days) on photosynthesis, metabolism and whole-cell protein abundances in response to loss of TRX*f*1, TRX*m*1*m*2 or NTRC.

In the following, the T-DNA mutant lines of TRX*f*1, TRX*m*1*m*2 and NTRC will be abbreviated as *trxf*, *trxm* and *ntrc* (cf. chapter 3.1.1). The lines have been characterized in previous studies (cf. chapter 1.2, 1.3, 1.4) and prior to all experiments, the lines were tested once for homozygosity (data not shown). During the tests, the *trxm1.1* turned out to carry a T-DNA insertion polymorphism called WiscDsLox, not SALK (data not shown) (compare Thormählen et al., 2017). Nevertheless, the kind of insertion is of no particular importance for the following experiments.

As a prerequisite, the effects of a plant's developmental state on different cellular processes have to be considered. Inspecting the expression pattern throughout the plant's lifespan, the TRX isoforms in our study as well as NTRC appear to be permanently and equally expressed in young and old rosette leaves under control conditions (Winter et al., 2007), eventually allowing for coherent and unambiguous conclusions.

3.1 Photosynthetic (de-)acclimation to short-term high light

Other than investigating the short-term role of TRXs and NTRC to regulate photosynthesis in dark-light shifts (Thormählen et al., 2013, 2015), the initial interest was based on short-term responses (minutes to hours) especially under conditions changing from medium light (ML) to high light (HL). In general, rapid short-term kinetics should resemble the nature of a fast redox relay system (Bräutigam et al., 2009). Therefore, plants were grown in the LED percival (CLF Plant Climatics GmbH, Germany) for 14 days at a photoperiod of 16 h under moderate light (ML; 80 µmol photons m^{-2} s^{-1}) (cf. chapter 2.2.1.1) (Garcia-Molina et al., 2020). Approximately 100 seeds were sawn out on soil to form a lawn like appearance building a dense cushion of leaves. This facilitates harvesting of a great number of plants at once and likewise lowers the variance of the sample. After 14 days the seedlings were subjected from ML to HL (450 µmol photons m^{-2} s^{-1}) for 3 h starting at the middle of the photoperiod (acclimation), following a 3 h de-acclimation under ML.

3.1.1 Deficiencies in Thioredoxin *f* and NTRC affect photosynthetic efficiency during dark-light transitions rather than during short-term high light (de-)acclimation

To study the effects of deficiencies in TRX*f*, TRX*m* or NTRC on photosynthesis, chlorophyll fluorescence experiments were initially performed. During these experiments, moderate and high actinic light was applied on the seedlings copying the intensities in the growth chamber. Preliminary trial runs with wild type (WT) using the Imaging PAM showed that a 3 h illumination could be reduced to 20 min to yet maintain a photosynthetic steady state (data not shown).

Figure 3.1.1 shows the photosynthetic measurements including all genotypes. To begin with, kinetics of Φ II in dark-adapted WT plants were analyzed (**Figure 3.1.1 A**). After the onset of actinic ML, starting with a strong saturating light pulse (cf. chapter 2.2.1.4), Φ II transiently decreased as expected, since all photosynthetic reaction centers were now closed, limiting photosynthesis for a short period of time. After that, levels of Φ II stabilized quickly and reached a value of 0.64 after 20 min (t_0 = 0.83). Following the first phase, HL was applied for 20 min, which led to a decrease of Φ II to a stable value of 0.28, with a very short adaption process right after the shift, leading to a temporary drop to 0.18. Hereafter, actinic light was switched to ML again, leading to a transient rise in Φ II to 0.63 after further 20 min. In the final phase, a slower adaption to ML, following the HL phase, was noticed. In sum, Φ II in WT plants,

regarding steady state, was almost identical before and after the shift to HL. Kinetics of PQ reduction practically followed Φ II kinetics in an inverse manner; open reaction centers cause a total oxidation of PQ in the dark. After the onset of ML, PQ reduction increased steeply and nearly stabilized after 20 min to 0.27 (**Figure 3.1.1 C**). After a shift to HL, PQ reduction became quickly stable and reached 0.70 after 20 more minutes. Following a shift to ML, PQ reduction slowly reached a plateau at the end of the experiment, which was slightly lower as before the HL shift (0.22). NPQ increased as ML was switched on to almost stable values after 20 min (0.97). After HL was switched on, NPQ first steeply and then continuously increased the following 20 min (final value at the end of the HL phase: 2.84). Following that, NPQ decreased after ML was turned on again; compared to the other parameters, NPQ did not reach the same level in this last ML phase (1.22) compared to the initial ML phase.

Next, a delay in activation of photosynthesis from dark to light due to lack of TRX*f*1 and NTRC could be seen, which has also been shown in previous studies (Thormählen et al., 2017). However, WT-like adjustments of Φ II and PQ reduction in all mutants were noticed after a shift from ML to HL and from HL back to ML (**Figure 3.1.1 A** and **C**). Also similar to earlier reports, NPQ started with a higher rate in *ntrc*, relative to WT, after light was switched on, and plateaued very quickly at a value of 1.30, which indicates photo-inhibition. After the onset of HL, NPQ further increased, temporarily higher than WT levels, but stabilized after 20 min to WT levels again (2.83). When HL was finally switched to ML again, NPQ kinetics were then WT-like. There were no substantial differences in NPQ between *trxf* and *trxm* found, compared to WT.

To sum up, photosynthetic yield decreased with short-term increasing light intensities, while PQ reduction and NPQ increased with increasing intensities in all genotypes. In this process, and beside the observed irregularities in *ntrc*, Φ II levels and kinetics before and after the HL phase were highly comparable across all genotypes; the same applied for the HL phase as well. As no considerable dissimilarities in PQ reduction were found, it was concluded, that under given conditions, TRXs and NTRC might – at most – only fine-tune photosynthesis when changing from one light intensity to another, which is unexpected to previous research focusing on the pivotal role of TRX*f* and NTRC on dark-light transitions.

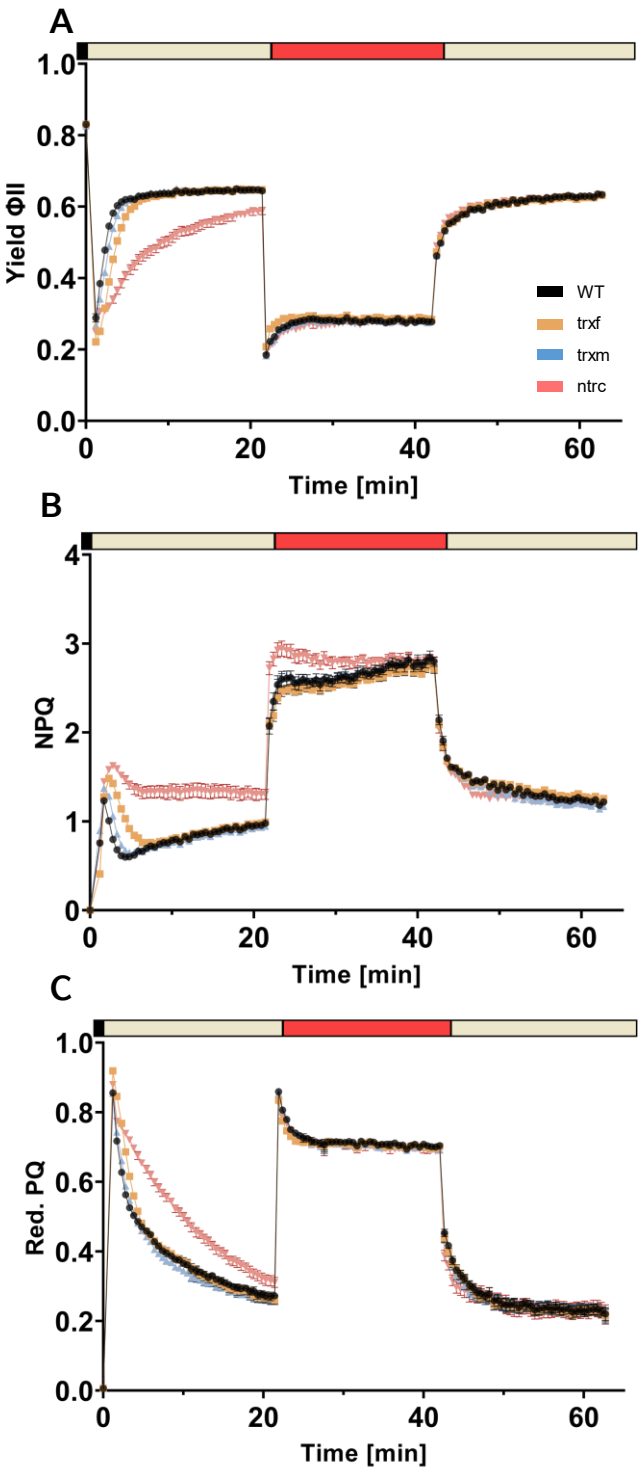

Figure 3.1.1. Transient changes in photosynthetic parameters of photosystem II in WT, *trxf*, *trxm* and *ntrc*.
(A) Yield. (B) NPQ. (C) red. PQ (1-qL). Plants were grown for 14 days at a photoperiod of 16 h and 80 µmol photons m^{-2} s^{-1}. In the middle of the photoperiod dark-adapted plants (30 min) were illuminated with and measured under actinic ML (80 µmol photons $m^{-2}s^{-1}$) for 20 min follow by 20 min HL (450 µmol photons $m^{-2}s^{-1}$) phase and a final ML phase again. Beige bar, ML; red bar, HL. Results are the mean values ± SE, n = 8.

3.1.2 Deficiencies in Thioredoxin *f* and NTRC affect the CBC

Next, metabolites of the CBC were measured, since this pathway is directly connected to photosynthetic light reactions, where resistances in fluxes at each of the redox-regulated steps should be additionally revealed (Knuesting & Scheibe, 2018). **Figure 3.1.2** illustrates the experimental setup and harvest points in this project. Regarding the CBC metabolites, the time points t_0, 15 min, 3 h, 3 h 15 min and 6 h were sampled.

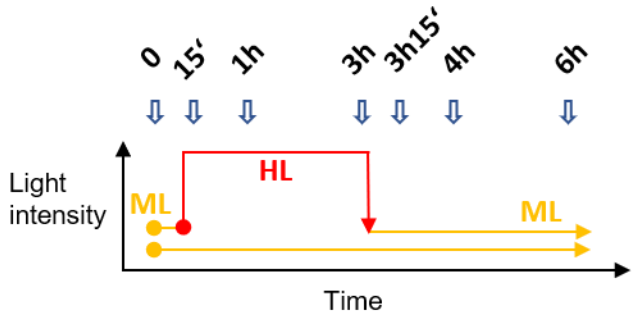

Figure 3.1.2. Experimental setup for short-term (de-)acclimation studies.
Plants were initially grown for 2 weeks under a photoperiod of 16 h light/8 h dark and ML (80 µmol photons m^{-2} s^{-1}). In the middle of the photoperiod, plants were then shifted to HL (450 µmol photons m^{-2} s^{-1}) for 3 h and returned to ML to grow for further 3 h. Particular harvest or measurement time points as indicated are mentioned in the text.

To begin with, an unsupervised clustering to spot genotypic (dis-)similarities between WT and the mutants was carried out. Therefore, a principal component analysis (PCA), including samples and metabolites, from either acclimated (15 min to 3 h) or de-acclimated (3 h to 6 h) HL treated plants, together with the respective control (ML) group was performed. In the de-acclimation phase, the 3 h time point was included to represent "t_0" for the following time points. A PCA serves to simplify complex data and to represent (clusters of) samples on only few descriptive dimensions. The loadings show how the original variables (metabolites) influence the explanatory components. Further, close metabolites are positively correlated, opposite ones (from the origin [0,0]) are negatively correlated (Abdi & Williams, 2010). A clear separation of HL and control samples could be noticed in the acclimation phase (**Figure 3.1.3**). Further, distinct groups of mutant lines and WT were identified, meaning that even under control conditions the effects of an impaired redox metabolism on the CBC were apparent. These effects were strongest for *trxf* and *ntrc*, relative to WT. Strong associations of 3-phosphoglycerate (3PGA) and RuBP with *trxm* and WT and sedoheptulose-1,7-bisphosphate (SBP), ribose-5-phosphate (R5P), fructose-1,6-bisphosphate (FBP), sedoheptulose-7-phosphate (S7P), G6P, G1P, and F6P with *ntrc* and *trxf* were

identified. In the de-acclimation phase, a very similar pattern compared to the acclimation phase was observed (**Figure 3.1.4**); *trxm* and WT were very much alike, *trxf* and *ntrc* segregated further away, indicating a special role in CBC regulation for these two factors; even the loadings were similar to the previous acclimation phase. Summarized, this could mean that there might be constant perturbations of one or several of the respective metabolites, especially of SBP and FBP. The general influence of TRXs and NTRC on the CBC was shown to be generally strong, being highest for NTRC, with clear differences between HL and ML.

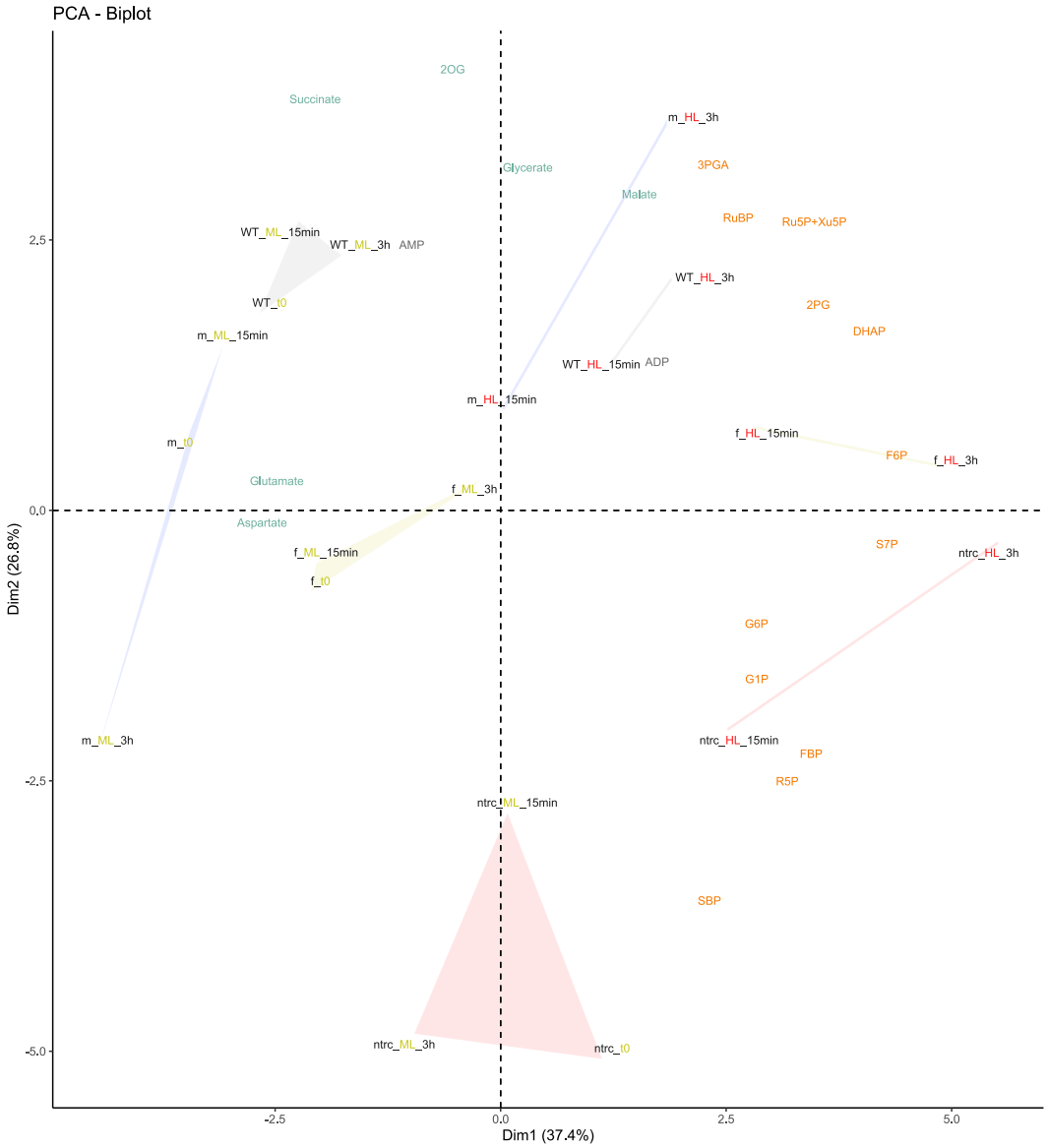

Figure 3.1.3. Clustering of WT, *trxf*, *trxm* and *ntrc* samples for LC-MS based metabolites during HL acclimation (t_0 – 3h).
The variance explained by the single components is given in parentheses. Clustering was done with the "FactoMineR" and "factoextra" packages in R. The cumulative variance explained by PC1 and PC2 is 64.2 %. Amino acids are labelled pink; sugars are labelled blue; organic acids are labelled green. Black, WT; yellow, *trxf*; blue, *trxm*; red, *ntrc*. f, *trxf*; m, *trxm*.

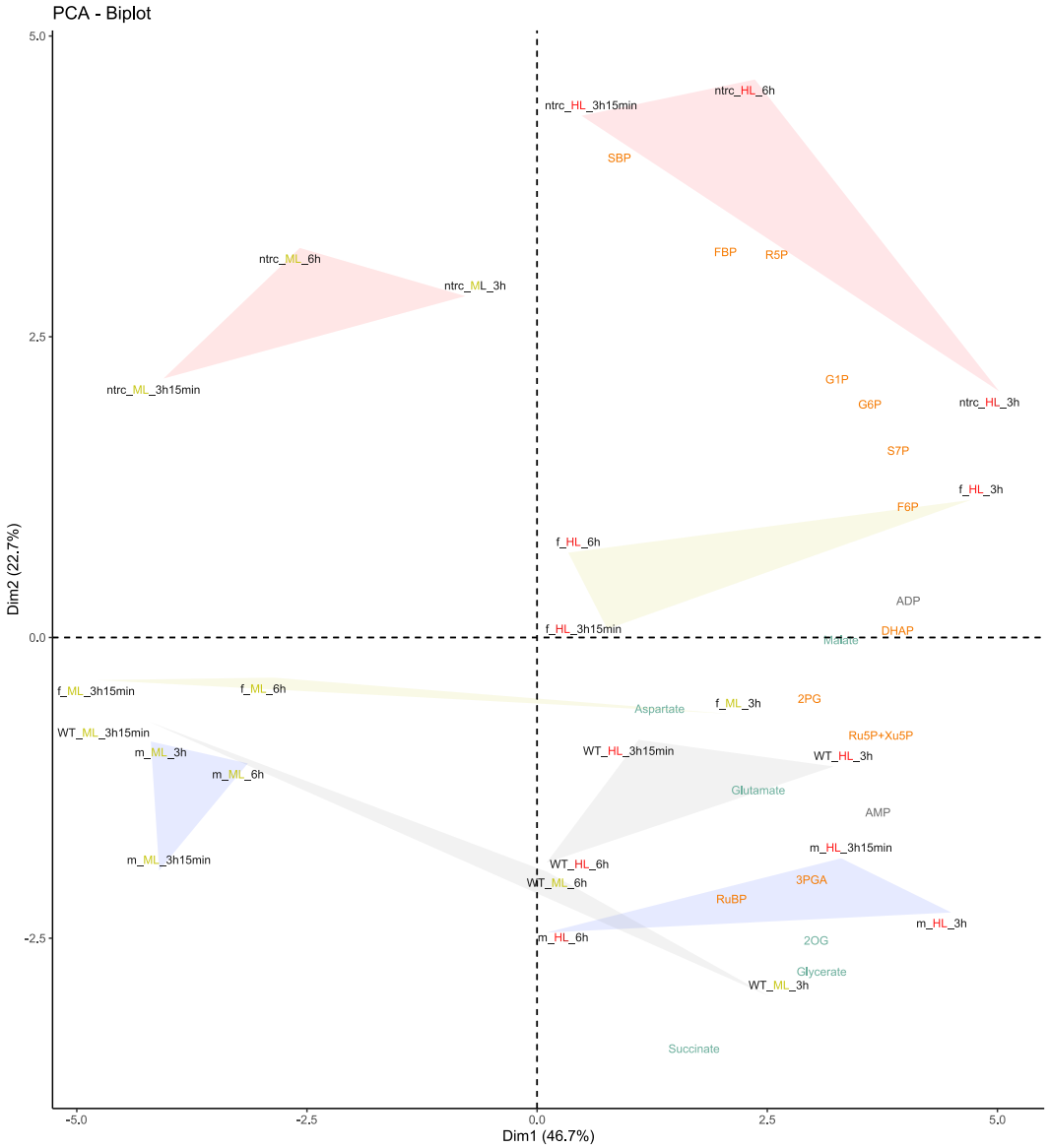

Figure 3.1.4. Clustering of WT, *trxf*, *trxm* and *ntrc* samples for LC-MS based metabolites during HL de-acclimation (3h – 6h).
The variance explained by the single components is given in parentheses. Clustering was done with the "FactoMineR" and "factoextra" packages in R. The cumulative variance explained by PC1 and PC2 is 69.4 %. Amino acids are labelled pink; sugars are labelled blue; organic acids are labelled green. Black, WT; yellow, *trxf*; blue, *trxm*; red, *ntrc*. f, *trxf*; m, *trxm*.

Figure 3.1.5 illustrates a simplified CBC, where statistics for each metabolite and sample were included. First, an excessive accumulation of FBP and SBP (more than 1.5-fold) became apparent, especially in *ntrc*. This indicates a specific bottleneck in CBC activation via NTRC. Besides that, significant changes under HL were scarce. However, RuBP and 3-PGA, key metabolites for fixation and subsequent reduction, were rather down-regulated in the mutants, so a clear disbalance between the stages of the CBC is brought to light. As outlined before, SBP and FBP have been shown to be significantly altered in *ntrc* and *trxf*. Further, these two metabolites, along with R5P were found to be notably up-regulated under HL. Apart from that however, there were no major effects of TRXs and NTRC under HL, as many significant changes occurred in the control conditions as well. Descriptive analyses and detailed lists of statistics regarding the metabolome can be found in **Supplement Table 5.4.1** and **Supplement Table 5.4.2**.

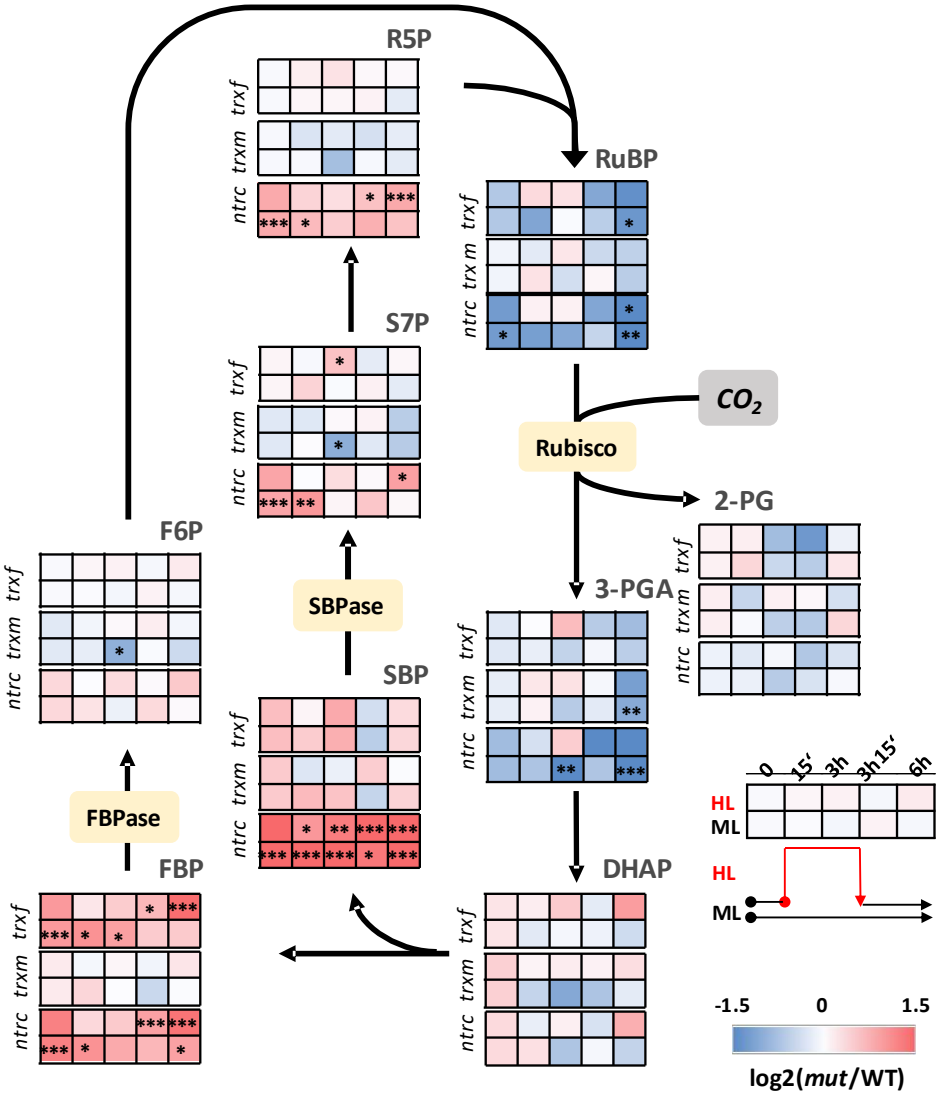

Figure 3.1.5. Simplified pathway of CBC under short-term HL (de-)acclimation. Significance levels within one condition and genotype were evaluated by using a one-way ANOVA with a *post-hoc* Tukey test and are labelled with different asterisks (* $0.01 < p < 0.05$, ** $0.001 < p < 0.01$, *** $p < 0.001$). Significances for t_0, sampled under ML, were inscribed under ML only. Ru5P and Xu5P were not distinguishable and not included here.

To draw a full picture of CBC changes in the mutants (phosphorylated intermediates only), a final cluster analysis was performed. This analysis shall complement the preceding ones, which segmented the data into the acclimation phases, now including all time points. The analysis corroborated that the effect of TRX*f* deficiency grows, compared to WT, is smallest in *trxm* and biggest in *ntrc* (**Figure 3.1.6**). This is most likely due to missing CBC enzyme-activation via TRX*f* and NTRC (Lemaire et al., 2007; Michelet et al., 2013; Thormählen et al., 2015). The hierarchical version of this PCA revealed 3 clusters (**Figure 3.1.7**). Whereas the first PCA highlights the genotypic effect, the second one not only identifies a distinct *ntrc* cluster (cluster 2) but further exposes the relation between control and treated samples; here it becomes apparent that de-acclimated HL samples somewhat return to the starting value (t_0) (within cluster 1) and acclimated HL samples correlate closer to each other (cluster 3), but are clearly dissimilar to the control and de-acclimated samples.

It was concluded, that under HL there is an important short-term role of NTRC in CBC regulation, and a smaller role of TRX*f* and TRX*m* and that over-accumulation of SBP and FBP might lead to an impediment in the cycle that causes shortcomings elsewhere in the cylce.

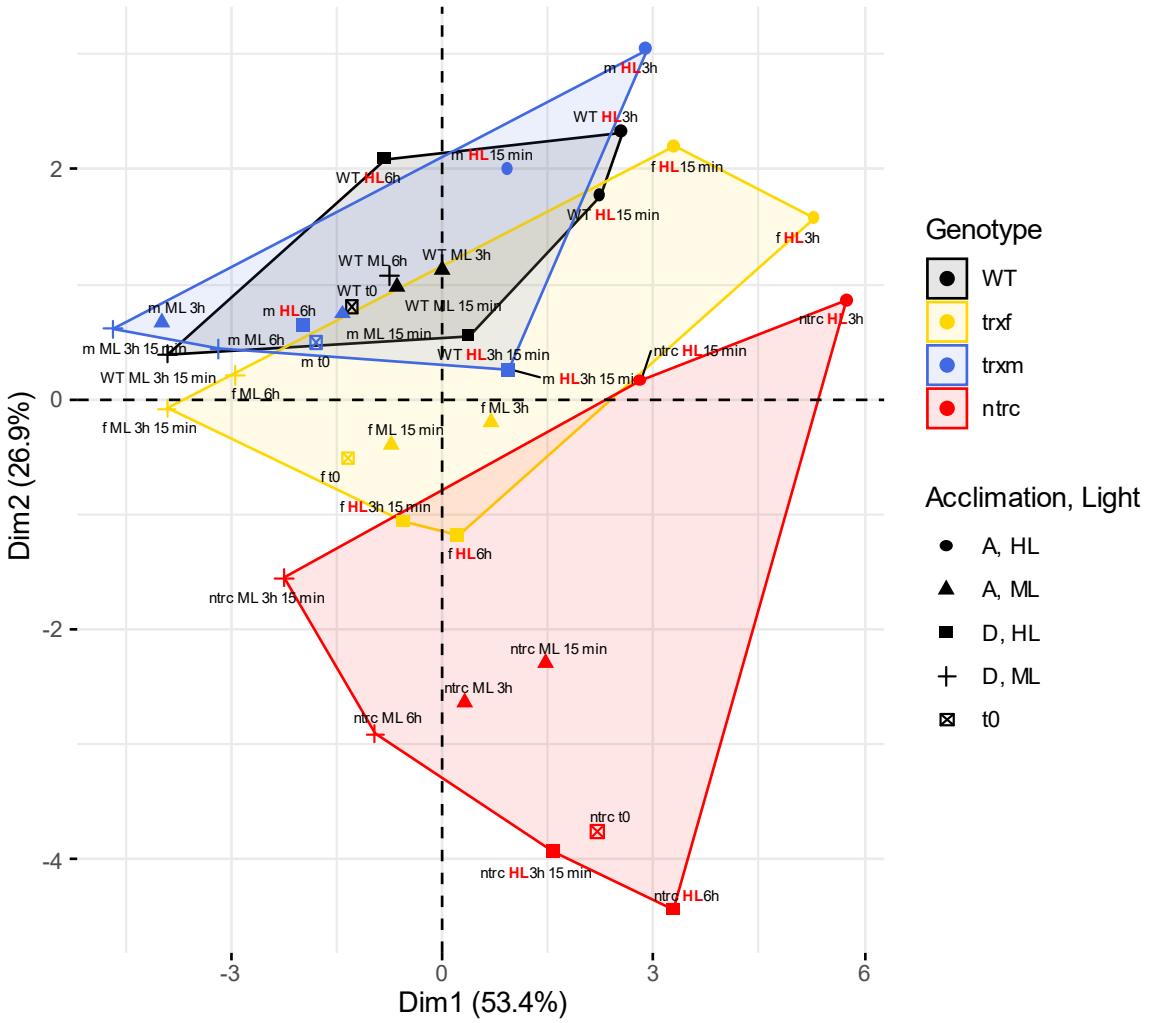

Figure 3.1.6. Complete PCA of Calvin-Benson Cycle metabolites during HL kinetics. The variance explained be PC1 and 2 is given in parentheses. The cumulative variance explained is 80.3 %. Clustering was done with the "FactoMineR" and "factoextra" packages in R. A, acclimation; D, de-acclimation; ML, medium light; HL, high light. f, trxf; m, trxm.

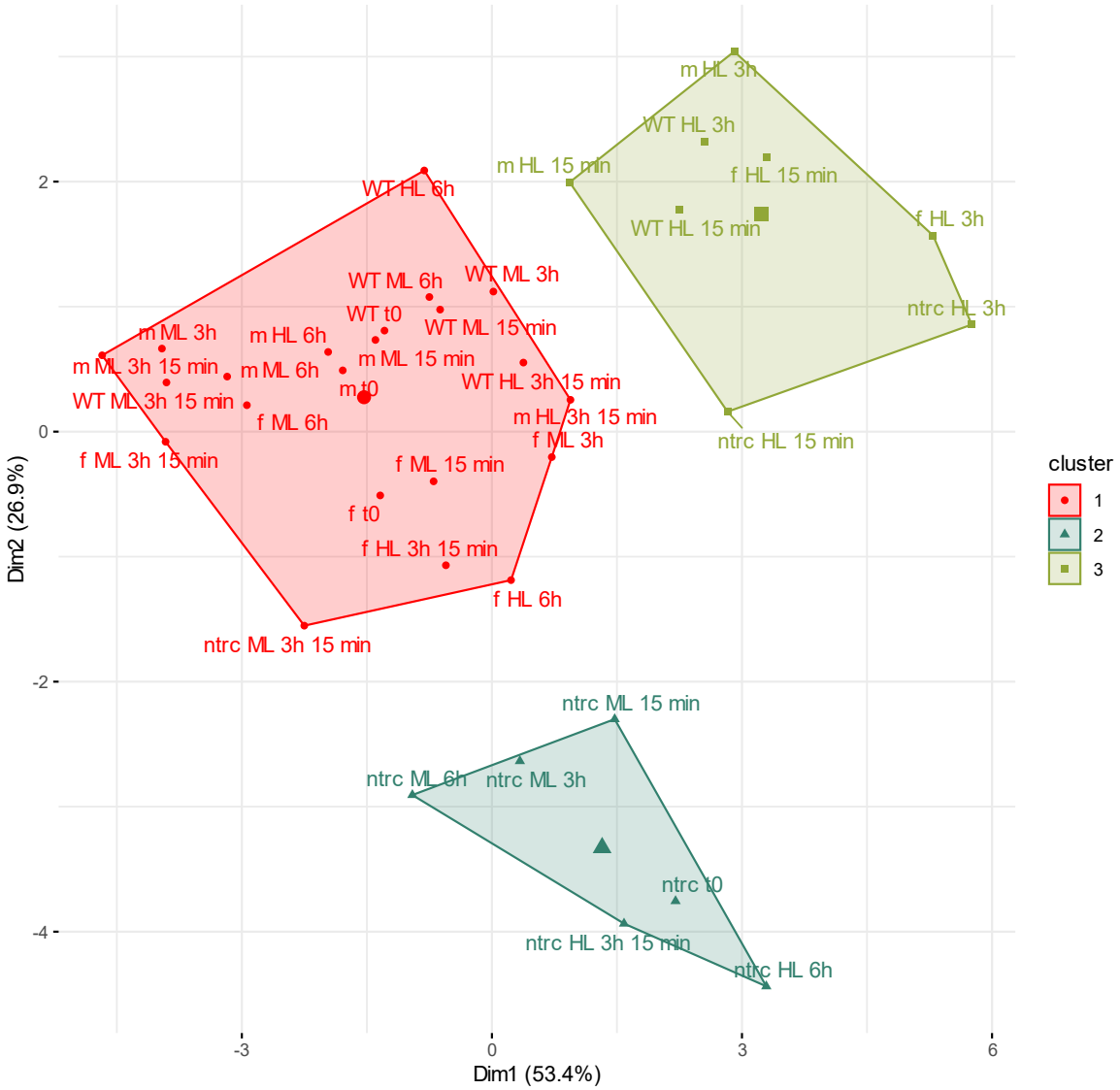

Figure 3.1.7. Clustered PCA of Calvin-Benson Cycle metabolites during HL kinetics. The variance explained be PC1 and 2 is given in parentheses. The cumulative variance explained is 80.3 %. Cluster numbers are arbitrary. Clustering was done with the "FactoMineR" and "factoextra" packages in R. ML, medium light; HL, high light; f, *trxf*; m, *trxm*.

3.1.3 Deficiencies in Thioredoxins and NTRC had only slight effect on global metabolite levels

Next, to gain insight into the profile of central metabolites, including sugars, amino acids and organic acids, we performed a gas chromatography time-of-flight mass spectrometry (GC-TOF-MS) analysis (cf. chapter 2.2.3.2). Compared to the previous chapter, all time points were harvested during this experiment (cf. **Figure 3.1.2**) First, two separate PCAs were performed as before, including all samples from the acclimation and de-acclimation phase, respectively. The HL acclimation relative to ML was analyzed first. There was a clear separation between control and HL samples in the mutants and a slight overlap in the two WT clusters in the middle and late time points (ML 1 h & 3 h) (**Figure 3.1.8**). Nearly all metabolites clustered together with HL samples. In ML a separation of genotypes according to PC2, in HL according to PC1, was noticed, so interpretation of PCs is ambiguous here. Compared to WT, *ntrc* and *trxf* seemed to undergo stronger changes during the acclimation. The late HL time points (3 h) showed to primarily involve amino acids and organic acids, the shorter time points (15 min, 1 h) also included sugars. This might give a first hint to the role of individual compound classes in redox-dependent HL acclimation. The de-acclimation followed a similar pattern; the prior HL treated samples clustered along PC1 and distinguished between the control samples (**Figure 3.1.9**). The genotypic differences were small due to large overlapping of samples. However, there was some dispersion observable regarding middle and late time points, especially between *ntrc* and WT and among the mutants; this was also seen for ML, from which we concluded that natural metabolite oscillation might be very present at this time frame and condition. For this reason, we continued to analyze HL and ML separately. Descriptive analysis and detailed lists of statistics regarding the metabolome can be found in **Supplement Table 5.4.3** and **Supplement Table 5.4.4**. However, they show that HL effects could be hardly elaborated, as significances were found both under HL and ML, partially overlapping. Resuming the genotypic effect, we concluded a stronger, but moderate, role of NTRC in regulating central metabolism in both HL and ML compared to TRX*f* and TRX*m*.

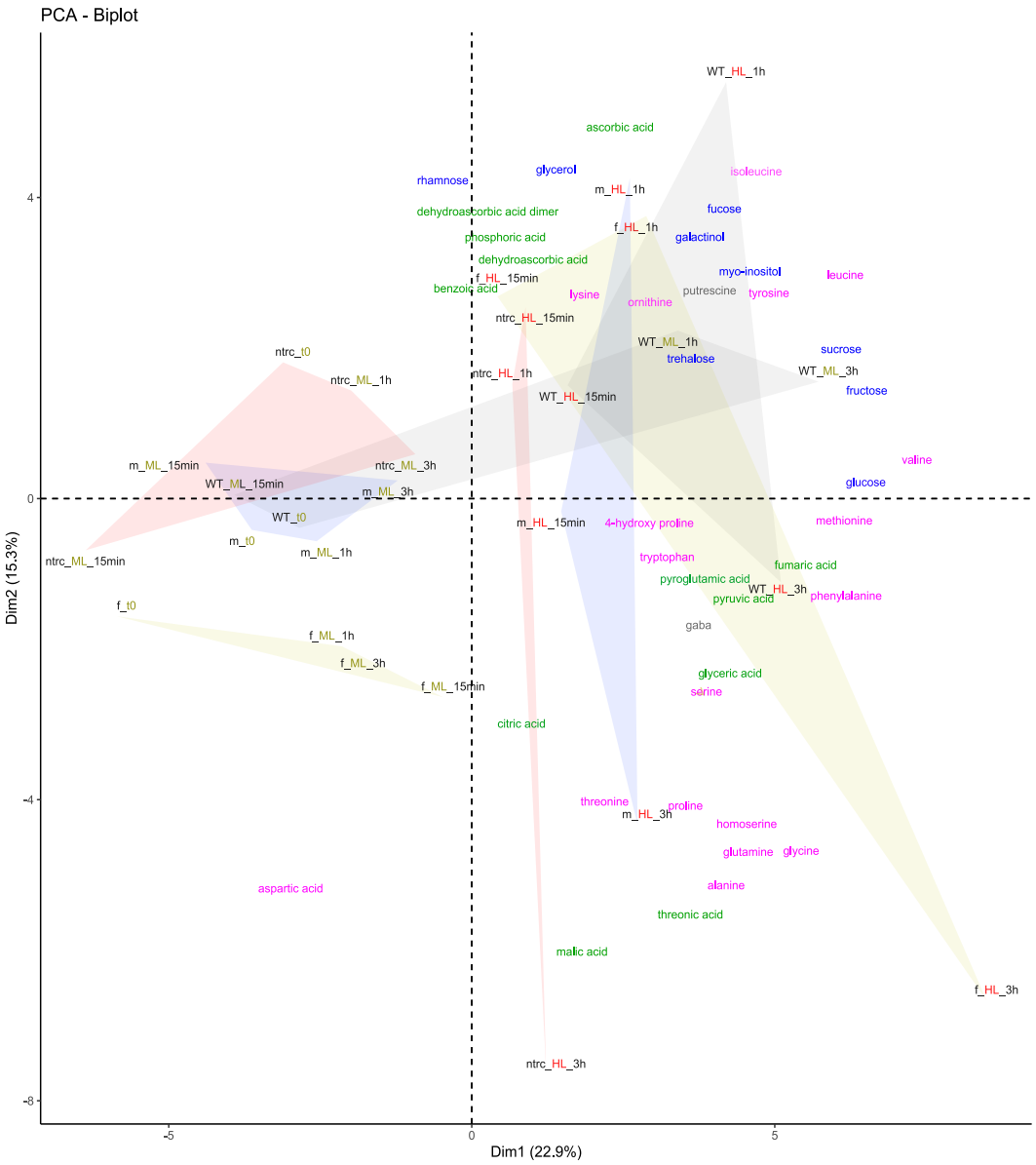

Figure 3.1.8. Clustering of WT, *trxf*, *trxm* and *ntrc* samples for GC-MS based central metabolites during HL acclimation phase (t_0 – 3h).
Only the most important metabolites are plotted. The variance explained by the single components is given in parentheses. The cumulative variance explained by PC1 and PC2 is 38.2 %. Clustering was done with the “FactoMineR” and “factoextra" packages in R. Amino acids are labelled pink; sugars are labelled blue; organic acids are labelled green. Black, WT; yellow, *trxf*; blue, *trxm*; red, *ntrc*. f, *trxf*; m, *trxm*.

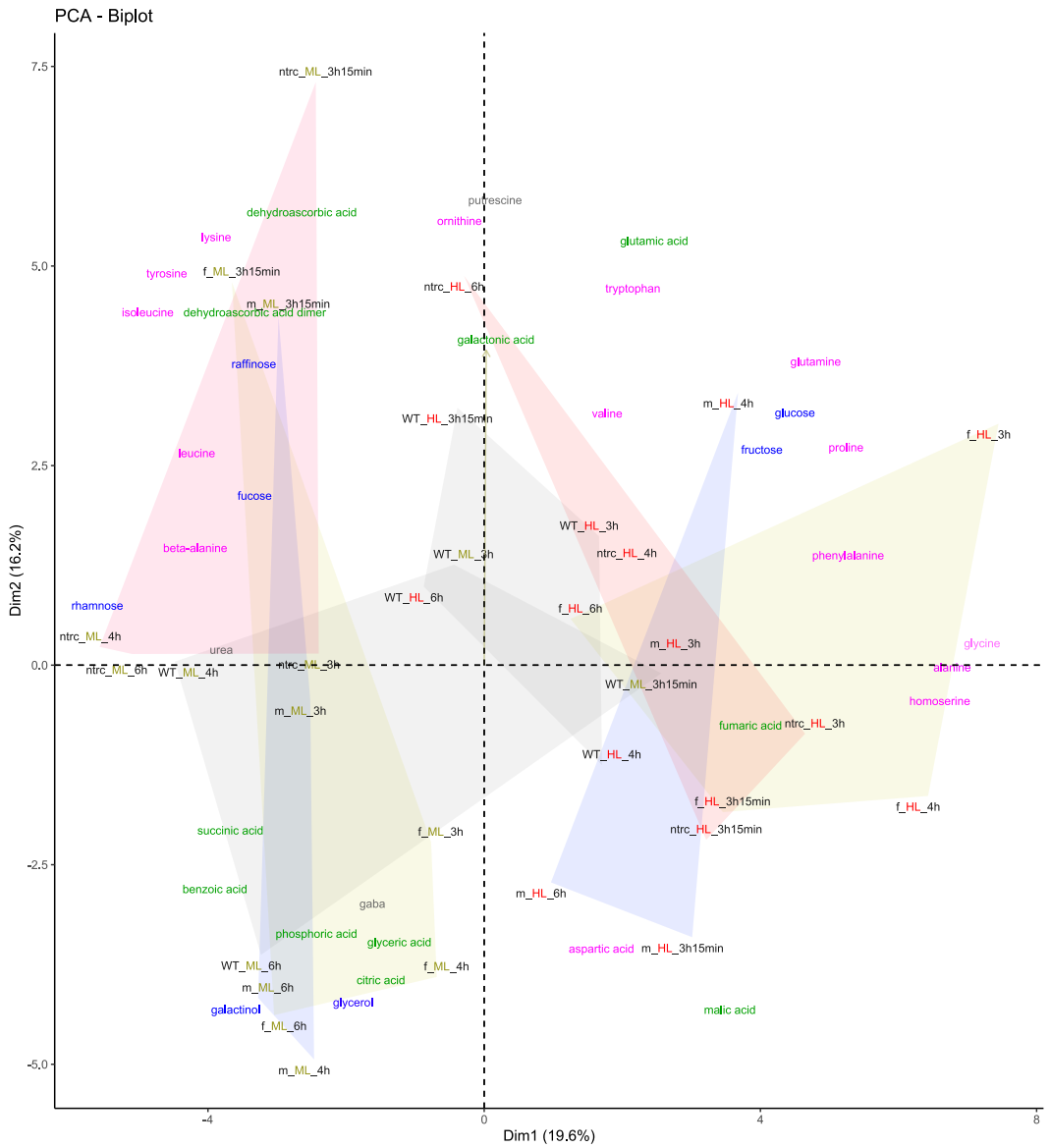

Figure 3.1.9. Clustering of WT, *trxf*, *trxm* and *ntrc* samples for GC-MS based central metabolites during HL de-acclimation (3h – 6h).
Only the most important metabolites are plotted. The variance explained by the single components is given in parentheses. The cumulative variance explained by PC1 and PC2 is 35.8 %. Clustering was done with the "FactoMineR" and "factoextra" packages in R. Amino acids are labelled pink; sugars are labelled blue; organic acids are labelled green. Black, WT; yellow, *trxf*; blue, *trxm*; red, *ntrc*. f, *trxf*; m, *trxm*.

Starch levels were determined from the insoluble pellets from the GC-MS analysis and are given as ratio between HL and ML (**Figure 3.1.10**), to herein segregate true HL events from circadian oscillations in the control group (Garcia-Molina et al., 2020). This was done because of the fact, that starch is progressively synthesized in plants during the photoperiod until night falls. We observed a rise in starch over time in all lines due to higher light but noticed a very diverse genotypic effect. Starting the experiment from the middle of the photoperiod, starch levels plateaued in WT after 3 h, meaning that WT might already prepare for the night period; starch levels rose and quickly stabilized in the de-acclimation phase only (69 % increase after 6 h). In *trxf*, starch peaked under 3 h HL and decreased thereafter; in *trxm* starch peaked shortly after HL passed and fell thereafter as well. In both TRXs lines starch levels were increased about 44-48 % after 6 h. In *ntrc*, starch levels went up after 3 h HL but peaked one hour later under ML and even decreased after 6 h below the 15 min value. This shows that short-term HL acclimation and de-acclimation might trigger different mechanisms for starch production and depletion when plants lack specific thiol-redox control, although a redundancy within the TRX/NTRC system cannot be excluded at this point. While *ntrc* showed lower average levels of starch (given in µmol C_6 equivalents/ gFW) in both ML (WT 9.28; *trxf* 8.66; *trxm* 9.11; *ntrc* 7.64) and HL (WT 16.12; *trxf* 15.62; *trxm* 16.24; *ntrc* 13.57), there were no significant changes between *ntrc* (as well as *trxf* and *trxm*) and WT within one light condition and time point determined.

Therefore, it is hypothesized, that at least *trxf* and *trxm* might stabilize starch levels until dawn to have enough supplies to sufficiently feed on during the night-time. Although a tendency of lower starch levels was apparent in *ntrc*, probably due to disturbed activation of starch biosynthesis, a significant role of the TRX/NTRC system in regulating starch metabolism during HL (de-)acclimation could not be concluded.

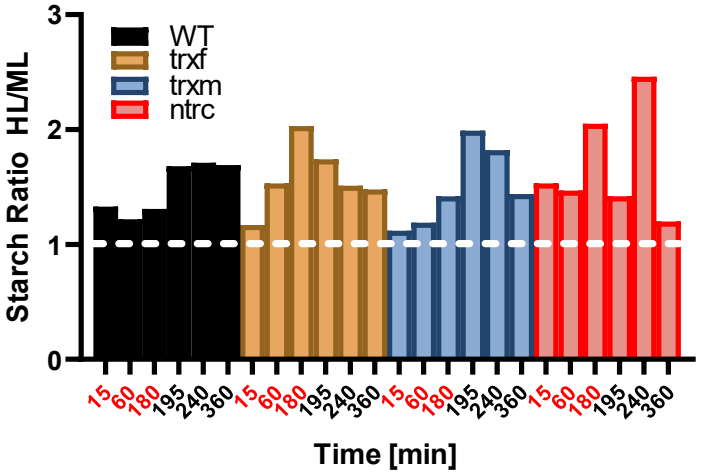

Figure 3.1.10. Time-resolved changes in starch content during HL (de-)acclimation in WT, *trxf*, *trxm* and *ntrc*.
Acclimation (red letters): 15min.– 3h; de-acclimation (black letters): 3h 15min – 6h. Results are the ratios of mean values between HL und ML, n = 5 biological replicates. t_0 before the treatment is considered as 1.

After that, a more heuristic approach was pursued to further dissect the driving forces of (de-)acclimation regarding central metabolites, since common statistical approaches were not satisfactory. For this, the dynamics in *ntrc* were investigated, being the most intriguing candidate in comparison to WT due to the strong phenotype (cf. chapter 1) and the results so far (cf. chapter 3.1.1, 3.1.2). Following a biomarker analysis (https://www.metaboanalyst.ca) (Chong et al., 2019; Pang et al., 2021) with a significance threshold of $p < 0.01$, common or distinct features (metabolites) were sought in every combination of light and phase in *ntrc* relative to WT (i.e. *ntrc* HL acclimation, *ntrc* HL de-acclimation, *ntrc* ML acclimation, *ntrc* ML de-acclimation). GABA, glycerate and erythritol/erythrose were found in all groups, indicating that NTRC might regulate these metabolites during the entire time-course, independent from light. This hypothesis is supported by GABA, glycerate and erythritol/erythrose being significantly changed in *ntrc* in almost every time point under ML and HL (**Supplement Table 5.4.4**). Moreover, GABA and glycerate were also determined significant in *trxf* and *trxm* in the late de-acclimation phase under HL. However, the respective biological roles remain unclear up till now. Next urea, myo-inositol, fumarate, asparagine, maltose, serine and galactinol were found to be of significance in *ntrc* under HL de-acclimation. However, they do not appear in same or close pathways, making a further interpretation difficult. Under control conditions, beta-alanine, rhamnose and phosphoric acid played role in the de-acclimation phase. Using the

biomarker analysis, there were no metabolites exclusively detected in ML or HL acclimation; it also did not return any significances in *trxf* and *trxm* relative to WT. Summarized, except for sugar build-up in the early minutes and hours and few individual significant hits which cannot be classified at the current moment, abundant and significant HL events were rather rare. Beyond that, the biomarker analysis did not return convincing further results. Therefore, meaningful separation of real HL events from control light due to strong oscillations of central metabolites in ML were not possible, indicating a minor role of the TRX and NTRC system in regulating the central metabolome in response to short-term HL (de-)acclimation.

3.1.4 Thioredoxins and NTRC do not alter LHCB2 phosphorylation

In sessile plants in particular, light changes entail a sophisticated interplay of different factors to cope with potential adverse environmental effects most commonly coming from excess light. One strategy to dissipate excess energy is via regulated NPQ. Another factor on the shorter-term scale is state transition (qT), mediated via the Serine/threonine-protein kinase STN7 (AT1G68830), which moderates LHCII migration between PSII and PSI to balance light-harvesting between the two photosystems (Bonardi et al., 2005). Under HL and PSII favoring light (Bräutigam et al., 2010; Puthiyaveetil et al., 2012), PQ is more reduced than in ML, which in turn activates phosphorylation of LHCII via STN7 and hence migration of P-LHCII from PSII to PSI. However, the same HL condition should also reduce TRXs, which are attributed to inactivate STN7 (Rintamäki et al., 2000; Lemeille et al., 2009; Rochaix, 2013; Ancín et al., 2019). Here, a possible involvement of TRXs in state transition using immunoblot assays was proved, assuming that under HL a higher phosphorylation rate of LHCB2 in the mutants should be seen. For this experiment, the same batch of samples and time points were used as for the metabolomics.

Following the ground state (state 2; WT 53 %, *trxf* 51 %, *trxm* 35 %, *ntrc* 41 % phosphorylated) we saw a swift decline in LHCB2 phosphorylation upon HL illumination in all lines (state 1; WT 23 – 31 %, *trxf* 24 – 28 %, *trxm* 25 – 32 %, *ntrc* 16 – 22 %) (**Figure 3.1.11 A**). After 3 h HL acclimation, P-LHCB2 levels increased again (state 2; WT 62 %, *trxf* 84 %, *trxm* 66 %, *ntrc* 64 %). However, there was no statistically significant difference observed in the mutants, relative to WT. After 6 h treatment, the levels nearly normalized to the initial values (WT 40 %, *trxf* 44 %, *trxm* 45 %, *ntrc* 36 %). A rise in P-LHCB2 after 3 h & 15 min could be seen under constant ML too, which remains completely obscure (**Figure 3.1.11 B**).

In the light of PTM, it makes sense to define the basal level of proteins as well, especially when dealing with extreme values; moreover STN7 abundance and activity was shown to be redox-dependent (Wunder et al., 2013). Therefore, the PhosTag approach (cf. chapter 2.2.2.2) allowed for additional, simultaneous determination of total LHCB2 abundance, to better evaluate the extend of LHCB2 phosphorylation in the background of redox regulation. Along with a strong and light-independent fluctuation in protein level in all genotypes, it was not possible to establish any relationship between protein abundance and PTM, though.

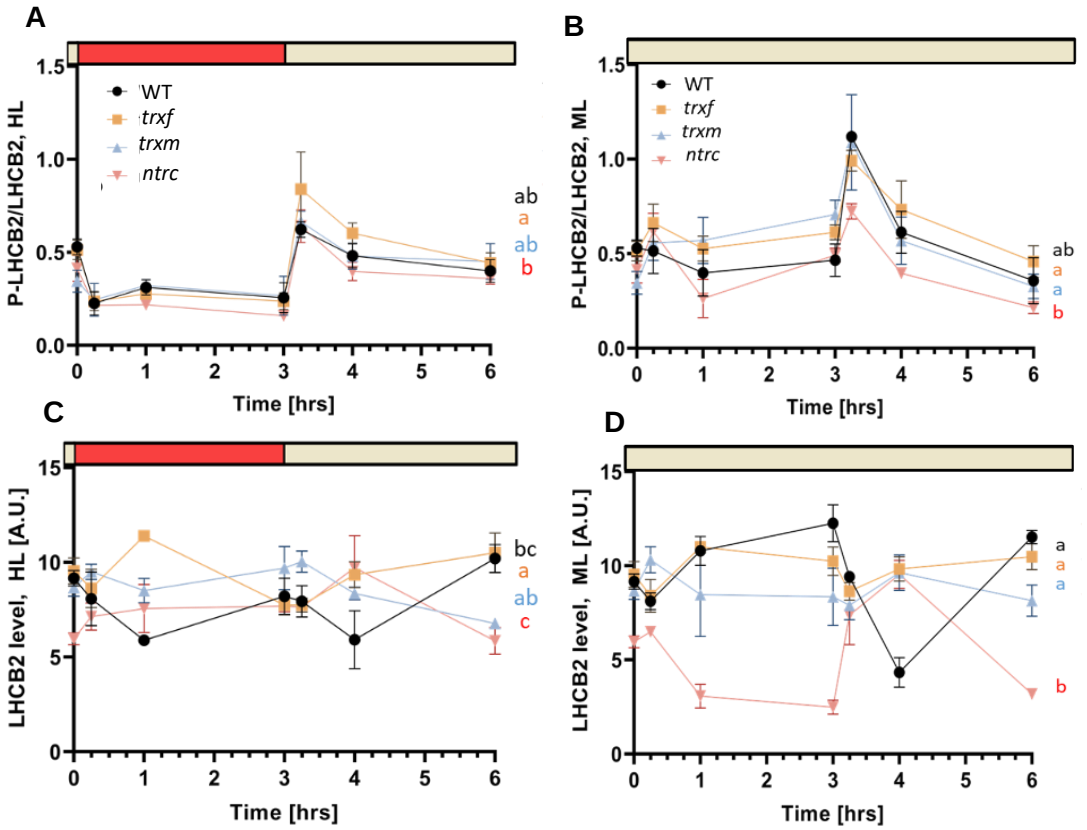

Figure 3.1.11. Transient changes in LHCB2 phosphorylation and abundance in HL (de-)acclimated WT, *trxf*, *trxm* and *ntrc*.
(A, B) LHCB2 phosphorylation given as ratio between phosphorylated and unphosphorylated forms. (C, D) LHCB2 protein levels. Seedlings were grown for 14 days and a photoperiod of 16 h under ML (80 µmol photons m^{-2} s^{-1}) and then shifted in the middle of the photoperiod to (A, C) HL (450 µmol photons m^{-2} s^{-1}) or (B, D) left in ML. Significance levels within one condition were evaluated by using a two-way ANOVA with a *post-hoc* Tukey test ($p < 0.05$) and are labelled with different letters. Red, HL; beige, ML.

Although LHCB2 phosphorylation appeared not to be influenced by TRXs or NTRC, the abundance of results gathered allowed for a more profound analysis. Thus, a novel approach was pursued to connect the cellular and plastidial metabolic state with phosphorylation states from light-harvesting protein LHCB2 in the thylakoid membranes. For this, HL treated samples from all genotypes and time points were pooled, to have a large and robust enough sample size and a simple correlation analysis was performed. To compensate for (still) existing irregularities in cellular responses due to disruption of thiol-redox regulators, the significance threshold was set to 0.01 and only medium to high correlations were considered (**Figure 3.1.12**, dashed lines). Under given conditions, aspartate, benzoate and glycerol were significantly and highly positively correlated to LHCB2 phosphorylation. Leucine and isoleucine, which are obviously intercorrelated, were among the significantly negatively correlated variables. CBC metabolites near RuBisCo within the cycle (Ru5P+Xu5P, RuBP, 2PG, DHAP) correlated strongly negatively; intercorrelation can be assumed here, too.

Of minor or no significant correlation to LHCB2 phosphorylation were the LHCB2 abundance, sugars and organic acids in general.

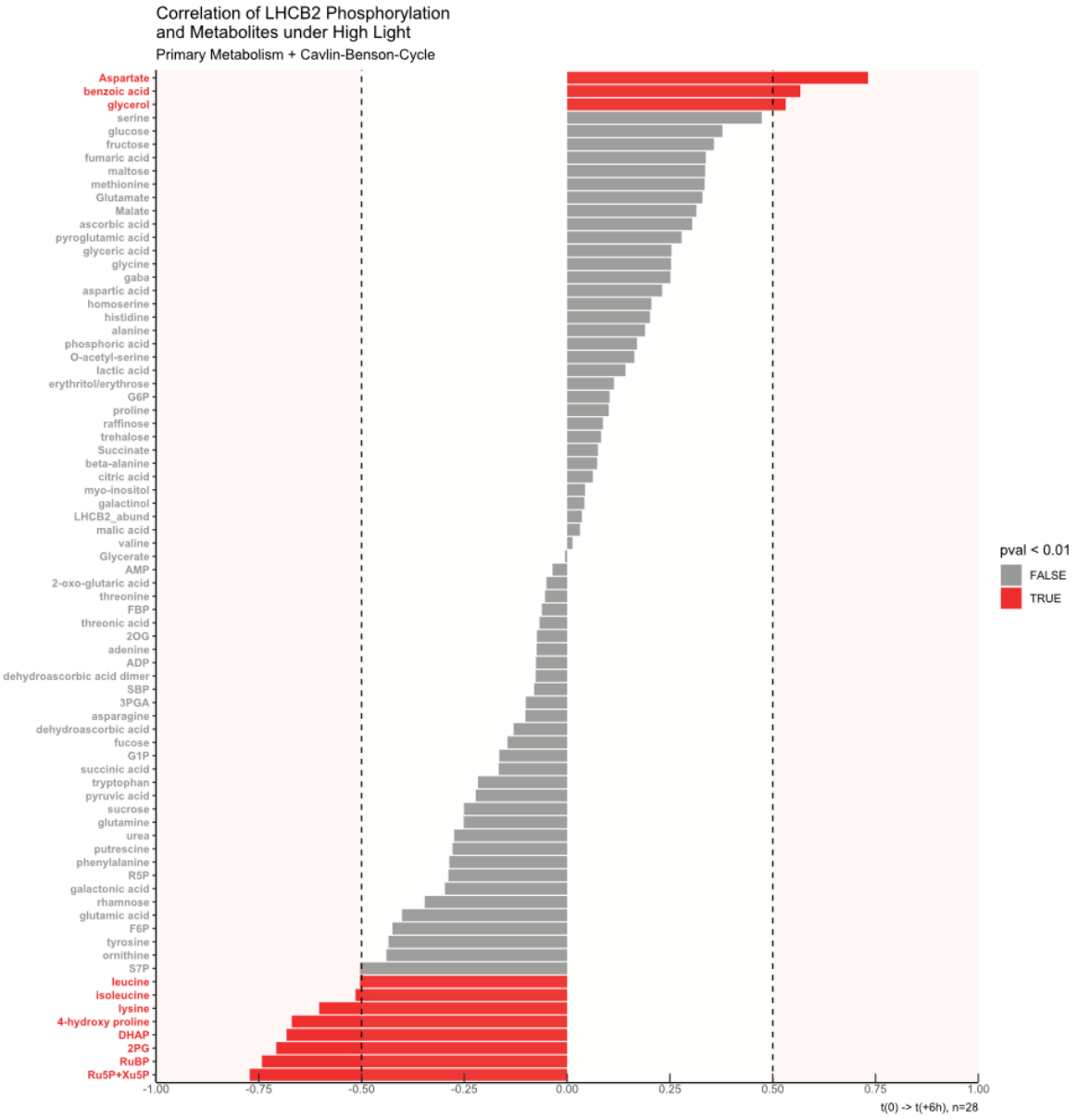

Figure 3.1.12. Correlation of metabolism and LHCB2 phosphorylation during short-term HL (de-)acclimation.
Red bars indicate a significant correlation (p < 0.01). The x-axis represents the Pearson correlation. Metabolites starting with capital letter were analyzed by LC-MS, otherwise with GC-MS. Results are the mean of n = 28 independent samples.

The correlation of LHCB phosphorylation and metabolism most strikingly revealed a negative relationship between few CBC metabolites, mainly from the regeneration and fixation phase (Ru5P+Xu5P, RuBP) as well as from the oxygenase reaction of RuBisCo (2-PG), therefore connecting the CBC with photosynthetic light reactions as stated previously. A tentative hypothesis might be that a limitation of RuBisCo could cause LHCB2 phosphorylation to increase. A sophisticated partial correlation could be calculated to underscore effects of single metabolites; however, this is quite a challenge with more than 3 variables and out of the scope of this thesis. Instead, **Supplement Figure 5.1.3** visualizes simple pairwise interactions of the beforementioned metabolites. It could be seen that there were strong and many significant correlations detected, yet most pairs fail to build a straight line of data points, which is simple visual evidence for a linear relationship, meaning a genuine (linear) correlation cannot be ascertained in our case. Nevertheless, rather confident pairings included P-LHCB2 and aspartate, aspartate and other central metabolites, leucine and isoleucine, and the CBC intermediates among each other.

Eventually, LHCB2 phosphorylation and STN7 activity appeared not to be mediated via the TRX and NTRC system in response to changes between ML and HL. Although significant correlations between LHCB2 phosphorylation and CBC metabolites and aspartate were calculated, it was concluded, that a simple correlation analysis might not be the best model to represent this kind of sophisticated data and is thus lacking the potential to fully elaborate the biological significance of the present results.

3.1.5 Correlation of metabolite profiles

Figure 3.1.12 showed a correlation plot of metabolites measured by GC-MS and LC-MS during HL (de-)acclimation against the LHCB2 phosphorylation during HL (de-)acclimation. **Figure 3.1.13** gives a pairwise correlation of the same set of metabolites omitting the comparison with LHCB2 phosphorylation. The idea of combining the central metabolites with CBC intermediates was to identify stable hubs and metabolite pairs during HL (de-)acclimation. Correlation in general can be performed under less stringent conditions compared to regression analysis for instance. Due to the experimental design however, the mean values from all genotypes (WT, *trxf*, *trxm* and *ntrc*) throughout acclimation and de-acclimation were taken to have a large enough sample size and represent the full dynamics of HL dependent metabolism. However, as can be seen there were more blank cells than significant correlations between metabolites. This can be interpreted as i) there is simply a larger number of various uncorrelated metabolite pairs or ii) the genotypic differences strongly influence the outcome. On the other hand, pseudo- or multicollinearity might connect (groups of) metabolites with others, where in fact no real bonding exists. To compensate for all that, the significance threshold was lowered to $p < 0.01$ and a second analysis was run without *ntrc* (**Supplement Figure 5.1.5**), because lack of NTRC is supposed to have the greatest overall influence on metabolism among the mutants, thereby potentially lowering the genotypic influence and creating a more homogenous sample set.
In the end, besides from a few simple conclusions however, like the strong inter-correlation of CBC intermediates or the presence of more positively than negatively correlated pairs, the tools for an exhaustive analysis of these data are lacking up to this moment, rendering biological interpretation difficult. Nevertheless, some observations will be discussed in a larger context later on.

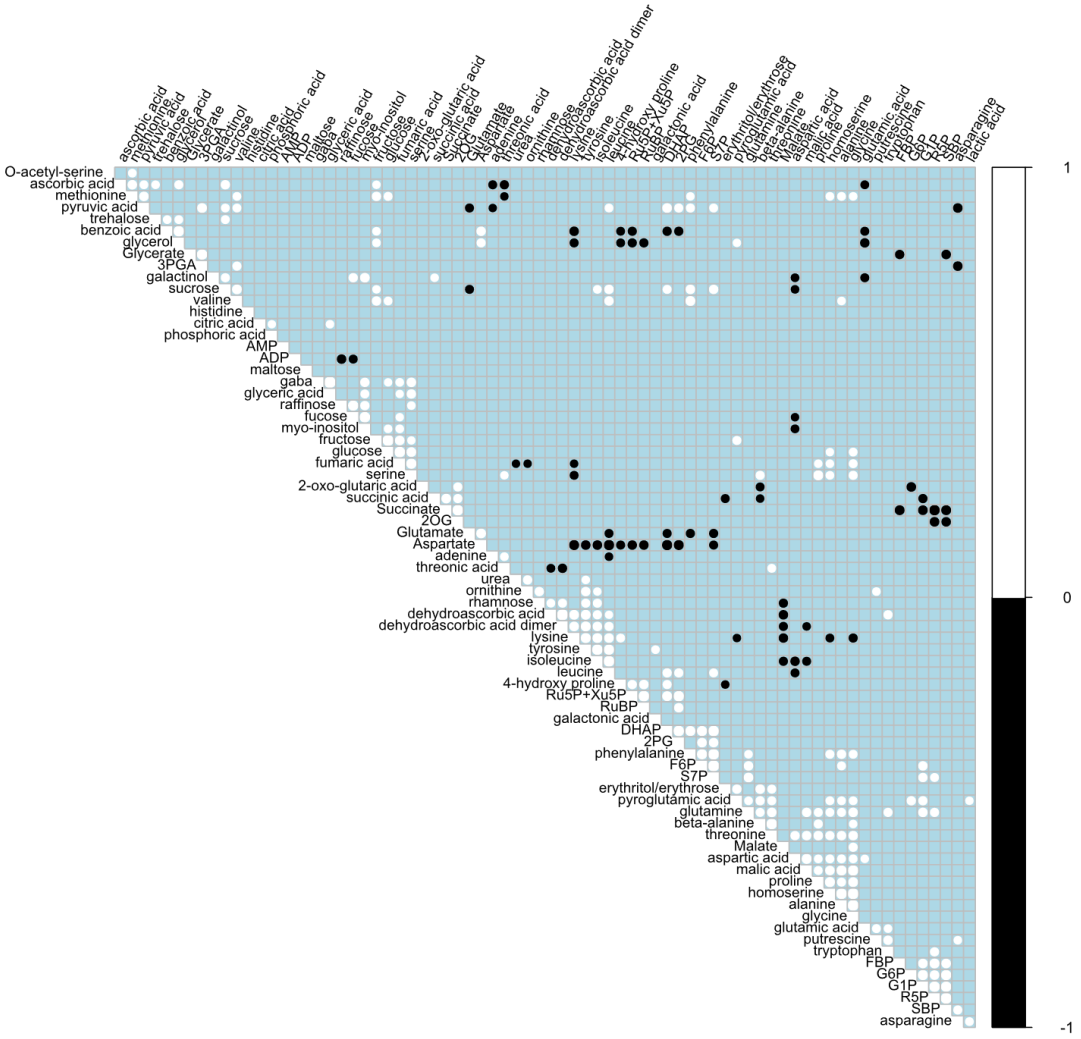

Figure 3.1.13. Correlogram of combined central metabolism and Calvin-Benson Cycle metabolites including WT, *trxf*, *trxm* and *ntrc* samples during short-term HL (de-)acclimation.
Positive correlations are shown in white, negative correlations are shown in black. Non-significant correlations (threshold $p < 0.01$) are shown in light blue/blank. Samples are ordered according to Ward's method (R package "corrplot").

Summarizing, the role of TRXs in regulating photosynthesis and metabolism in response to short-term HL (de-)acclimation was found to be largely insignificant, whereas the influence of NTRC tended to be slightly higher, especially with respect to CBC regulation. Here, bottlenecks at the site of FBPase and SBPase were revealed, indicating a key role of NTRC in CBC regulation under both HL and ML. STN7 activity was not influenced by the TRX and NTRC system in response to light switches between ML and HL, whereby a significant negative correlation between LHCB2 phosphorylation and the CBC should be mentioned; nevertheless, the biological interpretation and reliability, due to the applied model, proves difficult. The findings further suggest that the metabolite profiles of central metabolism and the CBC essentially operate separately.

3.2 Photosynthetic acclimation to fluctuating light

In the section above, it was shown that deficiencies in TRX*f*, TRX*m* and NTRC had little to no substantial effects on photosynthetic efficiency during short-term HL (de-)acclimation in the time frame of several hours. However, under natural conditions, there are also more rapid fluctuations in light intensities in the time frame of seconds to minutes, which is called fluctuating light (FL). In the following experiments, the acclimation responses of WT and redox mutants in FL were investigated. To determine the yet unknown time frame of redox-dependent acclimation to FL, the quick, easy and non-invasive technique of chlorophyll *a* fluorescence was chosen to measure photochemistry in PSII. Therefore, 3 weeks old plants grown in ML (125 µmol photons m^{-2} s^{-1}) were shifted up to 7 days to FL (1 min 50 µmol photons m^{-2} s^{-1}, 5 min 500 µmol photons m^{-2} s^{-1}; Ø 125 µmol photons m^{-2} s^{-1}) and measured repeatedly under rapid actinic light fluctuations (1 min HL, 5 min LL), mimicking the conditions in the plant growth chamber.

Before the shift from ML to FL (t_0), the photosynthetic parameter ΦII decreased in the first LL phase, while NPQ and PQ reduction inversely increased relative to the relaxed state in dark-adapted plants (**Supplement Figure 5.2.1**). During the subsequent HL phase, the dynamics changed and PQ and NPQ further elevated, while ΦII dropped. Over the course of the experiment, the parameters stabilized with each fluctuating cycle and changes in dynamics were found to be negligibly small towards the end of the experiment, assuming a quasi steady state conditions 20 min after the onset of actinic light. Regarding the mutants, a typical dark-light phenotype in the beginning of the measurement was observed, especially in *trxf* and *ntrc*, which is due to attenuated enzyme activation and has been observed earlier (cf. chapter 3.1.1; Thormählen et al., 2017). Besides that, the *trxf* and *trxm* mutants showed WT-like behavior, while a strong restriction in photosynthesis was observed in *ntrc*.

Next, the focus was now on each last cycle between LL and HL at the end of the experiment under quasi steady state conditions as mentioned before, which will be the reference for further conclusions. Here, the WT showed an average increase of ΦII in the HL phase and a decrease in the subsequent LL phase already after 3 h compared to t_0 (**Figure 3.2.1**). This pattern even intensified when plants were acclimated for several days. Intriguingly, PQ reduction increased in the LL after 3 h to eventually drop in both the HL and LL phase to a level lower than before the shift. NPQ levels increased only after 3 days of acclimation, most notably in the LL phase. In *trxm*, we observed a higher ΦII in the beginning of the LL phase after HL, reaching 6 - 7 % after day 4,

relative to WT. The *ntrc* mutant showed a decrease of ΦII in both HL and LL and a strong reduced PQ pool under LL throughout the entire experiment. Loss of NTRC influenced on NPQ, especially under HL; the effect increased when long-term adapted. After 3 to 4 days, all mutants showed a slight imbalance in ΦII following the HL phase. PQ reduction state was notably changed within 3 days in all genotypes, whereas little change between long- and short-term was observed in *ntrc*; like in WT, PQ reduction was also decreased under the levels prior to the shift in *trxf* and *trxm* after 3 to 4 days. This observation might not be trivial, since a balanced redox poise has been suggested to be of importance for long-term gene expression (Pfannschmidt, 2003; Bräutigam et al., 2009; Queval & Foyer, 2012).

It was concluded, that WT originating from ML increasingly adapted photosynthetic parameters to FL acclimation, starting already 3 h after the shift from ML to FL, whereas *ntrc* seemed to rapidly forfeit dynamic acclimation strategies to retain a balanced redox poise when exposed to FL, which demonstrates that NTRC is crucial to sustain optimal photosynthesis in acclimation to FL (Thormählen et al., 2017). TRX*m*1*m*2 appeared to be negative regulators of ΦII in the LL phase, supporting results of previous studies (Thormählen et al., 2017), whereas there were no substantial effects of TRX*f* observed. According to our evaluation, the time frame of completed acclimation to FL took at least 4 days.

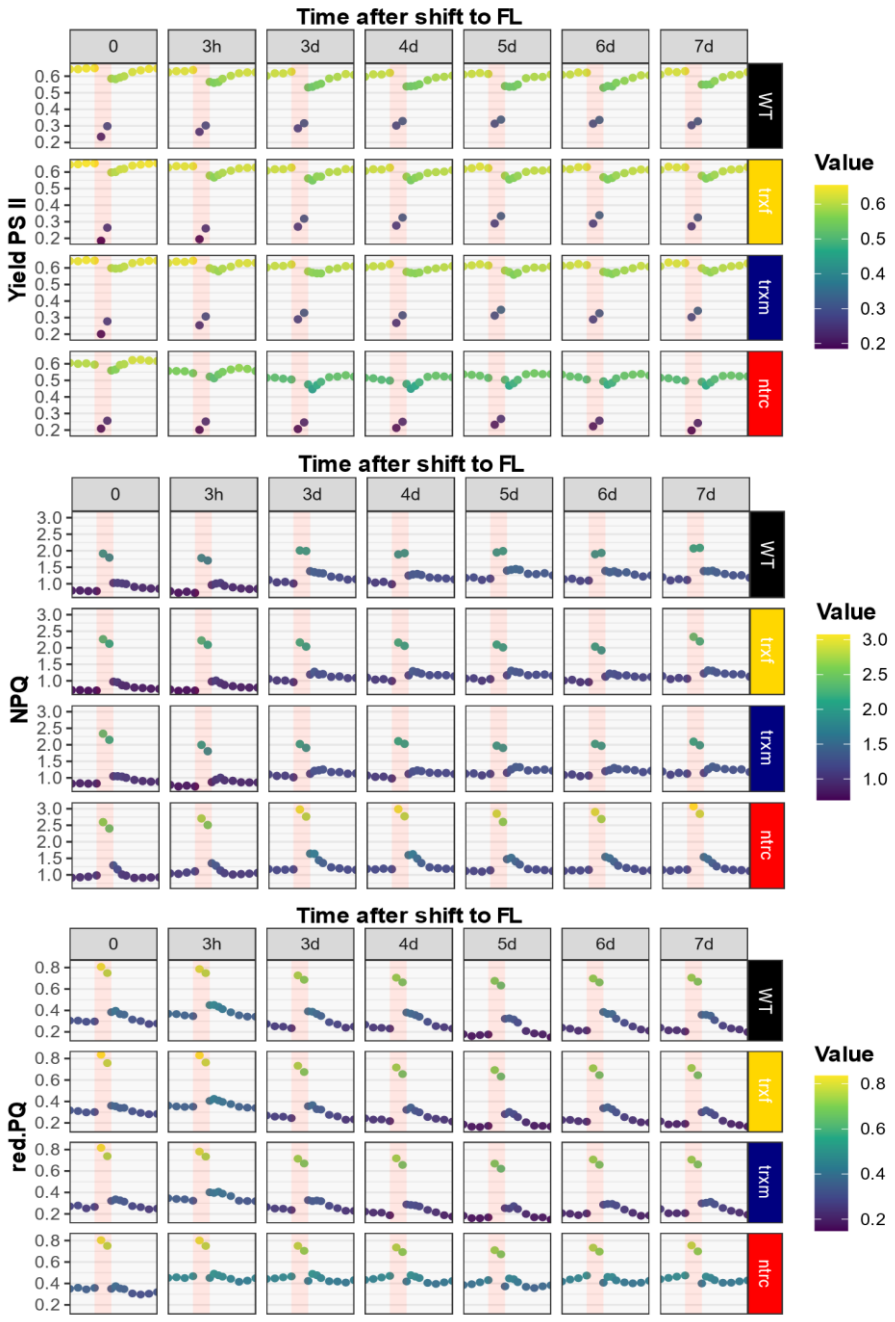

Figure 3.2.1. Transient changes in photosynthetic parameters of photosystem II in WT, *trxf*, *trxm* and *ntrc* under FL.
Top row: effective yield (ΦII). Middle row: NPQ. Bottom row: red. PQ (1-qL). Plants were grown for 3 weeks in ML at a photoperiod of 12 h and 125 µmol photons m^{-2} s^{-1} and grown for one further week in FL (1 min HL, 500 µmol photons m^{-2} s^{-1}; 5 min LL, 50 µmol photons m^{-2} s^{-1}; Ø 125 µmol photons m^{-2} s^{-1}). Dark-adapted (30 min) plants were put under actinic fluctuating light similar to the regime in the FL growth chamber and repeatedly measured before the shift (t_0) up to 7 days after the shift. Shown is a scope of the quasi-steady state after dark-adaption (~ 20 min). Results are the mean, n = 5 biological replicates. Red, HL phase; grey, LL phase.

3.3 Long-term acclimation responses

As shown in the chapter before, effects of TRX*f*, TRX*m* or NTRC on light acclimation responses are operating in a time frame of several days rather than a few hours. This chapter is therefore aimed to elucidate the roles of the Fd- and NAPDH-dependent TRX system in long-term acclimation responses using four different light regimes: ML, FL, HL and LL. Higher light intensities were used for the HL conditions to bring the system more to its limits. To avoid possible negative effects of this increase in light intensity, the photoperiod was decreased from 16 h to 12 h (cf. chapter 2.2.1.1). Since growth and photosynthetic parameters were improved in HL compared to ML in the WT (see below), these conditions were found to be beneficial for WT plants.

3.3.1 Deficiencies in Thioredoxin *m* and NTRC mediate dynamic responses under fluctuating- and high light

In the present experiment, plants were initially grown at a 12 h photoperiod for 3 weeks under ML (control; 250 µmol photons m^{-2} s^{-1}) and shifted for up to 10 days to FL (1 min HL, 900 µmol photons m^{-2} s^{-1}; 4 min LL, 90 µmol photons m^{-2} s^{-1}; Ø intensity 250 µmol photons m^{-2} s^{-1}), HL (900 µmol photons m^{-2} s^{-1}) or LL (90 µmol photons m^{-2} s^{-1}) (cf. chapter 2.2.1.1) (**Figure 3.3.1**).

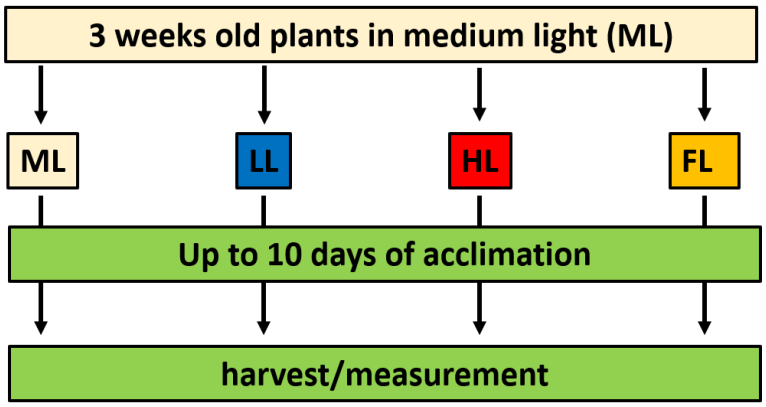

Figure 3.3.1. Experimental setup for long-term acclimation studies.
Plants were initially grown for 3 weeks under a photoperiod of 12 h light/12 h dark and ML (250 µmol photons m^{-2} s^{-1}) and then shifted to FL (1 min HL, 900 µmol photons m^{-2} s^{-1}; 4 min LL, 90 µmol photons m^{-2} s^{-1}; Ø intensity 250 µmol photons m^{-2} s^{-1}), HL (900 µmol photons m^{-2} s^{-1}), LL (90 µmol photons m^{-2} s^{-1}) or left in ML, to further grow for up to 10 days. Harvest or measurement time points are mentioned in the text.

In the beginning, the phenotypes were characterized. Lack of TRX*f* and TRX*m* caused WT-like phenotypes (**Figure 3.3.2**). As already known, *ntrc* exhibited a pale phenotype (Pérez-Ruiz et al., 2006) under normal conditions, which was also observed under all other light regimes. The leaf shape of all lines was altered in HL and LL relative to ML; under HL the leaves were curled and the petiole was less developed, under LL it was noticeably larger in comparison to the blade. FL grown plants seemed to be similarly shaped to ML. Regarding the growth, leaf sizes of ML grown WT, *trxf* and *trxm* increased about 20% every day during this vegetative phase (**Figure 3.3.3**). FL adapted WT, *trxf* and *trxm* had a smaller growth rate (~15 %), HL adapted plants had a higher growth rate of over 30%. LL levels were little higher than in ML; this might be due to the fact, that the plants from this batch were smaller before the shift to LL, compared to ML, so they might have experienced a relative increase in average growth during acclimation. Lastly, under all conditions *ntrc* showed a significant growth retardation relative to the other lines, the lowest being under FL (less than 10 %).

In summary, NTRC deficiency resulted in a severe and significant growth retardation under ML and LL, which even exacerbated under HL and FL, while lack of TRX*f* and TRX*m* led to WT-like phenotypes and growth rates in all light conditions.

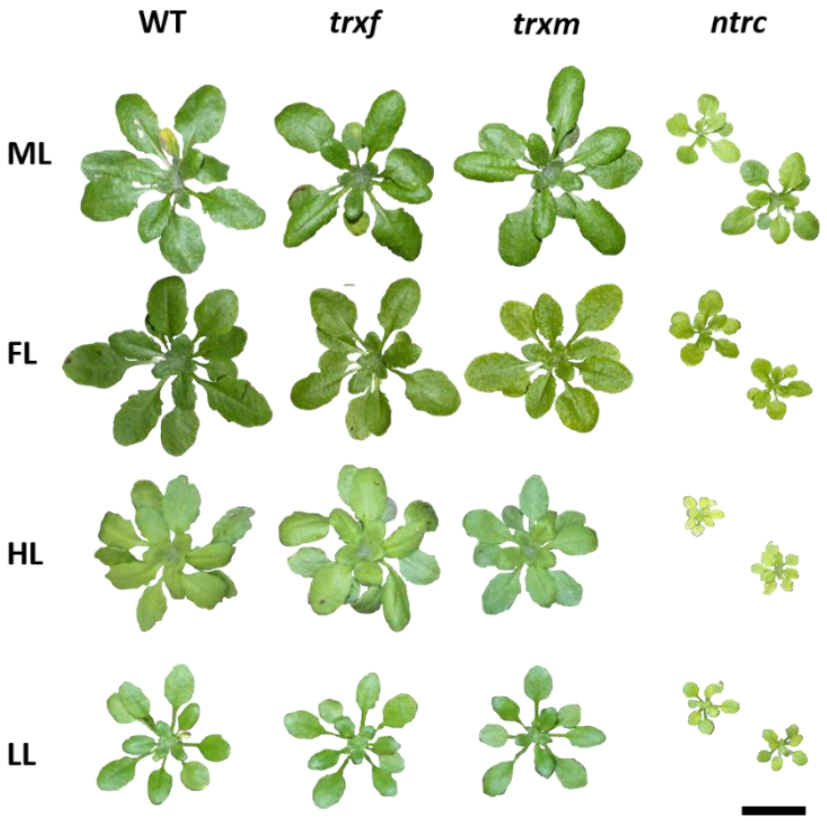

Figure 3.3.2. Phenotypes and respective sizes of fully adapted WT and redox mutants *trxf*, *trxm* and *ntrc* grown under different light conditions.
Pictures were taken of fully acclimated plants from different batches (initial 3 weeks of growth under ML [250 µmol photons m^{-2} s^{-1}] at a 12h photoperiod plus one added week under either ML, FL [1 min HL 900 µmol photons m^{-2} s^{-1}, 4 min LL 90 µmol photons m^{-2} s^{-1}; Ø 250 µmol photons m^{-2} s^{-1}], HL [900 µmol photons m^{-2} s^{-1}] or LL [90 µmol photons m^{-2} s^{-1}]). Leaf color might not be fully comparable due to slight variations in illumination during photography. Leaf size is also subject to a certain variability. However, the *ntrc* mutant exhibited a pale phenotype in every light condition and HL plants were bigger in general (see **Figure 3.3.3**). The black bar indicates a size of 2 cm.

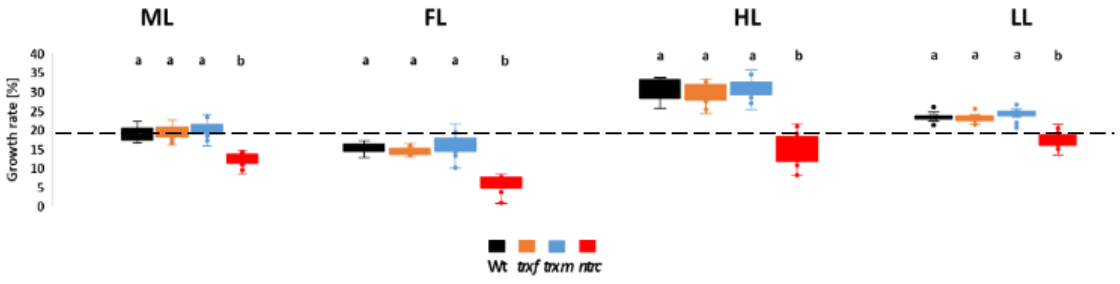

Figure 3.3.3. Growth rates of fully adapted WT, *trxf*, *trxm* and *ntrc* grown under different light conditions.
Measurements were performed every 2 days for 10 days total. The rate was calculated from curve fitting within exponential growth. Significance levels within one condition were evaluated by using a one-way ANOVA with a *post-hoc* Tukey test ($p < 0.05$) and are labelled with different letters.

The maximum quantum efficiency of PSII (Fv/Fm) is frequently measured to monitor oxidative stress, with a reference value of 0.84 in many mature leaves, meaning that 84 % of the incident photosynthetic active radiation (PAR) is absorbed (Baker, 2008). To begin with, Fv/Fm was close to 0.83 to 0.84 in all WT batches before the shift (**Figure 3.3.4**). After the shift, values of ML, FL and LL adapted plants were fluctuating but stabilized during the time course of the whole experiment (0.85 in these conditions after 10 days). Under HL, Fv/Fm declined rapidly after 3 h (0.80), eventually to fully recover after 10 days (0.83). The biggest overall changes were observed in HL and took place latest 3 h after the shift from ML, which finally lasted for the remaining period. This immediate and long-lasting effect in HL may indicate a strong and longer-term adaption on photosynthesis level. Regarding the mutants, there were no changes in *trxf* detected compared to WT. Lack of TRX*m*1*m*2 led to a decrease in all conditions, except in LL. This could mean that TRX*m*1*m*2 are positive regulators of Fv/Fm under non-limiting light conditions. Further, the results point to bottlenecks in photochemistry, especially in *ntrc,* where Fv/Fm significantly decreased under all conditions, which supports findings of Pérez-Ruiz et al. (2006). Lack of NTRC not only induced an incipient decrease before the shift, but magnified further down-regulation of Fv/Fm in HL (t_0: 0.80, day 10: 0.73) and FL (t_0: 0.82, day 10: 0.80).

Summarized, TRX*m* and NTRC, but not TRX*f*, are indispensible of stabilizing Fv/Fm under different light conditions, especially under HL and FL.

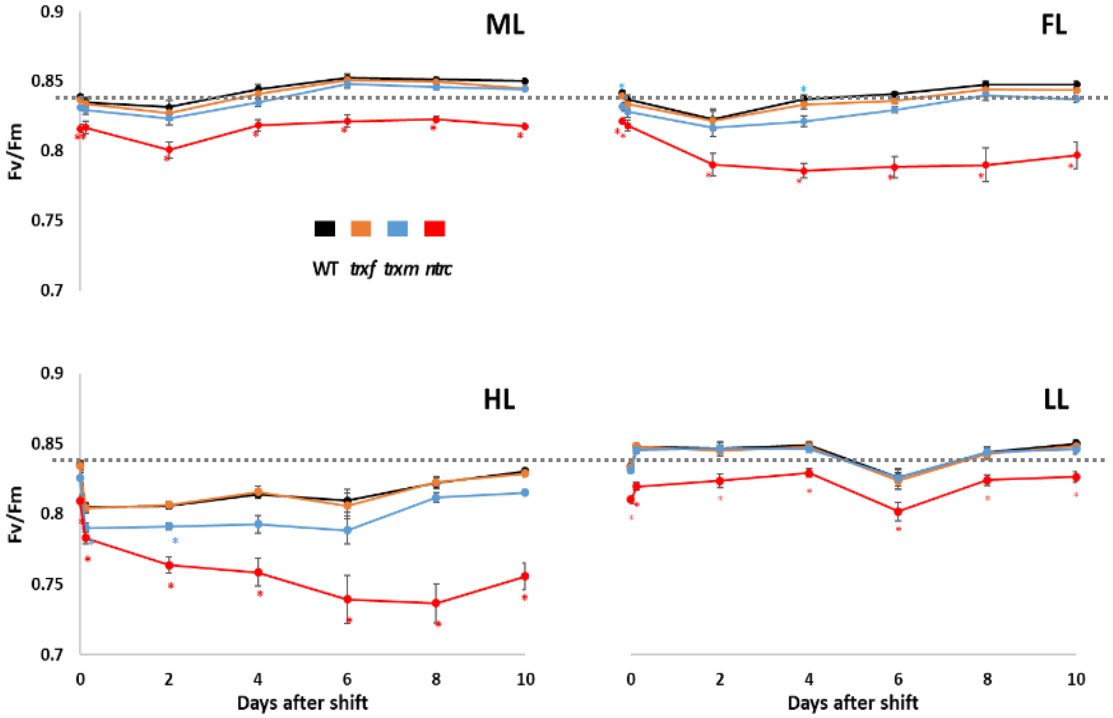

Figure 3.3.4. Changes in maximum quantum yield of photosystem II (Fv/Fm) in WT, *trxf*, *trxm* and *ntrc* grown under different light conditions.
Measurements were performed prior to the shift and subsequently every 2 days after the shift from ML to FL, HL or LL. Significance levels, relative to WT, within one condition were evaluated by using a one-way ANOVA with a *post-hoc* Tukey test (* $p < 0.05$). The dashed line indicates the dark-adapted WT level in ML.

Next, the effects of deficiencies in TRX*f*1, TRX*m*1*m*2 or NTRC on long-term acclimated plants were investigated, that have been fully acclimated (7 days) to ML, FL, HL or LL, by measuring photosynthetic performance under rapid actinic light fluctuations (1 min HL, 4 min LL), equivalent to the FL acclimation conditions in the growth chambers. In WT, short-term exposure (from ML) to FL led to low ΦII and to high NPQ and PQ reduction in the HL phase (**Figure 3.3.5**); in the LL phase, inverse effects were observed. When pre-exposed to HL, the intensity of these photosynthetic parameters increased, while they decreased when fully acclimated to FL. LL acclimated plants exhibited ML like dynamics, except for NPQ, which was markedly lower during the HL phase. Under ML, loss of TRX*f* and TRX*m* had no substantial influence on ΦII, NPQ and PQ. Most changes occurred when knocking out NTRC, leading to a reduced ΦII, while NPQ was increased both in the HL and LL phase. Plants pre-exposed to FL instead showed clear changes in all three parameters: the NPQ was increased in the mutants, compared to WT, at the cost of a lower ΦII. This effect was overall strongest in *ntrc* and was accompanied by a heavy over-reduction of PQ. Loss of TRX*m* on the other side increased photosynthetic efficiency in the LL phase, presumably due to a lower PQ redox state ensuring an efficient electron transport. Loss of NTRC and TRXs seemed to increase the quenching capabilities under HL, compared to WT. This effect also appeared to override the oxidation of PQ in *trxm*, leading to a lower ΦII when HL acclimated. However, compared to FL it is obvious that other factors in the mutants might contribute to a lowered ΦII in HL. LL adapted plants reacted similar to ML grown plants, with almost identical ΦII, yet LL adaption lowered NPQ in all genotypes, especially in the HL phase, while PQ redox states in the mutants corresponded to that of WT.

Summarized, different acclimation environments generate different photosynthetic outcome, where the least effects were observed in *trxf*, with TRX*f* being mainly important for CBC enzyme activation, followed by TRX*m*, negatively affecting and positively affecting ΦII in FL and HL, respectively. Most strikingly, photosynthesis deteriorated in *ntrc* when exposed to FL and HL, thus concluding that NTRC might act as key modulator for dynamic and beneficial acclimation in FL and HL.

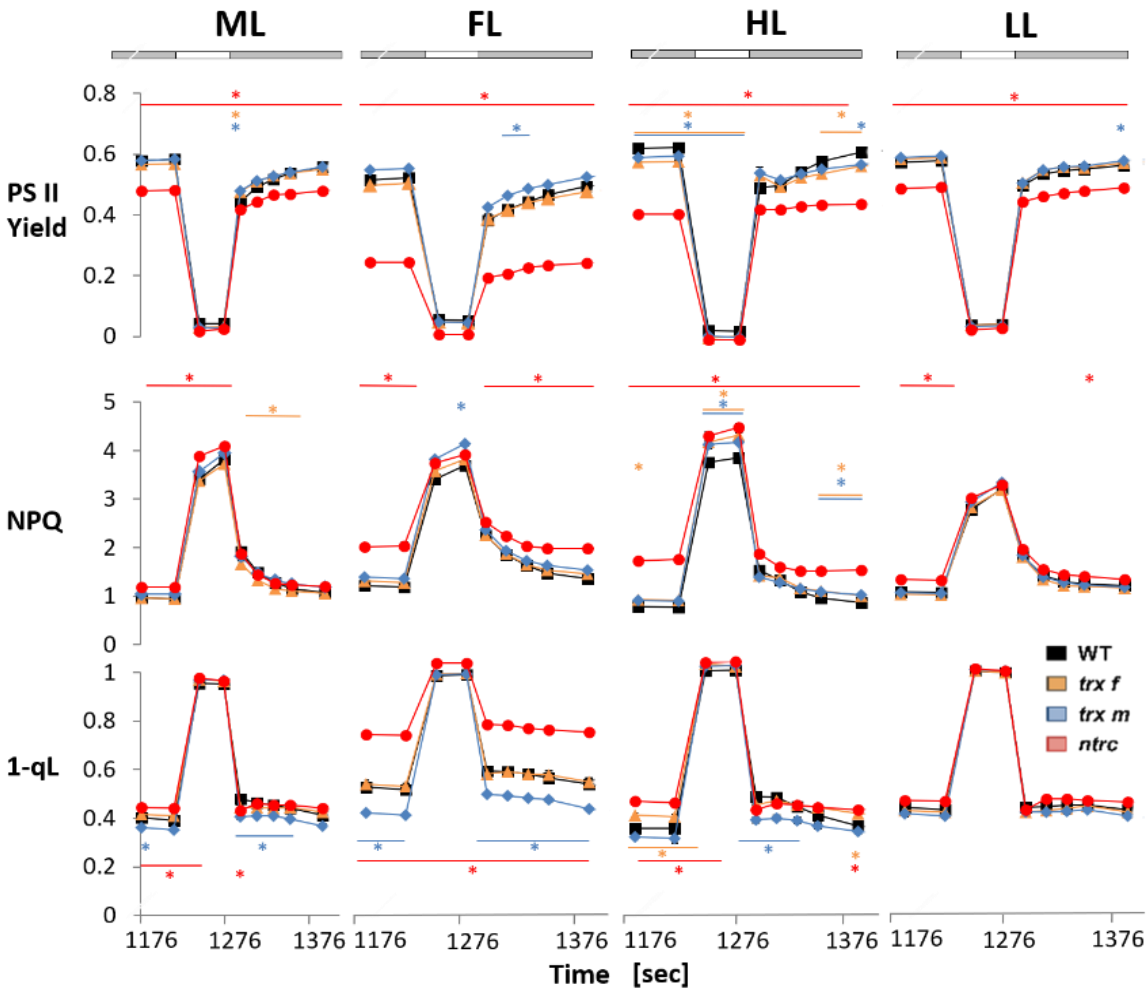

Figure 3.3.5. Changes in photosynthetic parameters of photosystem II in fully acclimated WT, *trxf*, *trxm* and *ntrc* grown under different light conditions.
Top row: effective yield (ΦII). Middle row: NPQ. Bottom row: red. PQ (1-qL). Dark-adapted (30 min) plants were put under actinic fluctuating light similar to the regime in the FL growth chamber. Shown is a scope of the quasi-steady state after dark-adaption (~ 20 min). Results are the mean ± SE, n = 6-12 biological replicates. Significant changes, relative to WT, within one condition were evaluated by using a one-way ANOVA with a *post-hoc* Tukey test (*$p < 0.05$). The grey bar indicates the LL, the white bar the HL phase of FL.

Measurements of electron transport rates (ETR) at progressively increasing light intensities was done to investigate the possible range of action, in the sense of photosynthesis, when plants were pre-exposed to different long-term light regimes, comparable to the experiment above. Our results showed similar dynamics of WT in ML, FL and HL, demonstrating an increase in ETR with increasing light intensity (**Figure 3.3.6**). LL adapted plants were limited in higher light intensities though; this has been observed before (Walters, 2005; Walters & Horton, 1994) and is due to the inability of LL acclimated plants to re-arrange their machinery to increasing light in a rapid and timely manner. Loss of TRX*f* and TRX*m* seemed to regulate ETR slightly positively when FL adapted, contrary to constant light regimes. NPQ in WT and TRXs mutants was very much alike in all light conditions. In *ntrc*, acclimation to all lights had a significant impact on the ETR in low, and more severely, in higher light intensities. Lack of NTRC started to limit ETR at 230 µmol photons $\cdot m^{-2} \cdot s^{-1}$ in FL, HL and LL. However, a recovery to WT levels under LL was slightly noticeable, compared to the other light conditions. NPQ coincided with changes in ETR in all genotypes, except *ntrc*; here an overly elevated NPQ was seen, especially distinct from WT from 35 to 100 µmol photons m^{-2} s^{-1}. Chlorophyll content is a common marker for studying acclimation (Walters & Horton, 1994; Bailey et al., 2004; Walters, 2005). Under short day, chlorophyll was significantly decreased in *trxf* and *ntrc* (Thormählen et al., 2015). We measured chlorophyll indirectly as absorption, which is an integral component of the ETR calculation. Here we found out, that absorption levels were lowered in *trxf* and *trxm*, respectively, under ML (-1 %; -6 %), HL (-2 %; -6 %) and LL (-7 %; -2 %) and increased in FL (2 %; 0.4 %), relative to WT. This could explain a better ETR in these lines under FL. In *ntrc*, levels were – in accordance with the pale phenotype – shrinking by 9 % (ML), 8 % (FL), 11 % (HL) and 8 % (LL), compared to WT.

Summarized, there were no substantial effects of TRX*f* and TRX*m* in regulating ETR observed, whereas NTRC is needed to ensure full electron transport in all light conditions tested.

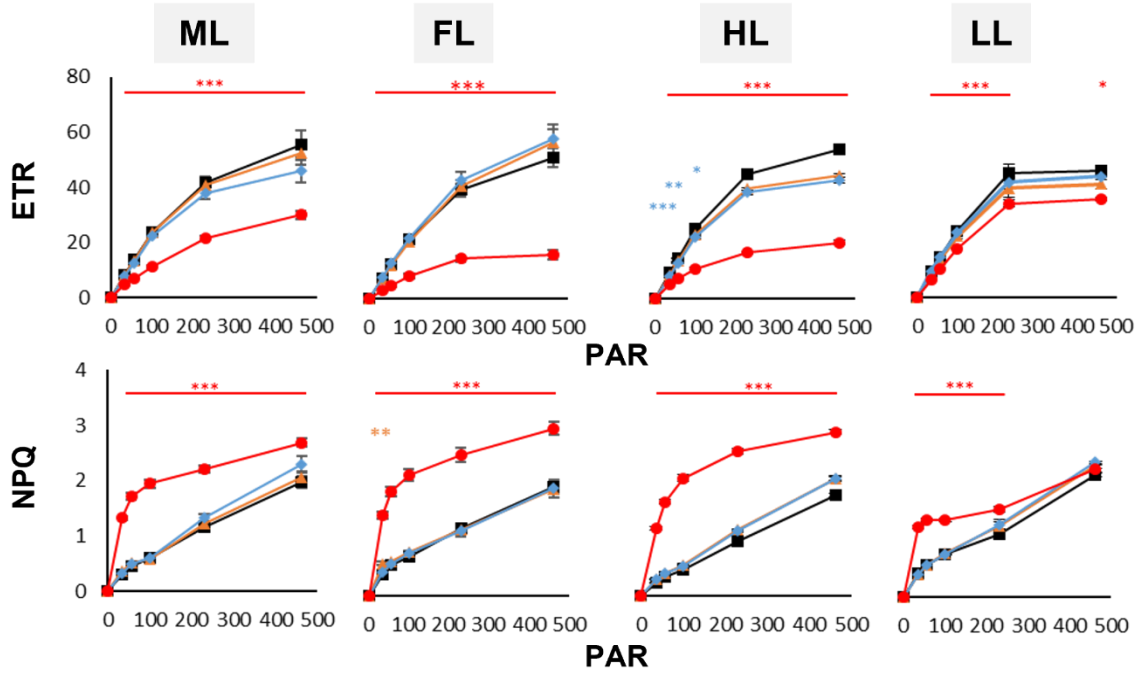

Figure 3.3.6. Changes in electron transport and NPQ as a function of light intensity in fully acclimated WT, *trxf*, *trxm* and *ntrc* grown under different light conditions. After dark-adaption (30 min) chlorophyll absorption was measured to calculate electron transport rate (ETR= 0.5 × PAR × Abs. × Φ II; top row) and NPQ (bottom row). Results are the mean ± SE, n = 5-12 biological replicates. Significant changes, relative to WT, within one time point were evaluated by using a two-way ANOVA with a *post-hoc* Tukey test (* $0.01 < p < 0.05$, ** $0.001 < p < 0.01$, *** $p < 0.001$). PAR; photosynthetic active radiation in µmol photons $\cdot m^{-2} \cdot s^{-1}$.

3.3.2 Acclimation to different light regimes involves large dynamics in the metabolome

3.3.2.1 NTRC deficiency has a significant effect on central metabolism

A targeted GC-MS analysis was performed next to establish a profile of central metabolism. This profile is intended to provide information on how light-dependent redox modulators affect central metabolism after 7 days of (full) acclimation in different light conditions. This includes primarily soluble sugars, amino acids, and organic acids. At first, a PCA showed that the samples were clearly divided by light (**Figure 3.3.7 A**). ML was sandwiched between LL and HL; the latter showed the largest confidence ellipses (95%) amongst the clusters, which is due to a strong deviation in *ntrc* under HL, compared to the other genotypes. Next, the FL clusters (FHL and FLL), whose ellipses slightly overlapped, clearly delimited from other light conditions. The most significant metabolites clustered towards FL and HL. Organic acids and amino acids seemingly play a major role in FL and HL, respectively. The genotypic effect however was little, only *ntrc* moved away from the cloud of points but showed the least variance (**Figure 3.3.7 B**). Sugars like glucose, which were located near higher light conditions, and pyruvic acid, a precursor for the tricarboxylic acid cycle (TCA cycle), showed in opposite directions, which is only natural since glucose depletion yields in a rise in pyruvic acid as part of the glycolysis. Citric acid, however, is orthogonal to glucose, which could mean that the respective pathways are independent.

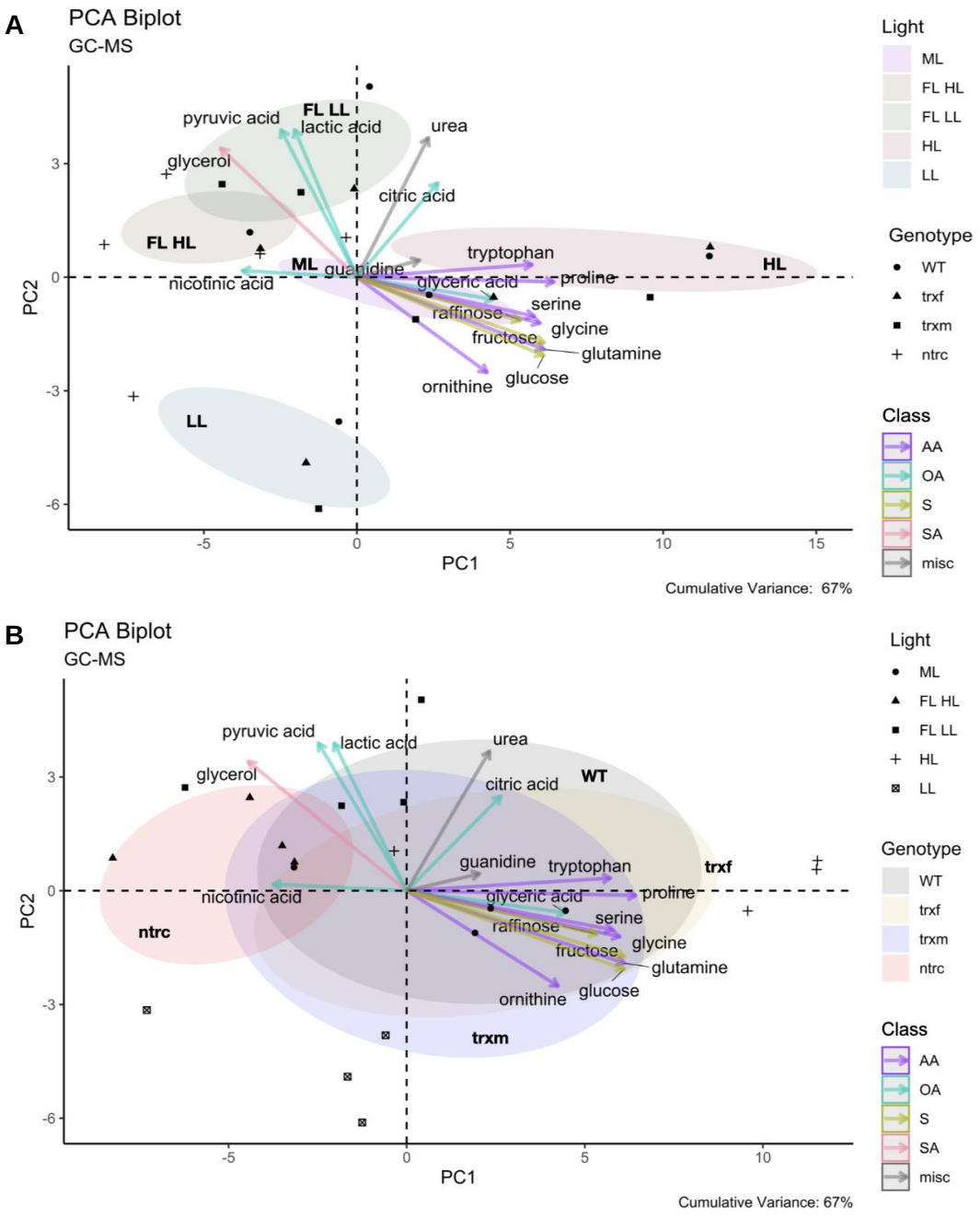

Figure 3.3.7. Cluster analysis of fully acclimated WT, *trxf*, *trxm* and *ntrc* samples for GC-MS based central metabolites.
(A) According to light. (B) According to genotype. Only the most important metabolites were plotted. The cumulative variance of PC1 and PC2 is 67 %. The clustering was done with the package "factoextra" and "FactoMineR" in R. AA, amino acid; OA, organic acid; S, sugar; SA, sugar alcohol; misc, miscellaneous.

Figure 3.3.8 shows a heat map of central metabolites based on GC-MS analysis. The rows (metabolites) were clustered according to their compound class. Here, amino acids and sugars on the one side, and organic acids, sugar alcohol and miscellaneous metabolites on the other side showed the closest relation. For the columns (samples) the hierarchical clustering algorithm (metric: correlation; linkage: Ward's method) identified 5 distinct clusters. A, D and E constitute unified clusters of the lines WT, *trxf* and *trxm* under HL, ML and LL, respectively. C is a mixed cluster of samples from both FHL and FLL. Here, in 3 out of 5 cases *trxf* and WT were highly correlated. This becomes apparent in other experiments too, which is why we will focus more on *trxm* and *ntrc* in future evaluations. Cluster B exclusively included samples from *ntrc* under every light condition examined. In this cluster there was almost no change in metabolite levels between the single samples detectable, which indicates a dramatic loss of metabolic plasticity when NTRC is knocked out. Regarding the expression values, metabolites in HL samples of WT, *trxf* and *trxm* – but not *ntrc* – formed an outgroup and were increased on average compared to other light conditions. Down-regulated metabolites in this group (pyruvic acid, lactic acid, nicotinic acid, aspartic acid, glycerol) were up-regulated in the other light conditions. Interestingly citric acid was concertedly up-regulated in the mutants under FHL and down-regulated in FLL compared to WT (**Supplement Figure 5.3.1**).

The effects of each genotype on metabolism in all light conditions pooled is depicted in **Figure 3.3.9**. This density-like summary helps to identify general bottlenecks in metabolism that may sustain throughout all conditions. We found mostly similar or overlapping pattern between *trxf* and *trxm* as well as WT. The biggest changes however were found in *ntrc*. Proline for instance serves as a stress marker (Verslues & Sharma, 2010) and showed no dynamic change in *ntrc* following a change in light intensity. In the *ntrc* mutant, compounds of every category were found to have little to no change, most notably proline, tryptophan, serine, 2-oxo-glutaric acid, glycine and fructose. To mention are also raffinose, which serves as a signaling molecule for stress (Wienkoop et al., 2008) and myo-inositol, which was recurrently observed to be strongly down-regulated in redox relevant studies (Thormählen et al., 2015; Hou et al., 2019). Specifically sugar and amino acids were strongly down-regulated after loss of NTRC, while loss of TRX*f* and TRX*m* led to WT-like metabolite levels.

It is hypothesized, that the general depletion of amino acids and organic acids might be an expression of critical carbon and nitrogen starvation in the case of *ntrc*.

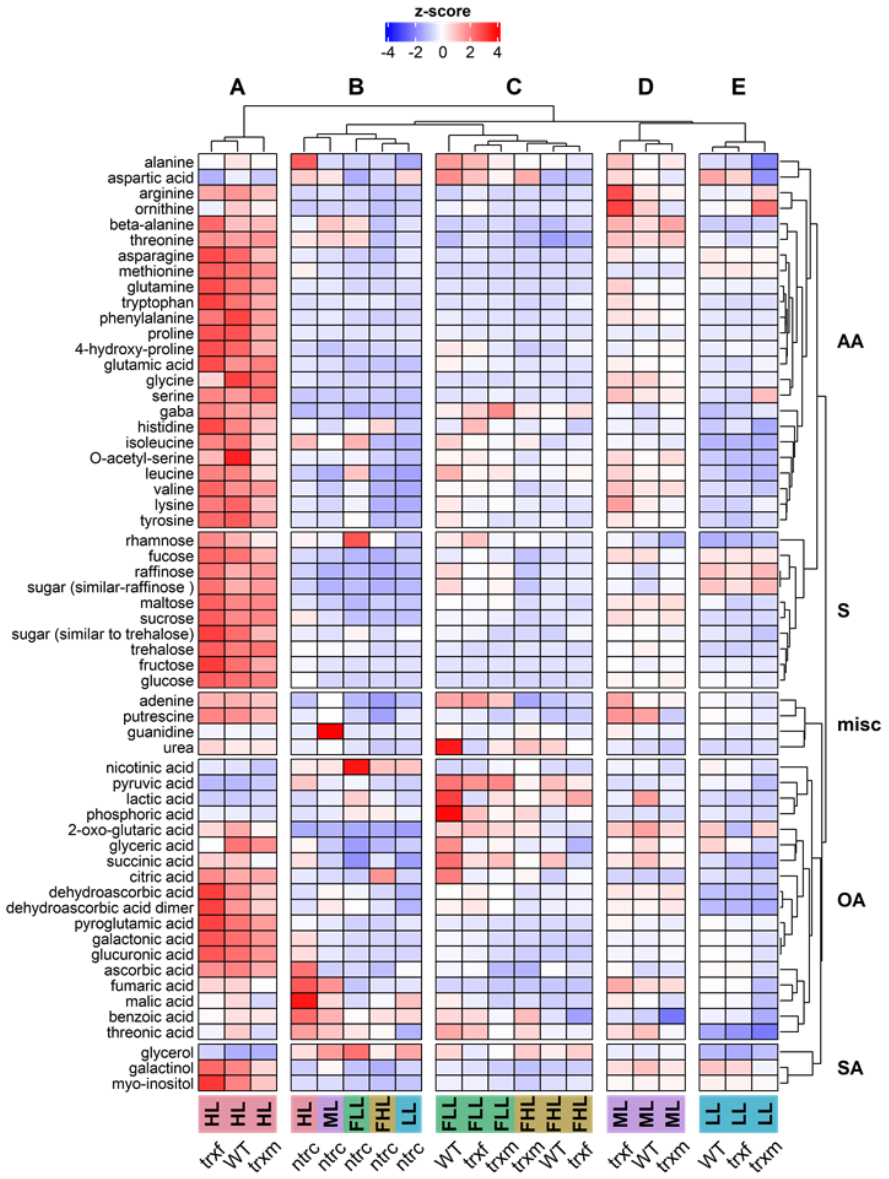

Figure 3.3.8. Heat map of standardized GC-MS based central metabolites in fully acclimated WT, *trxf*, *trxm* and *ntrc* grown under different light conditions.
AA, amino acid; S, sugar; misc, miscellaneous; OA, organic acid; SA, sugar alcohol. The heat map was generated with R package "ComplexHeatmap".

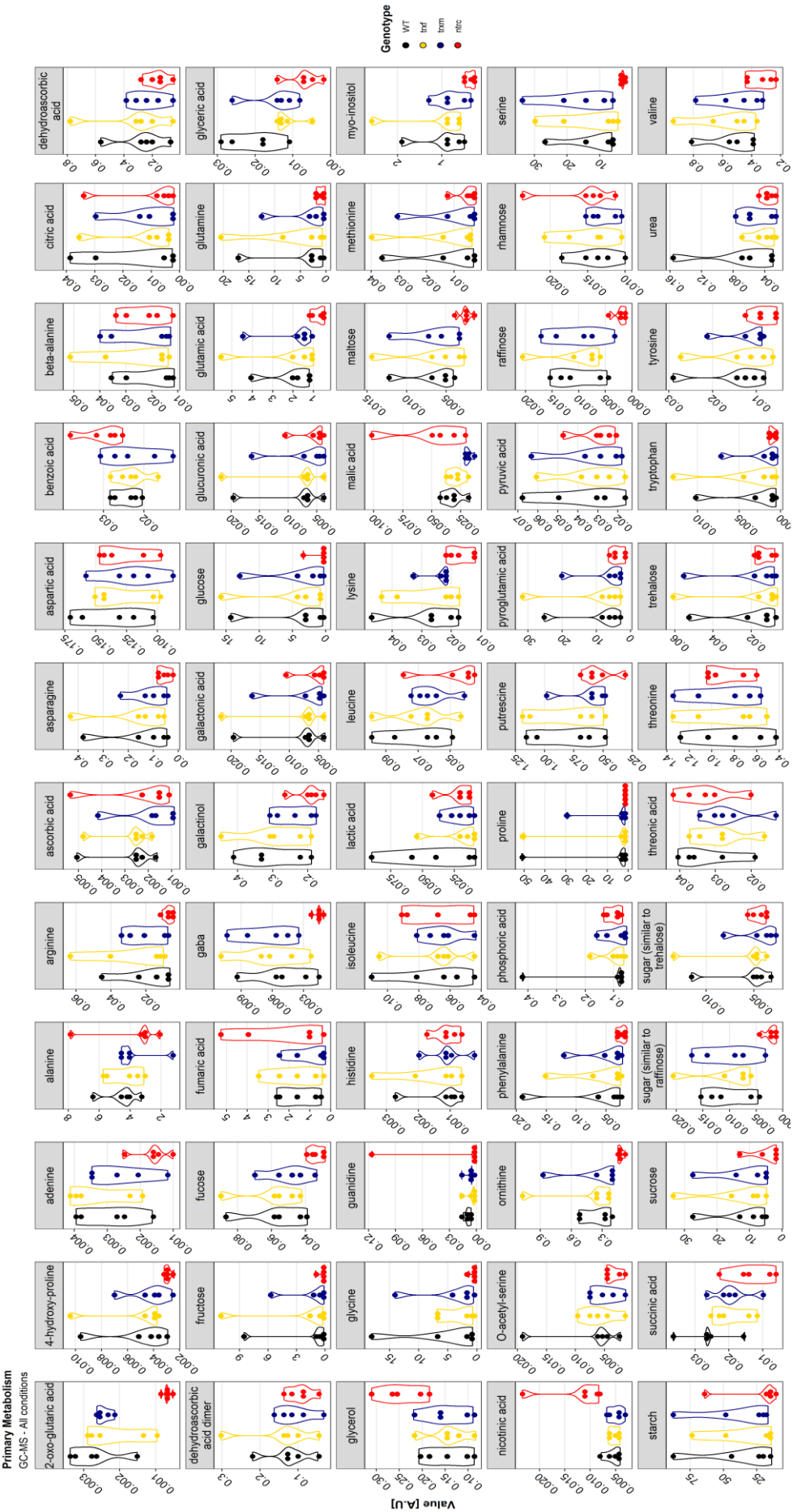

Figure 3.3.9. Overview of GC-MS based central metabolism in fully acclimated WT, *txf*, *txm* and *ntrc*.
Shown are the pooled mean values across all light conditions (ML, FHL, FLL, HL, LL). Values are in arbitrary units.

Lastly, a biomarker analysis (https://www.metaboanalyst.ca/) (Chong et al., 2019) pooling all light conditions, comparable to **Figure 3.3.9**, revealed a role of myo-inositol, ornithine, serine, fucose, raffinose and an undefined sugar similar to raffinose in *ntrc* compared to WT, while all metabolites were down-regulated on average (FC < 0; threshold AUC > 0.9) (**Table 3.3.1**). The AUC classifies metabolites according to their values, with high values being a strong indicator of reliably separating the control (WT) from the treated (*ntrc*) group. Given **Figure 3.3.8**, **Figure 3.3.9** and **Supplement Figure 5.3.3**, it is apparent that these metabolites exhibit little to zero dynamics in response to varying light conditions in *ntrc*, meaning NTRC might strictly regulate these metabolites or concomitant pathways.

Table 3.3.1. Biomarker analysis of central metabolites in *ntrc* relative to WT.
Analysis was performed with MetaboAnalyst (https://www.metaboanalyst.ca/) with pooled samples across all light conditions. AUC, area under the curve; FC, log2-fold change.

Metabolite	AUC	*p* value	FC
myo-inositol	0.968	3.81×10^{-08}	-1.30
ornithine	0.950	6.43×10^{-08}	-1.30
serine	0.916	4.67×10^{-07}	-1.74
fucose	0.909	5.28×10^{-07}	-0.64
raffinose	0.902	2.09×10^{-06}	-1.91
sugar (similar to raffinose)	0.902	2.09×10^{-06}	-1.91

In summary, long-term acclimation to different light intensities entails distinct metabolic responses in WT, along with WT-like responses in *trxf* and *trxm*, while exposing that metabolic re-adjustments are largely restrained in *ntrc*, especially under HL, indicating that NTRC is substantial to ensure the full range of metabolic dynamics in response to long-term changing light intensities.

3.3.2.2 Loss of Thioredoxins and NTRC affect Calvin-Benson-Cycle

To complete the metabolite profile, CBC intermediate metabolites were measured by LC-MS/MS using metabolite standards to obtain absolute values. Similar to the central metabolism, the analysis began with unsupervised clustering using PCA. Other than the results concerning central metabolism, a stronger genotypic effect was detected (**Figure 3.3.10 B**). Similar to the central metabolism, the light clusters segregated between HL and FHL and between LL and FL, respectively (**Figure 3.3.10 A**), indicating the prompt response of the metabolome to fast changing environments as outlined in the introduction. The FL regime branched a little more into the two sub conditions where FLL formed a clear outgroup to all other conditions; the other conditions clustered more closely together. Most contrasting to the central metabolism, HL showed here the smallest confidence ellipses of all conditions, which means, that only little genotypic effect is to be expected here. The PCA loadings (metabolites) concentrated on ML and HL. Strong negative correlations between FPB & SBP and ADP & AMP & shikimate were revealed. The former pair is strongly associated with *ntrc*, where regulation via NTRC has been highlighted earlier (Geigenberger et al., 2017).

The hierarchical clustering revealed 5 clusters, of which the FL clusters (A and B) formed two distinct but close related groups relative to the other light conditions and are the only cluster where all genotypes were included (**Figure 3.3.11**). Expression pattern of cluster A and B were very similar and differed only selectively. Especially carbohydrate synthesis (CHS) under FHL and CBC intermediates under FLL were down-regulated on average, whereas energy metabolites ADP and AMP and shikimate, which serves as a proxy for Erythrose-4-phosphate, were up-regulated in the entire FL. Strong up-regulations of 2PG in WT and *ntrc* under FHL were found, as well as an evident accumulation of SBP and FBP in *ntrc* under FLL, where all other CBC metabolites in this group were found to be diminished. This appears to be a bottleneck within the cycle, indicating a key role of NTRC in tight regulation of the CBC. Cluster E consisted of LL *trxf* and *trxm*, although TRX*m* and TRX*f* seemed to have partly opposing roles in CBC under LL. Highly correlated samples of HL WT, *trxf* and *trxm* could be found in cluster D, where expression was above average. Cluster C included samples of *ntrc* under constant light. Here, a great similarity between ML and LL was observed with extreme increases of CBC intermediates of over 16-fold compared to other samples (**Supplement Figure 5.3.6**). This underlines the role of NTRC in regulating photosynthesis particularly under lower light conditions (Thormählen et al., 2015; Naranjo et al., 2016; Nikkanen et al., 2016).

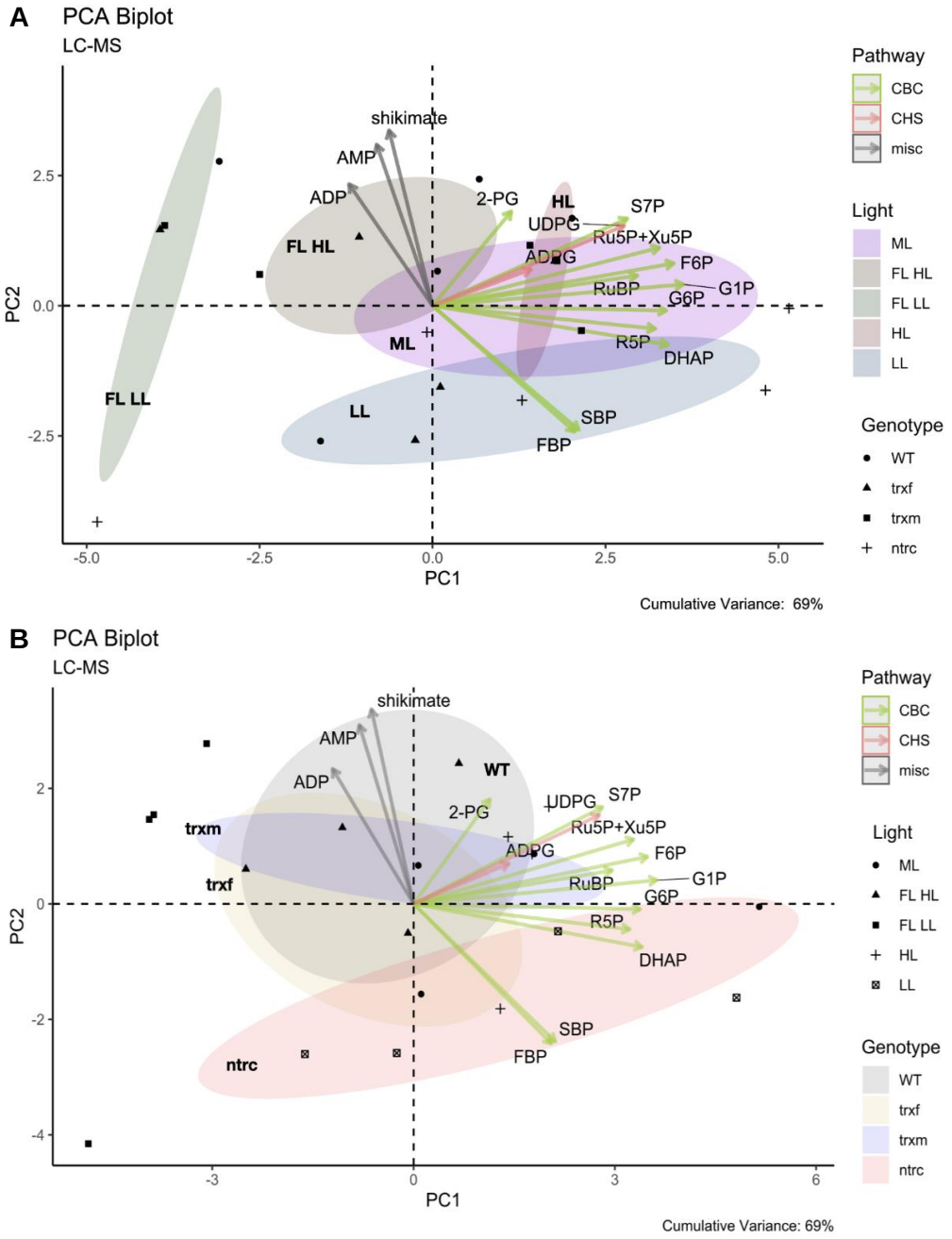

Figure 3.3.10. Cluster analysis of fully acclimated WT, *trxf*, *trxm* and *ntrc* samples for LC-MS based metabolites.
(A) According to light. (B) According to genotype. The cumulative variance explained by PC1 and PC2 is 69%. The clustering was done with the packages "factoextra" and "FactoMineR" in R. CBC, Calvin-Benson-Cycle; CHS, carbohydrate synthesis; misc, miscellaneous.

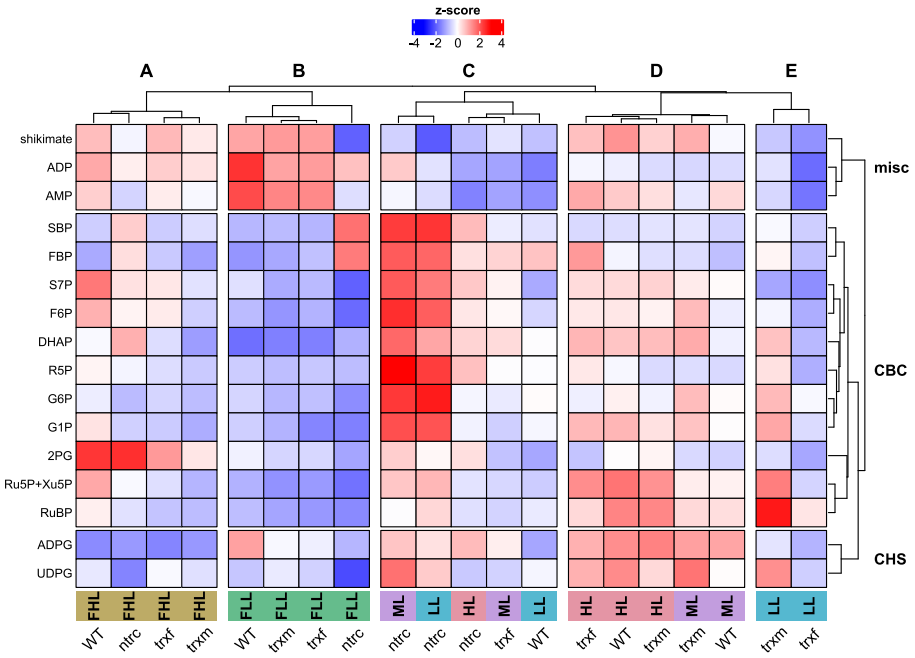

Figure 3.3.11. Heat map of standardized mean values of LC-MS based metabolites in fully acclimated WT, *trxf*, *trxm* and *ntrc*.
The heat map was generated with R package "ComplexHeatmap". CBC, Calvin-Benson-Cycle; CHS, carbohydrate synthesis; misc, miscellaneous.

A detailed analysis of the CBC under FL including absolute values and statistics is shown in **Figure 3.3.12**. As outline before, a significant accumulation of FBP and SBP in *ntrc* could be detected. Under FL HL, FBP and SBP were relatively increased 2.3- and 3.3-fold, respectively. Further significant changes in *ntrc* were associated with FL LL and scattered throughout every stage of the CBC (shikimate -56 %; SBP 1004 %; S7P -54 %; RuBP -60 %; 3PGA - 76%). Besides that, *trxf* showed a change in RuBP and 3PGA under FL LL, too. A significant bottleneck at FBP/FBPase, which is a known target for TRX*f*1 (Thormählen et al., 2015; Geigenberger et al., 2017) was also revealed. There were no significant changes detected in *trxm* compared to WT. Interestingly, overall similar expression patterns were observed between the lines when pooling the light conditions to explicitly examine the genotypic effect (**Supplement Figure 5.3.5**). This is different output compared to the results gained from the central metabolism, where a clear HL phenotype was seen due to loss of NTRC. Further, it shows that G6P, R5P and SBP for instance, did not change in WT, irrespective the light condition. On the other hand, some metabolites were more or less neither responding to intact (WT) nor impaired (mutants) redox regulation in the individual conditions: S7P, G6P, F6P and DHAP under HL; R5P and RuBP under FLL; ADPG under FHL. This is also backed up by statistics, depending on the model used (**Supplement Table 5.4.8**;

Supplement Table 5.4.9). For R5P and SBP we could thus conclude a possible crucial pacemaker role in the CBC (Hammel et al., 2020).

Summarized, the results showed that adjustments of CBC metabolites in response to long-term changing light intensities were dependent on the TRX/NTRC system especially under LL and ML, indicating different *in vivo* roles of TRX*f*, TRX*m* and NTRC in the CBC regulation. Sustained accumulation of SBP and FBP in *ntrc* could moreover indicate a missing reduction of respective enzymes, leading to impediments of the whole cycle, in particular under FLL.

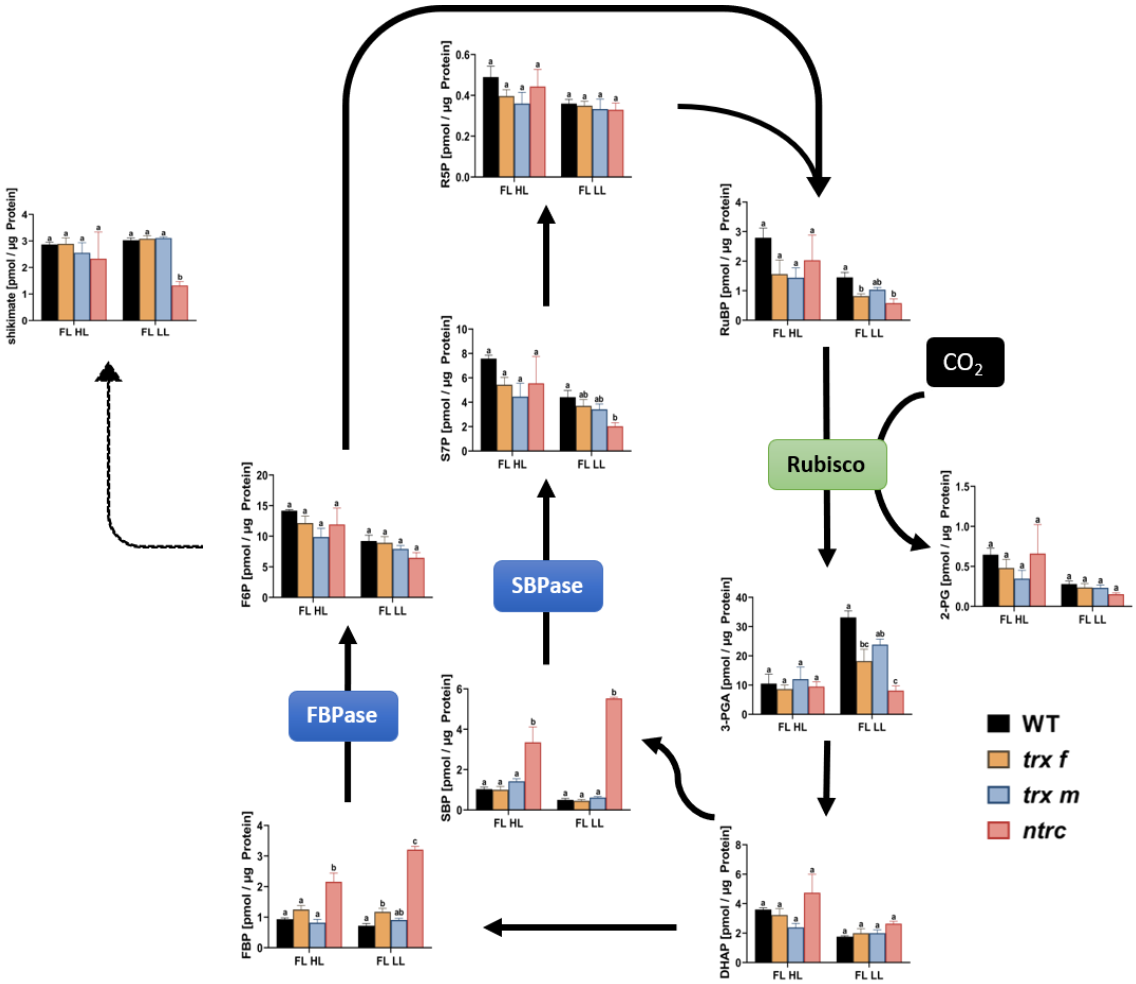

Figure 3.3.12. Simplified pathway of Calvin-Benson Cycle under fluctuating light in WT, *trxf*, *trxm* and *ntrc*.
Shikimate is shown as a proxy for Erythrose-4-Phosphate. Redox regulated enzymes are highlighted. Results are the mean ± SE, n = 3 biological replicates. Significance levels within one condition were evaluated by using a one-way ANOVA with a *post-hoc* Tukey test ($p < 0.05$) and are labelled with different letters.

3.3.2.3 Loss of thioredoxins has moderate effect on carbohydrate synthesis

Next, metabolite ratios were calculated to spot additional resistances in metabolic flow. Focusing on carbohydrate synthesis, genotypic differences were rather small, however light effects were seen (**Figure 3.3.13**). An up to 7-fold increase of G1P relative to ADPG in FL HL was detected, compared to ML (**Figure 3.3.13 A**). In ML and HL, G1P/ADPG ratios were smaller than in LL, which might indicate a strong pulling force to keep starch synthesis operating under constant moderate to high light intensity. This holds true for ML and HL as starch levels were increased here (**Figure 3.3.14**). In FL LL, electron pressure might be too low to fully activate the CBC. Except for ML, there were no statistical significances within one light condition detected. G6P/G1P ratios were at a similar and constant level in favor of G6P in every sample (**Figure 3.3.13 B**). In HL, G6P/G1P ratio was significantly higher in *ntrc* relative to WT. Next, the oxygenase reaction of RuBisCo producing 2PG should be at a low rate, under HL conditions. Under constant lights ML, HL and LL high levels of the acceptor molecule RuBP were found compared to 2PG in all genotypes but *ntrc*, where significantly reduced ratios were detected (**Figure 3.3.13 C**). Under FL, RuBP/2PG ratios were at very low absolute levels in all genotypes. This might be a convincing hint to a serious involvement of photorespiration under FL conditions.

Starch levels (as µmol hexose equivalents g^{-1} FW) were similar between FL and LL in all lines (10-20 µmol) (**Figure 3.3.14**). Under ML, starch was elevated in WT and TRXs mutants (40-50 µmol), but significantly lower in *ntrc* (20 µmol), indicating that FL, which has the same average light intensity as ML, is not sufficient to fully activate starch biosynthesis in WT. Starch was overall highest under HL in every genotype, with a slight but significant decline in *ntrc* (70 µmol) compared to WT (90 µmol).

In summary, our results revealed a putative role of photorespiration under FL, which is largely independent from redox-regulation. Moreover, FL conditions turn down starch synthesis, in comparison to constant light with the same average light intensity, showing similar starch levels as in LL acclimated plants. Further, TRX*f* and TRX*m* were not important to activate and stabilize starch biosynthesis in response to varying light conditions, while NTRC is needed regulate photorespiration and starch biosynthesis, especially under ML and HL.

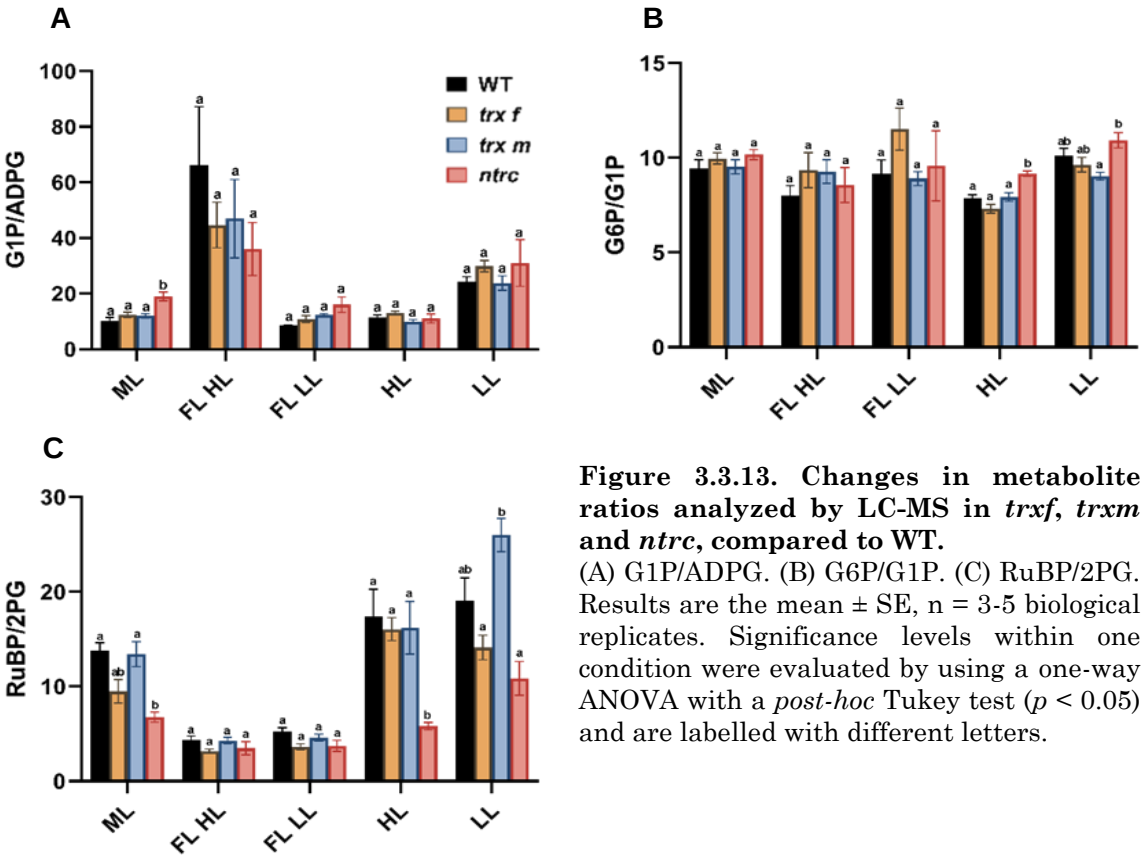

Figure 3.3.13. Changes in metabolite ratios analyzed by LC-MS in *trxf*, *trxm* and *ntrc*, compared to WT.
(A) G1P/ADPG. (B) G6P/G1P. (C) RuBP/2PG. Results are the mean ± SE, n = 3-5 biological replicates. Significance levels within one condition were evaluated by using a one-way ANOVA with a *post-hoc* Tukey test ($p < 0.05$) and are labelled with different letters.

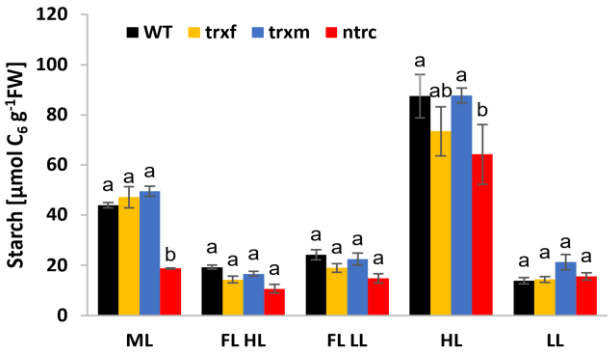

Figure 3.3.14. Changes in starch content in *trxf*, *trxm and ntrc*, compared to WT.
Results are the mean ± SE, n = 4-5 biological replicates. Significant changes within one condition were evaluated by using a two-way ANOVA with a *post-hoc* Tukey test and are labelled with different letters ($p < 0.05$). C_6, hexose equivalents; FW, fresh weight.

3.3.2.4 NTRC deficiency disrupts correspondence between metabolites

By investigating the linear correlation between metabolites across all light conditions (defined as Pearson correlation coefficient r), we found that sugars and amino acids were strongly connected in WT (**Supplement Figure 5.3.8**). Positive correlations in general outnumbered negative ones. It further appeared, that central metabolites barely correlated with CBC metabolites, pointing to mostly distinctly operating networks within the cell. However, the CBC intermediates Ru5P & Xu5P and FBP indicated sugar states by showing positive correlations with the main sugars fructose ($r_{FBP, fructose} = 0.730$), sucrose ($r_{FBP, sucrose} = 0.692$), maltose ($r_{FBP, maltose} = 0.736$) and glucose ($r_{FBP, glucose} = 0.732$). These associations between metabolites seemed to be lost in NTRC deficient plants (**Supplement Figure 5.3.9**); sugars were found to be only partly correlating with amino- and also some organic acids. Further, Ru5P & Xu5P and RuBP negatively correlated with some close related amino acids ($r_{RuBP, leucine} = -0.750$, $r_{RuBP, lysine} = -0.701$, $r_{RuBP, isoleucine} = -0.593$, $r_{RuBP, tyrosine} = -0.574$, $r_{RuBP, valine} = -0.615$) as well as with rhamnose ($r_{RuBP, rhamnose} = -0.777$). However, since these amino acids are strongly inter-correlated and were mostly down-regulated and very low in abundance in *ntrc* compared to WT, caution has to be taken in interpretation.

Summarized, we postulated that the central- and CBC metabolism might be distinctly operating systems, tenuously connected via FBP and glycolysis. A simple linear correlation, however, might fail to depict the real underlying ties between the two systems and to corroborate our hypothesis.

3.3.3 Acclimation to different light regimes involves large re-adjustments of the proteome

3.3.3.1 Clustering revealed a strong light effect but little genotypic effect on protein abundance

Proteins directly regulate cellular functions, so measurements of single protein abundance were performed to provide significant hints to the adjustment of cellular functions during different environmental perturbations (Wegener et al., 2010). Plant material was taken from the same batches as for analyzing the metabolomics. A very important prerequisite for data processing was to have at least two valid values for each sample in general, and in each light condition separately, to be able to perform proper statistics. After processing the raw data, a total of 4023 peptides remained. Relative abundances were taken from MaxQuant's *label-free quantification* output. These were translated into 2964 unique gene loci (uniport.org) to be analyzed in-depth. The most peptides were detected in LL, followed by ML, HL and FL (**Supplement Figure 5.3.10**). First a PCA was performed; samples were clustered according to genotype and light. The analysis showed little genotypic effect of *trxf* and *trxm*, but a large effect for *ntrc* relative to WT (**Figure 3.3.15 A**). Confidence ellipses of WT, *trxf* and *trxm* were largely overlapping and extended along PC1; the *ntrc* cluster was almost orthogonal to all other groups along PC2, indicating a distinct role of NTRC in the proteome adjustment. Light clusters were more distinct, too; here, FL formed a clear outgroup compared to other conditions (**Figure 3.3.15 B**). ML and LL clusters were overlapping; HL showed the highest variance. The cumulative variance explained by PC 1 and PC 2 was 61 %, thereby representing the data quite sufficiently.

Next, a heat map was generated to illustrate general regulation pattern across all samples and light regimes (**Figure 3.3.16**). The biggest and most noticeable effects were found in WT and *trxf* under HL, which formed an outgroup compared to other clusters. Here, nearly each half of the proteins was either outstandingly up- or down-regulated, respectively. Further, the change in expression here was above (below) average, indicating that HL has a substantial effect on WT and *trxf*, and a minor effect on *trxm* and *ntrc*. LL samples of WT, *trxm* and *trxf* were closely correlated. Under FL, *ntrc* clustered with WT and *trxm*, from which can be concluded that here no big proteomic difference might to be expected between the mutants and WT. Further, the *ntrc* mutant formed a distinct cluster within ML, HL and LL, suggesting little to zero dynamics in the proteome adjustment in response to changing light intensities.

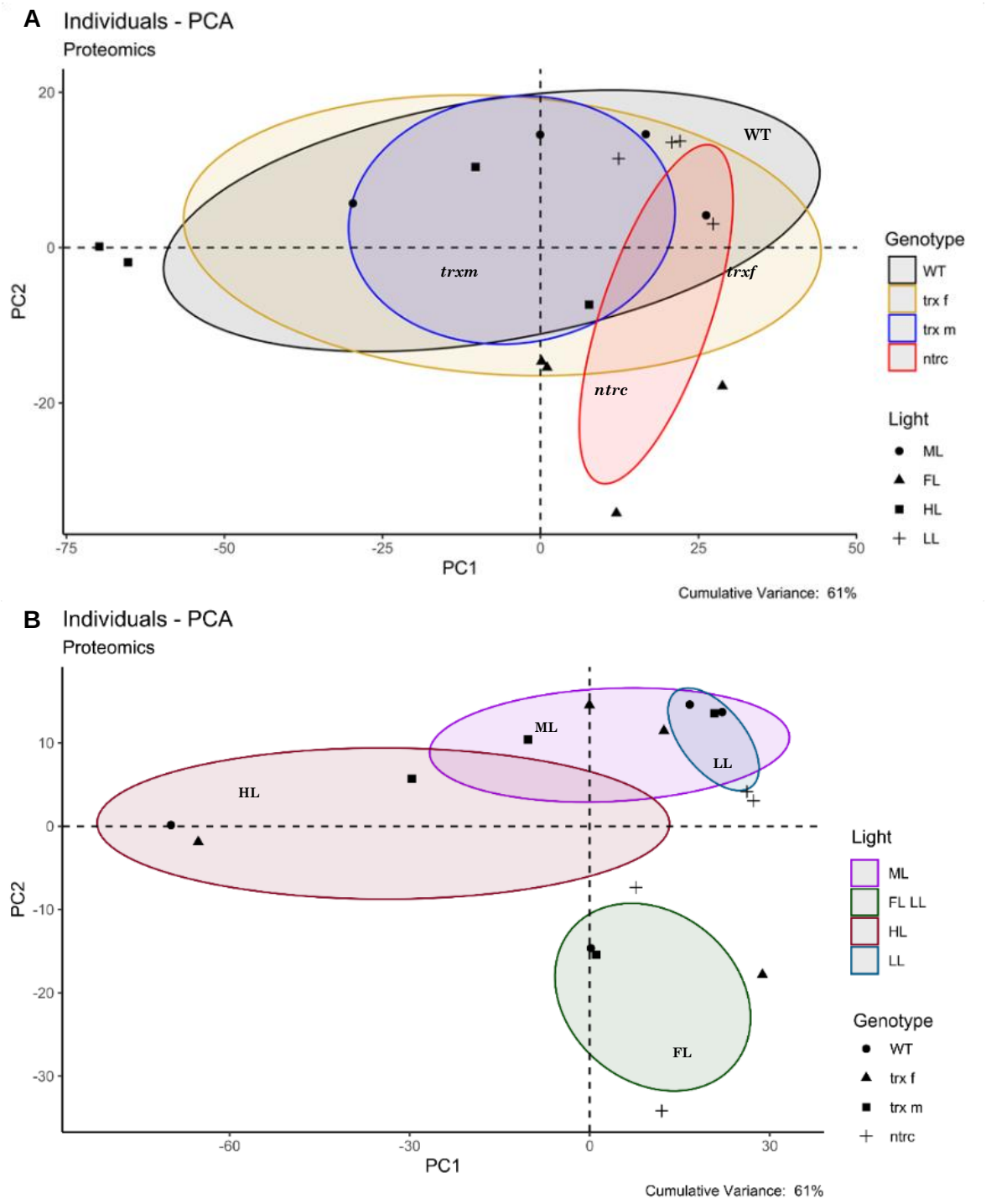

Figure 3.3.15. Cluster analysis of proteomics in fully acclimated WT, *trxf*, *trxm* and *ntrc* grown under different light conditions.
(A) According to genotype. (B) According to light. The cumulative variance explained by PC1 and PC2 is 61 %. Plot was generated with R package "factoextra" and "FactoMineR".

Cluster 1 mainly represents translation and anabolic processes around ribosomes and the nucleus, cluster 2 represents stimuli responses and catabolism with focus on thylakoids (**Figure 3.3.17 A** and **B**) (analysed with "agriGO" and "REVIGO") (Supek et al., 2011; Tian et al., 2017). The two clusters and the hereby associated annotations, in terms of gene ontology (GO), notably behave contrary.

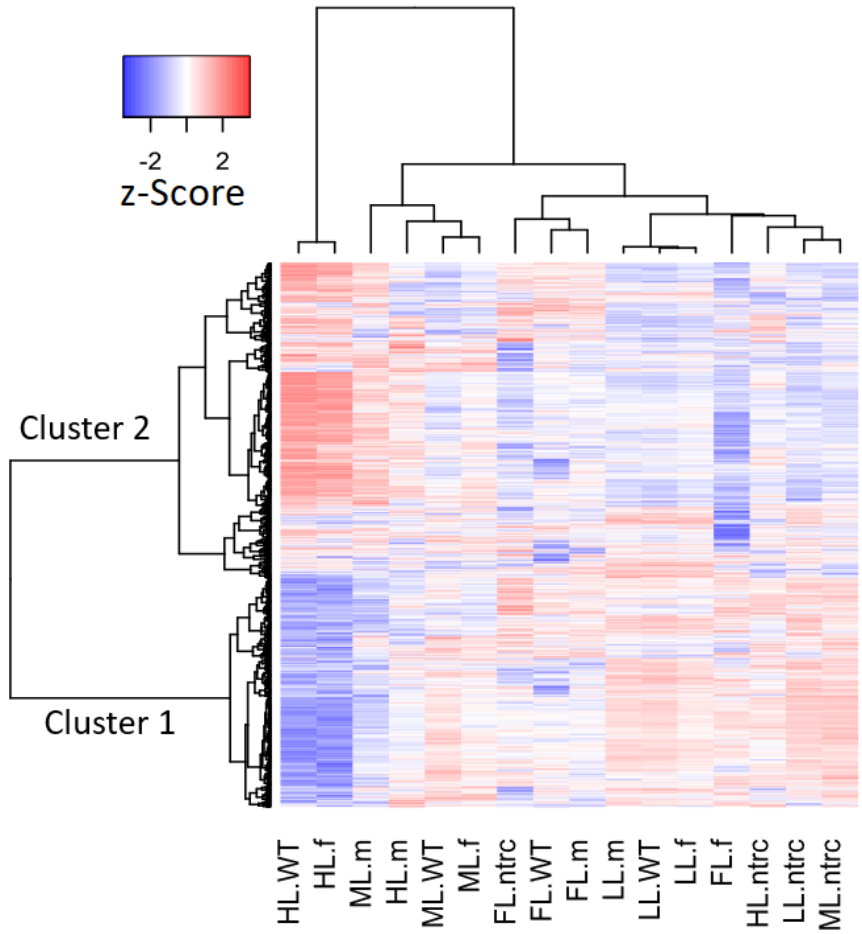

Figure 3.3.16. Representative heat map of standardized protein abundances in fully acclimated WT, *trxf*, *trxm* and *ntrc*.
Only valid peptide hits common in all light regimes were incorporated. FL samples were harvested under the LL period of FL. Blue color indicates down-regulation. Red color indicates up-regulation. The plot is separated in two clusters. The row clustering (proteins abundance) outlines the overall adjustment, the column clustering indicates the relation between different samples. Clustering distance: correlation; clustering method: Ward's method. Heat map was generated with R package "gplots" (Warnes et al., 2016). f, *trxf*; m, *trxm*.

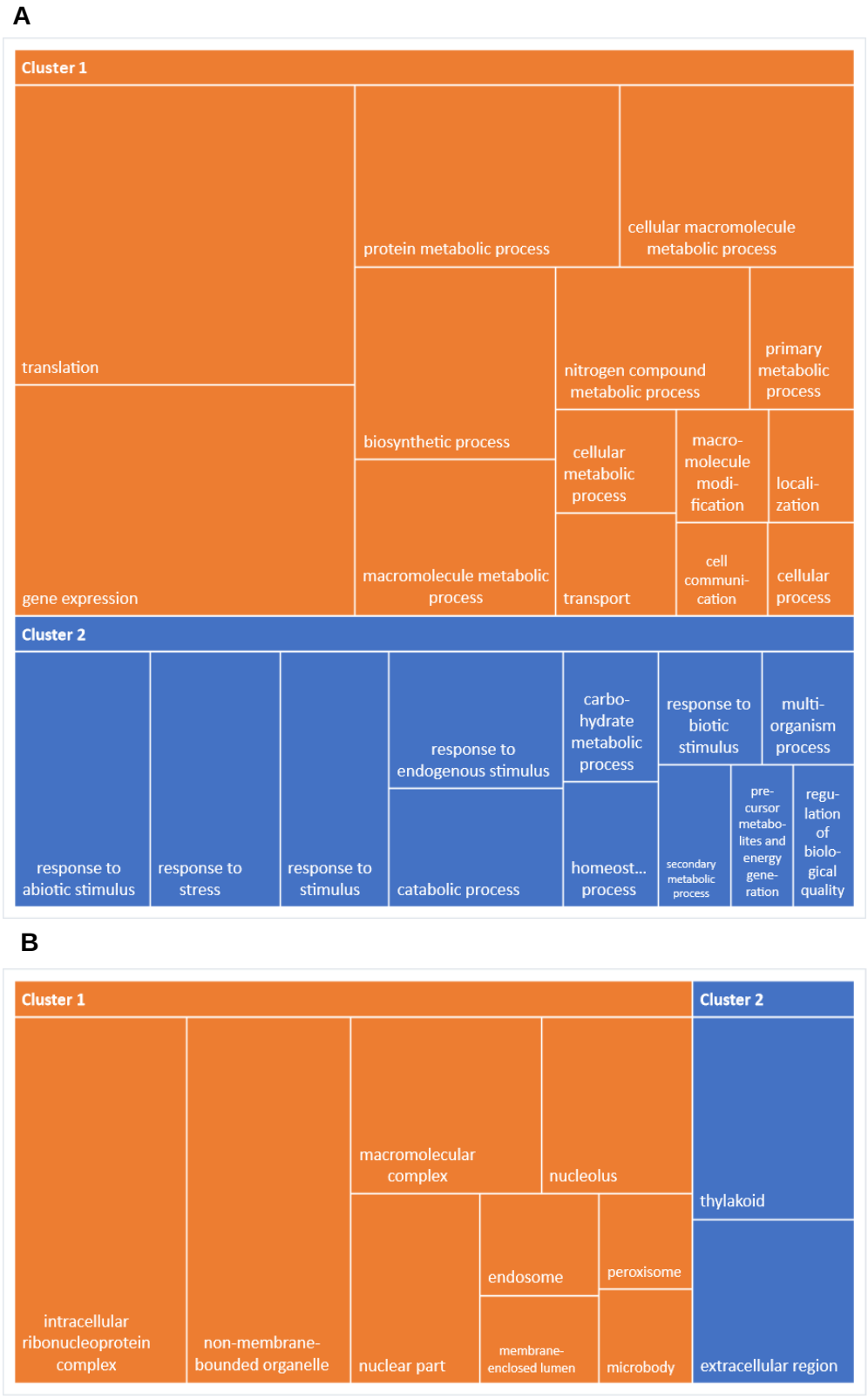

Figure 3.3.17. Treemap of significant (FDR < 0.05) GO terms regarding proteomic changes.
(A) biological process ("BP"); (B) cellular compartment ("CC"). A list of complete GO terms was created with "agriGO" and sent to "REVIGO" to remove redundant terms (Supek et al., 2011; Tian et al., 2017). The size of the boxes equals the -$\log_{10}$(FDR). Cluster 1 and 2 are corresponding to **Figure 3.3.16**.

3.3.3.2 Light acclimation involves oxidoreductases in the wild type

In the next analysis, processes only in the WT were investigated in detail. As significance test a repeated t-test with a Benjamini-Hochberg correction was applied to reduce the rate of type I (false positive) errors (Benjamini & Hochberg, 1995). 737 proteins were significantly ($p < 0.05$) regulated in HL, 419 in LL and 133 in FL, relative to ML (**Figure 3.3.18 C**). Based on FL, the distinct overlap between HL and LL, respectively, was almost identical (28 respectively 35 proteins). We also found a greater number of proteins overlapping in FL and LL compared to exclusively found proteins in FL (61 > 44), already indicating that FL acclimation had a low impact on significant changes in protein abundances in WT. However, changes took place in the plastid more frequently under FL (45 %) than under HL (33 %) or LL (38 %) (**Figure 3.3.18 A** and **B**).

Next, the common significant changes between FL, HL and LL (relative to ML) were explicitly examined. Only two terms were found to be of significance regarding the biological process (BP) in WT: *oxidation-reduction process* (GO:0055114; $p = 0.04\%$) and *single-organism metabolic process* (GO:0044710; $p = 1.10\%$). Protein changes exceedingly involved following cellular compartments (CC): *chloroplast stroma* ($p = 6 \times 10^{-8}$), *thylakoid membrane* ($p = 1.5 \times 10^{-6}$) as well as the *cytoplasm* ($p = 1.6 \times 10^{-6}$). **Table 3.3.2** displays a list of candidates found in the GO term *oxidation-reduction process*; 4 out of 9 proteins were found in the plastid, two of which are involved in photosynthesis (PGR5-like protein 1A and NDH subunit U).

In summary, this first analysis with WT samples already underlines the idea of an integral role of redox regulation in light acclimation processes, mainly occurring in the chloroplast.

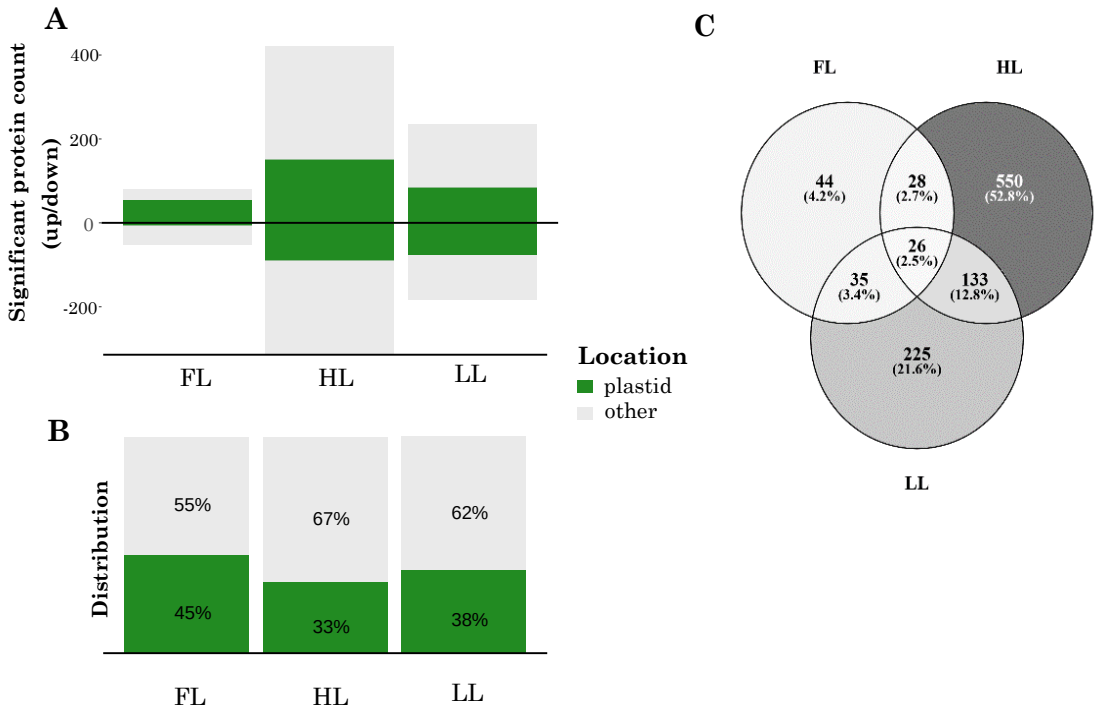

Figure 3.3.18. Overview of proteomic changes in WT.
(A) Number of significantly regulated proteins. (B) Distribution of significantly changed proteins across cell compartments. (C) Venn diagram of distinctly and conjointly changed proteins across FL, HL and LL, relative to ML. Only valid peptide hits common in all conditions were incorporated. Significances were tested with a repreated t-test following Benjamini-Hochberg correctin ($p < 0.05$). The subcellular location was defined with SUBA4 (Hooper et al., 2017).

Table 3.3.2. Significant and common protein changes in FL, HL and LL (relative to ML) linked to *oxidation-reduction process* (GO:0055114) in WT.
Significances on protein level were tested with a repeated t-test following Benjamini-Hochberg correction ($p < 0.05$). Prior to that, GO term enrichments were evaluated with "agriGO" (FDR < 0.05). Location (consensus) was determined with SUBA4.

Locus	Protein names	Location
AT1G76680	12-oxophytodienoate reductase 1	cytosol
AT3G24503	Aldehyde dehydrogenase family 2 member C4	cytosol
AT4G39330	Probable cinnamyl alcohol dehydrogenase 9	cytosol
AT1G17990	Putative 12-oxophytodienoate reductase-like protein 2A	cytosol
AT1G79440	Succinate-semialdehyde dehydrogenase	mitochondrion
AT2G45770	Cell division protein FtsY homolog	plastid
AT5G21430	NAD(P)H-quinone oxidoreductase subunit U	plastid
AT4G22890	PGR5-like protein 1A	plastid
AT1G06690	Uncharacterized oxidoreductase	plastid

3.3.3.3 Wild type plants are mostly affected by high light

MapMan offers ontology-driven analyses and was designed to cover plant-specific pathways and processes (Usadel et al., 2009; Klie & Nikoloski, 2012). Since the biggest effects were revealed in HL, cell functions in WT under HL (relative to WT ML) were illustrated (**Figure 3.3.19**). The functional categories (MapMan bins) are of different size; fairly normally distributed bins harbor a larger number of proteins (e.g. *regulation of transcription*, *protein synthesis*, *hormones*).

A strong up-regulation could be observed in *stress* and *redox processes*. *Protein synthesis* and *transport* was strongly down-regulated. A detailed analysis of *protein synthesis & amino acid activation* can be found in **Figure 3.3.20**. This detailed mapping convincingly shows that processes from RNA to protein metabolism were heavily decreased. This is in line with the previous mentioned observations (**Figure 3.3.16**; **Figure 3.3.17**). No striking changes in FL or LL (relative to ML) were observed (**Supplement Figure 5.3.11**).

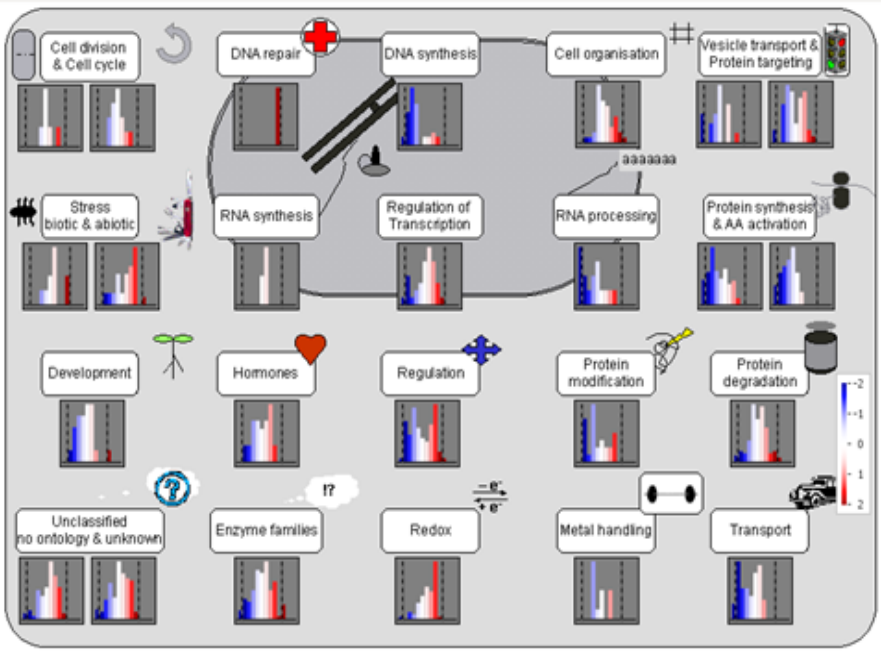

Figure 3.3.19. Proteomic responses in WT under HL, relative to ML.
Relative abundances are shown as log2-fold changes ranging from -2 (blue) to 2 (red). White, no change. Graph was generated with MapMan.

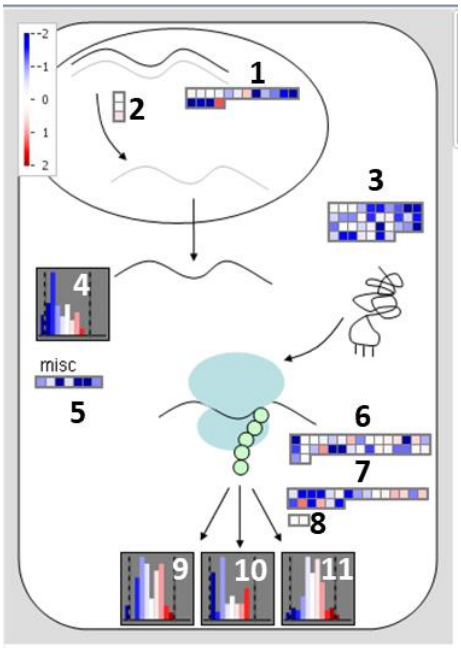

Figure 3.3.20. MapMan illustration of RNA and protein metabolism in WT under HL, relative to ML.
1) RNA processing 2) RNA Transcription 3) Amino acid activation 4) Ribosomal protein 5) Ribosome biogenesis 6) Protein synthesis – initiation 7) Protein synthesis – elongation 8) Protein synthesis – release 9) Protein targeting 10) Posttranslational modification 11) Protein degradation. Relative abundances are shown as log2-fold changes ranging from -2 (blue) to 2 (red). White, no change. Graph was generated with MapMan.

To potentially explain the findings from chlorophyll fluorescence measurements (cf. chapter 3.3.1) on protein level, thereby linking the CBC via the TRX/NTRC system, the light reactions in the thylakoids were investigated next. **Figure 3.3.21** shows a heat map of photosynthetic subunits of core proteins (PSII, PSI), light-harvesting complexes (LHCs), electron shuttling (NDH, Cyt b_6f, PC) and energy production (ATPase) in WT. In FL, relative to ML, only little change was observed in the core subunits and electron transport, but an increase in PSII assembly and stabilizing units (PSBO, PSBP, PSBQ, PSB27, PSB28) and a strong decrease in LHCs (LHCI, LHCII) could be detected. In HL, core units of both photosystems as well as LHCs, NDHs and Cyt b_6f complex were strongly down-regulated. In detail, core proteins PSBA, PSBB, PSBD, PSAA. PSAD, PSAF AND PSAL, as well as PETB and PETC, were significantly down-regulated in HL, relative to ML. On the other side, a strong increase in almost every domain under LL was noticed, which has been observed before (Walters & Horton, 1994), including significant changes of PSBC, PSBH, PSBO, PSBR, PSAD, PSAE, PSAG and PSAL. This shows that the WT takes thorough measures to adapt to different light environments by accurately adjusting proteins vital for full photosynthetic functionality: under HL as protective mechanism from excess light (balanced with optimal quantum yield), under LL to fully utilize photochemistry as energy source for down-stream anabolic processes.

Differentially increased proteins under HL down-stream the light reactions included chloroplastic triosephosphate isomerase (AT2G21170), ß-amylase (AT4G00490), probably to increase the pool of soluble carbohydrates to cope with stress, TRX*h5* (AT1G45145), a mediator for electron transport and distribution (Vandereyken et al., 2018), chloroplastic fructose-bisphosphate aldolase (AT4G38970), Phosphoglycerate kinase (AT1G56190), RuBisCO activase (AT2G39730) and Mg-chelatase (AT4G18480) for chlorophyll biosynthesis.

Taken together, redox- and stress response processes increased, while translation decreased in WT under HL. Photosynthetic proteins were mildly affected under FL and strongly influenced under LL and HL. The most and biggest protein changes were found under HL, possibly influencing photosynthesis to a higher degree than in FL or LL (cf. chapter 3.3.1).

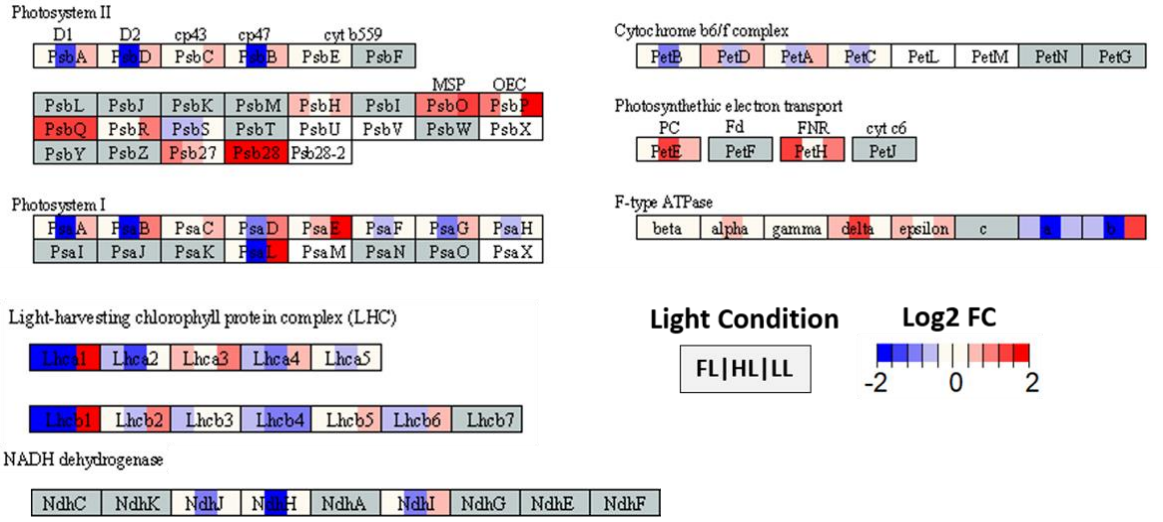

Figure 3.3.21. Heat map of photosynthetic subunits in WT.
Each box represents one protein, where the log2-fold change was calculated in the following order: FL/ML, HL/ML, LL/ML. Blue color, down-regulation; red, up-regulation; white, not present in *Arabidopsis;* grey, blank. The figure was generated with R package "pathview".

3.3.3.4 Loss of NTRC strongly affects proteomic re-adjustment in all light regimes

The results above showed that changes in protein levels involved in redox processes are a common feature in light acclimation responses (cf. chapter 3.3.3.2). It was therefore interesting to address proteomic changes due to knockout of redox modulators TRX*f*, TRX*m* or NTRC in comparison to the respective WT in each light condition.

Only few changes were observed in *trxf* in general, with a highest of 18 exclusively, significantly changed proteins under FL (**Figure 3.3.22**); however, here nearly all proteins were down-regulated and located in the plastid. In other light conditions there were only few changes found, predominantly in the cytosol. In *trxm* a similar pattern was noticed under FL, where all 6 significant proteins were down-regulated, the plastid ones being Glyceraldehyde-3-phosphate dehydrogenase isoforms 1 & 2 (AT1G79530 & AT1G16300) and RNA polymerase-associated protein 3 (AT3G48500). As summarized in chapter 3.3.3.1, the cluster analyses showed a humble change in protein abundance in *trxm* under FL, which means that improved photosynthesis under LL phase of FL (cf. chapter 3.3.1) must be explained otherwise. Interestingly, numerous and strong changes in *trxm* under ML were found, which is also in line with the previous cluster analyses; 164 and 149 proteins were significantly up- and down-regulated, respectively, 34 % of which were located in the plastid. Further, large intersections between *trxm* and *ntrc* were found under HL (40 shared compared to 7 exclusive proteins in *trxm*). There were only minor changes under LL in *trxm*. If grown under FL, HL or LL, loss of NTRC showed a substantial alteration in protein abundance. The numerically biggest changes occurred in HL (227; 27 % in plastid), followed by LL (145; 42 % in plastid) and FL (41; 39 % in plastid). Under ML, a number of 65 proteins were exclusively found in *ntrc* and thus much lower than in *trxm* (231 exclusive proteins).

Summarized, most protein changes were revealed in *ntrc*, particularly under HL, indicating a different role in translation processes compared to WT, where overall significant changes affected the cytosol noticeably more than the chloroplast.

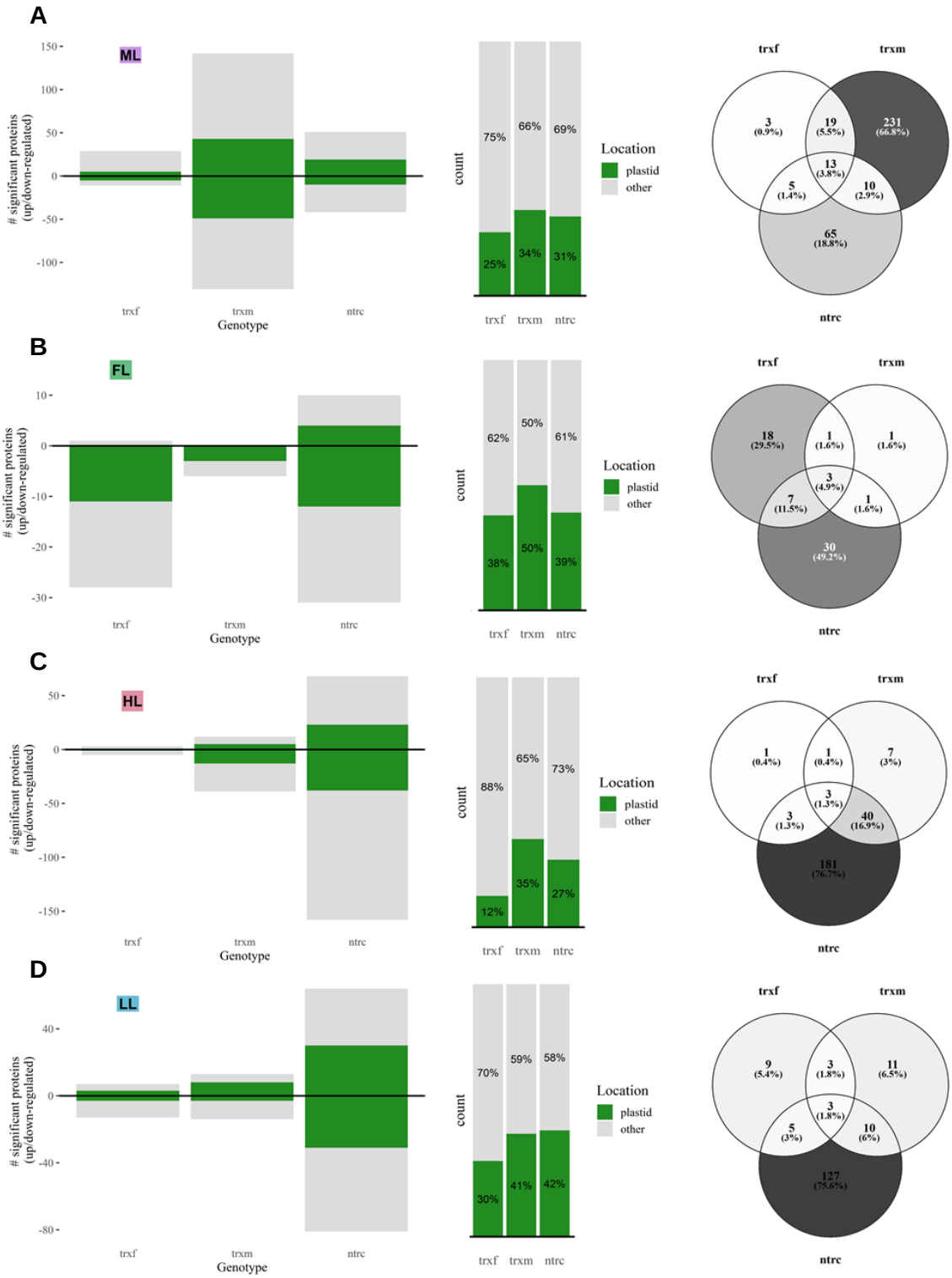

Figure 3.3.22. Overview of significantly ($p < 0.05$) up- or down-regulated proteins in *trxf*, *trxm* and *ntrc*, relative to WT.
Summary and distribution of significantly changed proteins across cell compartments and Venn diagrams of commonly and exclusively changed proteins in (A) ML, (B) FL, (C) HL and (D) LL.

A detailed list of highly significant protein changes ($p < 0.001$), regarding the entire data set, is given by **Table 3.3.3**. This list contains information about the light conditions, the subcellular location and the direction of regulation (up/down). As can be seen, the only other significant hit, besides exclusively involving *ntrc*, is TRX*m*2 down-regulation in *trxm* under HL. As outlined in the beginning of this chapter, only few changes were detected under FL, where however all proteins were up-regulated; two of three proteins were found in the plastid: LOW PSII ACCUMULATION 1 (AT1G02910), which is part of PSII and Alternative NAD(P)H-ubiquinone oxidoreductase C1 (AT5G08740), which is involved in electron transport. Contrary, the majority of proteins under HL and LL is down-regulated. Plastid localized proteins are COLD-REGULATED 15A (AT2G42540), Superoxide dismutase 1 (AT4G25100), important for light response, CBS domain-containing protein 2 (AT4G34120) and 30S ribosomal protein (AT5G24490) in HL and Photosystem I chlorophyll a/b-binding protein 3-1 (AT1G61520), a light-harvesting compound, Beta-amylase 3 (AT4G17090), for starch processing, Protochlorophyllide reductase B (AT4G27440), crucial for photosynthesis and chlorophyll, CBS domain-containing protein 2 (AT4G34120) and Ferredoxin-dependent glutamate synthase 1 (AT5G04140), involved in ammonium assimilation and glutamate biosynthesis, under LL. An intriguing TRX-activating protein – CBSX2 (cystathionine ß-synthase domain), which stabilizes cellular redox homeostasis and modulates plant development (Yoo et al., 2011), – was found significant in both HL and LL and has been reported to interact with NTRC (González et al., 2019). Brief descriptions of each protein were taken from https://www.uniprot.org.

Table 3.3.3. Significantly changed proteins ($p < 0.001$, t-test with Benjamini-Hochberg correction) in *trxm* and *ntrc*, compared to WT.
Red, up-regulated; blue, down-regulated. Annotation was taken from Uniprot (https://www.uniprot.org/). Subcellular localization (consensus) was determined with SUBA4. There were no significances detected in *trxf* below the mentioned threshold.

Light	Location/ Genotype/ Locus	Protein name	*p* value (%)	Expression
ML	**plastid**			
	ntrc			
	AT1G71500	Rieske (2Fe-2S) domain-containing protein	0.084	↑
	AT4G34120	CBS domain-containing protein CBSX2	0.035	↓
	AT5G04140	Ferredoxin-dependent glutamate synthase 1	0.008	↑
	vacuole			
	ntrc			
	AT5G22580	Stress-response A/B barrel domain-containing protein	0.037	↓
FL	**endoplasmic reticulum**			
	ntrc			
	AT3G09260	Beta-glucosidase 23	0.036	↑
	plastid			
	ntrc			
	AT1G02910	Protein LOW PSII ACCUMULATION 1	0.032	↑
	plastid, mitochondrion			
	ntrc			
	AT5G08740	Alternative NAD(P)H-ubiquinone oxidoreductase C1	0.036	↑
HL	**cytosol**			
	ntrc			
	AT2G30870	Glutathione S-transferase F10	0.056	↓
	AT3G44860	Farnesoic acid carboxyl-O-methyltransferase	0.065	↓
	AT3G44870	AtPP-like protein	0.065	↓
	mitochondrion			
	ntrc			
	AT3G15020	Malate dehydrogenase 2	0.023	↓
	AT4G00860	AT0ZI1 protein	0.038	↓

Table 3.3.3 (continued)

HL	**peroxisome**			
	ntrc			
	AT1G19570	Glutathione S-transferase DHAR1	0.053	↓
	AT4G23600	Cystine lyase CORI3	0.057	↓
	plastid			
	ntrc			
	AT2G42540	Protein COLD-REGULATED 15A	0.062	↓
	AT4G25100	Superoxide dismutase [Fe] 1	0.007	↓
	AT4G34120	CBS domain-containing protein CBSX2	0.081	↓
	AT5G24490	30S ribosomal protein	0.047	↑
	trxm			
	AT4G03520	Thioredoxin M2	0.003	↓
LL	**cytosol, plasmamembrane**			
	ntrc			
	AT1G20450	Dehydrin family protein	0.047	↓
	AT3G53990	Adenine nucleotide alpha hydrolases-like superfamily protein	0.015	↓
	endoplasmic reticulum			
	ntrc			
	AT3G09260	Beta-glucosidase 23	0.012	↑
	mitochondrion			
	ntrc			
	AT2G26080	Glycine dehydrogenase (decarboxylating) 2	0.005	↑
	nucleus			
	ntrc			
	AT1G20440	Dehydrin COR47	0.038	↓
	peroxisome			
	ntrc			
	AT1G35720	Annexin D1	0.025	↓
	AT1G76180	Dehydrin ERD14	0.014	↓
	plastid			
	ntrc			
	AT1G61520	Photosystem I chlorophyll a/b-binding protein 3-1	0.030	↓
	AT4G17090	Beta-amylase 3	0.038	↓
	AT4G27440	Protochlorophyllide reductase B	0.091	↓
	AT4G34120	CBS domain-containing protein CBSX2	0.018	↓
	AT5G04140	Ferredoxin-dependent glutamate synthase 1	0.046	↑

Table 3.3.3 (continued)

LL	**vacuole**			
	ntrc			
	AT5G22580	Stress-response A/B barrel domain-containing protein	0.019	↓

Next, specialized pathways and protein networks were analyzed more deeply. Therefore, the cluster of photosynthesis related proteins were chosen and concisely visualized with "pathview" (Luo et al., 2017).

First, no changes were noticed in *trxf* relative to WT regarding the shift from ML to other light conditions (**Figure 3.3.23 A**). Indeed, most changes (down-regulation) occurred in LHCs and PSI core subunits (PSAA, PSAB) under ML. In *trxm* the same down-regulation of LHCs and PSI core units was detected, beyond that PSII core units PSBA, PSBD and Cyt b_6f were affected, too (**Figure 3.3.23 B**). Apart from very few significant changes under ML, no significances in other conditions were detected in *trxm*. Next, a strong decline in PC in *ntrc* under every condition was seen (**Figure 3.3.23 C**), so electron transfer from Cyt b_6f to PSI might be heavily disturbed. This potential bottleneck in electron flow might fit to the observations of over-reduced PQ (cf. chapter 3.3.1). There were nearly no changes in PSII or PSI under ML, yet LHCBs but not LHCAs were down-regulated. Under FL, PSI was depleted and few LHCB and LHCA were down- and up-regulated, respectively. Moderate to strong increases in PSII and PSI core units as well as in NDH and Cyt b_6f were detected under HL. Further, LHCs were inconsistently changed, while PC and Fd were down-regulated. However, under HL, only PSBQ2 and PSAE were significantly down-regulated in *ntrc*. Eventually, little to no changes were observed under LL in *trxf* and *trxm*. In *ntrc*, a greater number of significant down-regulations were detected, including levels of PSI subunits (PSAC, PSAD, PSAE, PSAF, PSAL), PSII (PSBC, PSBO, PSBP, PSBQ) and light-harvesting LHCA3.

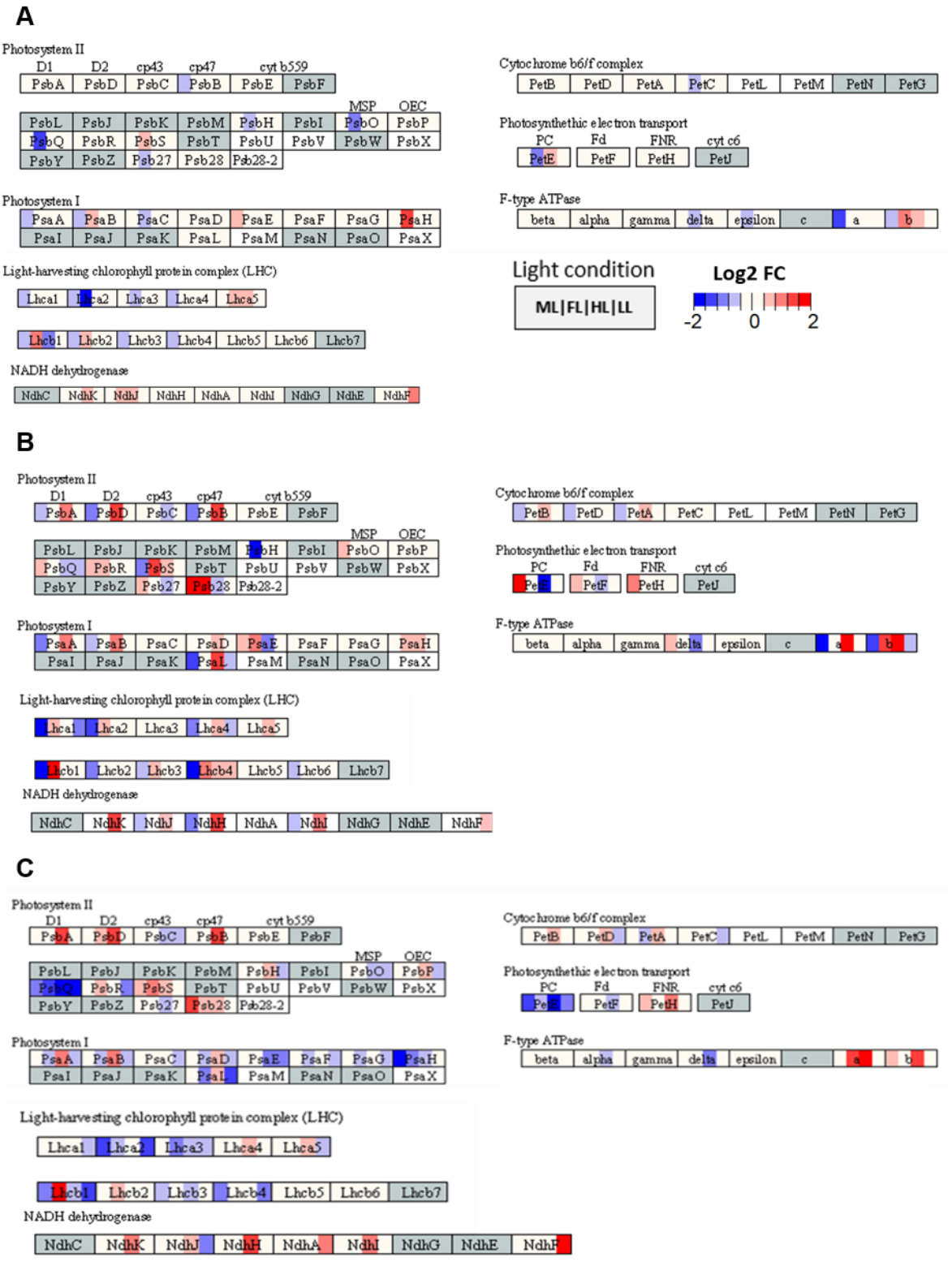

Figure 3.3.23. Changes of photosynthetic subunits in *trxf*, *trxm* and *ntrc*, relative to WT.

(A) *trxf*. (B) *trxm*. (C) *ntrc*. Each box represents one protein, where the log2-fold change was calculated in the following order: ML/ FL/ HL/ LL. Blue, down-regulation; red, up-regulation; white, not present in *Arabidopsis;* grey, blank. The figure was generated with R package "pathview".

Summarized, light shifts from ML to FL, HL or LL result in global proteomic adjustments and notably involve oxidation-reduction processes in the WT. The findings further suggest a bigger role of the cytosol in acclimation responses than the chloroplast. The overall biggest changes appeared in WT (and *trxf*) when HL acclimated, being connected to a decrease in translation and an increase of stress responses. Interestingly, the relevance of these processes almost inverted in every other light condition. Next, pre-exposure to FL did not have a great impact on the proteome. Following this, genotypic differences between WT and TRXs mutants were rather small across all light conditions, while NTRC deficiency resulted in frequent significant protein changes. However, relatively little to no dynamic acclimation response to all the different light regimes was attested in *ntrc*, emphasizing HL, where WT plants, but not *ntrc*, appreciably reacted with strong adjustments, indicating an extensive key role of NTRC in regulating the proteome and thus maintaining beneficial cellular processes.

3.3.4 NTRC does act upon protein abundance, but not gene expression in the chloroplast, under high light

The results from PAM measurements and proteomics under HL were quite captivating, because they revealed the biggest effects compared to other light conditions. Following the previous approach, MapMan figures were generated to illustrate changes in general cell functions, focusing on *ntrc* under HL, relative to WT (**Figure 3.3.24 A**), as striking changes in other light conditions and genotypes were not observed (**Supplement Figure 5.3.13; Supplement Figure 5.3.14**). Again, the more ponderous bins were prioritized, containing the majority of proteins. *Redox processes* seemed to be slightly decreased, while higher levels in protein abundance related to *protein synthesis & amino acid activation* were noted. **Figure 3.3.24 B** draws a detailed picture of protein synthesis processes; here strong increments of protein abundance in every subcategory were seen, especially linked to ribosomes.

Taken all findings together, however, protein synthesis turned out to be not substantially altered, as the WT heavily down-regulated these processes under HL. In fact, a lack of NTRC is associated with an extensive restriction in dynamic acclimation responses on protein level towards all light intensities tested, which will be further elaborated later on.

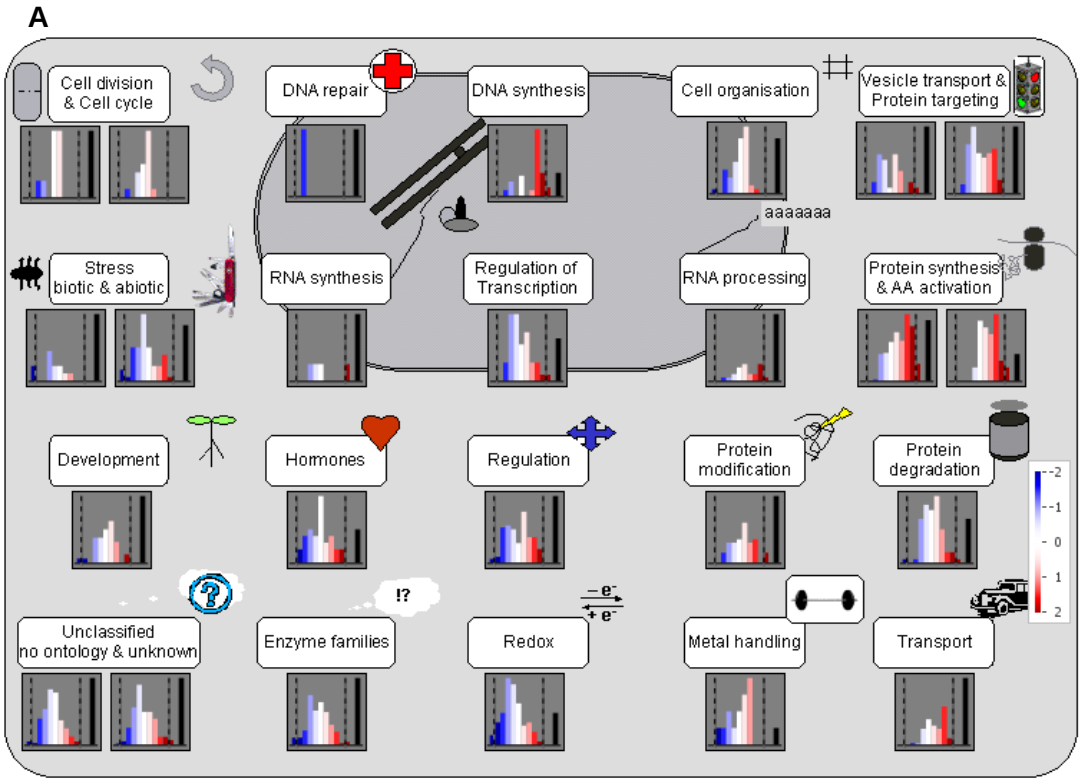

Figure 3.3.24. MapMan illustrations of changes in *ntrc* compared to WT under HL.
(A) Cell functions. (B) Protein synthesis. 1) RNA processing 2) RNA Transcription 3) Aminoacid activation 4) Ribosomal protein 5) Ribosome biogenesis 6) Protein synthesis – initiation 7) Protein synthesis – elongation 8) Protein synthesis – release 9) Protein targeting 10) Posttranslational modification 11) Protein degradation.
Relative abundances are shown as log2-fold changes ranging from -2 (blue) to 2 (red). White, no change; grey, not detected. Graphs were generated with MapMan.

Next, to critically compare if the findings from the proteomics aligned with gene expression, a targeted chloroplast ribosome profiling approach was used to quantitatively compare RNA abundance and translation output (Trösch et al., 2018). Plant material of *ntrc* was scarce so a new harvest had to be taken for the following experiment. Therefore, plants were grown for 3 weeks at a photoperiod of 16 h under ML (250 µmol photons m^{-2} s^{-1}) and one additional week under HL (900 µmol photons m^{-2} s^{-1}) (cf. chapter 2.2.1). After 4 weeks, WT and *ntrc* plants were sampled during the photoperiod. The day length and light-source differ from proteomics experiments but day length is according to the mentioned reference and is anyway more relevant in developmental- and particularly starch synthesis studies (Sulpice et al., 2009; Mugford et al., 2014) and in addition reduces the genotypic effect of NTRC disruption, showing a stronger phenotype under short-day conditions. Translation output and RNA levels were almost identical in *ntrc* and WT (**Figure 3.3.25 A** and **B**). A detailed analysis showed that the expression of individuals genes did not change more than 2-fold in the mutant compared to WT (**Supplement Figure 5.3.15**), which is considered insignificant.

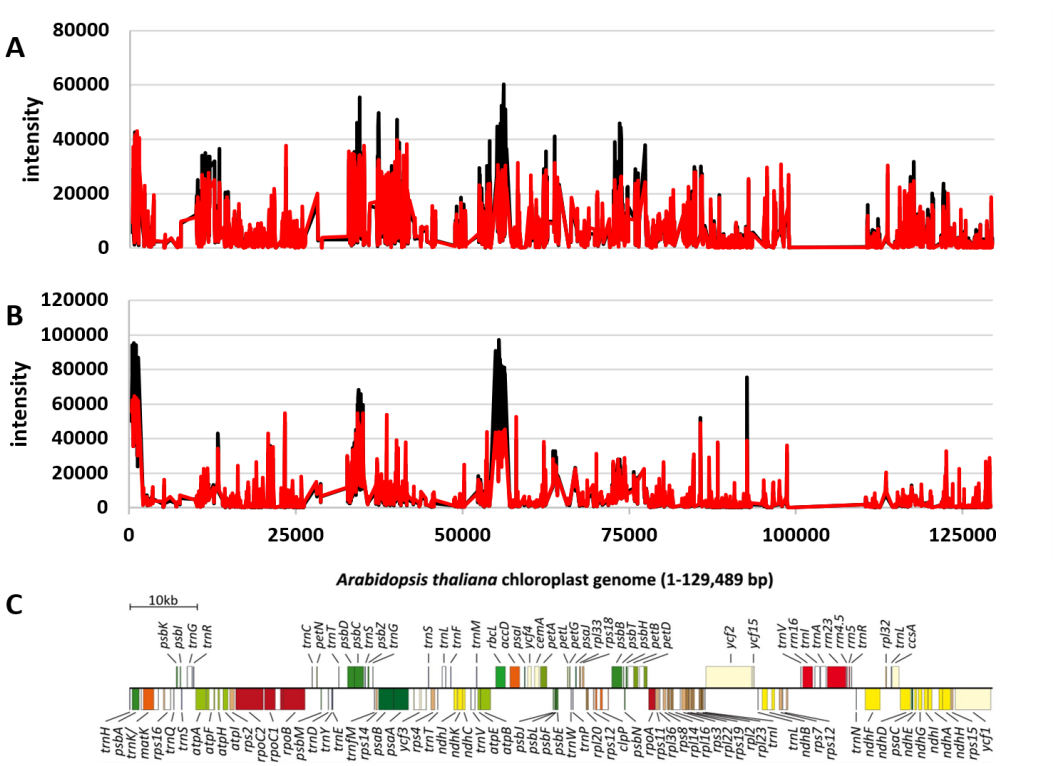

Figure 3.3.25. Changes in ribosome footprints and RNA levels in *ntrc* compared to WT under HL.
(A) Ribosome footprints. (B) RNA levels. (C) Full annotation of the *Arabidopsis* chloroplast genome aligned with (A) and (B). Plants were grown for 3 weeks at a photoperiod of 16 h under ML (250 µmol photons m^{-2} s^{-1}) and one additional week under HL (900 µmol photons m^{-2} s^{-1}). Values are the mean of n = 3 independent replicates. The x-axis represents the chloroplast genome in base pairs. Red, ntrc. Black, WT. bp, base pairs; kb, kilo base pairs.

Finally, network predictions of protein-protein interaction were performed. For this purpose, a list containing highly significant ($p < 0.001$) proteins changed in *ntrc* was created, relative to WT under HL, and NTRC itself was added as potential hub within this network (**Figure 3.3.26**). 8 out of 9 proteins were down-regulated, only Ferredoxin-dependent glutamate synthase (AT5G04140) was up-regulated, which was also previously up-regulated under both long-day and short-day in *ntrc*, relative to WT (Lepistö et al., 2009). Other direct interaction partners according to this analysis were malate dehydrogenase (AT3G15020), an important factor in the TCA cycle, and CBS domain-containing protein (AT4G34120), the above-mentioned redox regulator (cf. chapter 3.3.3.4) that was highly significantly down-regulated in ML, HL and LL, and lastly superoxide dismutase (AT4G25100), important in light responses; all of them are either found in plastids or mitochondria.

In summary, it could be seen that NTRC might be a small hub in the WT, connecting carbon and nitrogen metabolism as well as redox- and radical-quenching enzymes in different compartments. Moreover, NTRC might negatively regulate *protein synthesis and amino acid activation* in HL, relative to WT, as a trade-off for other processes (e.g. *redox*). On the whole however, the findings imply that NTRC deficiency entails complete loss of dynamic proteomic acclimation responses to all investigated light conditions. Furthermore, it has little to no effect on gene expression in the chloroplast, which is underlined by **Table 3.3.4**, summarizing that differentially expressed ribosomal subunits are over-represented in the cytosol ($p < 0.0006$, Fisher's exact Test).

Table 3.3.4 Number of differentially expressed (at least 1.5-fold) ribosomal subunits in different compartments in *ntrc* under HL, compared WT.
According to MapMan Bin 29.2.1.

	chloroplast	**cytosol**
down-regulated	9	7
up-regulated	18	102

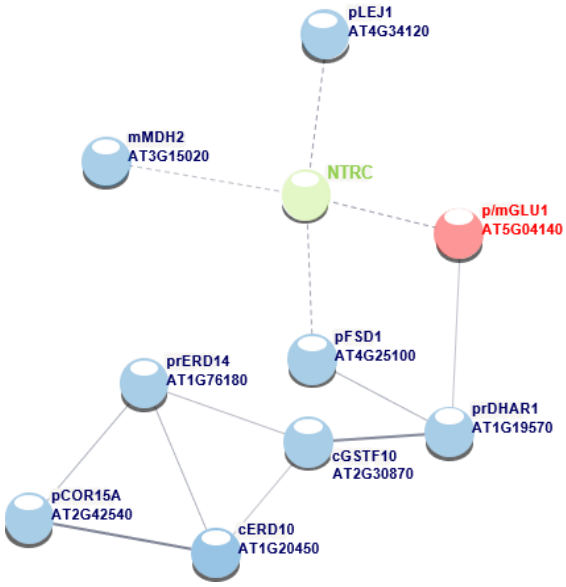

Figure 3.3.26. Network predictions of protein-protein interaction under HL.
The nodes represent NTRC among the significantly changed ($p < 0.001$, repeated t-test with Benjamini-Hochberg correction) proteins in *ntrc*, relative to WT. Down-regulated proteins are given in blue, up-regulated in red. Unconnected nodes were disregarded. The thickness of the edges indicates the degree of confidence of the interaction (Szklarczyk et al., 2019, 2021). Dashed lines indicate an interaction in the WT in the presence of NTRC. Distances are arbitrary. Trivial names are given in capital letters. The subcellular location (SUBA4, consensus) is given in small letters ahead the protein name. c, cytosol; m, mitochondrion; p, plastid; pr, peroxisome.

3.3.5 Redundancy within the Thioredoxin system plays a subordinate role

Supplement Figure 5.3.12 helps to clarify the question of redundancy within the thioredoxin protein family. TRX*m2* was strongly down-regulated in *trxm*. TRX*m4*, the only other detected *m*-isoform, was mostly up-regulated, but its expression was not significantly altered to hypothetically compensate for loss of TRX*m1* or TRX*m2*. TRX*f*1 as well as TRX*f*2 remained largely undetected (ML, FL and HL); under LL, expression of TRX*f*2 was not altered after loss of TRX*f*1, indication no compensatory role. The cytosolic isoform TRX*h*5, responsible for plant immunity (Jedelská et al., 2020), was significantly down-regulated in *trxm* and *ntrc* under HL. Thus, regarding the TRX protein family, there was some extra-plastidial change and potential co-regulation detectable, but not within the chloroplast.

In general, however, patterns of co-regulation or compensation, if any, reside within one light condition only and are found to be of little to no significance.

3.3.6 Total protein content is not affected by Thioredoxin and NTRC deficiencies

Lastly, total protein content according to Bradford (cf. chapter 2.2.2.1) was measured to complement and evaluate the metabolomics and proteomics data. Protein content was not significantly affected in the mutants compared to the respective WT in each light condition (**Figure 3.3.27**). Compared to other conditions, HL acclimated plants exhibited the highest protein contents. This shows that mechanisms regulating the turnover of protein synthesis and degradation are still intact under given light environments and practically independent from thiol-redox control, although a small tendency towards a decline in *ntrc*, compared to the other genotypes, was noticed.

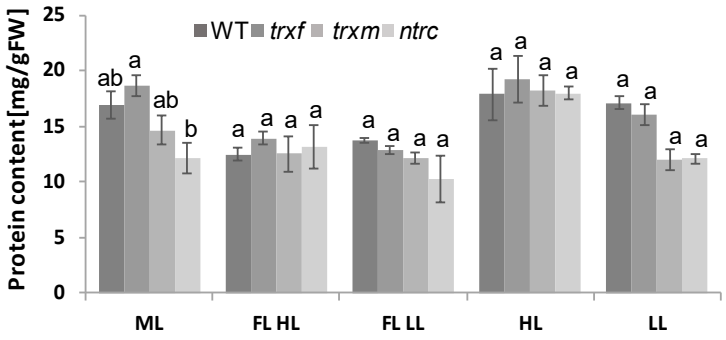

Figure 3.3.27. Changes in protein content in fully adapted WT, *trxf*, *trxm* and *ntrc* grown under different light conditions.
Samples were taken in the middle of the photoperiod. Values are shown as mean ± SE, n=3-5 biological replicates. Significance levels within one condition were evaluated by using a two-way ANOVA with a *post-hoc* Tukey test ($p < 0.05$) and are labelled with different letters. FW, fresh-weight.

4 Discussion

The objective of the present work was to investigate the *in vivo* roles of TRX*f*1, TRX*m*1 & *m*2 and NTRC in *Arabidopsis thaliana* in acclimation to various light regimes. Different light stimuli were applied, including various photoperiods, light intensities, discriminating between constant und fluctuating light regimes, and acclimation periods. The results showed that photosynthetic performance was mostly unaffected by TRX and NTRC deficiency when plants were shifted between ML to HL on a time scale of hours, while in *ntrc* the *a priori* severe phenotype deteriorated when mutants were acclimated for several days to FL or HL. Disruption of NTRC further resulted in a detrimental loss of metabolic and proteomic plasticity, revealing a key role of NTRC in photosynthesis and global cellular processes, especially under HL and FL, while a subordinate role of TRX*f* and TRX*m* in the long-term adaption to various light conditions was proposed. Moreover, the pivotal role of TRX*f* and NTRC in regulating the CBC has been highlighted as well. In the following, the results will be discussed in the context of pre-existing knowledge about thiol-redox biology, metabolism and photosynthesis.

4.1 Thioredoxins and NTRC marginally, but disparately, regulate cellular responses after short-term high light treatment

The kinetics experiments under HL served to elucidate the effects of TRXs and NTRC on photosynthesis and metabolism when facing fast changing environments (minutes to hours), thus untangling the *in vivo* roles of TRXs and NTRC in short-term HL acclimation (stimulation with stress) and de-acclimation (returning from stress to control conditions). The mode of action (i.e. enzyme activation) of the TRX system is based on ultra-short redox reactions and should therefore reveal a significant short-term role of TRXs and NTRC in dynamic photosynthesis, which has been demonstrated before (Naranjo, Diaz-Espejo, et al., 2016; Naranjo, Mignée, et al., 2016; Thormählen et al., 2013, 2015, 2017).

4.1.1 Thioredoxins and NTRC fine-tune photosynthesis

Our results showed that TRXs and NTRC modulate photosynthesis in dark-adapted plants (cf. chapter 3.1.1), thus agreeing with previous observations. TRXs and NTRC are needed to activate enzymes in the thylakoid membrane and the CBC, explaining

the initial retardation in photochemistry when coming from the dark (**Figure 3.1.1**). However, once stable, this modulation did not occur when plants were challenged with light-light switches between ML and HL, hence being a novel observation. This leads to the hypothesis that under given conditions, TRXs and NTRC, if at all, regulate the fine-tuning of photosynthesis upon light-light transitions, being in strong contrast to the necessary and well-known light-activation of photosynthesis after prolonged darkness.

4.1.2 Thioredoxin influence on STN7 activity is unlikely

The state transition kinase STN7, mediating the phosphorylation of LHCB2, is especially active under LL and PSII favoring light, while reducing PQ (Bellafiore et al., 2005). However, under HL, PQ is also reduced. This theoretically leads to a transition from photosynthetic *state 1* to photosynthetic *state 2*. This transition was not recorded in our experiments; we noticed a shift to *state 2* in all genotypes after the light was switched from HL to ML again (**Figure 3.1.11**), confirming STN7 to be more active under moderate levels of light. Therefore, the TRX and NTRC involvement in state transition under given conditions is, if at all, very marginal and not significantly different from WT. Furthermore, it was thought that under different PQ states, despite the difference in timescale between LHCII phosphorylation and transcriptional regulation, the latter being a long-term adjustment of photosystem complexes to counteract excitation imbalances, there might be a coupling revealed between short-term and long-term responses, using redox deficient mutants to modulate PQ (Rintamäki et al., 2000; Bonardi et al., 2005; Dietzel et al., 2008; Wagner et al., 2008; Rochaix, 2013). Following different approaches to prove a potential thioredoxin-dependent regulation in LHCII phosphorylation (Wunder et al., 2013; Ancín et al., 2019), our data does not support this hypothesis in the current state.

4.1.3 NTRC is a key regulator of central- and CBC metabolism

Figure 4.1.1 gives an easy-to-follow overview of changes in both central metabolism and CBC. It becomes evident, that starting from t_0, the HL treatment induces upward changes in central metabolism. However genotypic changes are not so apparent as the median of most curves is close to zero. On the other side the changes in the CBC after short-term HL appear in less bell-shaped curves with more asymptotic tails skewing to either left (down-regulation) or right (up-regulation), while a clear up-regulation has been noticed under HL. That implies that the CBC is generally affected under HL and redox deficiencies explicitly modulate certain metabolic responses on top. Especially

trxm and *ntrc* exhibited a flattened curve after turning off HL, indicating drastic changes in their metabolic states. It is thinkable that the central metabolism could act as a buffer for changes in cell homeostasis (Mettler et al., 2014). **Supplement Figure 5.1.4** for ML control can be directly compared as all samples were standardized concurrently leaving the t_0 time point fixed. What exact metabolites might be responsible for these adjustments is going to be discussed later on.

Instead of using predefined pathway analyses for our kinetics, which, on one hand, would be quite challenging with a number of time points and at that uneasy to comprehend, and on the other hand be limited by the number of metabolites detected, one first concentrated on the effects of metabolite classes in acclimation using data-reduction techniques (PCA) and correlation analysis; beyond that, it was attempted to circumvent this potential bias (Wanichthanarak et al., 2015), leading to a new approach by combining CBC – a rather exclusive analysis in the plant science field – and central metabolism with chloroplast PTM data regarding light-harvesting proteins (LHCB2 phosphorylation). This captures the purport of an integrative (systems) biology, using multiple measures trying to understand and predict biological phenomena. Summarized, sugars, organic acids and the LHCB2 abundance did not correlate with the phosphorylated form of LHCB2 (**Figure 3.1.12**). Intriguingly, CBC metabolites close to RuBisCo (Ru5P+Xu5P, RuBP, 2PG, DHAP) were significantly negatively correlated, indicating that an unprecedented relationship between chloroplast stroma metabolites and thylakoid PTM procured in the process of state transition. This result preliminarily indicates an inverse link between CBC/RuBisCo and LHCB2 phosphorylation. However, a TRX involvement could not be deduced from our data. Lastly, aspartate was shown to be positively correlated with P-LHCB; being responsible for plant nutrition and energy, stress response and as nitrogen carrier (Han et al., 2021), the role of aspartate in the present case still remains unclear.

The PCAs showed no outstanding differences between WT and the mutants regarding the GC-MS based central metabolite profile (**Figure 3.1.8; Figure 3.1.9**). The treated samples separated from the control groups as expected. Only the acclimation phase revealed a key role of sugars in the early time points (15 min – 1 h) in all genotypes. This makes sense since the early buildup of sugars is the prime step for further growth-related processes when energy is abundantly available. Regarding CBC metabolites, the lack of TRX*f* and NTRC led to distinct clustering of groups, validating a key role in regulating the CBC. This became also apparent, constructing a simplified model of the CBC, indicating significantly regulated metabolites (**Figure 3.1.5**). It showed, that an over-accumulation of intermediates in the regeneration phase might cause imbalances

in the whole cycle leading to a down-regulation in the fixation and reductive part. What is more, is that besides SBP, S7P and R5P are also up-regulated while RuBP is down-regulated in *ntrc*, allowing to conclude, that redox-activated phosphoribulokinase, converting R5P to RuBP, might be an additional bottleneck where the CBC is hampered (Marri et al., 2009, 2014; Nikkanen et al., 2016). Lastly, it was determined to some degree, if the HL treatment was reversible in the different genotypes. It turned out, that the HL and ML samples were fairly matching after 6h in WT and *trxm*, but not in *trxf* and *ntrc* (**Figure 3.1.7**), further indicating important roles of TRX*f* and NTRC in CBC regulation.

Deriving correlations within metabolites from PCA is not sufficient as i) only metabolites explaining the most variance were included to prevent over-plotting and ii) the genotypic effect can be ambiguous due to the dimension reduction, so additional correlation analyses were performed with the entire data set counting in all time points (**Figure 3.1.13**). The aim here was to reveal highly stable metabolic hubs and pathways, that are not influenced by light, time or redox regulation. Moreover, pooling samples of WT with or without mutant samples supports this approach and additionally reveals genotypic specifics, respectively. However, sophisticated methods for a deeper readout are still lacking to this point, so only a few observations could be made: expected correlations of some CBC intermediates and closely linked metabolites, like leucine and isoleucine or glucose and fructose, were detected. Furthermore, a major advantage was derived from the fact, that GC-MS based central metabolites and LC-MS based CBC metabolites were analyzed together, as they merged to interesting clusters. For instance, pyruvate positively correlated with 3PGA, DHAP, 2PG and S7P, where no inter-correlation could be determined. Phenylalanine also correlated with DHAP, S7P, F6P and pyruvate. G1P showed the most correlations with both CBC and central metabolites (positive: FBP, G6P, R5P, SBP, F6P, S7P, pyroglutamate and glutamine; negative: succinate), building the bridge between the CBC and starch/sucrose synthesis as substrate for AGPase. Aspartate was among the very few metabolites that negatively correlated with plenty of other metabolites, including the CBC (benzoic acid, glycerol, lysine, tyrosine, isoleucine, leucine, hydroxy proline, Ru5P+Xu5P, RuBP, DHAP, 2PG and S7P). Apart from known roles in nitrogen assimilation and as precursor for several other amino acids, the role of aspartate yet remains unclear. The correlated data have to be handled with care though, as fewer time points were originally considered for the CBC compared to the central metabolites. This and the fact, that LC- and GC-MS systems might exhibit different characteristics affecting the output (Stitt & Fernie,

2003), may have also led to different clustering of aspartate (LC-MS) and aspartic acid (GC-MS), although the original expression pattern was very similar.

Performing the same analysis without *ntrc* samples was hoped to identify potential NTRC-dependent targets in short-term (de-)acclimation to HL (**Supplement Figure 5.1.5**). However, there were no striking differences detected, meaning all before-mentioned observations including all genotypes were pretty much intact. Nonetheless, taking several other analyses additionally into account (**Figure 3.1.13**; **Figure 3.1.8; Supplement Figure 5.1.1**), a strong correlation of the sugars fructose, glucose, maltose and sucrose in WT, *trxf* and *trmx* were found over the entire time course in both HL and control plants. This correlation is disturbed in *ntrc* treated with HL, giving hints to NTRC regulating carbohydrate interconversion in environments, where short-termed, high levels of light-energy are available. This hypothesis is supported by measurements, showing a strong fluctuating starch turnover in *ntrc* (**Figure 3.1.10**). This phenomenon generally seemed to be more distinct in the mutants than in WT, latter one showing a rising, but stable level of starch, possibly preparing for the night-time to feed on starch reserves that had been build up during the day. However, one must say that meaningful starch studies make particularly sense in short-day conditions (e.g. 8 h light/ 16 h dark, compared to the present condition: 16 h light/ 8 h dark), when plants are forced to produce even more starch during the light-period for a prolonged dark-period (Sulpice et al., 2014). This could be the reason why no significant differences between *ntrc* and WT were found within each light condition under long-day, other than under short-day (Thormählen et al., 2015). Anyway, the findings still indicate that plants lacking chloroplast thiol-redox regulation, run another strategy than WT plants to coordinate the rate of photosynthesis and partitioning of end-product synthesis, which is important, as altering the allocation of amino acids, sugars and starch affects the rate of growth (Heyneke & Fernie, 2018). This strategy could be due to a higher active carbon metabolism in plants growing under long-day periods, including also a higher starch degradation capacity (Seaton et al., 2018). As there is evidence for starch degradation even in illuminated plants (Baslam et al., 2017), thiol-redox deficient plants might follow this strategy to produce energy and reducing equivalents for growth (Seaton et al., 2018); however, maltose levels do not really support this idea (**Supplement Figure 5.1.1**). Another hypothesis could be that exactly under long-day conditions, combined with HL, the regulatory properties of the key enzyme in starch synthesis (AGPase) are differentially changed (Seaton et al., 2018). Lastly, the phenotypic appearance of at least *trxf* and *trxm* did not allow the conclusion of a bigger

impact of a fluctuating starch metabolism. If these plant lines started into the night with a lower starch reserve, one could determine the levels and rate of starch and its degradation by sampling throughout the night to get a fuller picture.

Lastly, alternative carbon storage compounds like fumarate increased during HL but were also lowered in *ntrc* compared to WT (**Supplement Figure 5.1.1**), thus providing only a limiting source of carbon for growth and recovery under HL (Chia et al., 2000; Obata & Fernie, 2012; Garcia-Molina et al., 2020); a further observed disturbance in compatible solutes like putrescine (Akula et al., 2019) and galactinol and myo-inositol, that were shown to accumulate under HL (Garcia-Molina et al., 2020), might provoke additional osmotic stress on already affected NTRC KO plants. Interestingly, levels of glycerol were almost unchanged in *ntrc* compared to WT, and even increased after the HL phase, which could suggest an increased lipid metabolism, maybe to satisfy energy needs in sugar deprived mutant plants.

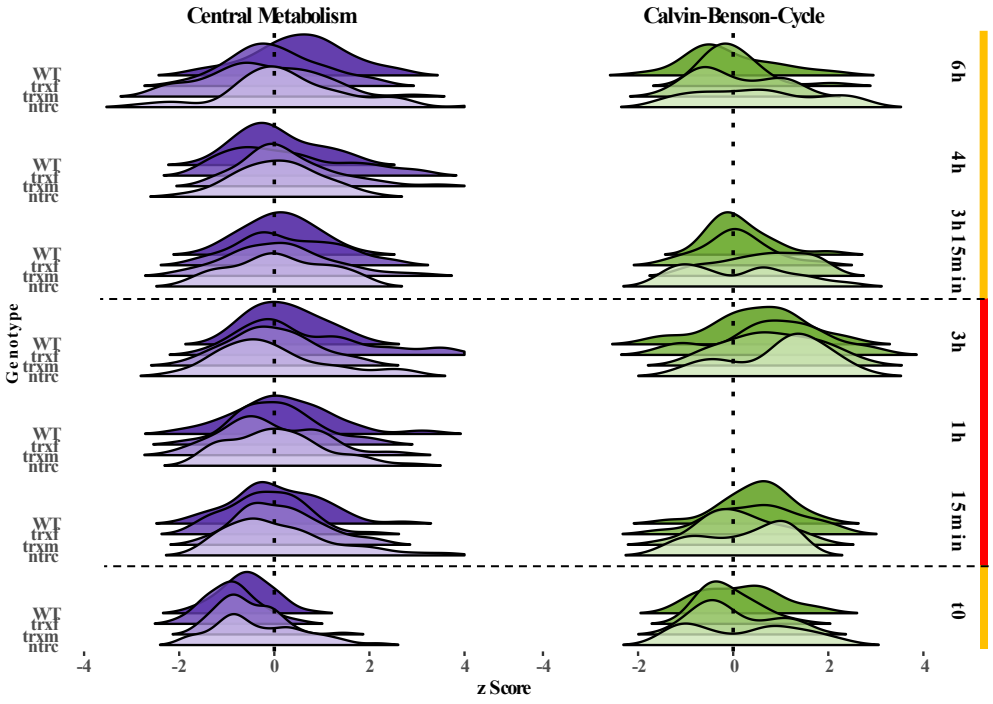

Figure 4.1.1. Time-resolved metabolic changes and distribution during HL acclimation (15 min – 3 h) and de-acclimation (3 h 15 min – 6 h).
HL and ML (**Supplement Figure 5.1.4**) samples were scaled together to directly compare changes starting from t0 (ML). Red bar, HL (450 µmol photons m^{-2} s^{-1}); orange bar, ML (85 µmol photons m^{-2} s^{-1}).

4.1.4 Redox regulation affects all compound classes

Next, a comprehensive study performing analysis of variance (ANOVA) tests was applied to ascertain significances within the large metabolomic output that was gathered. First, single metabolites were tested for significance, relative to WT. GABA and glycerate were found to be of importance in the de-acclimation phase in all mutants. Little is known about the glycerate pathway (Igamberdiev & Kleczkowski, 2018), however many glycerate derivates are connected to serine and photorespiration, glycolysis and fermentation. Being synthesized from glutamate, GABA is an important signaling molecule in response to various plant stresses, in modulating photosynthesis, and acting as a bypass for the TCA cycle in the GABA shunt (Li et al., 2021). Thereby, GABA functions as nitrogen storage, with a low abundance possibly expressing a nitrogen crisis, especially in *ntrc*. The biomarker analyses (cf. chapter 3.1.2) support the available data for GABA and glycerate being striking candidates for further research in conjunction with NTRC. Beta-alanine and threonine were significantly changed in *ntrc* at different time points. As a non-proteinogenic amino acid, beta-alanine is a generic stress response molecule and plays a role in the pantothenate (vitamin B5) pathway (Parthasarathy et al., 2019). However, since isoleucine and valine were not significantly altered, this pathway may not be affected in *ntrc*. The up-regulation mostly reflects stress the plant is experiencing when NTRC is knocked out. Threonine serves as precursor for branched-chain amino acids, that constitute important building blocks for proteins (Joshi et al., 2010), therefore in the human diet as well; changes in the equilibrium of these amino acids have only been reported for abiotic stresses excluding light so far, so a deeper understanding in our case is still missing.

The second analysis (**Table 4.1.1**) however, shows the summary of a linear model. This very simple model tries to predict metabolic output (response) based on genotype and acclimation (predictors) in an additive manner (*response* ~ *genotype* + *acclimation*), assuming the predictors are independent (Gareth et al., 2014). However, variables are seldomly independent, so that we can speak of an (additional) synergy or interaction effect. This can be expressed by *response* ~ *genotype* × *acclimation*. In other words, a change in *genotype* results in a change in *acclimation*, and vice versa. For the analysis, metabolites within single compound classes (amino acids, organic acids and sugars for central metabolism; phosphorylated metabolites for CBC) were pooled, as simplification and because these classes comprise a major part of the metabolites analyzed and thereby explain most of the variance. The creation of a formula including coefficients

was disregarded. Instead, we focused on *p* values describing the significance of each predictor. Single time points were pooled to the respective acclimation phase (acclimation or de-acclimation), which are constituted as *acclimation* in **Table 4.1.1**. Firstly, the statistical output revealed a constant acclimation effect under ML for every class of metabolites. This effect seemed not much different from HL. The genotypic effect receded under HL compared to ML, confirmed previous analyses. There was no interaction effect (*genotype* × *acclimation*) observed. This can be interpreted as follows: light phases were perceived be all genotypes, but responded to in mostly different ways. The striking genotypic effect in organic acids for example could be explained by their excessive down-regulation in *ntrc*. Although other models might be superior to represent the current data, our simple model is supported by similar results performing a 3-way ANOVA, with light as a third factor (**Supplement Table 5.1.1**).

Table 4.1.1 Summary of ANOVA based of linear regression model (response ~ genotype × acclimation) involving central metabolism and Calvin-Benson-Cycle metabolites.
Results are shown as *p* values. Significances ($p < 0.05$) are shown in bold. The analysis was done separately for HL and ML.

HL	amino acids	organic acids	sugar	Calvin-Benson-Cycle
Genotype	5.36×10^{-01}	**3.46×10^{-04}**	**1.51×10^{-02}**	8.48×10^{-01}
Acclimation	**1.36×10^{-03}**	**5.77×10^{-09}**	6.24×10^{-02}	**5.05×10^{-03}**
Interaction	2.68×10^{-01}	2.96×10^{-01}	2.49×10^{-01}	3.24×10^{-01}
ML				
Genotype	**3.96×10^{-03}**	**1.10×10^{-03}**	7.00×10^{-01}	**3.66×10^{-02}**
Acclimation	**1.95×10^{-02}**	**2.03×10^{-02}**	**4.64×10^{-02}**	**2.45×10^{-04}**
Interaction	4.27×10^{-01}	6.86×10^{-01}	3.34×10^{-01}	9.44×10^{-01}

4.2 Acclimation to fluctuating light takes several days

Regarding photosynthetic acclimation, little was known about the time frame of light acclimation in plants with or without thiol-redox regulation, which is an important prerequisite for further studies dealing with acclimation to dissect the short-term and long-term responses. In the previous chapter (cf. chapter 3.1), shorter term effects on photosynthesis in the mutants were investigated, responding to quick dark/light changes or changes between HL and ML in the range of minutes to hours. Fluctuating light comprises a more natural light source, simulating sun- and light-flecks or moving canopies shading leaves on lower leaf levels, and is nowadays a favored stimulus to test plant physiology and acclimation responses (Alter et al., 2012; Grieco et al., 2012; Armbruster et al., 2016; Kaiser et al., 2017; Thormählen et al., 2017;

Slattery et al., 2018; Schneider et al., 2019). To start simple, plants were grown in the lab scale in a controlled environment for optimal reproducibility allowing to draw coherent and unambiguous conclusions about acclimation mechanisms. Here we wanted to precisely document the progressive adjustment of WT to FL, on the scale of hours to days, and the respective roles of TRX*f*1, TRX*m*1*m*2 and NTRC in acclimation to FL by measuring photosynthesis via chlorophyll fluorescence.

Thormählen et al. (2017) showed that TRXs *m*1 and *m*2 as well as NTRC are both indispensable for photosynthetic acclimation in fluctuating light. However, measuring PSII performance, this experiment was amended by i) increasing the measuring frequency, ii) adding *trxf* as novel target and iii) looking specifically at the individual operating parameters of chlorophyll fluorescence of light adapted plants (F', Fm', Fo') under rapid fluctuations, to calculate Φ II, NPQ, which is tightly correlated to stress (Guadagno et al., 2018), and the redox-state of PQ, that is – different to NPQ – important for the LTR (Wagner et al., 2008; Bräutigam et al., 2009). Our results showed, that the short-term acclimation (starting-time t_0 to 3 days) appeared to be a sequential process, whereby an increase in Φ II during the HL phase and a decrease during LL in all genotypes was observed, except in *ntrc*. Regarding the transitions from the LL to HL phase of FL, it appears that TRX*f* and TRX*m* might have overlapping yet distinct functions in priming and stabilizing Φ II in the course from t_0 to 3 days after the shift from ML to FL. Coming from HL to the LL phase, TRX*m* seemed to negatively regulate Φ II and PQ reduction (cf. chapter 3.3.1 for similar results). PQ reduction peaked and stabilized already after 3 days in *ntrc*, pinpointing to a premature steady state in acclimation, compared to WT. This can be interpreted as an incipient inhibition effect. We concluded that stunted growth and inhibition effects due to NTRC deficiency might disrupt early acclimation responses to FL, making NTRC a compelling integrator of cell signals governing early light acclimation. All in all, our observations in longer-term acclimated plants (3 days to 7 days) were quite consistent with findings of Thormählen et al., 2017, showing a decrease in Φ II in *ntrc* due to over-accumulation of electrons in the photosynthetic chain (increased PQ reduction) (**Figure 3.2.1**). We also saw the same increase in Φ II in *trxm* during the HL subsequent LL phases. Further, a novel short-lived fluctuation of Φ II in all mutants during that very light cycle was noticed, which may be due to the illumination with a lower average light intensity. These fluctuations, however, seemed not to disrupt further quantum efficiency. Walters & Horton (1994) showed, that following a transition from HL to LL, changes in Fv/Fm were largely complete within 3-4 days. From our data we concluded

that acclimation to FL takes at least 4 days in the WT and that NTRC might constitute an early and central hub to ensure the full range of dynamic acclimation towards FL.

4.3 Thioredoxin *m* and NTRC are key protagonists for the long-term response to changing light environments

In the last part of the results (cf. chapter 3.3), acclimation responses in WT and TRX mutants were investigated, when dealing with longer-term light shifts from ML to either HL, LL or FL, to primarily monitor changes in photosynthesis, metabolite pools and protein abundances and therefore infer the respective *in vivo* roles of TRX*f*, TRX*m* and NTRC in response to changing light regimes. As a consequence, we would further elicit the role of the prevailing LL intensity in FL (Morales & Kaiser, 2020) and were able to directly compare Φ II of ML and FL grown plants, because of measuring them under the same average light intensity. The robustness and reproducibility of the GC-MS protocol (Lisec et al., 2006; Obata & Fernie, 2012) allows for perfect comparison of short- (cf. chapter 3.1 & 4.1) and long-term (cf. chapter 3.3 & 4.3) effects within present work. Moreover, light intensities were higher, compared to the previous chapters. Although reports described a limit for beneficial photosynthetic active radiation, being destructive or inhibitory when in excess (Bailey et al., 2004; Garcia-Molina et al., 2020), growth and treatment lights were chosen that still guaranteed observable and beneficial growth and acclimation responses in WT (Walters, 2005; Thormählen et al., 2017).

4.3.1 Photosynthesis is affected by NTRC and Thioredoxin *m*, but not Thioredoxin *f*

Determining Fv/Fm as a measure of acclimation capability, Thormählen et al. (2017) revealed a recovery in WT after shift from ML to FL after 10-day period, while Fv/Fm was found to be continuously lower under HL. Acclimation of *trxm* was mostly WT-like in FL. In HL, both *trxm* and *ntrc* showed a from WT significant different acclimation response. Our study revealed no potential photo-inhibition of PSII under ML, LL and FL in all genotypes, except for *ntrc*, which seemed to be unable to fully acclimate to FL, thus being in line with the above-mentioned study. All genotypes showed a lower Fv/Fm under HL, that did not recovery to starting values after 10 days. We concluded that *ntrc* failed to acclimate to both FL and HL, being more severely affected by the latter one than previously shown. TRX*f* and TRX*m* were shown to be of minor or no importance in stabilizing Fv/Fm.

Comparing photosynthetic performance and quenching parameters (Φ II, NPQ) as well as the PQ redox states in ML and FL acclimated plants (**Figure 3.3.5**), we found out, that i) there is some form of LTR in FL acclimated plants, ii) this response is specific for TRX*m*, but not TRX*f*, and iii) most profound in NTRC deficient plants. Further, changes in the mutants after HL adaption pointed to a similar significance of the redox system compared to FL acclimation. As already seen, the reduction of PQ in *ntrc* increased when FL adapted, leading to a severe electron accumulation within the electron transport chain (ETC). Electrons not used for photochemistry and being uncontrollably quenched act harmful on PSII (Eberhard et al., 2008). Although controlled quenching (NPQ) is not involved in acclimation, it becomes more important with increasing light intensities to fully dissipate excess energy as heat (Wagner et al., 2008), meaning *ntrc* is likewise increasingly affected by photo-inhibition. In FL acclimated plants, the HL phase of FL seemed to lead to an impaired relaxation of NPQ in the following LL phase in all genotypes; however, NTRC seemed not to play a role in NPQ during this HL phase. Although they showed an elevated baseline *a priori*, NPQ still significantly increased in HL acclimated *ntrc* mutant plants, supposing the need for NTRC in fast energy-quenching under HL. In addition, NPQ kinetics, including relaxation, generally worked as expected in HL acclimated plants, compared to FL for example. Most considerably, all genotypes except *ntrc* could keep up an overall high rate of Φ II, indicating a role of NTRC in maintaining beneficial PSII photochemistry and balanced energy-quenching especially in irradiances limiting photosynthesis (i.e. FL and HL) (Guinea Diaz et al., 2020). PQ redox states in *trxm* were more oxidized in ML, FL and HL, relative to WT, presumably leading to an efficient photosynthetic flow as recorded, especially in FL. We concluded that TRX*m* might act as a negative regulator of photosynthesis in FL, while its influence is limited to the light-reactions, as these ostensible improvements in the mutant did not influence sugar and starch levels (**Supplement Figure 5.3.3**) or growth (cf. chapter 3.3.1). Finally, levels of Φ II in the LL phase of LL grown plants were higher than of those grown under FL and even higher when HL acclimated; Φ II during the HL phases was comparable (low) among the different conditions. Taken together, this means that constant HL acclimation primes the plants to yield a better quantum efficiency at least under short-term fluctuations. Lastly, since acclimation to FL, HL or LL yield different photosynthesis phenotypes, the role of the prevailing low background light intensity cannot be explicitly concluded (Morales & Kaiser, 2020). Regarding the differences in duration of the HL and LL phases of FL, respectively (1 min HL, 4 or 5 min LL; cf. chapter 3.2 &

3.3), we could not observe striking differences in acclimation responses, further questioning the impact of the LL phase in FL (Morales & Kaiser, 2020).

ETR measurements showed, that WT plants operate on different levels to cope with various light stresses; a limitation at higher intensities in LL grown plants was obvious, because the existing proteome cannot sustain high energy fluxes (Mettler et al., 2014), most probably due to downwards adjustment of light-harvesting and -processing mechanisms; HL plants on the other side showed an increased tolerance to both HL and LL. The results further elucidated the distinct roles of TRXs and NTRC in regulating accurate ETR; whereas there were only subtle changes in *trxf* and *trxm* compared to WT, NTRC is needed to fully activate proper electron flow in both low and high actinic light when pre-exposed to either ML, FL, HL or LL. In summary, NTRC appears to be a key component in effective ETR in all light regimes tested, while ETR is regulated with very little TRX involvement.

4.3.2 Thioredoxin *m* and NTRC modulate the metabolome and proteome

A lot of metabolic studies in plants focus on abiotic factors like salt stress or drought and spared experiments on light as external stimulus (Carrera et al., 2021). We followed a different research rationale by studying the long-term acclimation responses of WT and thiol-redox-deficient plants to various light regimes, altering light intensities, and examining the metabolome and proteome, being closest to the phenotype than the genome or transcriptome (Hollywood et al., 2006). Moreover, specific metabolites can control enzyme redox-states and consequently activities and therefore lead local metabolite pools and fluxes into a newly adjusted steady state (Knuesting & Scheibe, 2018). Further, as outlined in the introduction, system-wide analyses are useful to break down acclimation processes and to concurrently ensure that prospective, targeted modifications, that make particularly sense in longer-term acclimated plants, occur with minimal trade-offs (Garcia-Molina et al., 2020).

Redox signaling downstream of PSI (NAPDH, thioredoxins, sugars etc.) is considered to transport information to the nucleus (retrograde signaling), triggering short- and long-term cell responses; thus, it is relatively obvious to thoroughly investigate these "primary signals" in a redox-compromised background (Dietz, 2015). Metabolic adjustments can hereby be considered as low to moderate acclimation responses. Greater imbalances in ROS, ascorbate or phytohormone levels could lead to more severe consequences such as cell death. Although metabolite changes in *ntrc* appeared to be quite extreme with no adverse consequences whatsoever, even under challenging light

conditions, metabolite levels of *trxm* and especially *trxf* were nearly WT-like in all conditions. These changes are going to be discussed in the following.

4.3.2.1 NTRC controls carbon and nitrogen metabolism

According to the above mentioned, we found large overlappings between WT and TRX*f* and TRX*m* deficient plants, but metabolic difference increased when knocking out NTRC (**Figure 3.3.7**). To begin with, nicotinic acid, which is part of the NAD(P) biosynthesis pathway (Pollak et al., 2007), and glycerol appeared to be of more importance in this mutant. The heat map analysis (**Figure 3.3.8**; **Supplement Figure 5.3.1**) indeed revealed elevated nicotinic acid and glycerol levels; latter could imply an elevated lipid metabolism due to a diminished sugar metabolism. Since the levels of both metabolites are significantly increased in almost every condition, it could also mean that NTRC might be involved in their regulation. In fact, research on NTRC and lipid metabolism is most widely missing.

The heat map and distribution analyses serve as representation for mean value comparisons; together with statistics (cf. chapter 5.4) they are powerful tools to detect important metabolic hubs in the context of light-dependent redox regulation. The results clearly showed a profound impact of NTRC in central metabolism in every light regime, disrupting an else sturdy carbon and nitrogen metabolism. The ponderous overall down-regulation of amino acids in every light regime, including important progenitor compounds and biomarkers for nitrogen like glutamine, aspartate and asparagine (Hildebrandt et al., 2015; Han et al., 2021), uncovered a systemic failure to build up a multitude of subsequent amino acids when NTRC is lacking. Further, 48 out of 59 central metabolites were significantly affected in HL. It is supposed that the metabolism already compromised in control conditions in *ntrc* is even exacerbated under HL. Interestingly, but not surprisingly, protein content was not significantly affected in *ntrc* relative to WT (**Figure 3.3.27**), as this would imply serious trouble for the plant to survive. However, we concluded, that protein turnover then might be stabilized by depleting the remaining pool of free amino acids, which was certainly detected (**Figure 3.3.8**), to satisfy the needs of a beneficial homeostasis. Although *ntrc* was shown to have normal energy-state levels (Thormählen et al., 2015), an inter-conversion of amino acids is more likely than costly and novel biosynthesis, also considering the deficit in precursor compounds. At the last, comparing the role of NTRC in leaf tissue and developing fruit metabolism, where amino acids are down- and up-regulated, respectively, seem to be highly distinct (Hou et al., 2019).

Regarding the CBC, which is tightly linked to the light reactions, acclimation to LL had no deteriorating effect on *ntrc*, compared to *ntrc* under ML whereby metabolites seemed to adapt to WT levels under FL (**Supplement Table 5.4.9**; **Supplement Table 5.4.8**). However, it became apparent, that FBP and SBP were severely affected (accumulated) by NTRC deficiency, which points to a massive impediment in the entire CBC regardless of the light environment, supporting a regulatory role of NTRC on SBPase *in vivo* (Geigenberger et al., 2017; Guinea Diaz et al., 2020). With respect to the other mutant lines, we saw, apart from the known and likewise bottleneck at FBP/FBPase in *trxf*, no substantial significances in *trxf*. Interestingly, the acceptor molecule RuBP was significantly increased in *trxm* under LL, possibly leading to a blockage in CO_2 fixation as well. This leads to the conclusion, that CBC targets might be tackled by different TRX systems and isoforms, depending on the light condition. Despite of the accumulation of SBP and FBP in *ntrc,* however, concentrations of CBC intermediates between WT and the mutants under FL were very much alike, suggesting that the CBC might play a minor role in acclimation to FL than previously thought. Thereto, protein levels of SBPase were not significantly affected. Nevertheless, SBPase was shown to have remarkable control over the CBC, especially on the PTM level (Harrison et al., 1997; Raines et al., 1999; Raines, 2003; Yoshida & Hisabori, 2018; Hammel et al., 2020), that might explain performance and growth in *ntrc* for the most part.

Although TRX isoforms *f* and *m* operate in the chloroplast, plastidial metabolites seemed to be concomitantly altered with cytosolic and even with mitochondrial metabolites (e.g. citric acid, lactic acid) in TRX deficient plants (**Supplement Figure 5.3.1**), leading to the conclusion, that TRXs, in line with their pleiotropic trait, might mediate a crosstalk between organelles. In this context, a recent study revealed an important role of TRX*m* in maintaining the chloroplast redox poise by exporting malate into the cytosol (Thormählen et al., 2017), which can be metabolized in the mitochondria to eventually produce ATP (Yamori, 2016). Well-studied communication relays mostly include compartment-spanning gene expression, however, other examples integrating metabolism are conceivable (Pesaresi et al., 2007). Regarding the connection between sink- and source tissues, an increased phloem loading with transport sugars like sucrose towards other tissues is lastly also very unlikely to explain low leaf sugar levels in *ntrc* (Hou et al., 2019).

The biomarker analysis imposingly identified metabolites, that help discriminate between control (WT) and treated (mutant) sample. Translated from human studies, this could mean that using **Table 3.3.1** for instance, helps to identify plants "suffering" from loss of NTRC. It further serves as a quantitative measure complementing the

visual representations, pinpointing to several metabolites, which expressions are completely declined after loss of NTRC, irrespective of the light condition. This could be hypothetically further used to create lists of biomarkers, describing genetic mutants, when no genetic tools are at hand, but moreover imposes the examination of related pathways in future studies. Myo-inositol, that has been shown to be repeatedly diminished in redox-deficient plants (Thormählen et al., 2015; Hou et al., 2019) and is expected to be elevated in WT under HL though (Obata & Fernie, 2012), constitutes a fine example of the limited use of photo-assimilates in down-stream cellular processes, when NTRC is missing. The role of NTRC and the properties of inositol-3-phosphate synthase, converting G6P to myo-inositol, might be worth investigating (Loewus & Murthy, 2000), as inositol-3-phosphate synthase transcripts were further shown to negatively correlate with biomass (Sulpice et al., 2009).

Again, it was attempted to find more general models, explaining the metabolic states in total, grouped by different compound classes (**Table 4.3.1**). Compared to the previous statistical approach (cf. chapter 4.1; **Table 4.1.1**) the results clearly show an overall consistent and highly significant effect of both the genotype and light on metabolism; the former might be prevalently attributed to NTRC (deficiency). Interestingly, interaction effects were observed, too. On metabolite level, this indicates a strong, yet unidentified, mutual relationship of the thiol-redox system and long-term light adaption processes.

Table 4.3.1 Summary of ANOVA based on linear model (response ~ genotype + light + genotype × light) involving central metabolism and Calvin-Benson-Cycle metabolites. Results are shown as p values. Significances ($p < 0.001$) are given in bold letters.

Predictor	amino acid	organic acid	sugar	CBC
Genotype	**$< 2.00\times10^{-16}$**	**2.07×10^{-07}**	**$< 2.00\times10^{-16}$**	**4.82×10^{-04}**
Light	**$< 2.00\times10^{-16}$**	**$< 2.00\times10^{-16}$**	**$< 2.00\times10^{-16}$**	**1.59×10^{-04}**
Interaction	**1.27×10^{-14}**	**7.48×10^{-06}**	**$< 2.00\times10^{-16}$**	3.66×10^{-02}

Correlation analysis in WT revealed large and stable hubs within the central metabolism and the CBC, respectively, which seem to operate largely independently from each other and from environmental light stimuli as well (**Supplement Figure 5.3.8**). We concluded, that WT does not present of lot of metabolic changes to changing light intensities, particularly in central metabolism. NTRC deficiency however shatters calculated correlations and thus might disrupt associated metabolites and pathways

observed in WT, regardless of the light regime (**Supplement Figure 5.3.9**). This on the other hand might also give the opportunity to study new NTRC targets.
Due to the measurement of relative abundances in GC-MS based metabolites, we could not calculate metabolite ratios like lactate/pyruvate for example, which would help to track the route of carbon utilization and energy production outside the chloroplast. Succinic- and fumaric acid, however, were found to be in similar ranges in *ntrc* compared to WT, probably allowing the TCA cycle to run quite consistently. Specific enzyme activity assays could shed further light on these questions (Stitt & Gibon, 2014). However, at least sugars levels were not indicative of any perturbations in metabolic cycles (Weiszmann et al., 2018).

4.3.2.2 Redox processes are important for light acclimation

Figure 4.3.1 summarizes the metabolome and proteome results together. It underlines the observation, that WT barely adjusts the central metabolism to changing light environments. Only in HL, WT (and *trxf* and *trxm*) plants activate metabolism and synthesize the bulk of organic acids, amino acids and sugars. The figure further clearly illustrates and corroborates previous observations, that most protein changes occurred in *ntrc* under HL, relative to WT, whereas the overall least changes happened in *trxf*, followed by *trxm*. In this context, any previously reported significances regarding chaperonin 60 subunit ß1 and ß2 for instance could not be detected (Fernández-Trijueque et al., 2019). However, intriguingly, NTRC and also TRX*m* deficient plants adjusted only little on protein level respecting all light conditions. Although these mutants show a similar idle behavior adjusting protein levels even in the same categories under HL, *ntrc* showed larger and more extreme changes relative to WT. The fewest significances were calculated for TRX*f* deficient plants, relative to WT, guiding further focus on the role of NTRC in protein adjustments. In summary however, despite exhibiting the most significant changes among the mutants, disruption of NTRC entailed a complete restriction of proteomic adjustments, especially under HL.
WT differentially expressed proteins in response to HL by up-regulating stress responses and CBC enzymes and down-regulating translation and photosynthesis, latter probably to save capacities being invested in other processes (e.g. stress control) (cf. chapter 3.3.3.3). Further, most absolute significant changes occurred in HL, while in FL more plastidial proteins were altered compared to HL (**Figure 3.3.18**). Taking LL into account as well, it was found that the key driving force of light acclimation in WT were indeed redox processes, especially in the chloroplast (cf. chapter 3.3.3.2). This

underscores our efforts to study plastidial thiol-redox-dependent acclimation responses to changing light regimes.

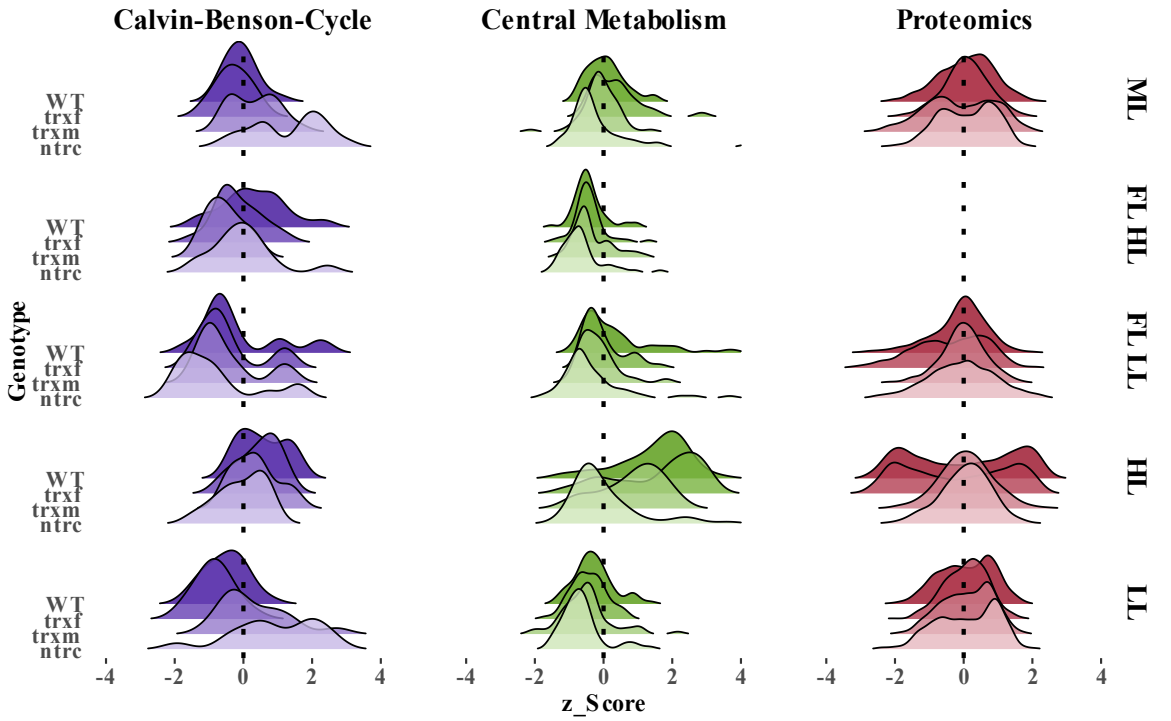

Figure 4.3.1. Overview of metabolic and proteomic changes in WT, *trxf*, *trxm* and *ntrc* in different light conditions.
In each category all variables were pooled and standardized across all light conditions to form the ridgeline shaped curves, expressing the density of changes within one sample compared to other samples.

4.3.2.3 NTRC is a central player to regulate protein adjustments

Significances in protein abundance calculated for ML and FL included minor changes in photosynthesis, CBC or electron transport. As discussed before, these changes might not substantially influence performance in *ntrc* relative to WT. However, NTRC appeared to be very important to counter-balance deficiencies under HL by a massive up-regulation of anabolic and biosynthetic processes; overall 272 proteins were significantly affected. It was found, that especially proteins involved in protein synthesis, predominantly ribosomal proteins, were greatly enhanced, compared to WT, at the trade-off of redox- and other processes (cf. chapter 3.3.3.4). Activation of cytosolic ribosomes seemed to be over-represented compared to plastidial ones. A follow-up experiment, recording little translation output in the chloroplast (cf. chapter 3.3.4), supports the idea of the chloroplast playing a minor role in protein synthesis in NTRC deficient plants. Although some processes on protein level might be activated under HL compared to WT, little change is achieved compared to other light conditions. Regarding

this and taking previous metabolomic analyses together, we concluded, that acclimation responses are entirely suspended in *ntrc*, even when they would be of most importance under HL. A functional promiscuity of NTRC (Jeffery, 2003; Chae et al., 2013), assigning a chaperone function apart from a reductase activity under HL and emphasizing the complexity and outreach of NTRC, might be responsible here. Moreover, evidence was found for NTRC being a potential hub, orchestrating and possibly regulating different enzymes all over the cell (cf. chapter 3.3.4) (Vandereyken et al., 2018). An intriguing candidate for further studies might also be chloroplast CBS domain-containing protein CBSX2 (AT4G34120), which was not detected under FL, but found highly significantly down-regulated under ML, HL and LL, playing a role in cell redox homeostasis (Yoo et al., 2011). One should also pay close attention to PETE (AT1G76100), that was down-regulated under all conditions as well. PETE is not a good indicator of electron flux in *Arabidopsis* though, compared to other plant species. However, it was increased in WT under HL and LL, relative to ML, and might serve some additional, yet to be determined, functions, apart from a known role as a copper storage protein (Schöttler & Tóth, 2014).

Although *ntrc* could not draw on sufficient reserves in form of sugars or amino acids for growth, the mutant could sustain a normal level of functional total proteins to control all necessary cell functions in order to survive (**Figure 3.3.27**). In the same way, it was surprising to find little explanation of the severe *ntrc* phenotype under FL on proteomic level; here only 41 proteins were significantly affected. However, three of them were highly significantly up-regulated: ß-glucosidase (AT3G09260), chloroplastic LOW PSII ACCUMULATION 1 (AT1G02910) and alternative NADH dehydrogenase (AT5G08740) (**Table 3.3.3**), two of which were found in plastids and important in photosynthetic electron flow, that might be worth further investigation. Nevertheless, it is questionable, if this retarded FL phenotype in *ntrc* considerably relies on proteomic changes. Under LL, *ntrc* exhibited a significant change in as many as 145 proteins. Functional analyses (e.g. over-representation of GO terms) with such a low number are meaningless though, however, a significant down-regulation of some PSI subunits was detected. In the CBC, there were no protein changes detected. Summarized, NTRC appears to be an important and multi-layered protagonist in light acclimation, especially under HL.

4.3.3 Thioredoxin and NADPH-dependent thioredoxin redundancy is debatable

A biological principle known as *guilt by association* states that genes with related functions tend to share functional properties (Gillis & Pavlidis, 2012). Combined with

reverse genetics, they provide a powerful tool for elucidating chloroplast functions (Armbruster et al., 2011). Transferred to our case, the diversity of the Fd-TRX system suggests a functional specificity for the different isoforms present in plants (Fernández-Trijueque et al., 2019). Our results from chlorophyll fluorescence and total protein changes (cf. chapter 3.3.5) in fully acclimated KO-plants corroborate this assumption rather than that of a redundant system. We concluded that TRXs *f* and *m* have distinct effects on single photosynthesis parameters, but still rather serve in their fine-tuning than playing a more significant role. This is rather not surprising, since the set of mutants used here do not represent the conventional genetic tools to dissect photosynthesis in the scope of the light reactions. NTRC on the other hand, showed a significant and beneficial effect in acclimation to FL earlier (Thormählen et al., 2017), which could be reproduced and detect in HL and LL as well. Nevertheless, as prime acceptors of photo-energy, the FTR and FNR system entail a feedback-regulation to the thylakoid reactions, with TRXs and NTRC being deleted, allowing energy to be accumulated in alternative sinks and components with limited capacities, causing detrimental effects on various cellular functions.

Regarding metabolites and related enzymes, the single and cooperative roles of TRX*f* and NTRC in regulating FBPase have been demonstrated before (Thormählen et al., 2015). Our data showed that while FBP is accumulated under all conditions in *ntrc*, indicating a missing activation of FBPase via NTRC, TRX*f* seemed to matter most in FBPase regulation under ML and HL (**Figure 3.3.11**). Further, WT and *trxf* levels of FBP were similar under FL, and (probable) functional TRX*f* seemed not to compensate the loss of NTRC or to restore CBC flow around FBPase in *ntrc*, indicating a minor role of TRX*f* and a bigger role of NTRC in CBC activation under FL (**Figure 3.3.12**) and a limitation of compensatory roles between the TRX- and NADPH-dependent TRX-system (cf. chapter 4.3.2.1). Also, a potential bottleneck in CO_2 fixation was noticed, revealing an accumulation of RuBP under LL, affected by disruption of TRX*m*. Lastly, the overview in **Figure 4.3.1** underlines the role of NTRC under moderate and little light, possibly rerouting photosynthetic electrons preferably via the FNR system into the CBC in conditions with little photo-chemical energy.

4.4 Outlook

Our methodology was confined to the principles of basic research by exploring and describing photosynthetic active organs and cells, where established high-throughput, quantitative small- and larger-scale studies were conducted, measuring protein levels, centralized metabolism, photosynthetic efficiency and specialized chloroplast

metabolism to get in-depth insight into metabolic switch points and bottlenecks and learn more about thiol-redox regulatory involvement in photosynthesis and cellular carbon reactions. Whilst marginally presenting the prospect of in-field application to potentially levering crop yields, biomass and plant resilience upwards, the results are also qualified to be reviewed under the aspects of systems biology (Deshmukh et al., 2014), from where new hypotheses and innovations can be derived.

Based on our results, we postulated a lower-ranking role of TRXs and NTRC in photosynthesis when plants are challenged with moderate, short-term fluctuations from ML to HL, but a substantial necessity for TRX*m* and NTRC to balance photosynthesis during rapid fluctuations under higher light intensities. In this context, however, a (thio)redox(in)-dependency of photosynthetic state transition guided by STN7 kinase, managing short-term and long-term responses to FL environments, is still one of the greater questions photosynthesis researchers try to solve. Its dissection involves sophisticated approaches, including site-directed mutagenesis of potentially entangled cysteine residues for instance (Shapiguzov et al., 2016). Latest studies described STN7 activity under diverse physiological stresses and genetic backgrounds by LHCII phosphorylation (Ancín et al., 2019), leaving direct interaction mechanism still unresolved. Future research needs to determine clear mechanisms to find out how redox signals are integrated to modulate STN7 activity and therefore photosynthetic state transition.

Next, instead of light intensity, different light qualities could be applied to further study acclimation programs, as well as altering the duration of the single phases in FL (Bailey et al., 2004; Morales & Kaiser, 2020; Walters, 2005; Walters & Horton, 1994). Also, limitations in abiotic factors can be cross-linked (Carrera et al., 2018); LED technology does not emit heat, however a rise in NPQ produces heat within the cell, especially in HL environments, which might be an appreciable point for future research. This study covered short- and long-term acclimation programs such as photosynthetic energy quenching, electron- and metabolite flows and proteomic adjustments. Although transcript abundances should not be extrapolated to that of protein abundances, and although the majority of acclimation processes are regulated at the PTM level (Eberhard et al., 2008), long-term acclimation studies could be supported by transcriptional analyses (Kolbe et al., 2006). In that respect though, redox-proteomics may even be a superior approach to confirm existing or discover novel TRX targets, but most importantly to understand regulatory dynamics in fluctuating environments (Rinalducci et al., 2008; Navrot et al., 2011; Wojdyla & Rogowska-Wrzesinska, 2015; Yang et al., 2016; Zaffagnini et al., 2019).

Further, it will be a challenging yet illuminating task to verify our calculations of linear correlations between selected central- and CBC metabolites and to link our data with veritable biochemical processes (Nägele, 2014). Finally, the *omics* data and enzyme kinetics could be combined in perspective to most appropriately describe co-regulations and the relationship to the underlying genotypes (Gibon et al., 2004, 2006; Glinski & Weckwerth, 2006) and – in case of NTRC as a potential hub in photosynthesis and cellular reactions – to increase the reliability of predicted or preliminary data on protein-protein-interactions (Vandereyken et al., 2018). Data interpretation could be therefore promoted by overlapping metabolites with corresponding enzymes (Wienkoop et al., 2008). Although our evaluation of the metabolite modules might be incomplete up to this point, we cannot exclude the presence of key factors connecting the – according to our understanding – distinctively operating metabolic networks of central and CBC metabolism. Further, if the FTR and FNR system are to be investigated more thoroughly, an induced and targeted knockout or silencing of TRXs and NTRC, augmented with flux studies and enzyme kinetics, are indicated as complementation, due to the complex pleiotropic effects of thiol-modifying thioredoxins (Stitt & Fernie, 2003). Alternatively, plants over-expressing NTRC were shown to gain overall fitness (Toivola et al., 2013; Nikkanen & Rintamäki, 2019; Guinea Diaz et al., 2020), which could be implemented, too. Therefore, enriching central modulators like NTRC, combined with targeted modifications (Deshmukh et al., 2014; Köhler et al., 2017; Kaiser et al., 2018; Slattery et al., 2018; Hammel et al., 2020) in different light regimes, has the potential to fuel plant growth and improve crop yields.

5 Supplement

5.1 Photosynthetic (de-)acclimation to short-term high light

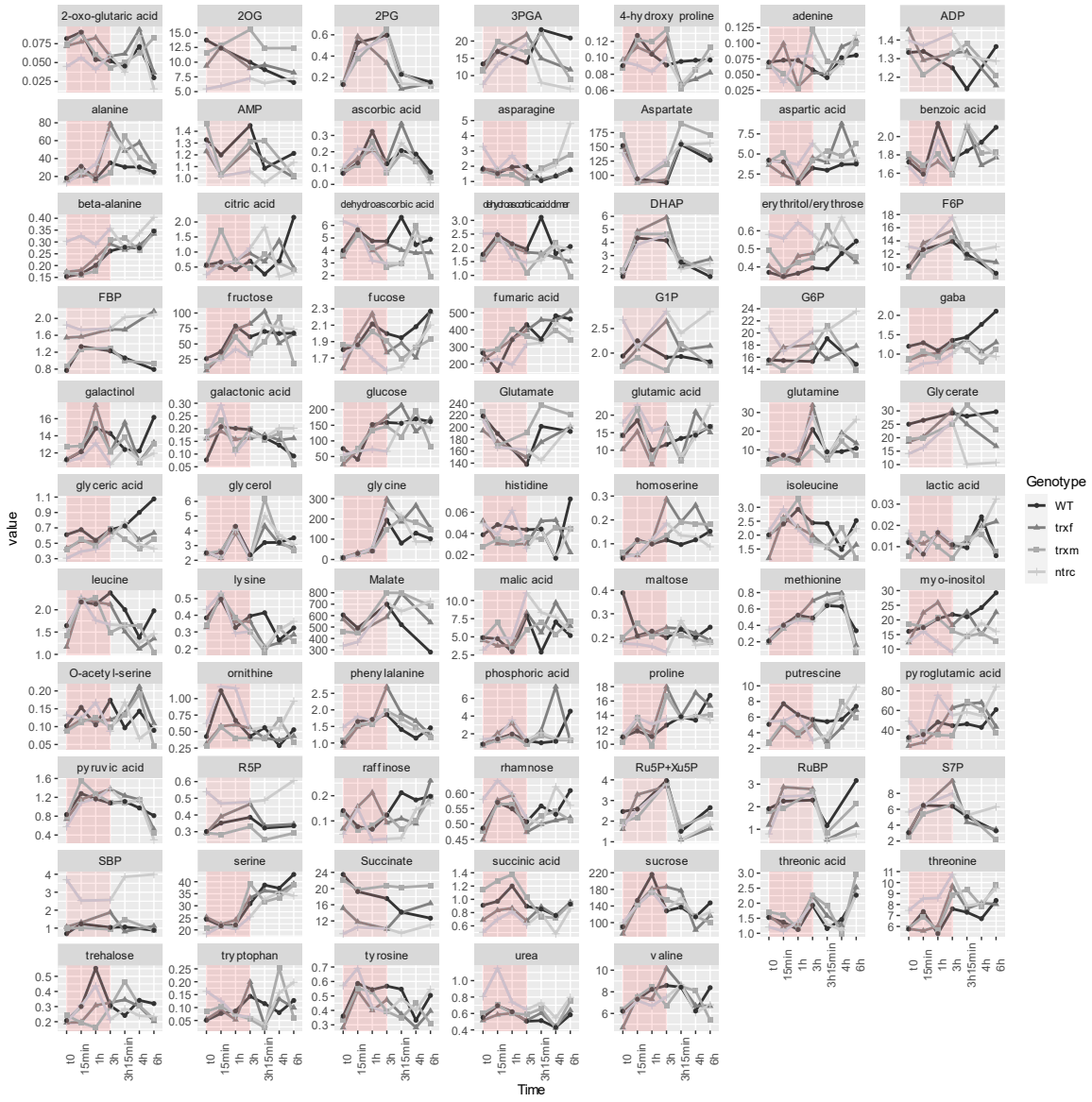

Supplement Figure 5.1.1. Kinetics overview of central- and CBC metabolism under short-term HL (de-)acclimation in WT, *trxf*, *trxm* and *ntrc*.
Metabolites with capital letters are LC/MS based and given in pmol/µg protein. Lower case metabolites are GC/MS based and given in arbitrary units. The red area indicates the HL acclimation phase. Values are shows as mean, n=3-5 biological replicates.

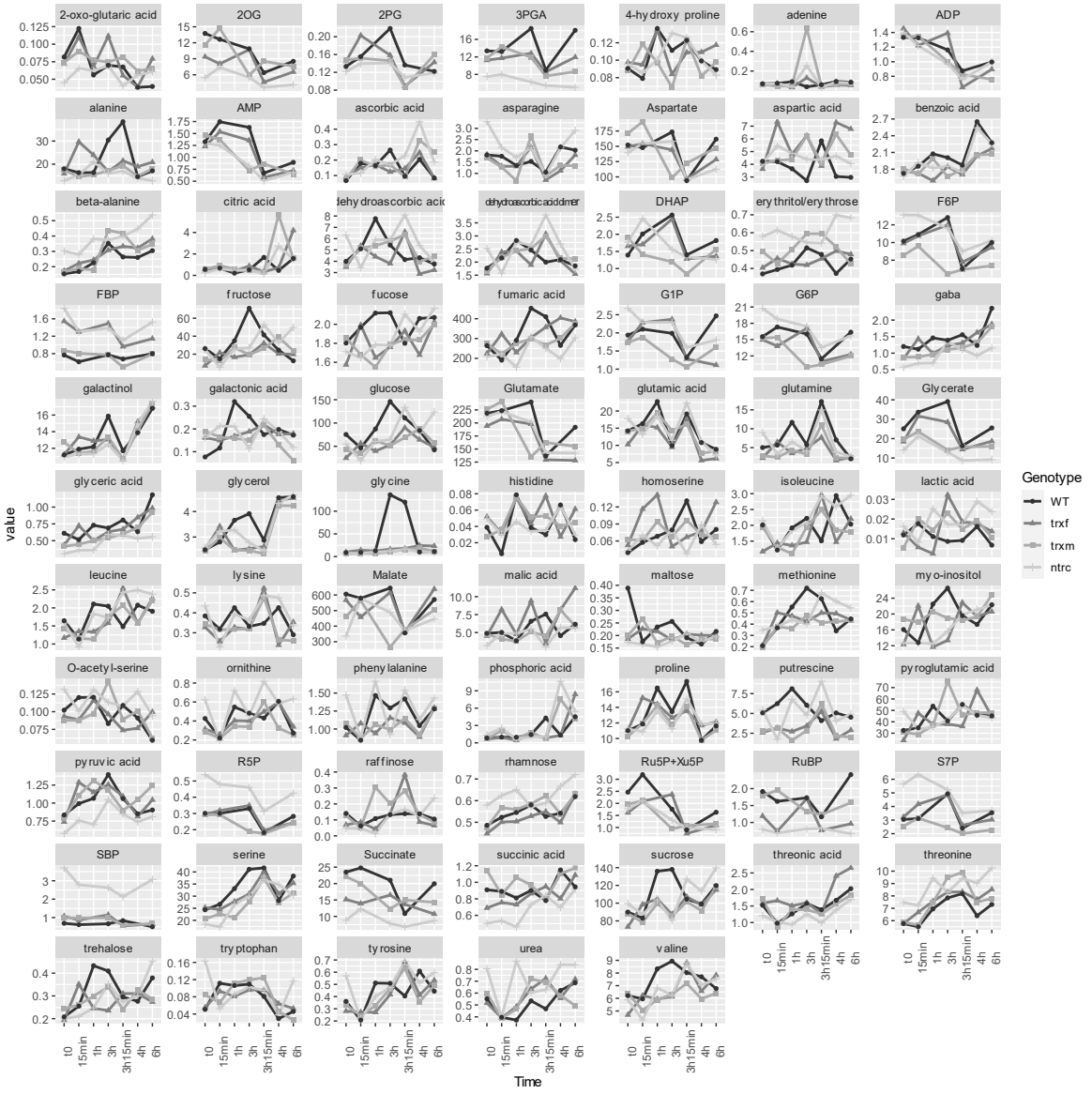

Supplement Figure 5.1.2. Kinetics overview of central- and CBC metabolism under ML in WT, *trxf*, *trxm* and *ntrc*.

This graph corresponds to **Supplement Figure 5.1.1** and serves as a control, where samples were grown and harvested under ML. Metabolites with capital letters are LC/MS based and given in pmol/µg protein. Lower case metabolites are GC/MS based and given in arbitrary units. Values are shows as mean, n=3-5 biological replicates.

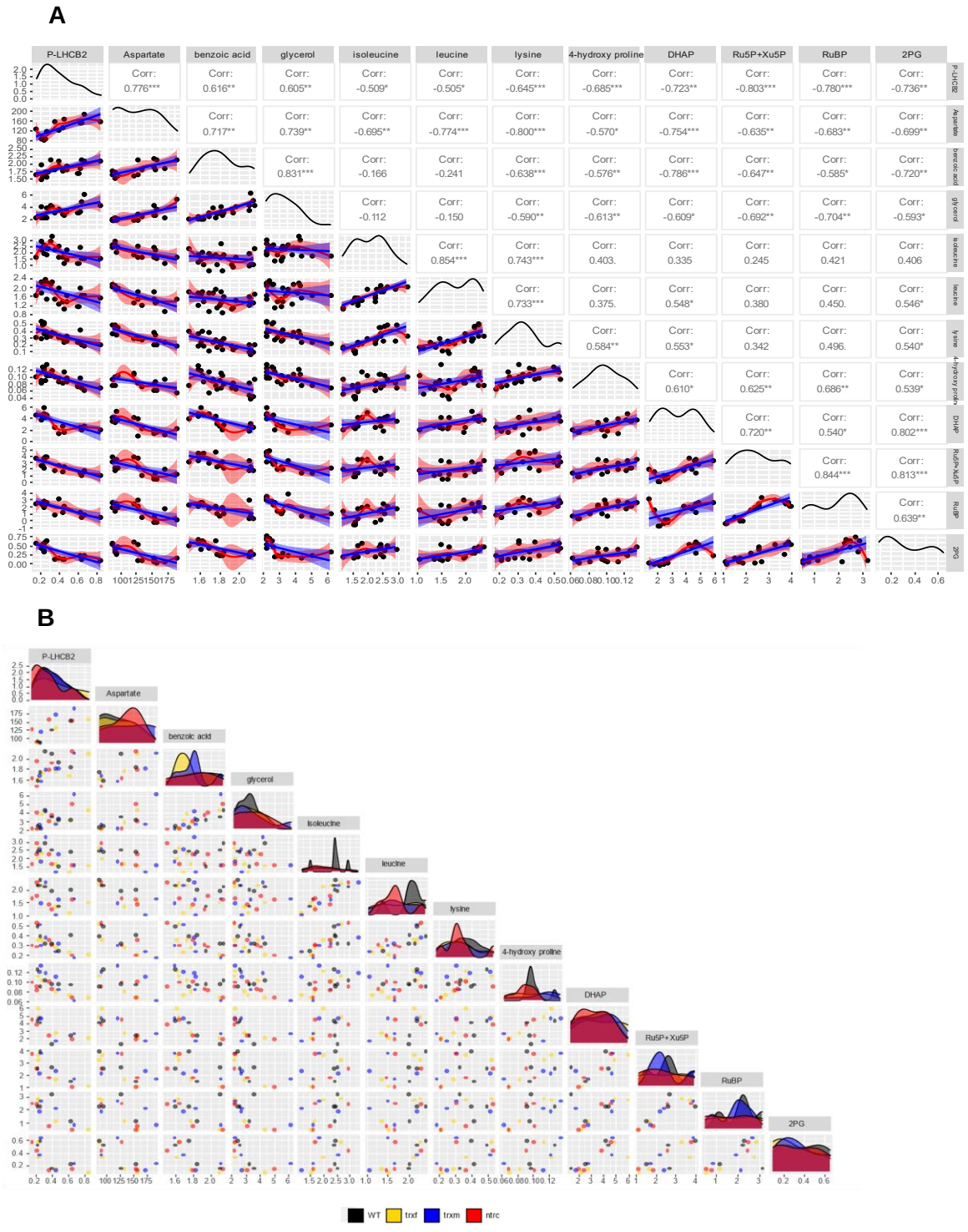

Supplement Figure 5.1.3. Scatter plot matrix of selected metabolites in HL (de-)acclimated samples.
(A) Scatter plot of each pair with Pearson correlation value and significance; red, locally estimated scatterplot smoothing; blue, linear model; significances are labelled with asterisks (* $0.01 < p < 0.05$, ** $0.001 < p < 0.01$, *** $p < 0.001$). (B) Scatter plot with density plots indicating genotypic effects on each metabolite and supports additional insights into each relation. The matrices were generated with R package "ggpairs".

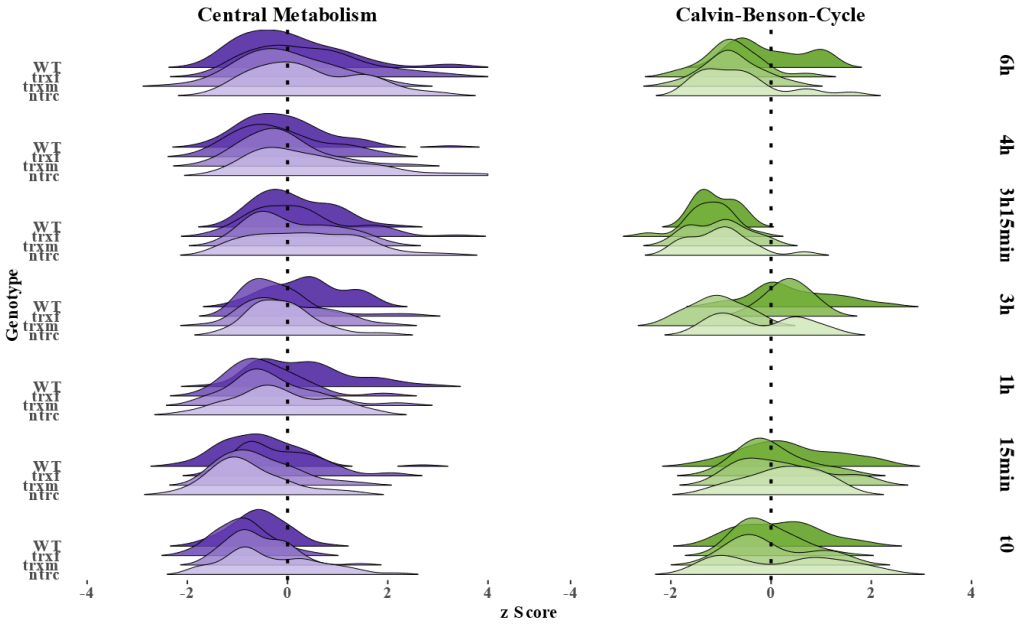

Supplement Figure 5.1.4. Time-resolved metabolic changes and distribution of control (ML) plants.
HL (**Figure 4.1.1**) and ML samples were scaled together to directly compare changes starting from t_0.

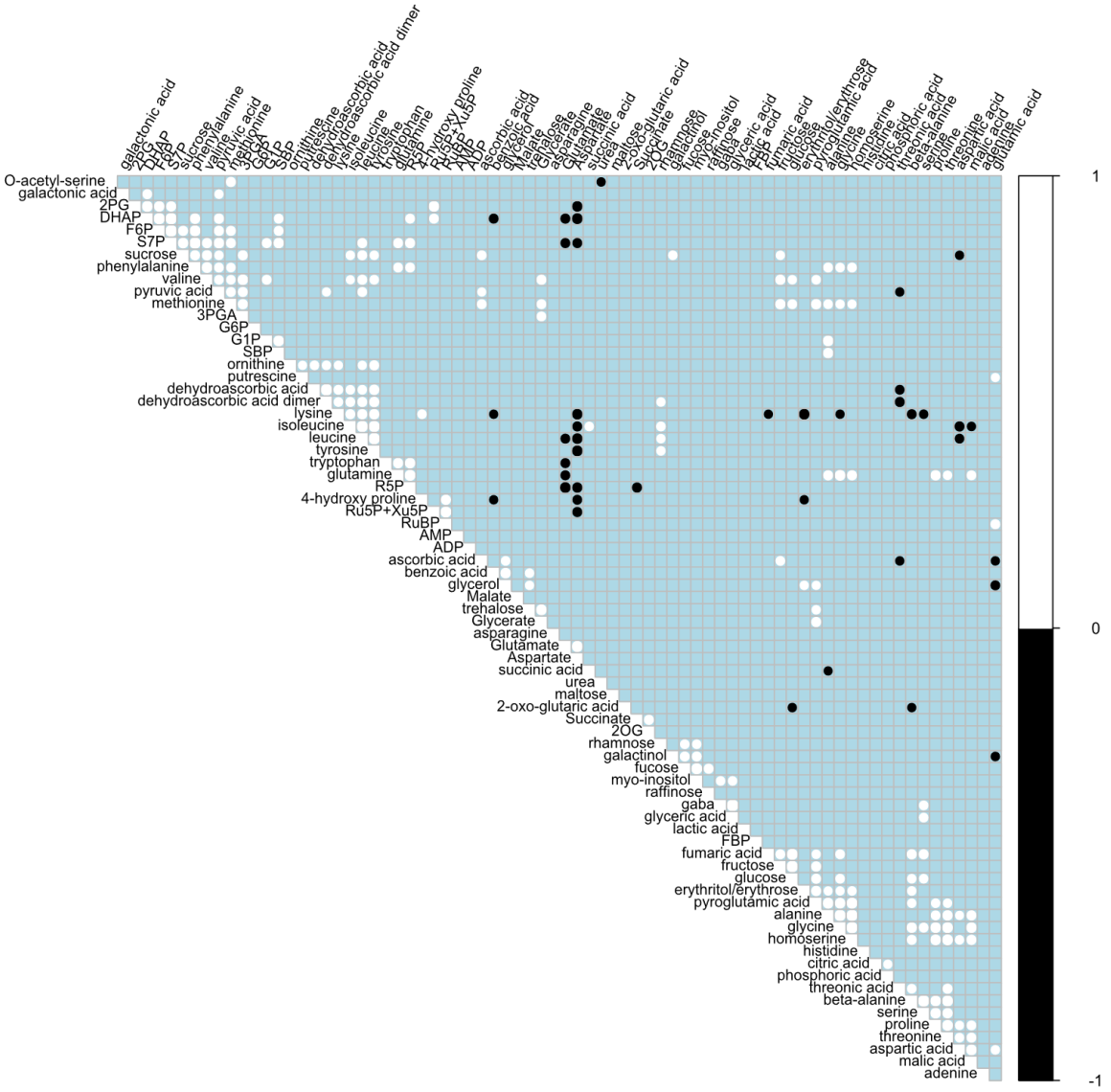

Supplement Figure 5.1.5. Correlogram of combined central metabolism and Calvin-Benson-Cycle metabolites including WT, *trxf* and *trxm* samples.
Positive correlations are shown in white, negative correlations are shown in black. Non-significant correlations (threshold $p < 0.01$) are shown in light blue. Samples are ordered according to Ward's method (R package "corrplot").

Supplement Table 5.1.1. Summary of ANOVA based linear model (response ~ genotype × light × acclimation) involving central metabolism and Calvin-Benson-Cycle metabolites.
Results are shown as p values. Significances ($p < 0.01$) are given in bold.

Predictor	sugar	organic acid	amino acid	CBC
Genotype	5.6×10^{-2}	**2.0×10^{-7}**	3.1×10^{-1}	8.8×10^{-2}
Light	**7.8×10^{-12}**	**1.3×10^{-5}**	**2.0×10^{-16}**	**6.5×10^{-10}**
Acclimation	**3.8×10^{-11}**	**2.0×10^{-16}**	**2.0×10^{-16}**	**1.7×10^{-5}**
Genotype × Light	2.3×10^{-1}	9.5×10^{-1}	7.8×10^{-1}	5.5×10^{-1}
Genotype × Acclimation	5.1×10^{-2}	**3.1×10^{-2}**	1.6×10^{-1}	6.7×10^{-1}
Light × Acclimation	**2.5×10^{-4}**	**1.4×10^{-3}**	**6.2×10^{-11}**	**4.9×10^{-3}**
Genotype × Light × Acclimation	3.8×10^{-1}	6.3×10^{-1}	6.5×10^{-1}	8.9×10^{-1}

5.2 Photosynthetic acclimation to fluctuating light

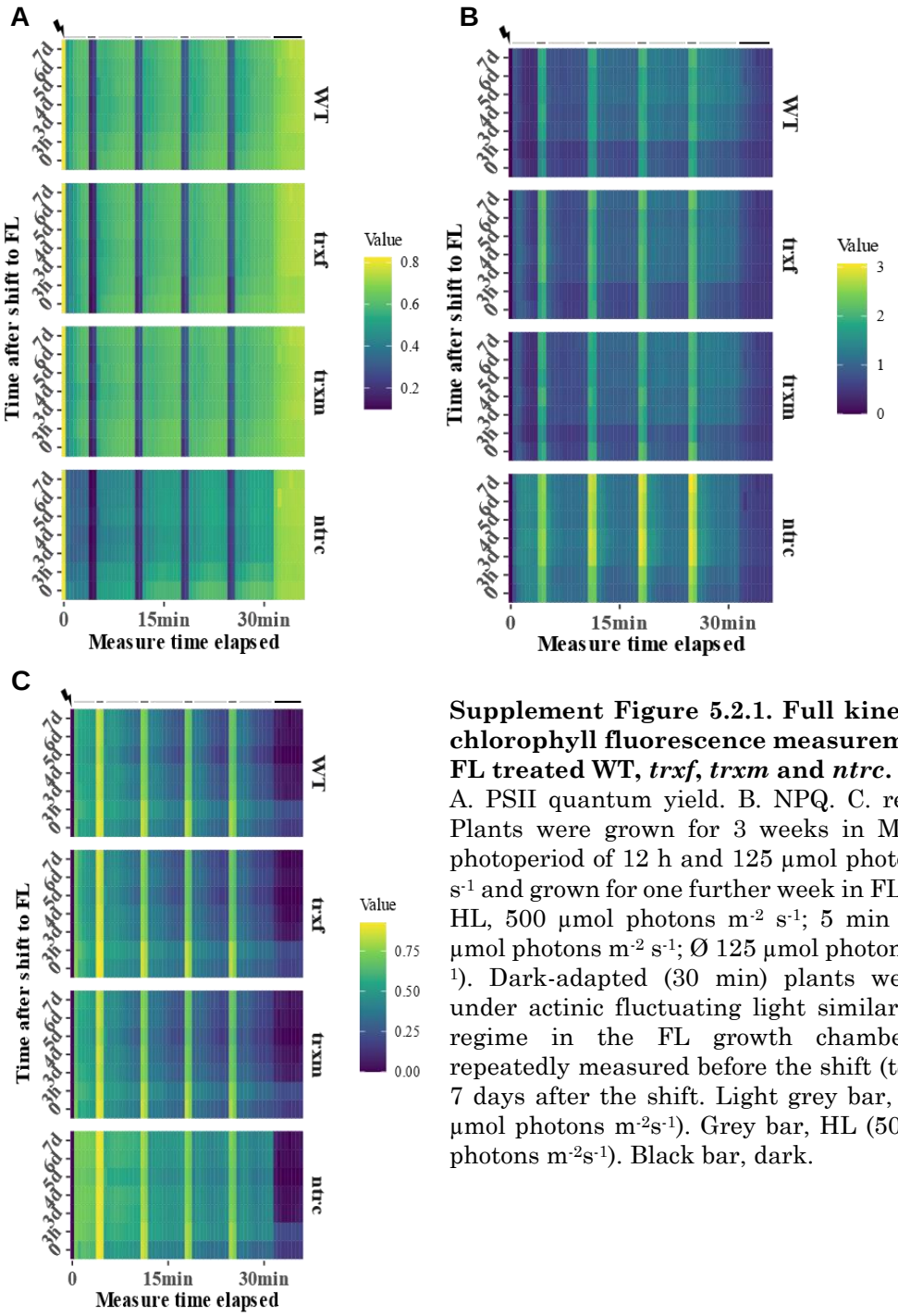

Supplement Figure 5.2.1. Full kinetics of chlorophyll fluorescence measurement in FL treated WT, *trxf*, *trxm* and *ntrc*.
A. PSII quantum yield. B. NPQ. C. red. PQ. Plants were grown for 3 weeks in ML at a photoperiod of 12 h and 125 µmol photons m^{-2} s^{-1} and grown for one further week in FL (1 min HL, 500 µmol photons m^{-2} s^{-1}; 5 min LL, 50 µmol photons m^{-2} s^{-1}; Ø 125 µmol photons m^{-2} s^{-1}). Dark-adapted (30 min) plants were put under actinic fluctuating light similar to the regime in the FL growth chamber and repeatedly measured before the shift (t_0) up to 7 days after the shift. Light grey bar, LL (50 µmol photons $m^{-2}s^{-1}$). Grey bar, HL (500 µmol photons $m^{-2}s^{-1}$). Black bar, dark.

5.3 Long-term acclimation responses

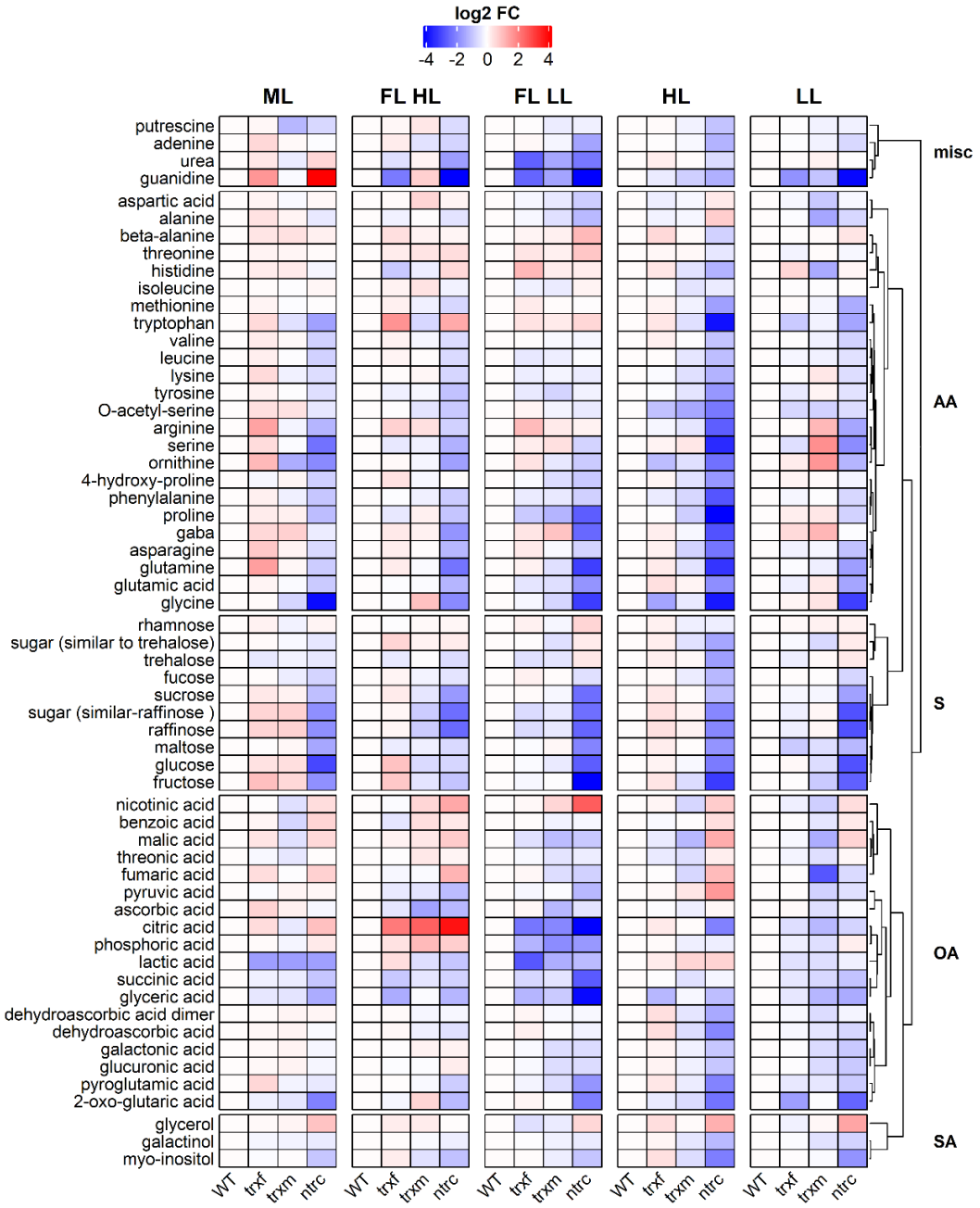

Supplement Figure 5.3.1. Log2-fold changes of GC-MS based central metabolites in *trxf*, *trxm* and *ntrc* relative to WT.
misc, miscellaneous; AA, amino acid; S, sugar; OA, organic acid; SA, sugar alcohol.

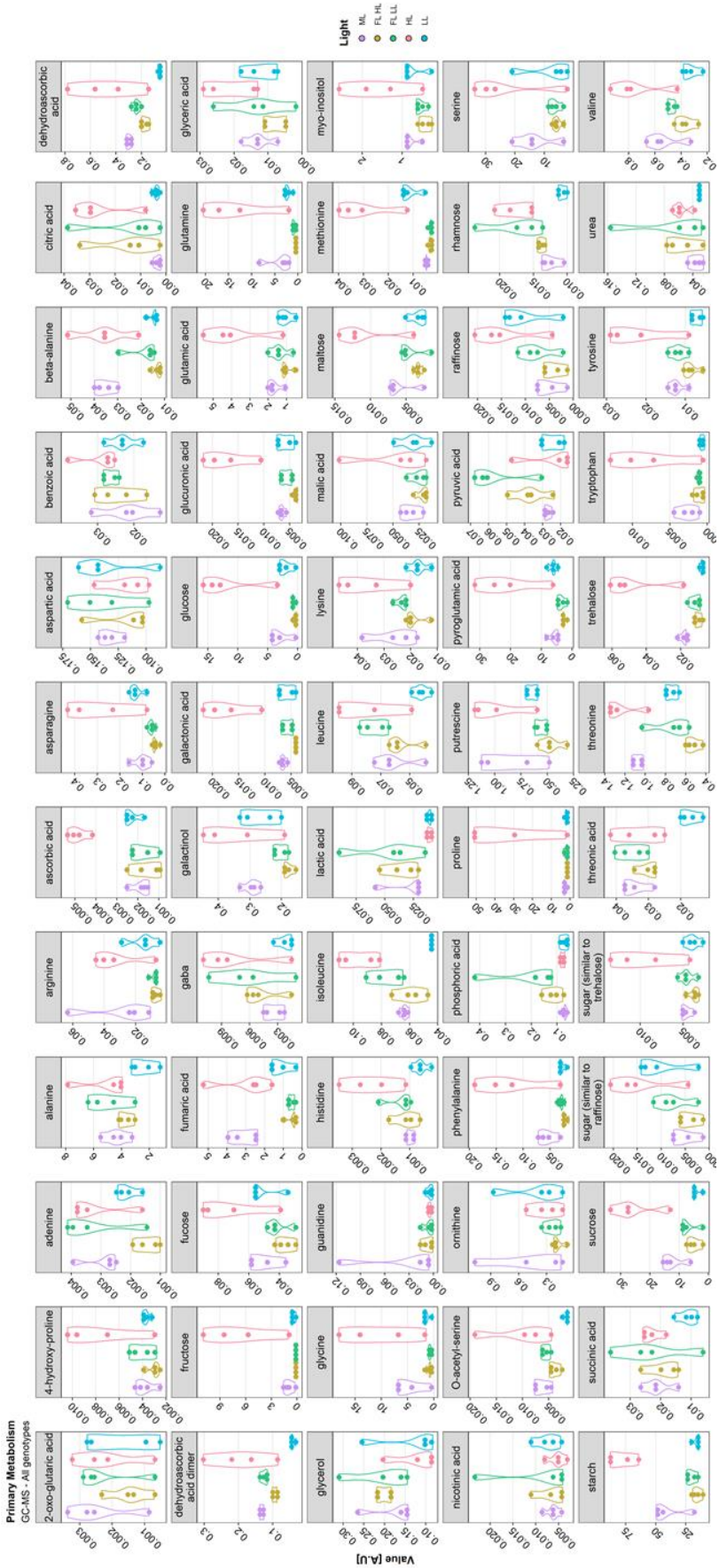

Supplement Figure 5.3.2. Overview of GC-MS based central metabolism in fully acclimated WT, *trxf*, *trxm* and *ntrc*.
Shown are the pooled mean values across all genotypes. Values are in arbitrary units.

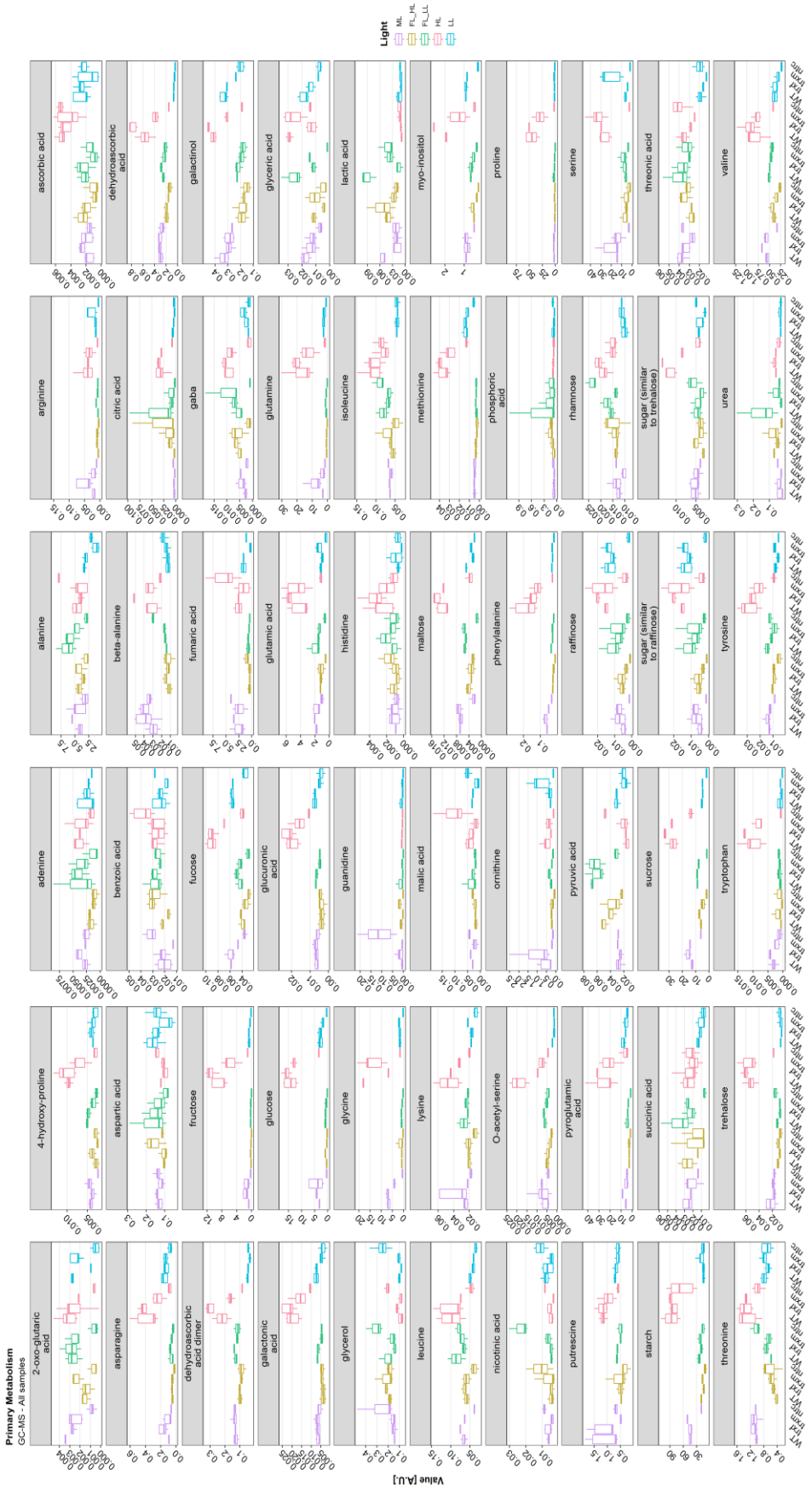

Supplement Figure 5.3.3. Overview of central metabolism based on GC-MS analysis in WT, *trxf*, *trxm* and *ntrc*. Results are shown as boxplots in arbitrary units, n = 3 – 5 biological replicates. Starch content was measured spectroscopically from the GC extraction residues.

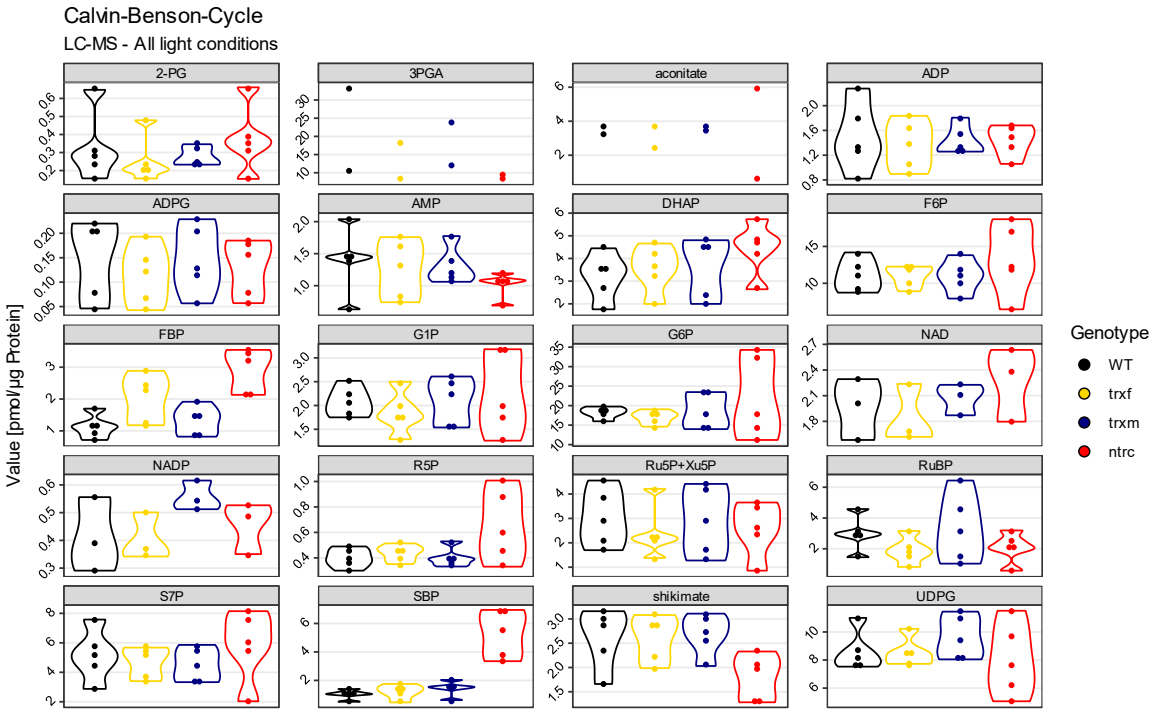

Supplement Figure 5.3.4. Overview of LC-MS based metabolites in fully acclimated WT, *trxf*, *trxm* and *ntrc*.
Shown are the pooled mean values across all genotypes.

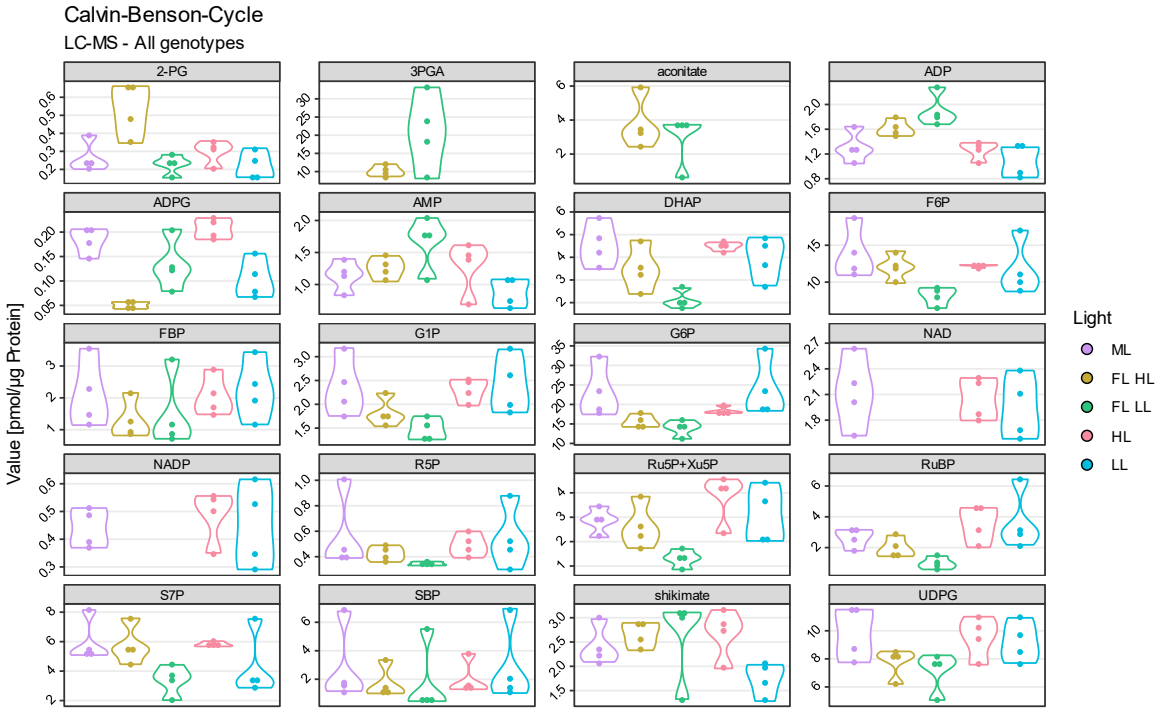

Supplement Figure 5.3.5. Overview of LC-MS based metabolites in fully acclimated WT, *trxf*, *trxm* and *ntrc*.
Shown are the pooled mean values across all light conditions.

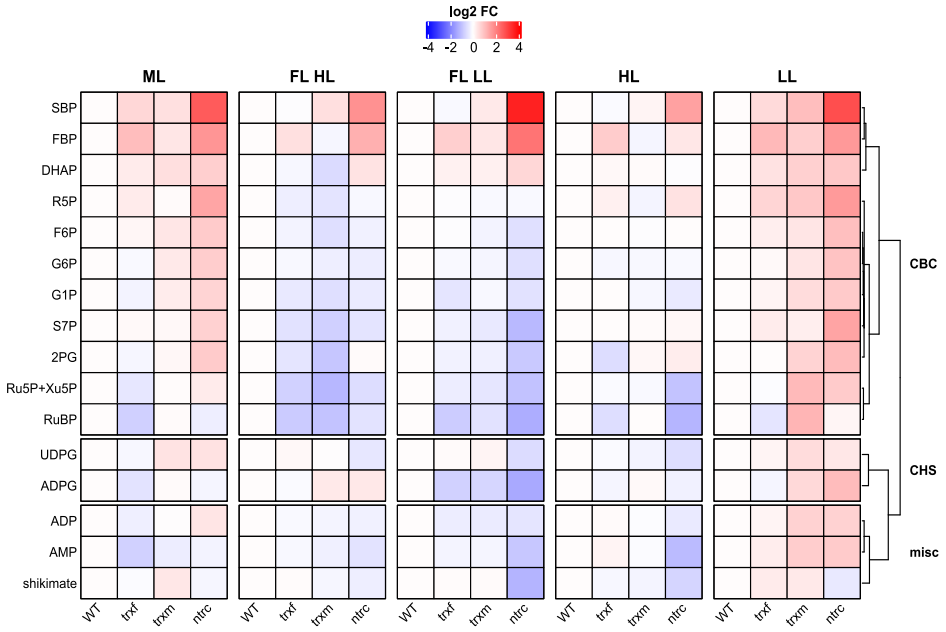

Supplement Figure 5.3.6. Log2-fold changes of LC-MS based metabolites in *trxf*, *trxm* and *ntrc*, relative to WT.
CBC, Calvin-Benson-Cycle; CHS, carbohydrate synthesis; misc, miscellaneous.

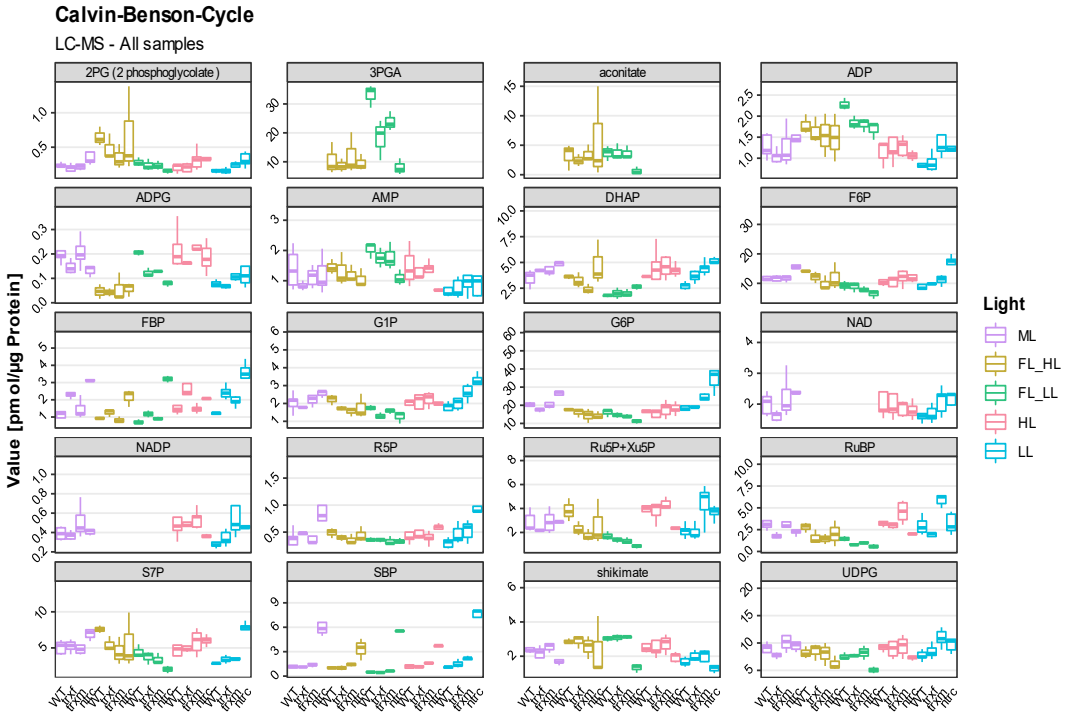

Supplement Figure 5.3.7. Overview of LC-MS based metabolites in WT, *trxf*, *trxm* and *ntrc*.
Results are shown as boxplots in pmol/µg protein, n=3-5 biological replicates.

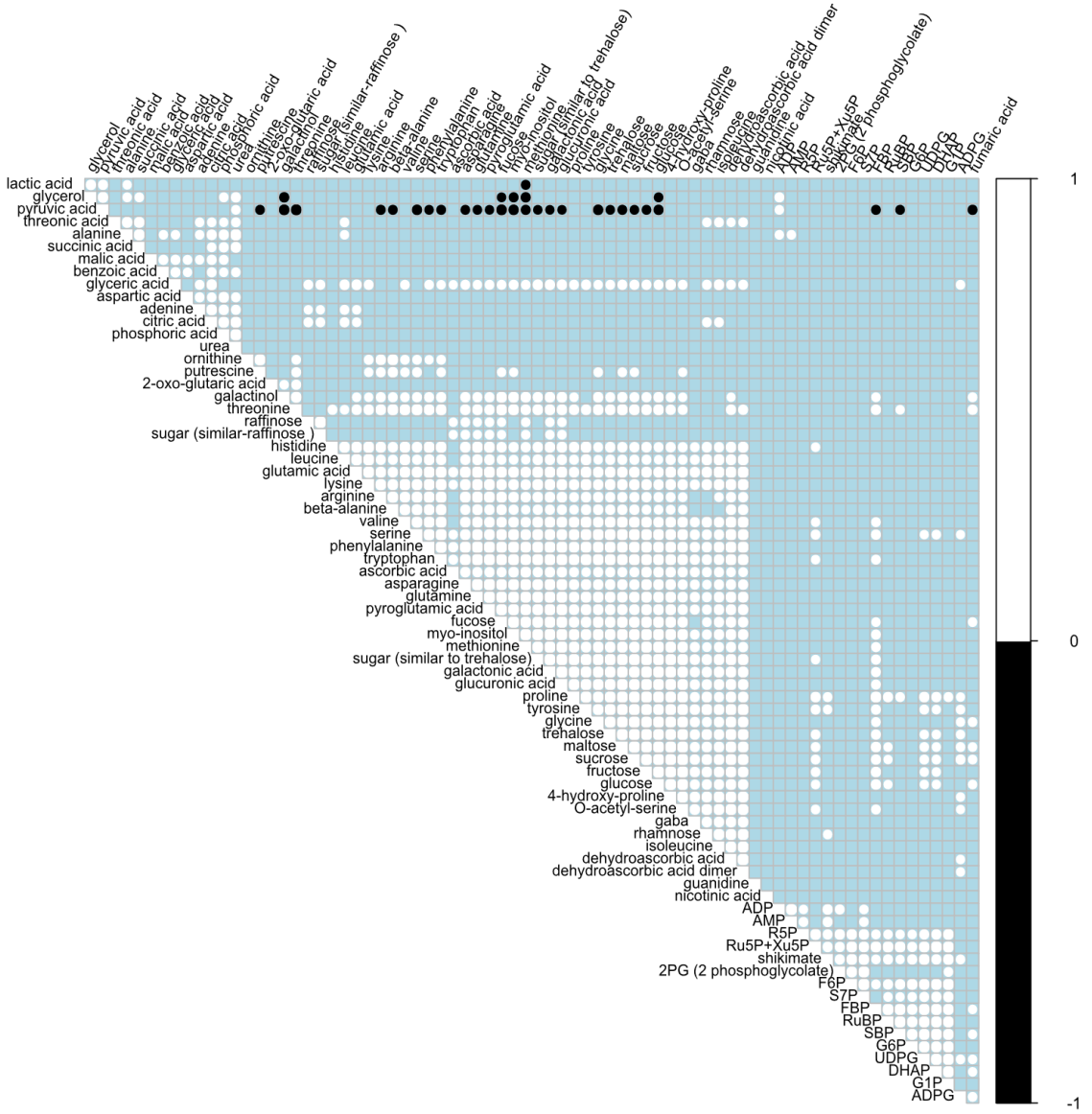

Supplement Figure 5.3.8. Correlogram of central metabolism and CBC metabolites in WT.

Biological replicates were combined from ML, FL HL, FL LL, HL and LL and analyzed with R package "corrplot". Positive correlations are shown in white, negative correlations are shown in black. Non-significant correlations (threshold $p < 0.01$) are shown in light blue/blank. Samples are ordered according to Ward's method. Detailed information can be found in the text.

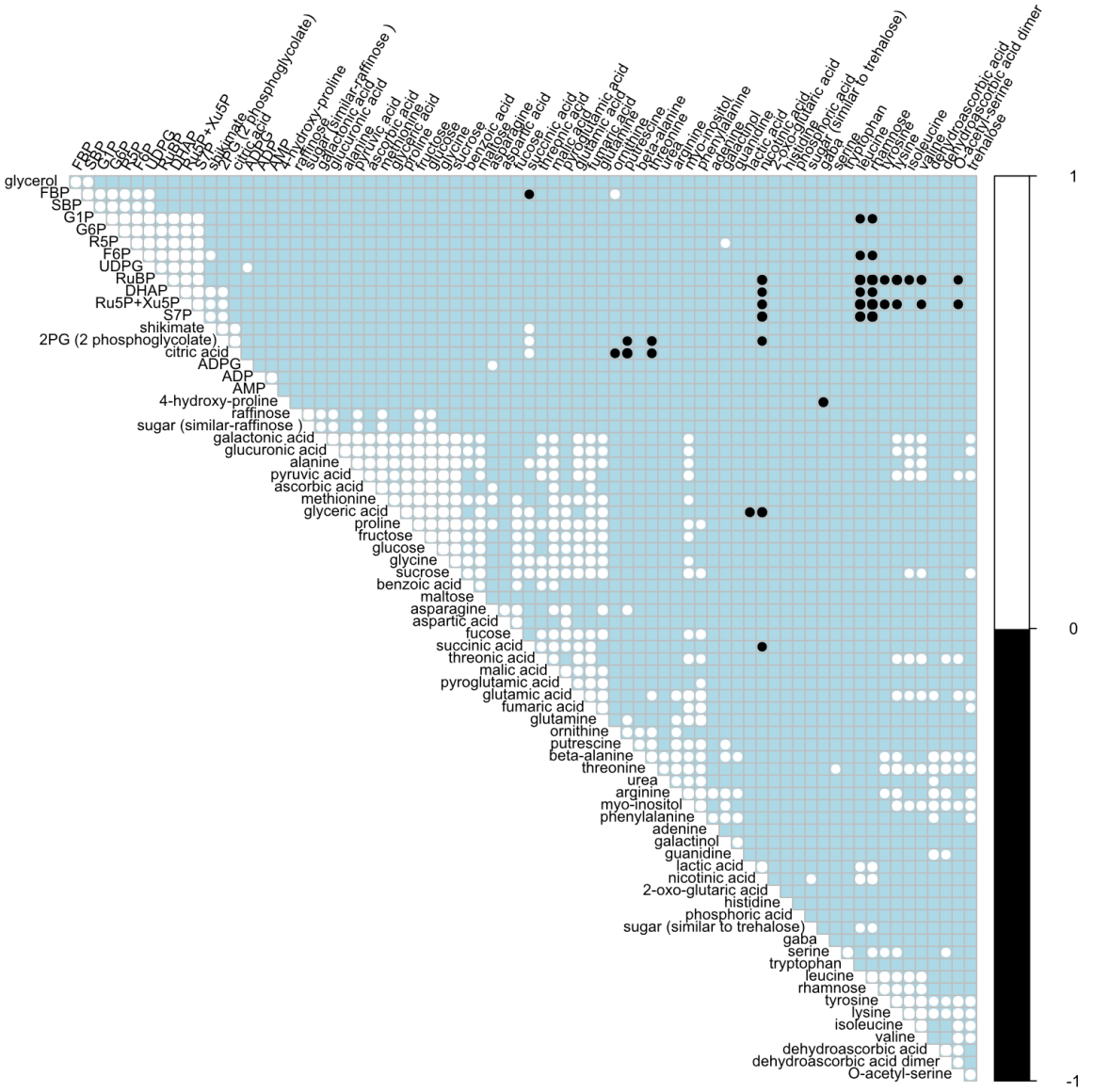

Supplement Figure 5.3.9. Correlogram of central metabolism and CBC metabolites in *ntrc*.
Biological replicates were combined from ML, FL HL, FL LL, HL and LL and analyzed with R package "corrplot". Positive correlations are shown in white, negative correlations are shown in black. Non-significant correlations (threshold $p < 0.01$) are shown in light blue/blank. Samples are ordered according to Ward's method. Detailed information can be found in the text.

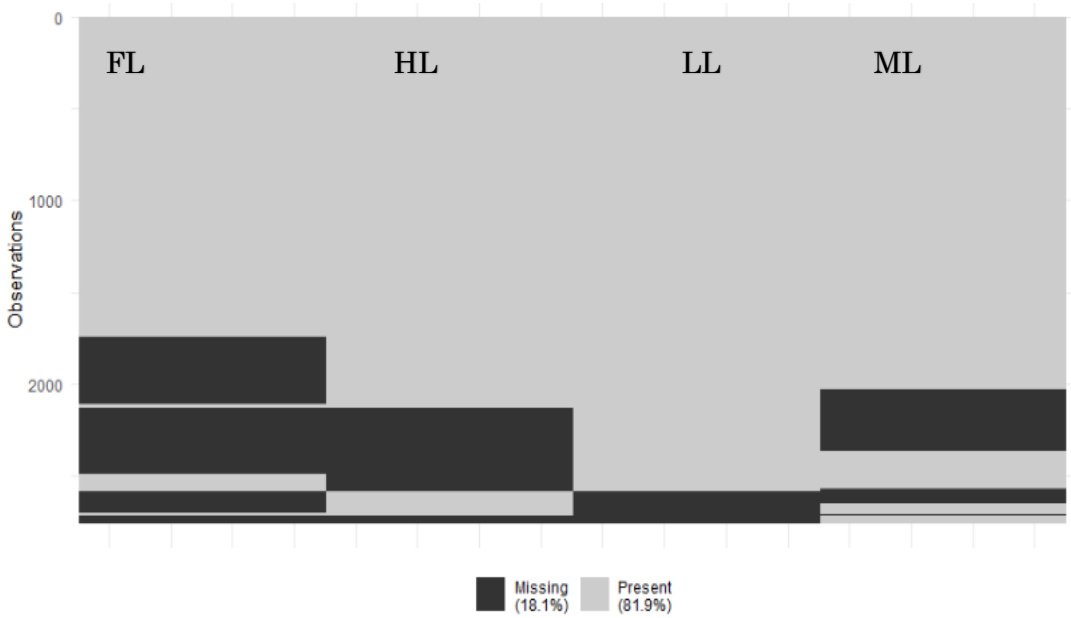

Supplement Figure 5.3.10. Comparison of present and missing peptides in different light conditions.
Generated with R package "visdat".

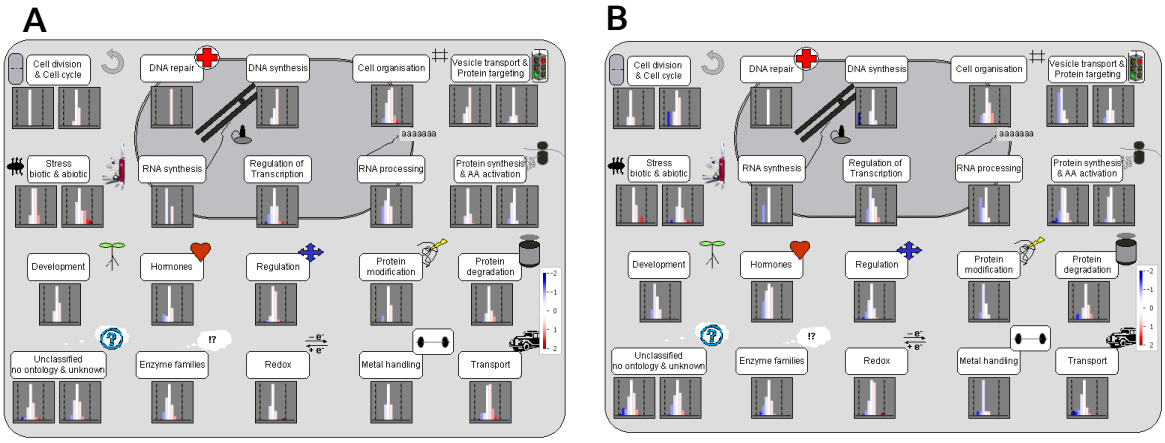

Supplement Figure 5.3.11. Changes in cell functions in LL and FL compared to ML in WT.
(A) LL. (B) FL. Generated with MapMan.

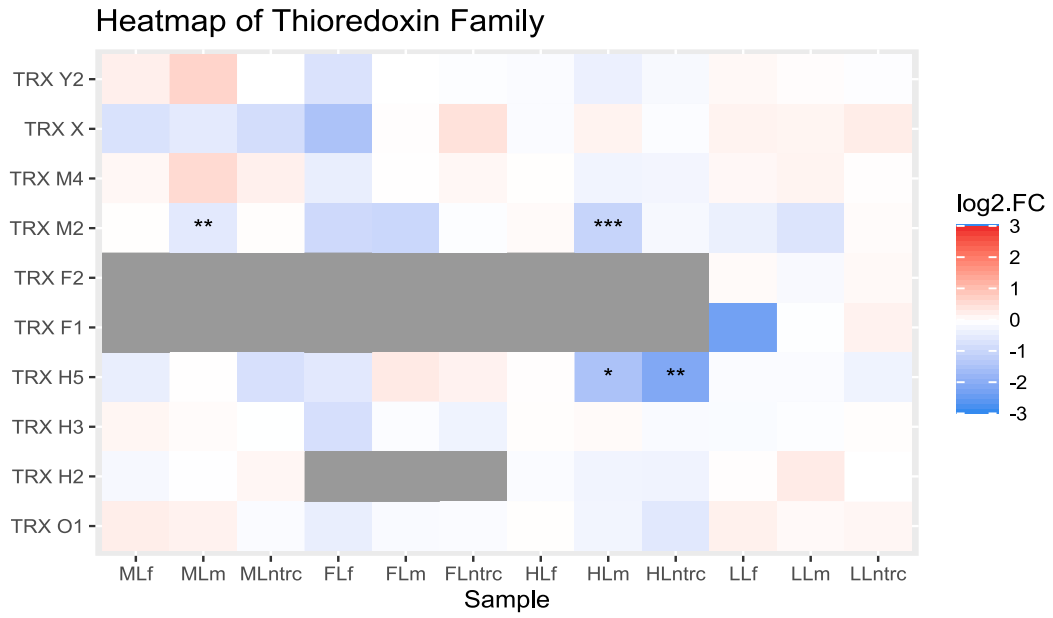

Supplement Figure 5.3.12. Protein changes of the Thioredoxin family in *trxf*, *trxm* and *ntrc*, relative to WT.
Values are log2 fold-changes relative to the respective WT in each light condition. Blue color indicates down-regulation. Red color indicates up-regulation. Some proteins are left undetectable (grey color) after data processing. Significances (multiple t-test with Benjamini-Hochberg correction) are shows as asterisks (* $0.01 < p < 0.05$, ** $0.001 < p < 0.01$, *** $p < 0.001$). f, *trxf*; m, *trxm*.

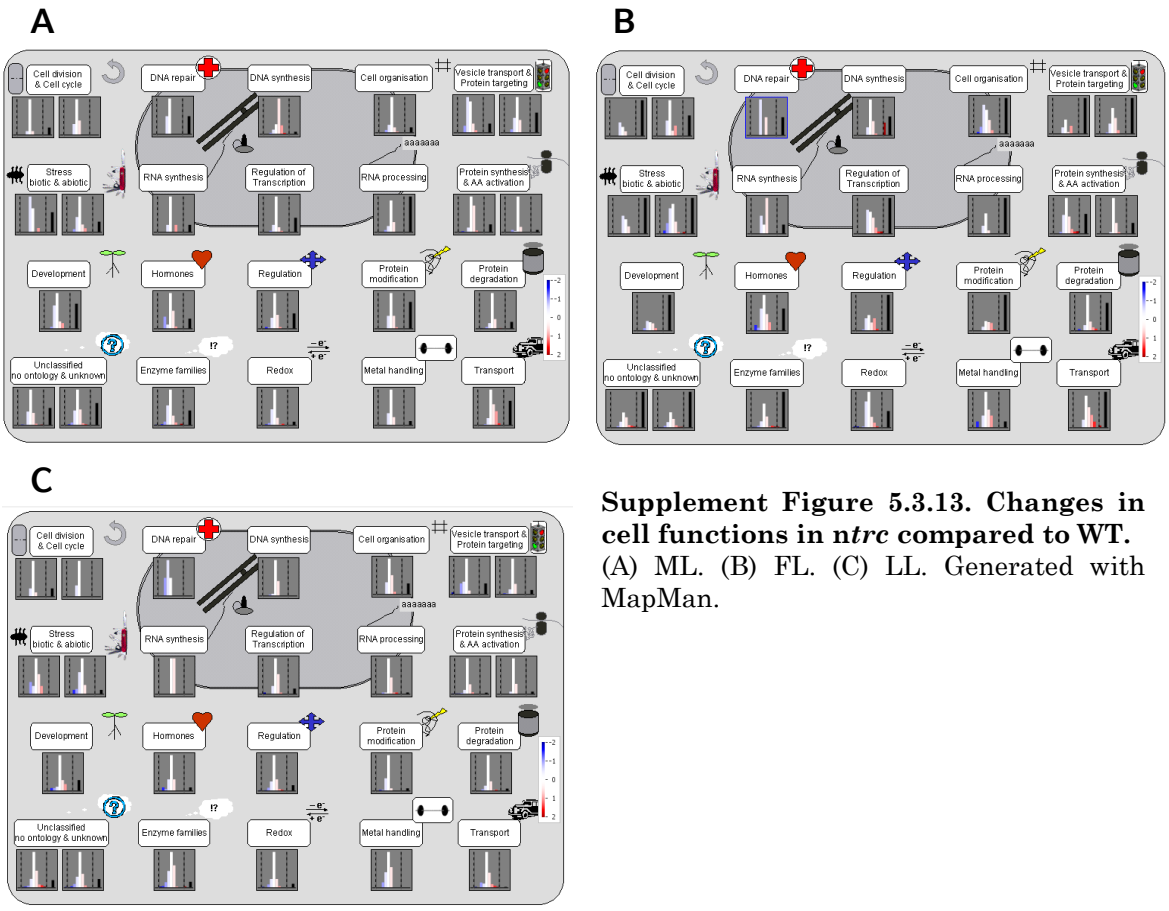

Supplement Figure 5.3.13. Changes in cell functions in n*trc* compared to WT. (A) ML. (B) FL. (C) LL. Generated with MapMan.

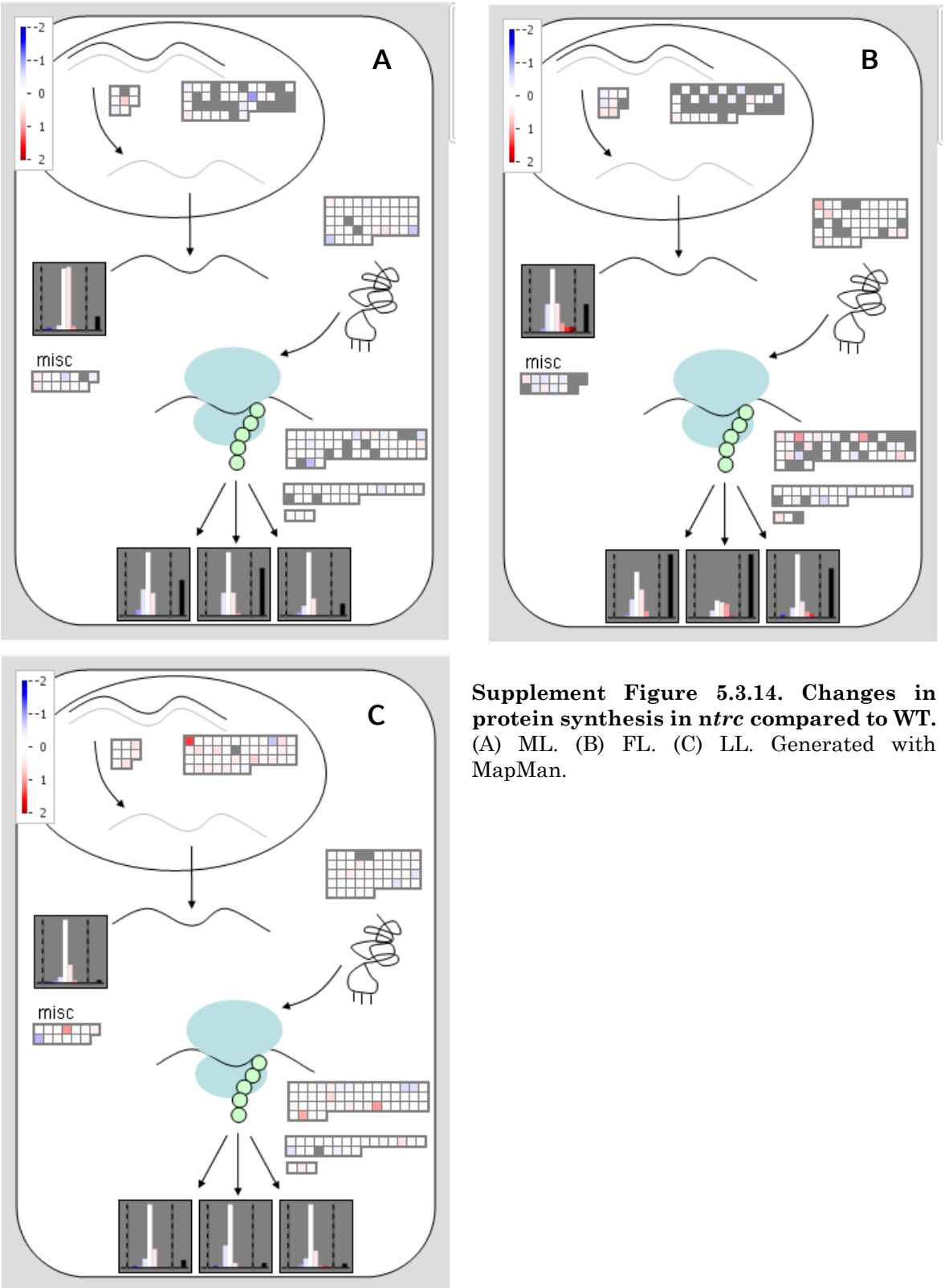

Supplement Figure 5.3.14. Changes in protein synthesis in n*trc* compared to WT. (A) ML. (B) FL. (C) LL. Generated with MapMan.

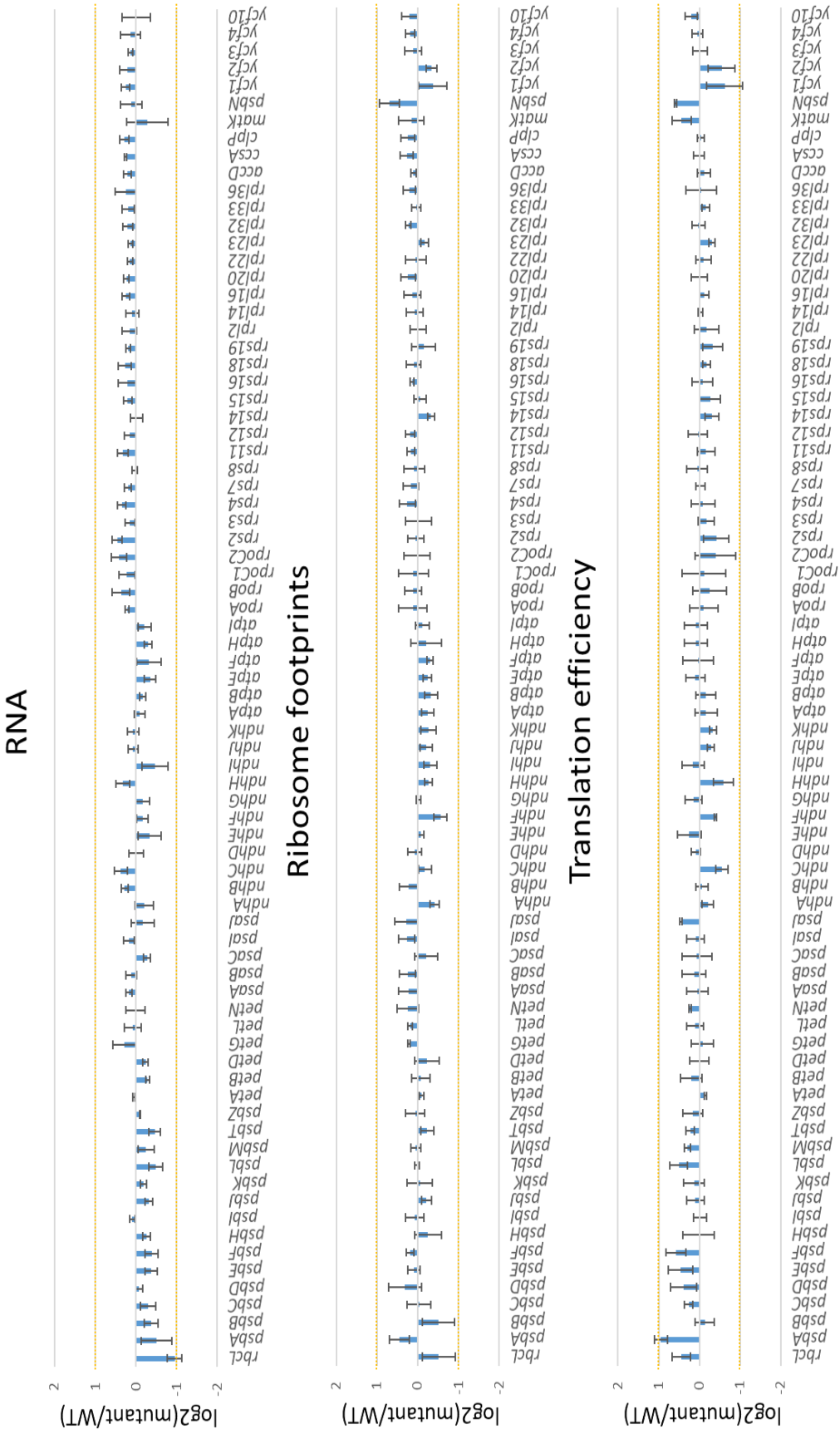

Supplement Figure 5.3.15. Changes in RNA, ribosome footprints and translation efficiency of chloroplast encoded genes in *ntrc* compared to WT under HL.

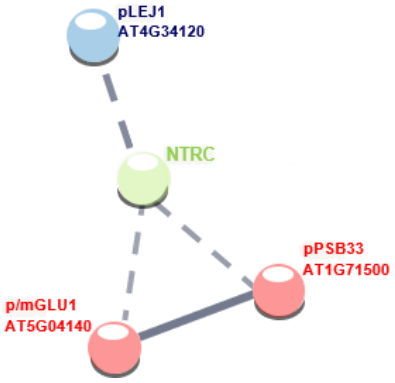

Supplement Figure 5.3.16. Network predictions of protein-protein interaction under ML.
The nodes represent NTRC among the significantly changed ($p < 0.001$, repeated t-test with Benjamini-Hochberg correction) proteins in *ntrc* relative to WT. Down-regulated proteins are given in blue, up-regulated in red. Unconnected nodes were disregarded. The thickness of the edges indicates the degree of confidence of the interaction (Szklarczyk et al., 2019, 2021). Dashed lines indicate an interaction in the WT in the presence of NTRC. Distances are arbitrary. Trivial names are given in capital letters. The subcellular location (SUBA4, consensus) is given in small letters ahead the protein name. m, mitochondrion; p, plastid.

5.4 Lists of raw data and statistics

Sample	N	Glutamate		Aspartate		Glycerate		Ru5P-Xu5P		Malate		Succinate		2OG		G6P		G1P		R5P		FBP		AMP		RuBP		S7P		DHAP		3PGA		2PG		SBP		ADP	
		mean	sd	mean	sd	mean	sd	mean	sd	mean	sd	mean	sd	mean	sd	mean	sd	mean	sd	mean	sd	mean	sd	mean	sd	mean	sd	mean	sd	mean	sd	mean	sd	mean	sd	mean	sd
WT HL 15 min	4	189.43	9.90	94.01	31.12	26.48	4.53	2.58	0.29	491.34	280.10	19.25	14.00	12.39	4.27	15.45	2.03	2.25	0.82	0.35	0.09	1.33	0.32	1.20	0.27	2.25	1.09	6.49	0.72	4.34	0.49	16.94	4.30	0.53	0.23	1.24	0.29	1.34	0.23
WT HL 3h	4	137.98	20.29	87.07	31.89	29.16	14.66	3.97	1.71	699.72	340.04	17.54	6.15	9.99	4.72	15.30	2.20	1.91	0.56	0.39	0.12	1.23	0.31	1.45	0.88	2.29	1.91	6.38	0.71	4.15	0.42	13.83	5.67	0.60	0.17	1.04	0.44	1.25	0.17
WT HL 3h 15 min	4	201.47	30.95	154.23	24.30	28.03	9.49	1.51	0.25	521.15	343.55	14.19	4.15	8.73	3.72	19.08	3.08	1.93	0.17	0.32	0.07	1.06	0.15	1.09	0.22	1.16	0.41	5.07	0.58	2.50	0.67	23.31	8.86	0.23	0.18	1.06	0.23	1.14	0.16
WT HL 6h	4	192.92	29.92	126.54	21.36	29.69	10.45	2.65	0.95	280.72	105.57	12.69	8.14	6.54	2.05	14.83	2.52	1.82	0.37	0.33	0.11	0.79	0.10	1.21	0.25	3.16	0.45	3.28	0.41	1.39	0.86	20.89	4.54	0.16	0.08	0.88	0.27	1.36	0.20
WT ML 15 min	4	223.49	29.06	147.75	32.72	33.63	14.26	3.19	0.95	579.17	389.36	24.77	11.00	12.65	6.58	17.32	1.75	2.10	0.78	0.30	0.04	0.61	0.12	1.75	1.04	1.62	1.26	3.11	0.83	2.01	0.91	13.22	5.41	0.16	0.08	0.61	0.27	1.33	0.28
WT ML 3h	4	240.26	50.42	173.31	66.86	39.10	22.19	1.76	0.23	644.49	200.40	21.03	5.61	10.86	2.87	16.04	3.75	1.99	0.33	0.33	0.15	0.77	0.21	1.63	1.17	1.73	0.19	4.93	3.88	2.56	2.00	18.49	7.75	0.22	0.29	0.66	0.22	1.16	0.16
WT ML 3h 15 min	4	136.61	25.60	94.00	15.07	16.28	2.07	0.90	0.23	356.32	224.77	10.87	4.95	6.39	1.70	11.46	2.49	1.32	0.67	0.18	0.05	0.68	0.20	0.67	0.17	1.17	0.54	2.40	0.35	1.40	0.46	8.97	1.65	0.14	0.01	0.83	0.40	0.87	0.08
WT ML 6h	4	191.72	70.56	161.61	28.96	25.51	10.19	1.63	0.27	570.98	216.08	19.94	16.12	8.53	2.28	16.37	6.55	2.47	1.20	0.28	0.11	0.80	0.33	0.90	0.26	2.41	0.77	3.54	2.14	1.82	1.50	18.06	7.78	0.12	0.06	0.50	0.17	1.00	0.21
WT t0	8	218.62	40.03	152.14	38.74	25.05	4.19	2.46	0.83	605.72	303.60	23.49	10.26	13.75	5.26	15.55	3.82	1.94	0.55	0.30	0.05	0.77	0.19	1.33	0.29	1.91	0.72	3.05	0.65	1.39	0.16	13.37	4.06	0.13	0.09	0.69	0.17	1.33	0.33
trxf HL 15 min	4	175.10	32.46	87.00	30.95	20.31	4.24	3.29	1.93	449.29	204.62	11.76	3.57	12.65	2.47	17.63	3.15	2.09	0.67	0.39	0.04	1.57	0.24	1.03	0.44	2.87	1.47	6.31	0.83	4.85	2.51	16.98	3.71	0.58	0.23	1.31	0.17	1.29	0.34
trxf HL 3h	4	150.00	25.55	92.18	49.84	30.18	14.94	3.68	0.51	587.94	425.70	10.03	3.29	8.98	2.49	18.06	2.47	2.65	0.55	0.47	0.03	1.74	0.42	1.26	0.54	2.78	1.50	9.61	1.75	5.93	1.75	21.87	6.33	0.34	0.15	1.88	1.08	1.33	0.28
trxf HL 3h 15 min	4	175.06	98.04	156.64	103.36	24.99	14.36	1.10	0.79	793.54	453.81	14.06	2.85	9.51	3.36	15.69	5.09	2.06	1.17	0.34	0.10	1.73	0.11	1.15	0.51	0.54	0.10	4.38	1.54	2.16	0.64	14.98	5.37	0.09	0.05	0.81	0.19	1.34	0.46
trxf HL 6h	4	200.51	54.69	133.04	52.19	16.87	7.60	1.64	1.12	540.09	519.97	16.37	3.43	8.23	3.30	17.86	3.66	2.15	0.40	0.35	0.08	2.17	0.77	1.01	0.44	1.18	0.35	3.43	0.75	2.73	0.86	11.74	3.99	0.14	0.06	1.12	0.43	1.16	0.50
trxf ML 15 min	4	207.12	37.75	154.19	40.11	31.62	9.07	2.09	0.85	458.17	202.08	13.94	3.23	8.05	2.16	13.81	2.59	2.28	1.29	0.32	0.08	1.30	0.33	1.54	0.45	0.74	0.41	4.17	1.21	1.70	0.91	11.72	6.09	0.20	0.11	0.86	0.25	1.22	0.24
trxf ML 3h	4	197.99	22.91	144.22	21.04	28.52	5.31	2.37	1.65	616.93	307.38	16.50	2.27	10.70	5.96	17.07	3.37	2.37	0.62	0.35	0.08	1.49	0.41	1.36	0.51	1.70	0.90	4.85	1.87	2.44	1.40	12.80	3.49	0.16	0.12	1.15	0.60	1.39	0.42
trxf ML 3h 15 min	4	129.32	29.18	96.61	28.45	14.42	6.09	0.75	0.27	362.11	239.90	13.69	7.59	4.62	2.15	10.99	2.90	1.28	0.38	0.20	0.04	0.96	0.07	0.58	0.16	0.77	0.28	2.63	0.50	1.28	0.36	8.56	1.71	0.09	0.06	0.55	0.16	0.65	0.12
trxf ML 6h	4	128.08	17.53	128.59	49.02	18.65	3.45	1.09	0.18	638.75	268.07	10.73	1.92	6.54	1.60	12.26	1.57	1.11	0.17	0.24	0.02	1.14	0.18	0.72	0.18	0.96	0.25	3.04	0.19	1.36	0.23	11.94	0.35	0.14	0.05	0.65	0.10	0.90	0.17
trxf t0	8	194.33	28.78	149.19	33.56	18.47	5.23	1.61	0.36	567.68	268.77	15.17	5.41	9.38	2.76	14.97	3.76	1.76	0.48	0.29	0.07	1.55	0.51	1.23	0.55	1.19	0.76	3.23	0.78	1.65	0.43	11.23	4.00	0.14	0.06	1.07	0.44	1.46	0.46
trxm HL 15 min	4	169.42	46.19	90.35	55.61	19.97	9.30	2.18	0.69	447.14	328.61	19.72	10.22	12.84	5.60	13.81	3.84	1.91	0.85	0.28	0.02	1.27	0.10	1.03	0.26	1.92	0.27	5.41	1.48	4.64	1.47	19.78	6.35	0.37	0.10	1.02	0.13	1.21	0.32
trxm HL 3h	4	190.78	41.11	120.06	51.07	25.13	8.66	3.85	1.44	799.42	371.01	20.65	8.02	15.54	6.15	17.57	4.38	1.65	0.63	0.33	0.07	1.29	0.43	1.32	0.36	2.68	2.01	6.60	3.46	4.66	2.63	16.73	7.42	0.65	0.38	0.94	0.21	1.32	0.34
trxm HL 3h 15 min	4	236.96	25.58	190.89	34.75	32.16	3.47	1.71	0.44	799.08	445.02	20.29	11.66	12.39	4.86	21.17	3.38	2.20	0.35	0.25	0.05	1.00	0.10	1.32	0.51	0.85	0.43	5.47	1.83	2.72	1.01	22.40	8.95	0.24	0.11	1.49	0.48	1.38	0.18
trxm ML 15 min	4	221.02	35.61	171.08	47.43	23.07	10.16	2.36	0.77	684.86	290.45	20.75	6.53	12.40	2.90	13.90	2.34	1.75	0.31	0.29	0.07	0.93	0.21	1.02	0.31	2.14	0.54	2.15	0.58	1.72	0.57	8.97	4.62	0.12	0.10	0.88	0.36	1.21	0.17
trxm ML 6h	4	241.09	65.62	190.03	74.06	23.60	5.09	2.11	0.78	565.05	197.28	20.02	4.05	14.69	2.37	15.40	4.78	1.88	0.79	0.29	0.10	0.80	0.35	1.37	0.32	1.95	1.67	3.14	1.31	1.41	0.47	14.32	9.27	0.15	0.07	0.98	0.45	1.35	0.30
trxm ML 3h	4	135.19	37.92	98.64	39.93	14.14	2.97	0.94	0.23	266.06	150.05	12.34	1.41	5.96	2.75	9.93	1.33	1.28	0.51	0.19	0.03	0.77	0.04	0.72	0.17	1.32	0.41	2.43	0.28	1.20	0.28	11.89	2.11	0.15	0.03	0.99	0.34	1.00	0.21
trxm ML 3h 15 min	4	162.35	41.12	122.48	43.12	15.71	7.90	1.08	0.53	378.24	253.40	14.98	6.03	8.53	4.48	10.42	1.25	1.05	0.23	0.18	0.04	0.49	0.14	0.86	0.47	1.23	0.33	2.01	0.79	0.84	0.14	7.65	0.91	0.09	0.04	0.59	0.19	0.82	0.26
trxm ML 6h	4	155.29	48.15	147.42	78.60	15.95	3.98	1.15	0.42	503.46	271.27	14.35	5.52	7.60	3.84	11.99	3.56	1.60	0.29	0.24	0.03	0.79	0.20	0.65	0.25	1.59	0.30	2.28	1.00	1.56	0.42	8.61	2.91	0.16	0.12	0.66	0.09	0.76	0.24
trxm t0	8	225.96	62.29	171.07	55.47	19.52	3.26	1.96	0.66	460.80	171.32	22.14	8.12	11.61	3.74	15.27	5.68	1.73	0.35	0.29	0.12	0.87	0.32	1.47	0.24	1.79	1.16	2.55	0.82	1.90	0.87	11.71	6.87	0.15	0.09	0.98	0.45	1.34	0.46
ntre HL 15 min	4	166.60	21.97	90.15	31.51	16.33	2.41	2.55	1.02	368.61	228.17	10.45	2.77	5.95	0.98	17.00	4.38	2.11	0.63	0.47	0.03	1.73	0.26	1.02	0.32	2.46	1.19	6.53	1.97	3.84	1.08	13.23	6.11	0.44	0.33	2.53	0.55	1.37	0.19
ntre HL 3h	4	162.49	15.68	127.87	27.05	25.97	12.70	3.76	1.69	712.55	165.99	10.06	2.86	7.26	0.69	20.29	4.94	2.85	0.85	0.48	0.11	1.76	0.24	1.06	0.37	2.49	1.75	7.99	1.56	4.57	1.80	19.37	16.10	0.57	0.28	2.57	0.60	1.43	0.41
ntre HL 3h 15 min	4	144.60	38.31	153.38	67.15	10.08	0.86	1.09	0.20	638.26	219.01	9.02	2.23	6.44	1.64	20.40	2.10	2.41	0.52	0.49	0.08	2.03	0.39	0.96	0.54	0.53	0.15	5.23	0.97	1.98	0.23	7.95	5.04	0.14	0.07	3.86	0.50	1.31	0.47
ntre HL 6h	4	202.29	30.58	156.49	49.79	10.72	3.78	1.84	0.35	723.37	396.64	11.02	1.25	7.30	1.30	23.59	3.67	2.85	0.41	0.61	0.04	2.08	0.17	1.14	0.56	0.79	0.28	6.30	1.03	2.41	0.61	6.16	1.47	0.13	0.08	3.99	1.55	1.29	0.44
ntre ML 15 min	4	221.73	48.01	154.35	40.92	21.26	17.23	2.10	0.82	577.28	345.56	12.30	5.55	7.37	2.90	18.79	4.42	2.29	0.14	0.48	0.12	1.31	0.44	1.25	0.33	0.70	0.16	6.34	1.59	2.46	1.18	7.98	2.17	0.14	0.11	2.79	1.67	1.22	0.38
ntre ML 3h	4	201.59	56.87	158.01	53.31	12.94	5.66	1.31	0.36	488.47	253.18	7.86	3.14	5.51	2.22	17.46	1.99	2.29	0.36	0.46	0.10	1.39	0.47	0.82	0.25	0.81	0.22	5.23	0.90	1.56	0.99	6.27	1.93	0.14	0.02	2.62	0.56	0.97	0.27
ntre ML 3h 15 min	4	142.84	5.17	95.61	28.36	8.75	1.77	0.99	0.32	371.05	267.47	6.84	2.19	3.64	1.24	13.54	3.52	1.60	0.33	0.31	0.10	1.11	0.20	0.51	0.13	0.82	0.34	3.52	0.50	1.34	0.07	5.48	0.85	0.11	0.06	2.13	0.50	0.76	0.19
ntre ML 6h	4	142.20	31.55	112.64	56.35	9.22	3.53	0.91	0.21	446.59	297.14	8.69	1.30	4.11	0.84	15.69	4.77	1.80	0.77	0.42	0.14	1.52	0.48	0.68	0.26	0.67	0.06	3.69	1.25	1.26	0.21	5.04	1.36	0.12	0.05	3.07	0.97	1.00	0.42
ntre t0	8	212.63	34.27	139.54	45.09	14.08	4.49	1.77	0.72	335.68	182.95	8.85	3.17	5.47	2.01	20.77	4.10	2.68	0.45	0.54	0.08	1.84	0.43	1.29	0.46	0.79	0.40	5.65	1.07	1.77	0.28	7.50	2.21	0.12	0.06	3.70	1.04	1.40	0.25

Supplement Table 5.4.1. Raw data of LC-MS based metabolite profile in WT, *trxf*, *trxm* and *ntrc* under short-term HL (de-)acclimation.

Samples were harvested after 14 days in the middle of the photoperiod under ML before the shift (t_0) and 15 min, 1h, 3h, 3h15min, 4h, 6h afterwards. HL samples after 3h represent the de-acclimation (ML again). Values are given as mean ± SD from n= 3 – 5 biological replicates.

Light	contrast	Time	Glutamate	Aspartate	Glycerate	Ru5P+Xu5P	Malate	Succinate	2OG	G6P	F6P	G1P	R5P	FBP	AMP	RuBP	S7P	DHAP	3PGA	2PG	SBP	ADP
ML	trxf - WT	t0	0.666	0.999	0.353	0.053	0.990	0.071	0.058	0.991	0.997	0.930	0.998	**0.000**	0.973	0.193	0.992	0.909	0.776	0.994	0.576	0.863
	trxm - WT	t0	0.986	0.843	0.508	0.422	0.660	0.978	0.595	0.999	0.604	0.897	0.997	0.921	0.930	0.985	0.861	0.563	0.881	0.990	0.755	1.000
	ntrc - WT	t0	0.992	0.947	**0.036**	0.158	0.149	**0.000**	**0.000**	**0.040**	0.109	0.064	**0.000**	**0.000**	0.999	**0.013**	**0.001**	0.769	0.052	0.995	**0.000**	0.976
	trxf - WT	15 min	0.948	0.997	0.984	0.088	0.905	0.110	0.234	0.572	1.000	0.973	0.992	**0.024**	0.917	0.309	0.640	0.946	0.965	0.890	0.934	0.965
	trxm - WT	15 min	0.936	0.565	0.288	0.100	1.000	0.748	0.833	0.894	0.887	0.947	0.999	0.849	0.656	0.916	1.000	0.698	0.986	1.000	0.821	1.000
	ntrc - WT	15 min	1.000	0.997	0.131	0.094	1.000	**0.049**	0.136	0.949	0.628	0.970	**0.019**	**0.023**	0.424	0.267	**0.003**	0.847	0.359	0.995	**0.000**	0.963
	trxf - WT	3h	0.501	0.808	0.243	0.551	0.999	0.775	1.000	0.981	0.965	0.788	0.989	**0.017**	0.833	1.000	1.000	0.996	0.287	0.801	0.657	0.725
	trxm - WT	3h	**0.004**	0.108	**0.000**	0.299	0.155	0.265	0.186	0.120	**0.004**	0.323	0.098	1.000	**0.032**	0.852	**0.034**	0.074	0.171	0.692	0.860	0.889
	ntrc - WT	3h	0.575	0.965	**0.000**	0.765	0.818	**0.034**	0.128	0.953	0.914	0.887	0.142	0.054	0.065	0.274	0.987	0.273	**0.001**	0.646	**0.000**	0.830
	trxf - WT	3h 15 min	0.995	1.000	0.987	0.988	1.000	0.933	0.883	0.998	0.977	1.000	0.995	0.625	0.993	0.860	0.995	0.996	0.999	0.888	0.905	0.743
	trxm - WT	3h 15 min	0.828	0.817	1.000	0.981	0.999	0.822	0.812	0.981	1.000	0.916	1.000	0.856	0.931	0.999	0.972	0.748	0.975	0.873	0.936	0.996
	ntrc - WT	3h 15 min	0.997	1.000	0.539	0.997	1.000	0.830	0.667	0.870	0.703	0.910	0.138	0.271	0.962	0.905	0.599	1.000	0.692	0.975	**0.014**	0.953
	trxf - WT	6h	0.158	0.741	0.615	0.646	0.981	0.218	0.842	0.437	0.990	**0.008**	0.912	0.467	0.950	**0.027**	0.943	0.842	0.226	0.989	0.984	0.969
	trxm - WT	6h	0.622	0.972	0.329	0.728	0.981	0.640	0.980	0.379	0.478	0.166	0.908	1.000	0.870	0.367	0.500	0.968	**0.020**	0.942	0.978	0.710
	ntrc - WT	6h	0.360	0.439	**0.024**	0.411	0.898	0.090	0.267	0.995	0.999	0.380	0.092	**0.016**	0.911	**0.005**	0.998	0.748	**0.001**	1.000	**0.000**	1.000
HL	trxf - WT	15 min	0.957	0.997	0.787	0.771	0.998	0.407	1.000	0.809	0.955	0.982	0.881	0.732	0.955	0.850	0.998	0.945	1.000	0.973	0.998	0.997
	trxm - WT	15 min	0.893	1.000	0.759	0.947	0.998	1.000	0.998	0.909	0.978	0.868	0.587	0.994	0.955	0.973	0.725	0.988	0.938	0.667	0.952	0.947
	ntrc - WT	15 min	0.850	0.999	0.425	1.000	0.956	0.267	0.061	0.920	1.000	0.989	0.136	0.306	0.944	0.993	1.000	0.949	0.874	0.927	**0.016**	0.999
	trxf - WT	3h	0.974	0.999	0.999	0.979	0.966	0.403	0.977	0.676	0.824	0.356	0.447	0.121	0.934	0.921	**0.016**	0.232	0.366	0.225	0.201	0.986
	trxm - WT	3h	0.255	0.772	0.929	0.999	0.975	0.915	0.133	0.792	0.995	0.930	0.716	0.992	0.976	0.957	0.996	0.946	0.935	0.979	0.995	0.989
	ntrc - WT	3h	0.822	0.637	0.963	0.992	1.000	0.408	0.697	0.190	0.234	0.164	0.313	0.097	0.624	0.993	0.415	0.969	0.673	0.998	**0.003**	0.854
	trxf - WT	3h 15 min	0.786	1.000	0.967	0.945	0.669	1.000	0.989	0.518	0.985	0.991	0.995	**0.023**	0.997	0.849	0.909	0.982	0.335	0.741	0.932	0.819
	trxm - WT	3h 15 min	0.595	0.711	0.924	0.992	0.654	0.582	0.468	0.829	0.887	0.932	0.545	0.990	0.888	0.977	0.980	0.995	0.998	1.000	0.739	0.718
	ntrc - WT	3h 15 min	0.198	1.000	**0.044**	0.941	0.961	0.702	0.796	0.949	0.998	0.711	**0.015**	**0.000**	0.981	0.845	0.999	0.942	**0.015**	0.914	**0.000**	0.873
	trxf - WT	6h	0.993	0.998	0.226	0.515	0.702	0.867	0.906	0.608	0.814	0.888	0.998	**0.000**	0.921	0.062	0.999	0.476	0.256	1.000	0.942	0.803
	trxm - WT	6h	0.753	0.569	0.749	0.979	0.342	0.342	0.102	0.981	0.994	0.998	0.844	0.923	0.935	0.551	0.696	0.984	0.085	0.994	1.000	0.904
	ntrc - WT	6h	0.987	0.819	**0.030**	0.681	0.264	0.985	0.990	**0.004**	0.169	0.113	**0.000**	**0.000**	0.995	**0.017**	**0.027**	0.691	**0.021**	0.996	**0.000**	0.987

Supplement Table 5.4.2. List of *p* values from LC-MS based short-term HL (de-)acclimated plants.
A 2-way ANOVA with *post-hoc* Tukey test was performed using the “emmeans” and “multcomp” packages from R. Values are given relative to the respective WT. Significances ($p < 0.05$) are given in bold.

Sample		WT_HL_15'	WT_HL_1h	WT_HL_3h	WT_HL_3h15'	WT_HL_4h	WT_HL_6h	WT_ML_15'	WT_ML_1h	WT_ML_3h	WT_ML_3h15'	WT_ML_4h	WT_ML_6h	WT_t0
N		5	5	4	5	5	4	5	5	5	5	5	5	9
adenine	mean	0.07	0.07	0.05	0.05	0.09	0.10	0.08	0.09	0.07	0.03	0.06	0.09	0.07
	sd	0.02	0.00	0.04	0.02	0.06	0.04	0.04	0.05	0.03	0.01	0.01	0.00	0.03
alanine	mean	31.32	17.09	57.27	41.51	29.84	24.63	16.35	16.39	17.34	20.32	15.14	17.13	18.04
	sd	15.16	5.95	28.16	6.68	11.19	9.48	1.15	2.48	1.57	4.28	3.04	6.00	5.33
beta-alanine	mean	0.16	0.20	0.22	0.23	0.27	0.33	0.17	0.23	0.40	0.27	0.24	0.30	0.15
	sd	0.05	0.05	0.04	0.06	0.05	0.08	0.05	0.02	0.16	0.07	0.04	0.02	0.05
ascorbic acid	mean	0.13	0.32	0.05	0.28	0.16	0.03	0.18	0.16	0.17	0.12	0.22	0.08	0.07
	sd	0.12	0.23	0.06	0.02	0.10	0.02	0.03	0.08	0.02	0.11	0.11	0.05	0.05
asparagine	mean	1.52	1.95	1.50	1.52	1.36	1.50	1.76	1.35	1.67	0.99	1.75	2.03	1.82
	sd	1.57	1.31	0.14	0.40	0.60	0.97	1.02	0.39	0.31	0.01	0.10	1.07	1.06
aspartic acid	mean	4.01	1.43	4.23	3.24	3.74	3.78	4.21	3.65	3.71	3.66	3.11	2.97	4.23
	sd	1.99	0.31	1.62	1.00	0.53	0.87	0.43	0.43	1.34	0.17	0.40	0.75	1.52
benzoic acid	mean	1.59	2.14	1.82	2.11	1.81	2.00	1.85	2.07	2.10	1.95	3.11	2.27	1.72
	sd	0.60	0.21	0.48	0.02	0.32	0.32	0.38	0.27	0.12	0.11	1.50	0.19	0.12
citric acid	mean	0.67	0.42	1.03	1.50	0.36	0.21	0.68	0.21	0.48	0.38	0.54	1.57	0.56
	sd	0.43	0.43	0.12	1.41	0.26	0.13	0.36	0.20	0.17	0.31	0.03	1.44	0.37
dehydroascorbic acid	mean	5.65	4.76	1.92	2.94	5.62	5.81	5.10	7.77	6.65	5.38	3.97	3.76	4.00
	sd	3.79	1.40	0.93	0.59	4.40	0.90	3.77	3.60	4.26	2.70	1.03	2.16	2.55
dehydroascorbic acid dimer	mean	2.48	2.15	0.86	1.62	2.11	2.15	2.16	2.83	2.84	2.71	2.13	1.86	1.77
	sd	1.36	0.62	0.42	0.26	1.51	0.33	1.30	0.65	1.45	1.12	0.47	0.91	0.94
erythritol/ erythrose	mean	0.35	0.36	0.35	0.47	0.47	0.58	0.39	0.42	0.50	0.48	0.45	0.45	0.37
	sd	0.11	0.10	0.07	0.09	0.13	0.09	0.13	0.08	0.06	0.06	0.14	0.13	0.14
fructose	mean	37.68	79.12	38.54	107.13	81.77	101.77	14.89	34.89	30.69	30.09	18.23	12.65	26.17
	sd	50.06	31.77	1.74	79.63	38.56	16.50	11.59	20.64	44.01	25.09	16.55	13.87	32.24
fucose	mean	1.86	2.12	1.45	1.76	2.23	2.44	1.97	2.12	2.18	2.03	2.06	2.07	1.80
	sd	0.66	0.41	0.05	0.20	0.58	0.33	0.72	0.86	0.78	0.37	0.61	0.55	0.57
fumaric acid	mean	162.46	342.31	414.66	361.22	490.04	602.79	190.95	291.10	420.95	338.46	218.53	368.35	264.13
	sd	26.79	125.70	64.91	42.73	118.78	141.29	62.20	169.47	227.07	166.99	49.38	185.33	47.73
galactinol	mean	12.14	14.86	11.30	13.78	12.09	14.73	11.89	12.19	13.05	11.65	14.93	16.80	11.20
	sd	4.47	0.75	0.21	0.48	1.64	2.08	3.58	0.25	0.93	0.46	3.84	3.43	2.57
galactonic acid	mean	0.21	0.20	0.14	0.16	0.16	0.12	0.12	0.32	0.19	0.22	0.20	0.17	0.08
	sd	0.07	0.11	0.04	0.04	0.02	0.08	0.14	0.03	0.16	0.06	0.04	0.07	0.07
gaba	mean	1.29	1.09	1.17	1.61	1.76	2.09	1.12	1.46	1.57	1.73	1.32	2.36	1.20
	sd	0.27	0.02	0.11	0.11	0.66	0.42	0.39	0.38	0.06	0.43	0.32	0.99	0.15
glucose	mean	40.81	152.46	108.80	209.90	196.16	235.09	46.46	87.07	72.86	96.45	71.38	42.46	75.38
	sd	41.38	49.96	14.49	120.01	69.27	29.44	26.55	46.99	87.48	57.78	53.97	34.31	81.11
glutamic acid	mean	18.48	10.08	11.70	8.83	16.51	21.34	16.31	22.76	12.34	18.44	10.71	8.84	14.23
	sd	4.66	1.30	4.21	3.41	6.92	2.67	6.88	10.36	5.01	9.15	8.06	5.54	6.34
glutamine	mean	7.22	4.57	33.70	8.04	10.93	15.25	5.67	11.68	3.64	12.35	4.34	2.04	5.02
	sd	2.92	2.30	15.31	3.60	2.15	3.00	4.70	5.35	3.35	10.89	5.40	1.74	4.75
2-oxo-glutaric acid	mean	0.09	0.05	0.06	0.05	0.07	0.04	0.12	0.06	0.09	0.05	0.03	0.04	0.08
	sd	0.00	0.02	0.02	0.02	0.02	0.03	0.02	0.00	0.01	0.02	0.01	0.03	0.05
glyceric acid	mean	0.68	0.54	0.60	0.91	0.88	0.99	0.52	0.73	0.69	0.88	0.69	1.18	0.61
	sd	0.13	0.00	0.06	0.16	0.32	0.20	0.18	0.17	0.12	0.20	0.14	0.49	0.09
glycerol	mean	2.53	4.31	2.16	4.64	2.90	2.86	2.81	3.66	3.00	2.62	5.18	4.58	2.50
	sd	0.16	0.50	0.12	0.67	0.54	0.50	0.33	1.40	1.05	0.10	1.53	0.42	0.35
glycine	mean	29.92	41.37	331.76	209.13	126.12	130.96	9.13	12.63	11.90	20.91	9.92	10.90	8.72
	sd	1.90	10.46	66.41	104.40	102.60	85.52	2.18	1.02	4.13	0.75	2.59	1.84	2.50
histidine	mean	0.05	0.05	0.01	0.04	0.02	0.06	0.01	0.08	0.03	0.03	0.08	0.02	0.04
	sd	0.01	0.02	0.01	0.03	0.01	0.03	0.01	0.07	0.01	0.01	0.03	0.01	0.03
homoserine	mean	0.12	0.10	0.20	0.15	0.12	0.16	0.06	0.07	0.08	0.06	0.05	0.08	0.04
	sd	0.05	0.05	0.07	0.01	0.05	0.07	0.02	0.02	0.03	0.03	0.02	0.02	0.03
myo-inositol	mean	17.40	20.38	10.17	17.76	26.81	32.44	12.79	22.51	23.55	21.34	20.92	22.33	16.09
	sd	11.96	5.16	0.24	7.31	14.58	1.53	5.41	13.07	15.37	6.72	13.95	9.58	8.88

Sample		trxf_HL_15'	trxf_HL_1h	trxf_HL_3h	trxf_HL_3h15'	trxf_HL_4h	trxf_HL_6h	trxf_ML_15'	trxf_ML_1h	trxf_ML_3h	trxf_ML_3h15'	trxf_ML_4h	trxf_ML_6h	trxf_t0
N		5	5	5	5	5	5	5	5	5	5	5	5	10
adenine	mean	0.10	0.03	0.05	0.02	0.11	0.13	0.07	0.03	0.05	0.06	0.05	0.06	0.06
	sd	0.06	0.03	0.03	0.01	0.10	0.07	0.01	0.00	0.00	0.03	0.03	0.02	0.04
alanine	mean	20.67	22.41	79.22	37.22	59.24	28.79	29.70	23.96	15.52	21.00	19.26	20.76	15.95
	sd	5.65	6.91	66.50	10.57	34.19	10.36	14.47	6.76	1.65	0.93	7.23	1.71	3.78
beta-alanine	mean	0.18	0.23	0.29	0.26	0.27	0.33	0.22	0.24	0.28	0.33	0.32	0.34	0.17
	sd	0.04	0.05	0.08	0.04	0.01	0.01	0.06	0.04	0.06	0.06	0.02	0.04	0.07
ascorbic acid	mean	0.16	0.21	0.14	0.40	0.19	0.05	0.15	0.17	0.16	0.17	0.27	0.11	0.09
	sd	0.08	0.08	0.01	0.31	0.05	0.00	0.08	0.05	0.07	0.02	0.20	0.03	0.09
asparagine	mean	1.71	1.83	1.16	1.30	1.29	2.16	1.32	1.31	2.48	0.91	1.04	2.00	1.84
	sd	0.09	0.70	0.68	0.44	0.38	1.21	0.25	0.61	0.52	0.66	0.53	0.35	0.66
aspartic acid	mean	2.37	1.70	4.51	2.39	9.30	3.86	7.35	4.79	3.62	3.00	6.46	4.56	3.63
	sd	0.90	0.24	3.73	0.63	6.39	0.69	3.42	2.74	1.31	0.54	5.53	1.65	0.95
benzoic acid	mean	1.63	1.73	1.61	1.96	1.67	1.72	1.73	1.60	1.92	1.67	2.09	2.24	1.77
	sd	0.20	0.23	0.07	0.04	0.20	0.30	0.21	0.06	0.01	0.15	0.30	0.14	0.27
citric acid	mean	0.47	0.72	0.95	0.50	2.25	0.40	0.83	0.40	0.56	0.13	0.93	4.82	0.56
	sd	0.34	0.54	0.95	0.26	1.65	0.28	0.63	0.21	0.35	0.01	0.60	3.92	0.29
dehydroascorbic acid	mean	5.61	3.99	4.51	4.64	4.66	4.97	5.36	4.42	5.75	9.09	2.86	3.56	3.51
	sd	2.80	1.25	2.70	1.98	2.50	3.46	1.03	0.12	3.19	0.13	0.23	1.93	2.26
dehydroascorbic acid dimer	mean	2.28	2.02	1.84	2.16	1.93	1.90	2.39	2.43	2.45	3.95	1.96	1.73	1.56
	sd	1.00	0.66	1.00	0.71	0.83	1.26	0.30	0.10	1.18	0.06	0.35	0.75	0.86
erythritol/ erythrose	mean	0.35	0.46	0.47	0.48	0.45	0.39	0.46	0.42	0.44	0.33	0.52	0.51	0.40
	sd	0.05	0.18	0.11	0.04	0.02	0.09	0.11	0.09	0.10	0.09	0.06	0.12	0.11
fructose	mean	31.02	73.42	82.53	119.30	69.98	76.98	21.70	16.66	53.56	43.44	20.33	24.77	7.16
	sd	24.57	54.54	68.57	79.61	58.22	45.79	19.01	15.81	46.16	27.27	1.15	28.47	2.73
fucose	mean	1.96	2.24	1.77	1.96	1.83	2.38	1.99	1.65	2.21	2.05	1.71	2.15	1.57
	sd	0.31	0.67	0.21	0.34	0.39	0.37	0.32	0.21	0.55	0.26	0.18	0.46	0.24
fumaric acid	mean	281.69	345.30	396.58	442.96	478.85	520.10	323.06	229.56	379.45	338.88	425.52	385.33	224.20
	sd	89.56	136.87	36.50	50.60	48.14	142.58	1.01	99.92	116.67	94.82	87.46	140.94	22.09
galactinol	mean	12.18	17.59	12.04	17.12	12.01	13.22	13.36	12.89	15.13	11.40	15.19	17.98	11.24
	sd	0.11	3.84	0.54	0.48	1.72	0.81	0.91	0.47	3.56	0.76	0.30	3.01	3.42
galactonic acid	mean	0.19	0.16	0.16	0.20	0.16	0.20	0.15	0.17	0.21	0.21	0.15	0.15	0.16
	sd	0.03	0.10	0.00	0.03	0.04	0.02	0.09	0.04	0.07	0.13	0.11	0.08	0.08
gaba	mean	0.98	1.02	1.18	1.27	1.13	1.13	1.43	0.99	1.35	1.25	1.74	2.07	0.84
	sd	0.14	0.11	0.24	0.18	0.14	0.28	0.56	0.26	0.54	0.30	0.49	0.31	0.17
glucose	mean	71.01	141.95	176.67	230.63	160.90	190.20	56.60	39.92	132.44	115.12	69.64	60.09	24.84
	sd	46.70	99.44	117.19	103.19	106.36	71.71	43.32	28.14	104.18	69.39	45.15	59.34	3.79
glutamic acid	mean	15.31	5.96	17.40	6.80	23.41	18.27	15.89	15.20	10.27	16.49	5.77	7.64	10.26
	sd	3.48	2.52	6.64	3.62	13.21	6.32	3.36	0.65	3.14	4.23	1.01	4.36	3.18
glutamine	mean	6.06	2.67	33.97	6.65	23.85	16.42	6.49	3.52	6.96	10.86	1.59	3.30	2.26
	sd	2.58	1.27	20.78	3.75	17.05	7.70	1.01	1.12	4.12	7.31	0.21	2.61	0.81
2-oxo-glutaric acid	mean	0.08	0.08	0.06	0.06	0.08	0.05	0.11	0.07	0.06	0.03	0.04	0.05	0.07
	sd	0.03	0.04	0.05	0.02	0.00	0.02	0.08	0.01	0.02	0.02	0.03	0.03	0.02
glyceric acid	mean	0.53	0.52	0.64	0.68	0.59	0.55	0.72	0.50	0.69	0.62	0.91	1.13	0.43
	sd	0.08	0.04	0.14	0.12	0.04	0.19	0.30	0.12	0.25	0.17	0.25	0.08	0.06
glycerol	mean	2.15	3.85	2.17	4.51	3.35	2.94	3.42	2.48	2.69	2.52	4.38	4.52	2.52
	sd	0.09	0.23	0.03	0.76	0.48	0.31	0.58	0.35	0.52	0.51	0.25	0.87	0.34
glycine	mean	32.14	52.53	298.46	185.69	269.03	123.99	14.03	12.31	17.89	19.51	26.86	24.46	9.85
	sd	3.47	4.38	128.19	121.67	135.40	71.86	6.07	3.17	7.04	4.09	13.08	4.81	2.32
histidine	mean	0.03	0.03	0.03	0.05	0.03	0.03	0.03	0.08	0.05	0.07	0.03	0.08	0.05
	sd	0.01	0.02	0.02	0.04	0.01	0.01	0.01	0.02	0.04	0.05	0.02	0.03	0.02
homoserine	mean	0.05	0.11	0.29	0.12	0.25	0.13	0.12	0.14	0.05	0.06	0.07	0.12	0.05
	sd	0.03	0.07	0.18	0.06	0.14	0.02	0.09	0.07	0.02	0.03	0.03	0.04	0.04
myo-inositol	mean	22.47	25.91	18.17	24.23	19.00	23.14	22.08	11.68	24.06	24.38	20.52	24.29	12.31
	sd	9.79	14.92	8.45	10.78	10.50	0.68	6.82	0.91	14.79	8.56	7.86	12.17	4.43

Sample		trxm_HL_15'	trxm_HL_1h	trxm_HL_3h	trxm_HL_3h15'	trxm_HL_4h	trxm_HL_6h	trxm_ML_15'	trxm_ML_1h	trxm_ML_3h	trxm_ML_3h15'	trxm_ML_4h	trxm_ML_6h	trxm_t0
N		5	5	5	5	5	5	5	5	4	5	4	5	10
adenine	mean	0.05	0.03	0.12	0.07	0.07	0.10	0.05	0.05	0.19	0.04	0.04	0.06	0.07
	sd	0.04	0.02	0.10	0.04	0.01	0.01	0.02	0.03	0.18	0.03	0.02	0.05	0.03
alanine	mean	27.64	15.88	23.71	60.28	53.78	28.78	14.60	15.43	16.21	22.61	15.15	18.70	17.43
	sd	12.89	2.38	7.27	36.19	35.25	0.77	0.81	6.95	4.79	5.45	2.70	3.34	4.54
beta-alanine	mean	0.16	0.18	0.31	0.28	0.25	0.33	0.19	0.18	0.33	0.32	0.30	0.38	0.17
	sd	0.02	0.01	0.08	0.04	0.08	0.05	0.02	0.09	0.07	0.03	0.06	0.09	0.05
ascorbic acid	mean	0.12	0.26	0.07	0.27	0.10	0.05	0.20	0.16	0.19	0.11	0.34	0.22	0.07
	sd	0.07	0.11	0.01	0.12	0.05	0.01	0.01	0.07	0.03	0.03	0.16	0.20	0.06
asparagine	mean	1.41	1.42	0.91	1.13	1.66	2.05	1.28	0.68	1.54	0.72	1.01	1.33	1.68
	sd	0.93	0.39	0.79	0.85	0.78	0.34	0.66	0.41	0.28	0.31	0.36	0.07	0.72
aspartic acid	mean	5.13	1.41	4.16	5.30	6.89	5.97	4.32	4.39	7.32	4.67	6.69	5.99	4.06
	sd	2.75	0.34	2.51	4.25	4.25	3.04	0.06	1.99	4.49	0.98	7.63	4.20	0.96
benzoic acid	mean	1.69	1.81	1.59	2.22	1.78	1.84	1.71	1.99	1.84	1.77	1.89	2.07	1.81
	sd	0.43	0.14	0.38	0.13	0.13	0.02	0.18	0.16	0.48	0.22	0.46	0.16	0.32
citric acid	mean	1.73	0.68	0.45	0.85	1.06	0.41	0.92	0.60	0.63	0.48	3.24	1.86	0.55
	sd	1.48	0.44	0.22	0.51	0.96	0.18	0.61	0.34	0.51	0.32	5.22	1.66	0.29
dehydroascorbic acid	mean	5.23	4.23	2.69	3.50	3.01	1.83	5.16	5.37	6.47	5.61	4.10	4.02	3.71
	sd	2.73	0.86	0.36	0.92	0.09	0.22	3.12	3.81	1.83	3.16	1.19	1.80	1.61
dehydroascorbic acid dimer	mean	2.31	2.04	1.10	1.65	1.27	0.91	2.19	2.43	2.82	2.72	2.14	2.00	1.65
	sd	0.85	0.49	0.28	0.12	0.31	0.10	1.09	1.38	0.19	1.20	0.43	0.63	0.48
erythritol/ erythrose	mean	0.38	0.42	0.45	0.57	0.45	0.46	0.43	0.51	0.54	0.55	0.47	0.39	0.49
	sd	0.13	0.10	0.12	0.01	0.14	0.01	0.07	0.05	0.04	0.07	0.11	0.12	0.06
fructose	mean	27.71	61.36	34.67	81.95	32.88	20.08	12.69	27.34	22.36	22.56	47.77	19.63	13.89
	sd	27.59	28.23	16.43	48.32	12.16	1.84	10.01	32.89	24.07	19.99	62.40	26.44	16.75
fucose	mean	1.84	2.02	1.91	1.72	1.46	1.96	1.68	1.55	1.90	1.87	1.86	1.89	1.86
	sd	0.43	0.25	0.10	0.26	0.10	0.20	0.33	0.86	0.35	0.45	0.51	0.49	0.39
fumaric acid	mean	285.32	402.58	361.91	460.56	395.72	379.34	222.50	274.83	362.35	383.31	328.74	343.95	274.53
	sd	144.85	99.41	94.37	11.47	29.27	83.95	84.46	163.53	83.51	33.20	191.99	153.08	86.01
galactinol	mean	12.83	15.39	12.15	14.78	9.42	13.32	11.40	11.63	14.57	11.42	14.38	16.29	12.72
	sd	2.37	2.20	2.35	2.29	0.53	0.65	1.68	6.01	1.02	2.71	3.15	4.19	1.84
galactonic acid	mean	0.23	0.12	0.20	0.18	0.12	0.03	0.16	0.16	0.15	0.18	0.13	0.07	0.19
	sd	0.09	0.10	0.00	0.01	0.01	0.02	0.05	0.13	0.11	0.09	0.08	0.06	0.12
gaba	mean	1.07	0.92	1.32	1.51	0.92	1.36	0.89	0.97	1.41	1.48	1.40	1.64	0.88
	sd	0.12	0.06	0.28	0.17	0.02	0.48	0.34	0.42	0.08	0.68	0.29	0.61	0.20
glucose	mean	74.52	133.64	146.84	184.35	101.37	93.86	34.71	61.74	59.65	72.15	107.55	46.87	42.38
	sd	69.86	51.29	76.14	75.87	35.36	41.36	19.76	70.70	61.82	50.44	114.96	56.79	46.66
glutamic acid	mean	21.71	7.52	15.93	9.05	15.14	15.77	14.95	19.44	14.41	18.47	8.81	7.52	14.11
	sd	4.75	4.08	4.44	2.56	5.37	6.50	6.49	2.40	0.61	4.49	3.59	4.59	5.58
glutamine	mean	5.84	3.22	11.36	6.35	11.38	6.97	2.45	4.33	3.39	5.48	2.78	1.90	2.85
	sd	1.77	2.00	4.61	2.61	3.92	0.92	0.88	3.00	1.09	3.23	2.96	1.75	2.11
2-oxo-glutaric acid	mean	0.09	0.06	0.04	0.06	0.07	0.08	0.09	0.08	0.14	0.09	0.06	0.08	0.07
	sd	0.02	0.02	0.02	0.03	0.04	0.06	0.04	0.00	0.07	0.05	0.06	0.05	0.04
glyceric acid	mean	0.55	0.47	0.69	0.78	0.49	0.66	0.45	0.50	0.70	0.75	0.74	0.84	0.41
	sd	0.08	0.01	0.15	0.05	0.01	0.22	0.19	0.23	0.06	0.33	0.11	0.33	0.12
glycerol	mean	2.63	4.17	2.16	4.40	2.75	2.61	2.97	2.49	2.43	2.52	4.25	4.30	2.45
	sd	0.31	0.10	0.12	0.14	0.09	0.17	0.13	0.25	0.29	0.23	0.30	0.30	0.34
glycine	mean	27.53	43.40	147.96	230.36	263.05	149.37	6.90	7.05	8.97	19.17	20.60	11.70	6.23
	sd	6.16	1.17	81.85	161.64	150.82	10.93	1.07	2.51	0.54	11.41	22.89	0.29	1.32
histidine	mean	0.03	0.03	0.04	0.05	0.07	0.05	0.04	0.08	0.07	0.06	0.04	0.04	0.03
	sd	0.02	0.01	0.04	0.03	0.04	0.04	0.02	0.02	0.04	0.05	0.02	0.02	0.02
homoserine	mean	0.11	0.10	0.14	0.21	0.24	0.17	0.06	0.09	0.06	0.10	0.07	0.08	0.06
	sd	0.07	0.04	0.05	0.11	0.12	0.04	0.00	0.08	0.02	0.08	0.04	0.04	0.02
myo-inositol	mean	17.74	20.64	16.17	20.72	11.01	15.27	17.91	20.59	22.80	21.12	21.81	21.44	18.68
	sd	8.43	7.10	4.48	10.91	2.12	4.47	11.61	18.94	12.77	12.06	12.95	15.38	9.30

Sample		ntrc_HL_15'	ntrc_HL_1h	ntrc_HL_3h	ntrc_HL_3h15'	ntrc_HL_4h	ntrc_HL_6h	ntrc_ML_15'	ntrc_ML_1h	ntrc_ML_3h	ntrc_ML_3h15'	ntrc_ML_4h	ntrc_ML_6h	ntrc_t0
N		5	5	4	4	5	5	5	5	4	5	5	5	10
adenine	mean	0.04	0.08	0.09	0.07	0.07	0.11	0.07	0.04	0.96	0.04	0.10	0.08	0.07
	sd	0.02	0.05	0.04	0.03	0.02	0.01	0.01	0.01	0.61	0.01	0.06	0.04	0.04
alanine	mean	23.03	33.36	66.15	69.43	28.72	26.92	15.46	21.04	17.29	16.74	12.75	12.92	12.93
	sd	8.50	17.73	16.83	10.76	7.94	13.60	3.32	8.59	7.45	2.69	1.35	0.65	1.68
beta-alanine	mean	0.33	0.29	0.40	0.34	0.35	0.44	0.28	0.38	0.55	0.50	0.47	0.54	0.30
	sd	0.03	0.09	0.16	0.04	0.04	0.08	0.07	0.08	0.20	0.11	0.14	0.16	0.09
ascorbic acid	mean	0.22	0.21	0.09	0.16	0.17	0.01	0.12	0.20	0.14	0.14	0.48	0.19	0.11
	sd	0.10	0.11	0.05	0.04	0.07	0.00	0.05	0.03	0.08	0.09	0.35	0.09	0.09
asparagine	mean	1.77	2.71	1.54	2.20	2.66	5.63	2.15	1.71	3.74	0.83	2.35	2.91	3.29
	sd	0.42	2.11	0.60	0.34	1.33	1.56	1.12	0.44	1.72	0.08	0.72	0.09	1.03
aspartic acid	mean	4.08	3.67	6.51	5.57	3.63	4.98	5.46	4.85	5.85	4.13	5.00	4.05	4.10
	sd	1.86	1.33	1.61	1.28	1.07	1.60	0.07	1.71	3.12	1.95	1.49	1.62	0.96
benzoic acid	mean	1.50	1.96	1.46	2.08	1.92	1.73	1.92	1.82	1.36	1.71	2.30	2.26	1.67
	sd	0.17	0.02	0.11	0.22	0.25	0.07	0.18	0.13	0.13	0.27	0.35	0.19	0.26
citric acid	mean	0.62	0.69	1.15	0.91	0.15	0.34	0.62	0.45	0.47	0.25	5.64	1.53	0.25
	sd	0.44	0.38	0.69	0.47	0.11	0.28	0.27	0.37	0.37	0.20	6.65	1.57	0.17
dehydroascorbic acid	mean	5.87	3.18	3.14	2.73	6.60	4.13	3.44	5.92	4.40	6.90	5.02	3.93	6.32
	sd	3.27	1.88	0.51	0.55	4.12	3.19	1.85	3.85	1.73	4.86	2.35	1.25	3.92
dehydroascorbic acid dimer	mean	2.53	1.60	1.56	1.75	2.51	1.68	1.58	2.77	2.21	3.26	2.55	1.74	2.52
	sd	0.97	0.69	0.34	0.31	1.34	1.05	0.68	1.47	0.80	1.90	0.81	0.21	1.42
erythritol/ erythrose	mean	0.56	0.65	0.62	0.65	0.71	0.52	0.61	0.58	0.66	0.63	0.71	0.68	0.58
	sd	0.08	0.13	0.06	0.04	0.02	0.14	0.11	0.12	0.11	0.09	0.06	0.19	0.08
fructose	mean	23.57	41.62	26.54	30.81	113.60	53.52	5.54	25.77	7.08	39.55	24.59	49.70	25.30
	sd	23.02	30.30	6.41	6.15	62.00	54.92	1.85	29.37	5.52	33.28	21.71	52.20	40.05
fucose	mean	1.87	1.69	1.58	1.57	1.88	1.96	1.65	1.79	1.49	1.81	1.76	2.17	1.71
	sd	0.41	0.34	0.15	0.30	0.42	0.33	0.28	0.36	0.25	0.42	0.12	0.41	0.35
fumaric acid	mean	229.62	195.30	277.30	247.90	413.06	294.25	221.58	155.44	181.04	184.55	192.68	302.63	207.93
	sd	68.21	1.52	51.38	54.03	19.71	73.96	32.99	22.88	83.77	38.30	2.10	140.59	77.55
galactinol	mean	11.42	13.15	10.50	12.03	11.07	11.93	11.30	11.33	11.75	9.12	13.96	17.63	10.98
	sd	2.26	2.21	2.07	3.14	1.63	0.47	2.08	1.20	1.85	0.85	1.13	3.80	0.73
galactonic acid	mean	0.29	0.11	0.19	0.15	0.24	0.19	0.21	0.21	0.17	0.25	0.18	0.12	0.16
	sd	0.13	0.08	0.06	0.05	0.05	0.05	0.02	0.06	0.04	0.12	0.04	0.06	0.10
gaba	mean	0.76	0.79	0.96	0.75	0.60	0.71	0.69	0.71	0.81	0.79	0.86	1.15	0.58
	sd	0.09	0.00	0.10	0.16	0.09	0.10	0.01	0.01	0.25	0.09	0.18	0.38	0.20
glucose	mean	66.72	73.12	58.71	60.16	211.05	100.86	19.68	60.51	21.64	91.17	52.77	123.61	54.95
	sd	58.81	58.05	15.20	14.94	107.37	89.68	1.07	59.87	14.24	71.70	42.75	116.24	70.08
glutamic acid	mean	22.88	15.51	17.02	5.80	15.24	21.23	13.21	18.57	12.43	16.83	7.21	7.13	17.78
	sd	7.84	13.13	4.77	1.11	5.23	12.64	5.73	2.14	3.13	3.97	4.46	3.24	7.52
glutamine	mean	6.25	9.69	23.00	3.29	20.82	25.03	3.27	6.52	3.45	15.17	2.40	2.70	9.00
	sd	1.64	10.72	5.85	0.43	4.54	20.82	0.66	5.52	1.55	14.27	1.73	2.10	11.65
2-oxo-glutaric acid	mean	0.06	0.04	0.06	0.04	0.09	0.01	0.07	0.06	0.03	0.05	0.06	0.06	0.04
	sd	0.02	0.02	0.06	0.02	0.03	0.00	0.04	0.02	0.01	0.04	0.03	0.03	0.04
glyceric acid	mean	0.39	0.42	0.54	0.38	0.31	0.34	0.36	0.36	0.38	0.42	0.49	0.56	0.31
	sd	0.06	0.05	0.07	0.09	0.05	0.02	0.00	0.03	0.12	0.05	0.03	0.13	0.07
glycerol	mean	2.14	4.06	2.16	6.80	4.10	3.07	3.23	3.28	2.40	2.35	3.98	4.66	2.59
	sd	0.05	0.30	0.22	4.25	0.73	0.68	0.35	1.03	0.04	0.09	0.16	0.44	0.46
glycine	mean	24.96	56.60	222.05	169.61	91.07	110.02	7.23	9.76	13.39	11.50	10.64	9.03	7.19
	sd	1.39	19.40	14.17	18.42	33.54	53.11	1.49	0.90	5.51	2.24	1.57	1.78	1.19
histidine	mean	0.04	0.06	0.03	0.03	0.02	0.04	0.03	0.05	0.04	0.05	0.06	0.03	0.05
	sd	0.01	0.03	0.01	0.02	0.02	0.02	0.00	0.00	0.01	0.03	0.00	0.01	0.05
homoserine	mean	0.06	0.12	0.17	0.17	0.13	0.11	0.07	0.05	0.07	0.05	0.09	0.05	0.04
	sd	0.02	0.06	0.04	0.04	0.07	0.06	0.06	0.02	0.04	0.02	0.05	0.03	0.02
myo-inositol	mean	16.14	12.34	8.75	8.67	15.93	11.46	12.67	12.49	10.31	15.50	14.95	22.30	12.68
	sd	7.49	4.55	0.85	2.45	5.83	4.23	3.70	3.90	3.76	6.91	5.98	11.68	5.93

Supplement Table 5.4.3. Raw data of GC-MS based central metabolite profile in WT, *trxf*, *trxm* and *ntrc* under short-term HL (de-)acclimation. Samples were harvested after 14 days in the middle of the photoperiod under ML before the shift (t_0) and 15 min, 1h, 3h, 3h15min, 4h, 6h afterwards. HL samples after 3h represent the de-acclimation (ML again). Values are given as mean ± SD from n= 3 – 5 biological replicates.

Sample		WT_HL_15'	WT_HL_1h	WT_HL_3h	WT_HL_3h15'	WT_HL_4h	WT_HL_6h	WT_ML_15'	WT_ML_1h	WT_ML_3h	WT_ML_3h15'	WT_ML_4h	WT_ML_6h	WT_t0
N		5	5	4	5	5	4	5	5	5	5	5	5	9
isoleucine	mean	2.40	2.93	1.46	1.63	1.70	2.32	1.22	1.92	2.62	2.21	2.79	2.04	2.01
	sd	1.54	1.55	0.15	0.46	1.03	1.40	0.27	0.60	1.75	0.87	1.31	0.54	1.57
lactic acid	mean	0.01	0.02	0.01	0.01	0.02	0.01	0.02	0.01	0.02	0.01	0.02	0.01	0.01
	sd	0.00	0.00	0.01	0.01	0.01	0.00	0.01	0.00	0.01	0.01	0.02	0.00	0.01
leucine	mean	2.17	2.13	1.76	1.63	1.47	1.50	1.13	2.11	2.36	2.07	2.55	1.90	1.64
	sd	0.85	0.81	0.38	0.38	0.71	0.61	0.21	0.05	1.20	0.54	1.35	0.30	1.16
lysine	mean	0.50	0.33	0.25	0.22	0.32	0.34	0.32	0.43	0.42	0.41	0.39	0.29	0.38
	sd	0.26	0.18	0.02	0.05	0.18	0.11	0.06	0.19	0.21	0.02	0.23	0.02	0.21
malic acid	mean	4.74	2.95	11.68	6.93	6.19	3.37	5.01	3.85	4.90	4.46	4.42	6.16	4.90
	sd	2.18	2.25	1.22	5.41	4.22	1.26	2.34	3.00	1.31	2.89	1.80	3.98	2.45
maltose	mean	0.21	0.23	0.17	0.30	0.20	0.27	0.18	0.23	0.21	0.20	0.18	0.22	0.39
	sd	0.02	0.08	0.04	0.09	0.08	0.04	0.01	0.00	0.06	0.06	0.06	0.07	0.49
methionine	mean	0.40	0.52	0.35	0.71	0.69	0.15	0.37	0.55	0.51	0.54	0.44	0.45	0.21
	sd	0.26	0.06	0.06	0.12	0.10	0.08	0.18	0.16	0.40	0.35	0.20	0.19	0.14
ornithine	mean	1.12	0.67	0.44	0.55	0.31	0.55	0.22	0.55	0.48	0.49	0.58	0.27	0.43
	sd	0.60	0.44	0.07	0.32	0.08	0.08	0.04	0.22	0.15	0.11	0.46	0.08	0.19
phenylalanine	mean	1.65	1.71	2.42	1.65	1.21	1.39	0.84	1.47	0.93	1.15	1.05	1.28	1.02
	sd	0.69	0.05	0.84	0.07	0.17	0.12	0.11	0.54	0.22	0.23	0.30	0.26	0.34
phosphoric acid	mean	1.42	1.97	0.61	1.93	0.82	2.36	0.98	0.97	0.56	0.73	1.18	4.51	0.83
	sd	0.82	0.61	0.12	0.81	0.20	1.80	0.58	0.11	0.22	0.53	0.65	2.79	0.58
4-hydroxy proline	mean	0.13	0.10	0.10	0.07	0.11	0.09	0.08	0.14	0.14	0.12	0.11	0.09	0.09
	sd	0.05	0.02	0.05	0.01	0.01	0.01	0.04	0.04	0.04	0.04	0.04	0.00	0.02
proline	mean	11.84	11.06	11.80	13.81	13.98	17.80	11.86	16.49	11.83	17.29	9.03	11.62	11.01
	sd	0.70	2.42	0.68	2.22	0.22	7.36	1.74	2.85	1.36	1.71	0.93	3.27	2.93
putrescine	mean	7.72	6.31	3.93	4.60	6.97	9.95	6.24	8.12	6.45	5.97	3.95	4.53	5.07
	sd	7.35	1.11	1.80	1.96	2.26	1.00	3.35	5.33	5.37	3.73	2.19	3.67	4.17
pyroglutamic acid	mean	35.42	48.13	52.97	58.25	46.08	62.02	34.72	53.67	28.05	48.03	45.13	45.23	32.46
	sd	2.40	20.27	29.06	12.25	10.87	5.95	15.69	4.41	8.48	30.07	28.28	26.02	15.58
pyruvic acid	mean	1.28	1.17	1.06	1.14	1.02	0.50	0.99	1.07	1.35	0.97	0.98	0.90	0.83
	sd	0.34	0.18	0.19	0.29	0.11	0.19	0.18	0.14	0.29	0.10	0.15	0.29	0.27
raffinose	mean	0.08	0.07	0.03	0.03	0.25	0.27	0.06	0.11	0.19	0.16	0.13	0.11	0.14
	sd	0.09	0.04	0.02	0.01	0.12	0.09	0.04	0.10	0.15	0.14	0.09	0.08	0.15
rhamnose	mean	0.57	0.55	0.38	0.51	0.54	0.54	0.52	0.55	0.61	0.55	0.55	0.62	0.49
	sd	0.23	0.05	0.03	0.03	0.16	0.05	0.10	0.13	0.14	0.02	0.01	0.06	0.07
serine	mean	21.70	22.06	27.15	34.68	37.38	42.54	26.64	33.11	39.31	40.78	33.13	38.30	24.36
	sd	2.04	0.57	3.95	0.05	0.89	8.67	5.62	8.54	12.47	7.44	15.29	9.98	6.89
O-acetyl-serine	mean	0.15	0.10	0.18	0.15	0.14	0.08	0.12	0.12	0.09	0.08	0.10	0.06	0.10
	sd	0.01	0.03	0.09	0.10	0.08	0.04	0.04	0.06	0.03	0.01	0.05	0.02	0.05
succinic acid	mean	0.97	1.20	0.84	0.82	0.77	0.98	0.89	0.81	0.97	0.94	1.07	0.94	0.91
	sd	0.05	0.56	0.06	0.24	0.26	0.41	0.05	0.10	0.18	0.17	0.03	0.26	0.13
sucrose	mean	153.33	215.92	131.57	176.80	115.40	158.32	83.13	135.94	78.78	114.37	102.38	119.76	89.97
	sd	50.70	8.03	3.69	54.24	28.82	17.29	17.90	26.86	21.78	13.18	45.96	36.80	30.97
trehalose	mean	0.30	0.55	0.17	0.29	0.35	0.32	0.25	0.43	0.47	0.31	0.32	0.38	0.21
	sd	0.02	0.46	0.03	0.11	0.18	0.07	0.14	0.16	0.25	0.11	0.11	0.16	0.10
threonic acid	mean	1.37	1.12	2.18	1.33	1.27	2.30	0.98	1.26	1.56	1.25	1.68	2.02	1.52
	sd	0.08	0.26	0.11	0.17	0.17	0.44	0.23	0.14	0.58	0.37	0.10	0.70	0.42
threonine	mean	7.36	5.34	8.11	6.86	6.79	8.13	5.50	6.95	7.42	8.10	6.50	7.31	5.77
	sd	0.18	0.48	0.60	0.44	0.05	1.25	0.13	0.78	0.73	1.09	1.06	0.35	1.18
tryptophan	mean	0.08	0.09	0.11	0.06	0.11	0.20	0.11	0.11	0.15	0.05	0.02	0.05	0.05
	sd	0.08	0.04	0.04	0.05	0.08	0.07	0.10	0.02	0.12	0.04	0.02	0.03	0.03
tyrosine	mean	0.59	0.54	0.36	0.49	0.37	0.46	0.21	0.51	0.59	0.52	0.60	0.44	0.36
	sd	0.36	0.30	0.07	0.17	0.19	0.17	0.02	0.27	0.38	0.19	0.35	0.09	0.26
urea	mean	0.69	0.62	0.49	0.53	0.40	0.53	0.40	0.37	0.61	0.53	0.64	0.69	0.55
	sd	0.03	0.11	0.02	0.08	0.07	0.13	0.04	0.08	0.15	0.12	0.13	0.20	0.06
valine	mean	7.31	8.23	7.70	8.78	6.82	7.75	5.96	8.33	8.50	8.83	7.52	6.77	6.21
	sd	2.65	2.12	1.64	1.90	1.38	2.08	2.45	2.72	4.31	0.80	2.33	0.88	3.34

Sample		trxf_HL_15'	trxf_HL_1h	trxf_HL_3h	trxf_HL_3h15'	trxf_HL_4h	trxf_HL_6h	trxf_ML_15'	trxf_ML_1h	trxf_ML_3h	trxf_ML_3h15'	trxf_ML_4h	trxf_ML_6h	trxf_t0
N		5	5	5	5	5	5	5	5	5	5	5	5	10
isoleucine	mean	2.63	2.29	1.99	1.80	1.22	2.40	1.44	1.36	2.55	3.10	1.47	2.71	1.17
	sd	1.24	0.58	0.44	0.32	0.21	1.50	0.32	0.21	1.34	1.78	0.05	1.48	0.31
lactic acid	mean	0.01	0.02	0.01	0.01	0.02	0.02	0.01	0.00	0.01	0.01	0.02	0.01	0.01
	sd	0.00	0.01	0.01	0.00	0.02	0.02	0.01	0.00	0.01	0.01	0.02	0.00	0.01
leucine	mean	2.26	2.17	2.12	1.63	1.15	1.44	1.35	1.34	2.42	2.46	1.57	2.60	1.17
	sd	0.78	0.74	0.65	0.07	0.04	0.34	0.36	0.21	0.99	0.87	0.07	1.14	0.33
lysine	mean	0.53	0.36	0.36	0.28	0.25	0.40	0.26	0.33	0.45	0.55	0.22	0.39	0.33
	sd	0.13	0.14	0.01	0.00	0.05	0.24	0.01	0.06	0.17	0.22	0.06	0.18	0.10
malic acid	mean	3.78	3.84	8.29	6.15	10.55	5.51	8.22	4.78	6.31	2.01	7.95	10.33	4.53
	sd	2.41	1.76	6.79	4.69	7.64	3.17	5.40	2.54	3.60	0.16	0.58	5.31	2.56
maltose	mean	0.20	0.22	0.24	0.27	0.19	0.18	0.23	0.22	0.20	0.22	0.21	0.21	0.19
	sd	0.10	0.04	0.01	0.12	0.06	0.01	0.00	0.03	0.03	0.05	0.01	0.05	0.06
methionine	mean	0.36	0.50	0.70	0.69	0.82	0.18	0.50	0.47	0.52	0.61	0.48	0.51	0.21
	sd	0.17	0.12	0.06	0.03	0.11	0.14	0.20	0.10	0.21	0.01	0.07	0.16	0.31
ornithine	mean	0.58	0.60	0.55	0.48	0.40	0.57	0.26	0.40	0.40	0.63	0.52	0.43	0.32
	sd	0.32	0.43	0.04	0.17	0.14	0.31	0.02	0.02	0.09	0.36	0.33	0.29	0.10
phenylalanine	mean	1.49	1.61	2.70	1.53	1.82	1.35	1.08	0.94	1.32	1.25	0.86	1.38	0.91
	sd	0.27	0.52	1.17	0.08	0.82	0.10	0.17	0.04	0.48	0.31	0.15	0.36	0.22
phosphoric acid	mean	2.06	3.19	0.86	2.34	10.86	1.61	0.94	0.44	1.68	0.98	1.55	9.13	0.63
	sd	1.91	2.44	0.26	1.78	7.51	0.90	0.20	0.10	1.30	0.48	0.61	6.11	0.39
4-hydroxy proline	mean	0.11	0.11	0.12	0.10	0.10	0.10	0.09	0.14	0.09	0.10	0.10	0.11	0.10
	sd	0.03	0.00	0.01	0.01	0.04	0.02	0.02	0.02	0.00	0.02	0.05	0.02	0.03
proline	mean	12.40	11.60	17.99	13.60	16.98	14.76	15.24	14.40	13.81	13.97	11.46	12.59	11.07
	sd	0.23	0.18	4.37	1.01	2.39	1.34	0.30	0.45	1.77	2.04	0.62	1.90	1.81
putrescine	mean	5.00	3.56	4.97	4.32	4.95	8.30	3.17	2.72	5.49	6.06	1.79	3.34	2.59
	sd	2.46	0.98	2.32	0.37	1.20	2.76	1.64	1.46	2.42	3.26	0.55	2.20	0.55
pyroglutamic acid	mean	27.48	39.60	62.72	50.95	70.81	51.81	47.59	37.69	33.99	40.42	59.49	48.64	23.80
	sd	7.43	10.34	36.60	11.02	36.38	19.41	18.41	17.57	10.24	18.02	44.80	14.33	8.07
pyruvic acid	mean	1.16	1.26	1.37	1.24	1.11	0.52	1.29	1.15	1.12	1.07	0.85	1.00	0.74
	sd	0.03	0.27	0.15	0.12	0.08	0.17	0.55	0.03	0.24	0.17	0.26	0.21	0.31
raffinose	mean	0.16	0.21	0.09	0.14	0.14	0.26	0.09	0.04	0.22	0.36	0.09	0.10	0.07
	sd	0.12	0.23	0.09	0.11	0.09	0.15	0.07	0.03	0.06	0.22	0.02	0.10	0.04
rhamnose	mean	0.58	0.59	0.47	0.51	0.50	0.54	0.50	0.50	0.60	0.59	0.50	0.67	0.45
	sd	0.06	0.03	0.05	0.07	0.09	0.01	0.03	0.07	0.09	0.05	0.05	0.13	0.10
serine	mean	22.34	24.06	33.31	34.55	37.54	37.95	24.49	27.75	34.10	40.39	31.96	39.13	25.27
	sd	4.34	1.66	2.58	5.53	0.74	6.70	5.98	4.66	1.90	3.51	6.08	1.49	7.17
O-acetyl-serine	mean	0.12	0.12	0.12	0.07	0.19	0.12	0.09	0.12	0.11	0.11	0.08	0.10	0.09
	sd	0.04	0.05	0.05	0.02	0.11	0.00	0.02	0.05	0.03	0.05	0.03	0.04	0.04
succinic acid	mean	0.83	0.87	0.68	0.77	0.66	1.08	0.76	0.73	0.82	0.94	0.79	1.01	0.69
	sd	0.05	0.02	0.22	0.07	0.15	0.33	0.13	0.04	0.15	0.60	0.23	0.26	0.13
sucrose	mean	143.84	180.83	186.00	186.35	95.74	117.34	98.61	104.62	106.73	115.93	103.02	124.72	73.33
	sd	30.74	46.04	38.70	42.04	29.43	6.24	13.71	47.47	37.85	25.13	14.78	33.50	14.20
trehalose	mean	0.20	0.31	0.33	0.31	0.26	0.22	0.35	0.25	0.35	0.25	0.31	0.29	0.19
	sd	0.02	0.14	0.01	0.04	0.02	0.03	0.02	0.09	0.15	0.11	0.05	0.05	0.09
threonic acid	mean	1.22	1.32	2.24	1.43	1.25	2.32	1.66	1.51	1.54	1.01	2.34	2.48	1.59
	sd	0.56	0.36	0.76	0.38	0.22	0.58	0.08	0.09	0.14	0.16	1.15	0.96	0.46
threonine	mean	5.60	6.02	9.69	7.34	8.02	8.06	6.68	7.56	7.71	7.60	7.44	8.25	5.78
	sd	0.54	1.08	3.86	2.04	2.04	0.63	1.55	1.40	0.89	0.76	2.29	0.37	2.06
tryptophan	mean	0.09	0.05	0.20	0.04	0.16	0.10	0.09	0.08	0.11	0.12	0.06	0.05	0.05
	sd	0.09	0.04	0.03	0.01	0.08	0.05	0.06	0.06	0.07	0.01	0.03	0.03	0.04
tyrosine	mean	0.54	0.40	0.47	0.42	0.35	0.55	0.27	0.27	0.64	0.65	0.41	0.62	0.28
	sd	0.28	0.13	0.14	0.10	0.17	0.31	0.12	0.06	0.28	0.27	0.03	0.35	0.11
urea	mean	0.59	0.60	0.52	0.55	0.45	0.69	0.39	0.49	0.60	0.57	0.54	0.70	0.52
	sd	0.16	0.21	0.06	0.12	0.04	0.11	0.15	0.14	0.19	0.22	0.15	0.30	0.14
valine	mean	7.55	7.31	10.17	8.23	6.65	7.88	6.22	5.94	8.11	8.81	6.24	8.83	4.69
	sd	1.85	1.02	3.41	0.32	0.60	2.47	0.05	0.28	2.44	2.92	1.99	2.15	1.02

Sample		trxm_HL_15'	trxm_HL_1h	trxm_HL_3h	trxm_HL_3h15'	trxm_HL_4h	trxm_HL_6h	trxm_ML_15'	trxm_ML_1h	trxm_ML_3h	trxm_ML_3h15	trxm_ML_4h	trxm_ML_6h	trxm_t0
N		5	5	5	5	5	5	5	5	4	5	4	5	10
isoleucine	mean	2.56	3.30	1.81	1.44	1.40	1.08	1.30	1.10	1.72	2.59	1.95	1.75	1.94
	sd	1.47	1.45	0.10	0.23	0.22	0.14	0.07	0.43	0.60	1.53	0.56	0.14	1.26
lactic acid	mean	0.02	0.01	0.00	0.01	0.01	0.01	0.02	0.01	0.04	0.01	0.02	0.01	0.01
	sd	0.01	0.01	0.00	0.00	0.01	0.01	0.02	0.00	0.03	0.01	0.02	0.01	0.00
leucine	mean	2.17	2.28	1.49	1.53	1.10	1.05	1.16	1.13	1.64	2.29	1.74	2.10	1.43
	sd	0.69	0.68	0.23	0.57	0.06	0.13	0.25	0.50	0.51	1.33	0.45	0.57	0.65
lysine	mean	0.52	0.39	0.30	0.16	0.22	0.22	0.32	0.32	0.33	0.49	0.28	0.25	0.34
	sd	0.24	0.13	0.03	0.02	0.03	0.03	0.05	0.19	0.11	0.25	0.14	0.03	0.15
malic acid	mean	6.96	3.33	5.97	6.60	7.31	7.06	4.09	3.79	6.51	4.81	6.21	6.54	4.80
	sd	0.91	1.78	2.27	4.62	3.52	3.44	1.83	1.27	4.64	3.03	4.74	2.72	2.14
maltose	mean	0.26	0.20	0.22	0.21	0.20	0.19	0.27	0.17	0.22	0.17	0.18	0.18	0.20
	sd	0.01	0.04	0.05	0.01	0.07	0.01	0.03	0.04	0.08	0.02	0.04	0.02	0.08
methionine	mean	0.37	0.48	0.47	0.86	0.73	0.09	0.38	0.36	0.48	0.47	0.42	0.42	0.20
	sd	0.14	0.09	0.16	0.26	0.20	0.06	0.09	0.18	0.04	0.17	0.19	0.14	0.14
ornithine	mean	0.56	0.40	0.40	0.41	0.33	0.28	0.22	0.35	0.36	0.42	0.31	0.26	0.28
	sd	0.26	0.18	0.09	0.13	0.04	0.06	0.06	0.05	0.10	0.08	0.16	0.13	0.03
phenylalanine	mean	1.57	1.57	1.96	2.33	1.53	1.12	0.87	1.06	0.90	0.97	0.95	1.28	1.08
	sd	0.38	0.29	1.00	1.16	0.49	0.13	0.15	0.56	0.12	0.12	0.19	0.10	0.24
phosphoric acid	mean	1.29	1.80	0.82	2.14	1.00	1.29	2.10	0.80	1.00	0.77	6.24	4.26	0.70
	sd	0.57	0.88	0.25	1.53	0.60	1.10	1.97	0.48	0.53	0.62	5.42	1.98	0.44
4-hydroxy proline	mean	0.12	0.12	0.13	0.06	0.07	0.10	0.12	0.10	0.08	0.13	0.07	0.11	0.09
	sd	0.03	0.01	0.05	0.01	0.01	0.06	0.06	0.06	0.02	0.02	0.03	0.03	0.03
proline	mean	13.64	9.76	16.77	14.33	15.61	14.98	11.96	14.22	11.23	13.08	10.42	10.79	10.27
	sd	1.92	1.79	0.20	2.10	4.61	1.57	1.34	1.73	0.98	2.77	0.44	2.10	1.51
putrescine	mean	5.32	3.95	5.65	2.02	4.49	5.89	3.17	1.62	2.58	4.54	2.38	1.99	2.80
	sd	3.55	1.83	2.05	0.04	1.15	0.72	0.33	0.61	1.52	1.64	1.12	0.14	1.90
pyroglutamic acid	mean	38.51	34.92	34.33	85.83	55.88	35.77	28.92	36.59	49.53	33.43	48.55	48.30	30.92
	sd	1.67	13.59	7.21	59.60	30.71	7.22	10.18	5.85	16.57	10.16	22.87	2.70	9.68
pyruvic acid	mean	1.56	1.27	1.09	1.11	1.12	0.45	1.11	1.31	1.47	1.10	1.04	1.30	0.79
	sd	0.03	0.04	0.17	0.19	0.22	0.03	0.01	0.10	0.34	0.06	0.36	0.34	0.28
raffinose	mean	0.06	0.08	0.12	0.07	0.05	0.22	0.05	0.30	0.23	0.33	0.16	0.07	0.13
	sd	0.04	0.04	0.05	0.05	0.03	0.09	0.03	0.40	0.24	0.42	0.09	0.05	0.11
rhamnose	mean	0.56	0.56	0.49	0.49	0.49	0.48	0.57	0.56	0.55	0.51	0.52	0.61	0.48
	sd	0.06	0.06	0.04	0.01	0.02	0.03	0.10	0.08	0.05	0.05	0.07	0.09	0.08
serine	mean	21.35	21.40	39.18	36.98	33.29	38.45	22.69	21.09	25.71	40.21	28.24	30.07	20.61
	sd	4.88	0.19	7.31	1.06	2.10	1.24	0.51	9.49	2.39	4.18	6.48	4.56	5.48
O-acetyl-serine	mean	0.11	0.13	0.10	0.18	0.22	0.05	0.09	0.10	0.13	0.07	0.11	0.06	0.09
	sd	0.02	0.03	0.01	0.13	0.14	0.01	0.02	0.03	0.05	0.04	0.03	0.02	0.02
succinic acid	mean	1.28	1.38	1.03	0.97	0.80	0.98	0.85	1.06	1.27	1.07	1.23	1.19	1.14
	sd	0.09	0.24	0.02	0.16	0.14	0.15	0.14	0.05	0.01	0.18	0.19	0.04	0.34
sucrose	mean	143.31	172.84	155.47	168.36	66.47	103.44	78.25	99.91	88.23	97.11	97.42	111.38	88.20
	sd	29.71	32.80	43.65	32.92	5.11	7.21	20.08	53.41	25.57	2.91	37.00	40.14	22.48
trehalose	mean	0.19	0.16	0.30	0.40	0.35	0.21	0.26	0.30	0.36	0.29	0.35	0.27	0.24
	sd	0.05	0.04	0.16	0.06	0.11	0.08	0.15	0.17	0.18	0.10	0.15	0.05	0.08
threonic acid	mean	1.61	1.17	2.27	1.81	1.22	2.87	0.87	1.39	1.49	1.52	1.59	2.00	1.71
	sd	0.42	0.14	0.27	0.37	0.25	0.16	0.13	0.29	0.32	0.61	0.69	0.59	0.73
threonine	mean	6.90	5.63	8.85	8.35	8.10	8.91	5.65	7.46	7.69	8.98	7.12	8.03	5.86
	sd	0.27	0.20	0.98	3.20	2.68	1.67	0.95	0.77	1.73	1.38	2.16	1.04	0.55
tryptophan	mean	0.10	0.07	0.06	0.03	0.14	0.06	0.07	0.11	0.14	0.09	0.05	0.03	0.08
	sd	0.10	0.08	0.04	0.03	0.04	0.02	0.06	0.08	0.09	0.04	0.03	0.03	0.06
tyrosine	mean	0.55	0.53	0.39	0.38	0.26	0.30	0.24	0.33	0.44	0.60	0.38	0.45	0.33
	sd	0.32	0.27	0.02	0.13	0.02	0.06	0.10	0.29	0.16	0.44	0.14	0.21	0.18
urea	mean	0.70	0.60	0.59	0.61	0.34	0.63	0.39	0.47	0.54	0.65	0.50	0.55	0.60
	sd	0.12	0.03	0.16	0.02	0.12	0.20	0.13	0.15	0.13	0.34	0.09	0.14	0.15
valine	mean	7.54	8.46	6.68	9.12	6.91	5.35	5.05	5.89	6.09	8.23	6.33	6.45	6.40
	sd	2.11	2.33	0.90	2.89	1.02	0.26	0.06	3.09	0.96	2.64	0.71	0.11	2.38

Sample		ntrc_HL_15'	ntrc_HL_1h	ntrc_HL_3h	ntrc_HL_3h15'	ntrc_HL_4h	ntrc_HL_6h	ntrc_ML_15'	ntrc_ML_1h	ntrc_ML_3h	ntrc_ML_3h15'	ntrc_ML_4h	ntrc_ML_6h	ntrc_t0
N		5	5	4	4	5	5	5	5	4	5	5	5	10
isoleucine	mean	2.93	2.23	1.67	1.61	2.19	1.91	1.28	1.83	1.74	2.64	2.10	2.95	2.15
	sd	1.19	1.03	0.20	0.08	1.21	0.92	0.10	0.60	0.43	1.28	0.55	0.65	1.07
lactic acid	mean	0.01	0.02	0.01	0.01	0.02	0.03	0.01	0.03	0.02	0.02	0.03	0.02	0.02
	sd	0.00	0.01	0.02	0.02	0.02	0.03	0.01	0.03	0.02	0.02	0.02	0.01	0.02
leucine	mean	2.28	1.76	1.57	1.61	1.57	1.32	0.92	1.83	1.40	2.18	1.92	2.38	1.59
	sd	0.91	0.76	0.19	0.11	0.90	0.56	0.21	1.15	0.49	1.03	1.11	0.40	0.86
lysine	mean	0.53	0.29	0.31	0.19	0.34	0.33	0.23	0.39	0.27	0.51	0.40	0.34	0.43
	sd	0.21	0.20	0.03	0.07	0.14	0.14	0.04	0.10	0.06	0.31	0.26	0.06	0.22
malic acid	mean	4.92	4.81	10.70	7.38	6.49	6.56	4.89	4.88	5.98	4.22	8.54	5.64	3.19
	sd	2.69	2.79	0.80	1.36	5.28	4.66	1.93	3.02	4.25	2.91	6.12	0.53	1.86
maltose	mean	0.17	0.16	0.14	0.19	0.19	0.15	0.16	0.15	0.14	0.17	0.17	0.20	0.17
	sd	0.03	0.04	0.05	0.10	0.07	0.02	0.05	0.02	0.04	0.02	0.07	0.05	0.08
methionine	mean	0.40	0.46	0.47	0.53	0.81	0.09	0.38	0.44	0.49	0.47	0.55	0.54	0.35
	sd	0.18	0.18	0.16	0.11	0.16	0.05	0.13	0.27	0.16	0.28	0.19	0.21	0.33
ornithine	mean	1.18	1.16	0.54	0.35	0.87	0.94	0.20	0.72	0.39	0.86	0.51	0.63	0.62
	sd	0.57	1.19	0.08	0.07	0.45	0.78	0.07	0.29	0.17	0.30	0.20	0.45	0.36
phenylalanine	mean	1.80	1.67	1.59	1.23	1.49	1.37	0.88	1.66	0.99	1.43	1.01	1.43	1.47
	sd	0.59	0.80	0.18	0.10	0.05	0.50	0.01	1.00	0.29	0.60	0.24	0.47	0.59
phosphoric acid	mean	1.55	3.56	1.47	1.38	1.79	0.83	2.54	0.60	2.61	0.69	12.81	5.40	1.38
	sd	1.04	2.04	1.43	0.52	0.89	0.45	2.67	0.29	0.85	0.19	1.04	1.47	0.72
4-hydroxy proline	mean	0.09	0.08	0.10	0.06	0.09	0.10	0.09	0.10	0.07	0.12	0.09	0.08	0.10
	sd	0.02	0.02	0.02	0.01	0.02	0.03	0.01	0.03	0.05	0.02	0.04	0.04	0.02
proline	mean	13.66	12.81	13.77	13.08	13.84	13.36	10.88	13.57	11.76	14.04	11.47	11.97	11.23
	sd	3.14	2.77	1.72	0.28	1.19	2.22	0.68	2.25	2.04	2.32	2.63	3.02	2.81
putrescine	mean	5.51	6.36	3.16	2.36	8.84	9.03	1.75	6.77	3.38	7.67	3.02	4.93	5.47
	sd	4.13	6.52	0.69	0.61	4.36	6.08	0.59	7.06	1.45	6.40	1.74	4.16	4.67
pyroglutamic acid	mean	31.56	75.46	49.26	51.33	66.07	79.57	33.35	35.63	92.13	53.08	41.24	43.65	49.21
	sd	7.10	43.17	8.41	10.05	25.49	56.48	8.34	11.50	38.11	33.83	3.72	11.91	33.94
pyruvic acid	mean	1.09	1.17	1.44	1.18	1.20	0.31	0.76	0.70	0.87	0.74	0.75	0.81	0.58
	sd	0.02	0.18	0.33	0.13	0.23	0.05	0.08	0.15	0.22	0.09	0.23	0.16	0.23
raffinose	mean	0.15	0.02	0.02	0.05	0.10	0.11	0.05	0.01	0.04	0.22	0.10	0.24	0.05
	sd	0.12	0.02	0.01	0.02	0.07	0.09	0.04	0.00	0.02	0.19	0.10	0.22	0.03
rhamnose	mean	0.64	0.60	0.55	0.55	0.63	0.59	0.62	0.65	0.60	0.67	0.68	0.72	0.58
	sd	0.11	0.14	0.03	0.03	0.01	0.03	0.07	0.10	0.11	0.19	0.07	0.09	0.08
serine	mean	21.40	20.35	25.67	28.33	34.54	34.89	17.34	26.55	28.54	36.80	28.15	30.32	18.42
	sd	2.85	10.07	0.83	4.37	1.94	4.13	1.72	6.45	5.45	2.50	2.94	6.84	2.19
O-acetyl-serine	mean	0.12	0.17	0.08	0.09	0.09	0.10	0.10	0.13	0.15	0.10	0.11	0.09	0.13
	sd	0.01	0.09	0.02	0.02	0.04	0.04	0.02	0.07	0.05	0.06	0.06	0.05	0.05
succinic acid	mean	0.70	0.82	0.56	0.58	0.49	0.74	0.53	0.46	0.48	0.54	0.60	0.92	0.50
	sd	0.14	0.30	0.03	0.11	0.19	0.23	0.10	0.10	0.12	0.09	0.04	0.54	0.14
sucrose	mean	143.43	174.36	130.18	115.53	139.52	113.20	87.18	103.77	75.67	114.43	101.98	139.71	99.53
	sd	34.23	51.72	3.33	13.28	51.69	37.50	19.36	61.85	25.69	35.27	33.35	52.17	42.64
trehalose	mean	0.31	0.44	0.23	0.43	0.22	0.21	0.21	0.25	0.24	0.25	0.26	0.45	0.20
	sd	0.16	0.04	0.11	0.31	0.07	0.07	0.08	0.14	0.02	0.02	0.08	0.24	0.11
threonic acid	mean	1.07	1.37	1.97	1.72	0.95	2.46	1.02	0.94	1.19	1.07	1.33	1.70	1.21
	sd	0.21	0.58	0.28	0.58	0.30	0.64	0.02	0.18	0.44	0.28	0.54	0.43	0.50
threonine	mean	8.54	8.59	11.24	10.22	8.28	10.46	7.24	9.43	11.45	10.53	9.25	10.26	7.47
	sd	0.44	0.45	1.90	1.52	0.48	1.12	0.88	1.07	4.00	0.57	0.25	2.12	1.09
tryptophan	mean	0.12	0.07	0.06	0.01	0.25	0.17	0.05	0.09	0.10	0.13	0.03	0.12	0.16
	sd	0.13	0.05	0.04	0.01	0.14	0.16	0.02	0.08	0.04	0.10	0.01	0.10	0.13
tyrosine	mean	0.69	0.42	0.37	0.31	0.49	0.49	0.22	0.40	0.40	0.70	0.38	0.60	0.57
	sd	0.40	0.33	0.09	0.03	0.26	0.34	0.01	0.18	0.10	0.47	0.15	0.20	0.33
urea	mean	1.15	0.74	0.68	0.81	0.64	0.88	0.40	0.87	0.79	0.77	0.87	0.84	0.81
	sd	0.17	0.19	0.20	0.28	0.15	0.19	0.02	0.29	0.28	0.23	0.29	0.21	0.20
valine	mean	7.19	6.72	7.13	7.64	7.28	6.18	4.28	6.81	5.32	7.58	5.89	7.53	5.89
	sd	2.22	2.21	0.93	0.25	2.65	1.41	0.81	3.47	1.62	2.45	1.18	0.80	2.86

Supplement Table 5.4.1. (continued)

Supplement Table 5.4.4. List of *p* values from GC-MS based short-term HL (de-)acclimated plants.

A 2-way ANOVA with *post-hoc* Tukey test was performed using the "emmeans" and "multcomp" packages from R. Values are given relative to the respective WT. Significances ($p < 0.05$) are given in bold.

Light	contrast	Time	2-oxo-glutaric acid	4-hydroxy proline	adenine	alanine	ascorbic acid	asparagine	aspartic acid	benzoic acid	beta-alanine	citric acid	dehydro ascorbic acid	dehydroa scorbic acid	erythritol/ erythrose	fructose	fucose	fumaric acid	gaba	galactinol	galactonic acid	glucose	glutamic acid	glutamine	glyceric acid	glycerol	glycine	histidine	homoserine	isoleucine
ML	trxf - WT	t0	0.936	0.968	0.998	0.792	0.964	1.000	0.939	0.990	0.954	1.000	0.979	0.967	0.879	0.453	0.716	0.847	0.147	1.000	0.175	0.277	0.370	0.682	0.150	1.000	0.969	0.758	0.888	0.249
	trxm - WT	t0	0.966	0.998	1.000	0.993	0.999	0.975	0.998	0.949	0.979	1.000	0.996	0.994	**0.039**	0.775	0.993	0.997	0.224	0.568	**0.034**	0.643	1.000	0.816	0.092	0.997	0.748	0.822	0.574	0.999
	ntrc - WT	t0	0.125	0.989	1.000	0.114	0.855	**0.000**	0.999	0.990	**0.001**	0.977	0.239	0.323	**0.000**	1.000	0.976	0.661	**0.002**	0.998	0.163	0.885	0.472	0.379	**0.002**	0.986	0.926	0.851	0.996	0.990
	trxf - WT	15min	0.953	0.875	1.000	**0.000**	0.971	0.750	0.138	0.941	0.732	0.999	0.999	0.982	0.757	0.981	1.000	0.209	0.535	0.799	0.937	0.994	0.999	0.995	0.274	0.331	0.483	0.514	0.097	0.984
	trxm - WT	15min	0.489	0.244	0.969	0.943	0.988	0.696	1.000	0.926	0.984	0.996	1.000	1.000	0.957	0.999	0.766	0.966	0.752	0.990	0.830	0.990	0.978	0.780	0.934	0.967	0.915	0.367	0.999	0.999
	ntrc - WT	15min	0.067	0.989	1.000	0.992	0.773	0.818	0.825	0.992	0.149	1.000	0.762	0.776	**0.004**	0.952	0.704	0.969	0.268	0.983	0.327	0.899	0.794	0.895	0.522	0.653	0.945	0.557	0.962	1.000
	trxf - WT	1h	0.952	1.000	0.807	0.077	1.000	1.000	0.863	0.149	0.985	0.998	0.205	0.913	1.000	0.732	0.391	0.798	0.189	0.973	**0.041**	0.614	0.118	0.083	0.197	**0.008**	1.000	0.997	**0.023**	0.807
	trxm - WT	1h	0.784	0.248	0.926	0.990	1.000	0.434	0.957	0.981	0.802	0.983	0.494	0.917	0.503	0.974	0.225	0.995	0.158	0.986	**0.025**	0.913	0.759	0.141	0.195	**0.009**	0.367	0.999	0.730	0.555
	ntrc - WT	1h	0.994	0.316	0.869	0.447	0.935	0.849	0.842	0.667	**0.017**	0.996	0.697	1.000	0.060	0.955	0.679	0.189	**0.009**	0.951	0.219	0.901	0.600	0.432	**0.009**	0.720	0.836	0.271	0.915	0.999
	trxf - WT	3h	0.729	0.069	0.984	0.937	0.999	0.259	1.000	0.861	0.139	1.000	0.952	0.918	0.806	0.570	1.000	0.927	0.785	0.573	0.975	0.415	0.928	0.765	1.000	0.833	0.304	0.608	0.558	1.000
	trxm - WT	3h	0.140	**0.029**	0.343	0.986	0.978	0.993	0.993	0.706	0.588	0.999	1.000	1.000	0.915	0.971	0.810	0.845	0.907	0.812	0.928	0.988	0.938	1.000	1.000	0.460	0.851	0.091	0.862	0.520
	ntrc - WT	3h	0.075	**0.012**	**0.000**	1.000	0.991	**0.000**	0.508	**0.012**	**0.026**	1.000	0.597	0.762	0.070	0.592	0.127	**0.006**	**0.014**	0.873	0.986	0.596	1.000	1.000	0.057	0.407	0.977	0.949	0.993	0.547
	trxf - WT	3h15min	0.688	0.623	0.976	0.996	0.861	0.998	0.969	0.598	0.707	0.995	0.134	0.181	0.122	0.875	1.000	1.000	0.180	0.999	0.997	0.963	0.939	0.972	0.119	0.993	0.977	0.083	0.994	0.479
	trxm - WT	3h15min	0.438	0.997	0.999	0.883	0.995	0.930	0.899	0.852	0.764	1.000	0.999	1.000	0.674	0.974	0.945	0.910	0.703	0.999	0.885	0.922	1.000	0.187	0.699	0.993	0.957	0.290	0.399	0.924
	ntrc - WT	3h15min	0.999	0.993	0.998	0.661	0.992	0.984	0.988	0.719	**0.000**	0.999	0.806	0.803	0.079	0.950	0.882	0.108	**0.001**	0.402	0.961	0.999	0.964	0.841	**0.001**	0.878	**0.034**	0.783	0.999	0.898
	trxf - WT	4h	0.967	0.956	0.994	0.552	0.862	0.385	0.101	**0.000**	0.475	0.983	0.914	0.993	0.771	0.999	0.645	**0.014**	0.278	0.998	0.803	1.000	0.462	0.850	0.236	0.131	**0.000**	**0.031**	0.659	0.149
	trxm - WT	4h	0.575	0.404	0.989	1.000	0.337	0.402	0.097	**0.000**	0.753	0.084	1.000	1.000	0.995	0.398	0.915	0.417	0.988	0.988	0.648	0.813	0.952	0.973	0.973	0.079	**0.020**	0.149	0.880	0.580
	ntrc - WT	4h	0.441	0.922	0.944	0.868	**0.001**	0.524	0.563	**0.002**	**0.000**	**0.000**	0.926	0.901	**0.001**	0.984	0.750	0.981	0.202	0.932	0.988	0.963	0.727	0.940	0.311	**0.007**	0.997	0.833	0.241	0.683
	trxf - WT	6h	0.990	0.788	0.975	0.649	0.988	1.000	0.693	0.999	0.931	**0.015**	0.999	0.997	0.820	0.903	0.995	0.994	0.620	0.885	0.977	0.968	0.985	0.983	0.973	0.998	**0.001**	**0.017**	0.363	0.696
	trxm - WT	6h	0.359	0.810	0.980	0.958	0.191	0.401	0.166	0.796	0.492	0.993	0.999	0.996	0.798	0.979	0.927	0.984	**0.014**	0.989	0.297	0.999	0.980	1.000	**0.016**	0.867	0.996	0.743	1.000	0.966
	ntrc - WT	6h	0.797	0.990	1.000	0.534	0.399	0.201	0.880	1.000	**0.000**	1.000	1.000	0.998	**0.002**	0.161	0.988	0.764	**0.000**	0.957	0.778	0.158	0.957	0.997	**0.000**	0.997	0.947	0.989	0.719	0.452
HL	trxf - WT	15min	0.893	0.855	0.792	0.863	0.975	0.990	0.712	0.994	0.975	0.969	1.000	0.981	1.000	0.995	0.972	0.126	0.176	1.000	0.969	0.917	0.867	0.996	0.249	0.896	1.000	0.634	0.520	0.981
	trxm - WT	15min	1.000	0.990	0.875	0.993	0.997	0.997	0.885	0.925	1.000	0.085	0.992	0.989	0.926	0.984	1.000	0.109	0.450	0.945	0.926	0.889	0.859	0.994	0.367	0.998	1.000	0.783	0.999	0.993
	ntrc - WT	15min	0.251	0.180	0.602	0.929	0.576	0.975	1.000	0.939	**0.000**	1.000	0.999	1.000	**0.005**	0.957	1.000	0.598	**0.003**	0.940	0.144	0.945	0.707	0.998	**0.003**	0.893	1.000	0.918	0.569	0.816
	trxf - WT	1h	0.385	1.000	0.462	0.980	0.327	0.997	0.998	0.056	0.831	0.900	0.955	0.995	0.410	0.997	0.948	1.000	0.970	0.138	0.698	0.996	0.747	0.985	0.996	0.837	0.996	0.727	0.995	0.721
	trxm - WT	1h	0.982	0.833	0.391	1.000	0.785	0.810	1.000	0.169	0.915	0.932	0.985	0.997	0.781	0.919	0.979	0.678	0.646	0.975	0.146	0.978	0.925	0.995	0.805	0.995	1.000	0.761	1.000	0.927
	ntrc - WT	1h	0.890	0.642	0.995	0.633	0.319	0.580	0.471	0.684	0.088	0.925	0.715	0.721	**0.000**	0.533	0.263	**0.037**	0.191	0.528	0.079	0.332	0.549	0.778	0.467	0.969	0.990	0.688	0.980	0.661
	trxf - WT	3h	0.999	0.530	1.000	0.432	0.595	0.952	0.998	0.630	0.292	0.999	0.358	0.292	0.255	0.445	0.573	0.989	1.000	0.945	0.942	0.523	0.559	1.000	0.941	1.000	0.924	0.558	0.261	0.842
	trxm - WT	3h	0.922	0.217	0.117	0.101	0.985	0.795	1.000	0.543	0.143	0.607	0.961	0.974	0.452	0.999	0.249	0.792	0.773	0.919	0.447	0.869	0.766	**0.001**	0.676	1.000	**0.005**	0.321	0.642	0.947
	ntrc - WT	3h	0.999	1.000	0.601	0.937	0.925	1.000	0.549	0.204	**0.000**	0.994	0.883	0.633	**0.001**	0.980	0.958	0.109	0.614	0.942	0.623	0.774	0.653	0.291	0.938	1.000	0.215	0.649	0.942	0.989
	trxf - WT	3h15min	0.985	0.518	0.768	0.989	0.298	0.983	0.946	0.776	0.923	0.119	0.665	0.722	0.999	0.972	0.826	0.430	0.107	**0.045**	0.732	0.971	0.960	0.994	**0.030**	0.995	0.966	0.819	0.898	0.992
	trxm - WT	3h15min	0.968	0.866	0.868	0.518	1.000	0.913	0.542	0.918	0.634	0.460	0.982	1.000	0.389	0.801	0.999	0.258	0.905	0.857	0.963	0.947	1.000	0.989	0.358	0.970	0.975	0.952	0.568	0.989
	ntrc - WT	3h15min	0.900	0.917	0.939	0.223	0.342	0.702	0.483	0.997	**0.044**	0.599	0.999	0.995	**0.049**	0.053	0.869	0.201	**0.000**	0.557	1.000	**0.017**	0.897	0.839	**0.000**	**0.002**	0.880	0.972	0.981	1.000
	trxf - WT	4h	0.973	0.926	0.871	0.144	0.971	0.999	**0.003**	0.826	1.000	**0.000**	0.917	0.987	0.982	0.974	0.310	0.997	**0.000**	1.000	1.000	0.875	0.338	0.084	**0.002**	0.837	**0.028**	0.797	**0.021**	0.860
	trxm - WT	4h	1.000	0.170	0.978	0.302	0.821	0.961	0.178	0.997	0.974	0.395	0.302	0.377	0.985	0.299	**0.007**	0.302	**0.000**	0.153	0.655	0.186	0.987	1.000	**0.000**	0.994	**0.038**	**0.008**	**0.039**	0.963
	ntrc - WT	4h	0.783	0.634	0.978	1.000	0.999	0.138	1.000	0.906	0.160	0.963	0.912	0.868	**0.001**	0.662	0.412	0.483	**0.000**	0.847	0.226	0.989	0.990	0.263	**0.000**	0.129	0.898	0.968	0.995	0.850
	trxf - WT	6h	0.823	0.995	0.858	0.992	0.983	0.726	1.000	0.375	1.000	0.976	0.952	0.969	**0.027**	0.834	0.996	0.472	**0.000**	0.669	0.293	0.802	0.894	0.997	**0.000**	0.999	0.999	0.216	0.975	0.999
	trxm - WT	6h	0.120	0.988	0.999	0.992	0.993	0.820	0.540	0.789	0.997	0.975	0.064	0.123	0.302	**0.033**	0.225	**0.001**	**0.000**	0.715	0.145	**0.028**	0.577	0.473	**0.001**	0.972	0.986	0.905	0.983	0.224
	ntrc - WT	6h	0.519	1.000	0.997	0.999	0.996	**0.000**	0.883	0.379	**0.032**	0.993	0.712	0.832	0.858	0.363	0.224	**0.000**	**0.000**	0.160	0.358	**0.040**	1.000	0.322	**0.000**	0.984	0.979	0.658	0.774	0.923

Light	contrast	Time	lactic acid	leucine	lysine	malic acid	maltose	methionine	myo-inositol	O-acetyl-serine	ornithine	phenylalanine	phosphoric acid	proline	putrescine	pyroglutamic acid	pyruvic acid	raffinose	rhamnose	serine	succinic acid	sucrose	threonic acid	threonine	trehalose	tryptophan	tyrosine	urea	valine
ML	trxf - WT	t0	0.998	0.544	0.870	0.994	**0.006**	1.000	0.843	0.967	0.689	0.917	0.994	1.000	0.349	0.784	0.827	0.713	0.791	0.990	0.117	0.691	0.992	1.000	0.994	0.999	0.887	0.974	0.450
	trxm - WT	t0	0.745	0.931	0.941	1.000	**0.013**	0.999	0.942	0.877	0.482	0.987	0.999	0.861	0.428	0.998	0.976	0.997	0.997	0.590	0.083	0.999	0.840	0.999	0.926	0.695	0.993	0.943	0.998
	ntrc - WT	t0	0.900	0.998	0.905	0.609	**0.003**	0.507	0.878	0.426	0.208	**0.045**	0.896	0.995	0.993	0.270	0.101	0.513	0.112	0.195	**0.000**	0.922	0.517	**0.037**	0.999	**0.002**	0.226	**0.014**	0.989
	trxf - WT	15min	0.531	0.972	0.931	0.340	0.927	0.756	0.455	0.641	0.993	0.745	1.000	**0.050**	0.444	0.741	0.221	0.994	0.980	0.953	0.752	0.880	0.139	0.522	0.596	0.972	0.973	1.000	0.998
	trxm - WT	15min	0.993	1.000	1.000	0.963	0.701	1.000	0.848	0.623	1.000	0.999	0.722	1.000	0.446	0.968	0.872	1.000	0.858	0.770	0.991	0.995	0.985	0.998	1.000	0.717	0.995	1.000	0.917
	ntrc - WT	15min	0.717	0.971	0.813	1.000	0.999	1.000	1.000	0.888	0.998	0.998	0.471	0.872	0.134	1.000	0.426	0.998	0.287	0.111	**0.046**	0.997	0.999	0.188	0.936	0.511	1.000	1.000	0.631
	trxf - WT	1h	0.761	0.400	0.767	0.962	0.997	0.936	0.318	0.998	0.728	0.118	0.961	0.373	**0.047**	0.591	0.946	0.893	0.883	0.559	0.932	0.439	0.863	0.893	0.077	0.935	0.389	0.760	0.327
	trxm - WT	1h	0.982	0.194	0.710	1.000	0.875	0.497	0.990	0.821	0.463	0.317	0.998	0.300	**0.011**	0.536	0.378	0.155	0.995	**0.020**	0.264	0.313	0.979	0.934	0.309	0.999	0.610	0.846	0.309
	ntrc - WT	1h	0.384	0.944	0.988	0.949	0.778	0.839	0.388	0.979	0.594	0.836	0.986	0.114	0.914	0.488	0.091	0.745	0.251	0.381	0.052	0.415	0.742	**0.024**	0.080	0.965	0.887	**0.000**	0.703
	trxf - WT	3h	0.956	0.999	0.994	0.882	0.998	0.999	1.000	0.856	0.935	0.346	0.728	0.421	0.966	0.966	0.445	0.989	0.992	0.583	0.684	0.539	1.000	0.987	0.357	0.760	0.989	0.999	0.993
	trxm - WT	3h	**0.044**	0.507	0.849	0.857	0.999	0.998	0.999	0.435	0.841	0.999	0.980	0.972	0.290	0.384	0.899	0.979	0.722	**0.012**	0.168	0.974	0.996	0.992	0.509	0.996	0.804	0.943	0.375
	ntrc - WT	3h	0.998	0.253	0.512	0.951	0.864	0.999	0.200	0.212	0.933	0.996	0.283	1.000	0.497	**0.000**	**0.020**	0.456	0.392	0.068	**0.005**	0.999	0.676	**0.000**	**0.028**	0.700	0.635	0.431	0.148
	trxf - WT	3h15min	1.000	0.855	0.497	0.574	0.995	0.945	0.963	0.827	0.724	0.967	0.996	0.055	1.000	0.932	0.913	0.136	0.892	1.000	1.000	1.000	0.872	0.939	0.860	0.381	0.806	0.986	1.000
	trxm - WT	3h15min	0.989	0.967	0.864	0.998	0.986	0.961	1.000	0.979	0.965	0.881	1.000	**0.008**	0.899	0.659	0.804	0.253	0.894	0.999	0.779	0.841	0.822	0.734	0.994	0.881	0.952	0.740	0.974
	ntrc - WT	3h15min	0.684	0.995	0.729	0.999	0.980	0.949	0.791	0.976	**0.041**	0.631	1.000	0.063	0.843	0.979	0.456	0.881	0.183	0.766	**0.021**	1.000	0.941	**0.028**	0.850	0.339	0.620	0.152	0.810
	trxf - WT	4h	1.000	0.191	0.368	0.258	0.985	0.990	1.000	0.748	0.962	0.853	0.987	0.243	0.722	0.671	0.836	0.965	0.868	0.992	0.180	1.000	0.160	0.699	0.997	0.792	0.602	0.836	0.799
	trxm - WT	4h	1.000	0.403	0.771	0.814	1.000	1.000	0.999	0.997	0.237	0.978	**0.000**	0.745	0.890	0.994	0.979	0.989	0.965	0.675	0.688	0.996	0.993	0.906	0.988	0.883	0.523	0.640	0.855
	ntrc - WT	4h	0.879	0.567	0.999	0.142	1.000	0.831	0.779	0.996	0.957	0.998	**0.000**	0.240	0.970	0.990	0.456	0.990	0.086	0.618	**0.004**	1.000	0.686	**0.010**	0.843	0.984	0.451	0.175	0.650
	trxf - WT	6h	1.000	0.493	0.781	0.135	1.000	0.964	0.990	0.368	0.672	0.973	**0.000**	0.878	0.938	0.993	0.916	1.000	0.815	0.997	0.962	0.995	0.472	0.697	0.658	1.000	0.662	0.999	0.465
	trxm - WT	6h	0.835	0.978	0.976	0.997	0.973	0.998	0.999	1.000	1.000	1.000	0.996	0.920	0.604	0.995	0.055	0.985	1.000	0.191	0.273	0.978	1.000	0.838	0.493	0.989	1.000	0.615	0.996
	ntrc - WT	6h	0.227	0.764	0.967	0.993	0.996	0.890	1.000	0.563	**0.049**	0.919	0.839	0.993	0.997	0.999	0.931	0.493	0.279	0.214	0.997	0.774	0.725	**0.005**	0.774	0.339	0.741	0.547	0.950
HL	trxf - WT	15min	0.932	0.996	0.985	0.977	0.999	0.965	0.749	0.836	0.163	0.971	0.955	0.984	0.524	0.962	0.699	0.532	0.999	0.995	0.760	0.972	0.931	0.279	0.650	0.991	0.985	0.607	0.997
	trxm - WT	15min	0.626	1.000	0.996	0.787	0.495	0.988	1.000	0.744	0.144	0.996	1.000	0.660	0.624	0.998	0.079	0.994	1.000	0.999	0.118	0.967	0.775	0.965	0.634	0.940	0.995	1.000	0.998
	ntrc - WT	15min	1.000	0.992	0.972	1.000	0.775	1.000	0.995	0.868	0.995	0.975	1.000	0.651	0.684	0.995	0.342	0.615	0.507	0.999	0.212	0.968	0.627	0.620	1.000	0.740	0.889	**0.000**	1.000
	trxf - WT	1h	0.999	0.999	0.978	0.983	0.994	0.996	0.695	0.993	0.994	0.993	0.757	0.986	0.515	0.954	0.825	0.065	0.823	0.876	0.081	0.372	0.849	0.896	**0.035**	0.891	0.756	0.997	0.874
	trxm - WT	1h	0.848	0.977	0.899	0.999	0.938	0.962	1.000	0.954	0.723	0.978	0.999	0.839	0.639	0.850	0.787	0.993	0.991	0.995	0.590	0.199	0.998	0.991	**0.000**	0.992	1.000	0.997	0.998
	ntrc - WT	1h	1.000	0.764	0.980	0.863	0.299	0.892	0.390	0.416	0.235	0.999	0.573	0.679	1.000	0.343	1.000	0.889	0.785	0.918	**0.033**	0.227	0.752	**0.007**	0.560	0.985	0.824	0.549	0.600
	trxf - WT	3h	1.000	0.796	0.600	0.540	0.291	**0.003**	0.447	0.497	0.979	0.883	0.997	**0.002**	0.961	0.943	**0.048**	0.723	0.355	0.136	0.674	0.090	0.995	0.425	0.360	0.315	0.879	0.996	0.226
	trxm - WT	3h	0.933	0.904	0.932	0.115	0.571	0.603	0.679	0.243	0.999	0.639	0.998	**0.018**	0.847	0.705	0.992	0.402	0.219	**0.000**	0.585	0.726	0.986	0.890	0.534	0.650	0.996	0.757	0.859
	ntrc - WT	3h	0.978	0.968	0.913	0.983	0.894	0.656	0.994	0.147	0.988	0.180	0.924	0.675	0.985	0.997	**0.019**	1.000	**0.023**	0.959	0.284	1.000	0.873	**0.026**	0.945	0.731	1.000	0.226	0.975
	trxf - WT	3h15min	0.779	1.000	0.903	0.988	0.876	0.997	0.579	0.227	0.994	0.984	0.987	0.999	0.999	0.970	0.806	0.249	0.999	1.000	0.984	0.971	0.976	0.960	0.999	0.950	0.960	0.999	0.968
	trxm - WT	3h15min	1.000	0.994	0.886	0.999	0.105	0.381	0.936	0.882	0.952	0.254	0.998	0.987	0.568	0.335	0.997	0.897	0.970	0.825	0.725	0.980	0.218	0.424	0.625	0.894	0.863	0.793	0.992
	ntrc - WT	3h15min	0.998	1.000	0.987	0.998	**0.038**	0.228	0.334	0.429	0.886	0.684	0.975	0.972	0.714	0.978	0.982	0.995	0.873	0.118	0.371	**0.044**	0.452	**0.009**	0.493	0.693	0.618	**0.018**	0.811
	trxf - WT	4h	0.917	0.822	0.885	0.266	0.969	0.469	0.417	0.646	0.988	0.335	**0.000**	0.230	0.742	0.433	0.872	0.285	0.832	1.000	0.829	0.801	1.000	0.591	0.698	0.725	0.999	0.957	0.999
	trxm - WT	4h	0.880	0.755	0.725	0.966	1.000	0.977	**0.013**	0.210	1.000	0.818	0.999	0.725	0.597	0.932	0.799	**0.007**	0.749	0.420	0.997	0.115	0.995	0.534	1.000	0.884	0.861	0.866	1.000
	ntrc - WT	4h	0.997	0.993	0.992	0.999	0.976	0.552	0.146	0.661	0.133	0.864	0.858	1.000	0.783	0.613	0.412	0.059	0.282	0.711	0.187	0.682	0.562	0.426	0.420	**0.019**	0.872	**0.041**	0.981
	trxf - WT	6h	0.439	0.999	0.910	0.831	0.134	0.996	0.313	0.740	1.000	1.000	0.939	0.266	0.861	0.935	0.998	1.000	1.000	0.369	0.899	0.287	1.000	1.000	0.695	0.258	0.943	0.310	1.000
	trxm - WT	6h	0.869	0.678	0.596	0.465	0.207	0.889	**0.010**	0.852	0.738	0.896	0.846	0.331	0.224	0.432	0.983	0.897	0.732	0.472	1.000	0.086	0.137	0.873	0.638	**0.039**	0.696	0.676	0.251
	ntrc - WT	6h	**0.015**	0.968	1.000	0.587	**0.014**	0.890	**0.001**	0.979	0.496	1.000	0.646	**0.044**	0.972	0.742	0.416	0.051	0.802	**0.039**	0.369	0.209	0.926	0.118	0.614	0.940	0.999	**0.002**	0.616

GC-MS Data (Primary Metabolism)	ML							
All arbitrary units	WT		trxf		trxm		ntrc	
N	N: 5		N: 5		N: 5		N: 5	
	Mean	SD	Mean	SD	Mean	SD	Mean	SD
2-oxo-glutaric acid	0.0034	0.0001	0.0028	0.0004	0.0025	0.0007	0.0009	0.0004
4-hydroxy-proline	0.0042	0.0005	0.0037	0.0007	0.0045	0.0008	0.0024	0.0001
adenine	0.0027	0.0006	0.0040	0.0005	0.0027	0.0001	0.0025	0.0007
alanine	4.1490	0.5282	5.5100	0.1859	4.5480	1.5080	3.2160	0.6552
arginine	0.0239	0.0133	0.0633	0.0528	0.0207	0.0113	0.0105	0.0001
ascorbic acid	0.0016	0.0006	0.0026	0.0004	0.0019	0.0008	0.0014	0.0005
asparagine	0.0940	0.0126	0.1662	0.0535	0.1039	0.0532	0.0616	0.0087
aspartic acid	0.1296	0.0185	0.1425	0.0076	0.1183	0.0166	0.1371	0.0190
benzoic acid	0.0204	0.0067	0.0220	0.0054	0.0128	0.0013	0.0317	0.0048
beta-alanine	0.0296	0.0068	0.0378	0.0131	0.0399	0.0054	0.0338	0.0026
citric acid	0.0026	0.0015	0.0037	0.0014	0.0020	0.0008	0.0050	0.0014
dehydroascorbic acid	0.2903	0.0403	0.3074	0.0283	0.3201	0.0573	0.2687	0.0506
dehydroascorbic acid dimer	0.1263	0.0147	0.1286	0.0024	0.1381	0.0170	0.1365	0.0129
fructose	0.8028	0.1485	1.5630	0.6615	1.1870	0.8438	0.2370	0.0110
fucose	0.0580	0.0013	0.0588	0.0076	0.0469	0.0016	0.0357	0.0034
fumaric acid	2.4540	1.2570	3.4460	0.1865	2.3700	1.2140	3.9490	0.2450
gaba	0.0028	0.0007	0.0042	0.0017	0.0045	0.0002	0.0022	0.0005
galactinol	0.3345	0.0492	0.2966	0.0502	0.2867	0.0396	0.2651	0.0168
galactonic acid	0.0064	0.0011	0.0066	0.0011	0.0070	0.0014	0.0057	0.0012
glucose	3.1510	0.3800	4.1650	0.2986	4.3330	2.8080	0.4257	0.0627
glucuronic acid	0.0064	0.0011	0.0066	0.0011	0.0070	0.0014	0.0057	0.0012
glutamic acid	1.8420	0.2498	2.0240	0.0845	1.7010	0.4645	1.0150	0.2282
glutamine	3.0430	0.3602	8.4180	5.0330	3.2140	1.8010	1.7190	0.2783
glyceric acid	0.0175	0.0035	0.0133	0.0051	0.0128	0.0034	0.0070	0.0019
glycerol	0.1429	0.0060	0.1478	0.0217	0.1564	0.0225	0.2647	0.1324
glycine	6.7150	0.7333	6.8350	1.1250	4.1860	0.6413	0.4684	0.0513
guanidine	0.0058	0.0043	0.0177	0.0162	0.0054	0.0028	0.1166	0.0747
histidine	0.0009	0.0001	0.0011	0.0007	0.0011	0.0007	0.0008	0.0004
isoleucine	0.0630	0.0009	0.0641	0.0061	0.0603	0.0047	0.0674	0.0021
lactic acid	0.0583	0.0341	0.0200	0.0098	0.0200	0.0087	0.0203	0.0099
leucine	0.0650	0.0072	0.0750	0.0011	0.0633	0.0005	0.0386	0.0014
lysine	0.0263	0.0058	0.0383	0.0182	0.0222	0.0005	0.0178	0.0016
malic acid	0.0294	0.0009	0.0379	0.0005	0.0208	0.0107	0.0430	0.0037
maltose	0.0069	0.0001	0.0067	0.0006	0.0072	0.0010	0.0026	0.0008
methionine	0.0048	0.0015	0.0053	0.0008	0.0046	0.0010	0.0047	0.0012
myo-inositol	0.8960	0.0321	0.8394	0.1718	0.8769	0.1936	0.4756	0.0216
nicotinic acid	0.0062	0.0007	0.0060	0.0023	0.0043	0.0015	0.0087	0.0010
O-acetyl-serine	0.0056	0.0020	0.0077	0.0049	0.0074	0.0008	0.0042	0.0010
ornithine	0.5148	0.3635	1.0740	0.9237	0.2064	0.0677	0.1429	0.0339
phenylalanine	0.0629	0.0045	0.0718	0.0131	0.0521	0.0019	0.0335	0.0032
phosphoric acid	0.0680	0.0301	0.0693	0.0245	0.0597	0.0185	0.0822	0.0255
proline	2.6760	0.5145	3.1810	0.8011	3.0430	1.2560	1.2930	0.0355
putrescine	1.0660	0.5885	1.1270	0.4737	0.4824	0.0336	0.6849	0.0696
pyroglutamic acid	5.8820	0.5344	8.7980	0.4637	5.0330	1.6090	4.5790	0.7966
pyruvic acid	0.0265	0.0059	0.0249	0.0031	0.0290	0.0006	0.0283	0.0005
raffinose	0.0047	0.0017	0.0072	0.0039	0.0074	0.0023	0.0014	0.0001
rhamnose	0.0123	0.0012	0.0138	0.0025	0.0105	0.0009	0.0136	0.0004
serine	14.6900	1.9660	20.8600	10.0200	13.7900	5.6520	3.1420	0.5110
succinic acid	0.0264	0.0053	0.0220	0.0011	0.0212	0.0095	0.0140	0.0008
sucrose	12.5600	0.8088	15.5400	2.3250	14.1200	0.6069	6.1440	0.1089
sugar (similar-raffinose)	0.0047	0.0017	0.0072	0.0039	0.0074	0.0023	0.0014	0.0001
sugar (similar to trehalose)	0.0051	0.0011	0.0052	0.0013	0.0046	0.0011	0.0038	0.0001
threonic acid	0.0375	0.0051	0.0340	0.0044	0.0285	0.0054	0.0372	0.0020
threonine	1.0180	0.0422	1.1330	0.1773	1.1030	0.2198	1.0460	0.0336
trehalose	0.0219	0.0081	0.0168	0.0020	0.0185	0.0029	0.0168	0.0019
tryptophan	0.0031	0.0013	0.0044	0.0006	0.0022	0.0009	0.0011	0.0008
tyrosine	0.0127	0.0009	0.0143	0.0026	0.0123	0.0010	0.0088	0.0004
urea	0.0312	0.0194	0.0394	0.0185	0.0249	0.0042	0.0471	0.0004
valine	0.5537	0.0322	0.6644	0.0096	0.5788	0.0469	0.3301	0.0026

GC-MS Data (Primary Metabolism)	FL HL								FL LL							
All arbitrary units	WT		trxf		trxm		ntrc		WT		trxf		trxm		ntrc	
N	N: 3		N: 3		N: 3		N: 3		N: 3		N: 3		N: 3		N: 3	
	Mean	SD	Mean	SD	Mean	SD	Mean	SD	Mean	SD	Mean	SD	Mean	SD	Mean	SD
2-oxo-glutaric acid	0.0015	0.0005	0.0013	0.0007	0.0023	0.0006	0.0007	0.0005	0.0027	0.0009	0.0029	0.0010	0.0026	0.0008	0.0006	0.0005
4-hydroxy-proline	0.0029	0.0009	0.0039	0.0010	0.0026	0.0002	0.0029	0.0008	0.0051	0.0003	0.0047	0.0007	0.0035	0.0011	0.0028	0.0005
adenine	0.0016	0.0010	0.0019	0.0003	0.0012	0.0005	0.0010	0.0008	0.0039	0.0041	0.0041	0.0019	0.0035	0.0021	0.0015	0.0016
alanine	4.2020	0.7626	3.5100	0.5521	4.1360	1.2100	3.0470	0.7406	6.4120	1.8710	5.7350	1.4720	4.4730	1.0070	2.9610	0.4395
arginine	0.0061	0.0016	0.0098	0.0035	0.0083	0.0050	0.0036	0.0024	0.0061	0.0007	0.0124	0.0018	0.0074	0.0033	0.0068	0.0023
ascorbic acid	0.0024	0.0012	0.0018	0.0011	0.0009	0.0005	0.0011	0.0011	0.0022	0.0009	0.0023	0.0015	0.0010	0.0009	0.0016	0.0010
asparagine	0.0460	0.0169	0.0533	0.0139	0.0460	0.0213	0.0208	0.0152	0.0621	0.0378	0.0749	0.0197	0.0570	0.0170	0.0376	0.0182
aspartic acid	0.1022	0.0084	0.1047	0.0260	0.1579	0.0616	0.1113	0.0063	0.1707	0.1056	0.1506	0.0668	0.1321	0.0563	0.0967	0.0290
benzoic acid	0.0222	0.0018	0.0165	0.0018	0.0308	0.0041	0.0276	0.0091	0.0284	0.0090	0.0282	0.0045	0.0240	0.0014	0.0252	0.0050
beta-alanine	0.0114	0.0039	0.0156	0.0030	0.0128	0.0030	0.0123	0.0073	0.0144	0.0007	0.0157	0.0015	0.0165	0.0018	0.0300	0.0015
citric acid	0.0026	0.0014	0.0108	0.0074	0.0141	0.0186	0.0339	0.0493	0.0387	0.0506	0.0086	0.0061	0.0105	0.0123	0.0020	0.0021
dehydroascorbic acid	0.1902	0.0500	0.2005	0.0349	0.1587	0.0140	0.1339	0.0493	0.2460	0.0273	0.2817	0.0241	0.2361	0.0478	0.2080	0.0441
dehydroascorbic acid dimer	0.0990	0.0183	0.1010	0.0082	0.0879	0.0095	0.0882	0.0295	0.1281	0.0152	0.1388	0.0032	0.1170	0.0090	0.1156	0.0256
fructose	0.1277	0.0244	0.2247	0.0505	0.0939	0.0479	0.0663	0.1040	0.2514	0.1273	0.2247	0.1054	0.2416	0.1906	0.0110	0.0039
fucose	0.0389	0.0062	0.0423	0.0013	0.0334	0.0077	0.0284	0.0035	0.0432	0.0070	0.0487	0.0052	0.0436	0.0055	0.0302	0.0044
fumaric acid	0.4492	0.3320	0.4012	0.0132	0.4141	0.3221	0.9919	0.6097	0.6881	0.4484	0.7275	0.1857	0.4676	0.1322	0.4064	0.0919
gaba	0.0051	0.0013	0.0063	0.0014	0.0058	0.0040	0.0016	0.0014	0.0055	0.0024	0.0071	0.0017	0.0104	0.0070	0.0011	0.0002
galactinol	0.1892	0.0540	0.1916	0.0639	0.1756	0.0170	0.1544	0.0428	0.2262	0.0046	0.2166	0.0332	0.1904	0.0332	0.1791	0.0343
galactonic acid	0.0039	0.0018	0.0038	0.0016	0.0044	0.0011	0.0043	0.0014	0.0069	0.0003	0.0063	0.0010	0.0047	0.0011	0.0046	0.0005
glucose	0.4512	0.0285	0.8521	0.1077	0.2974	0.1208	0.2826	0.2717	0.9054	0.4411	0.8399	0.3740	0.7129	0.5205	0.1552	0.0164
glucuronic acid	0.0037	0.0021	0.0035	0.0021	0.0035	0.0026	0.0043	0.0014	0.0069	0.0003	0.0063	0.0010	0.0047	0.0011	0.0046	0.0005
glutamic acid	1.2070	0.0614	1.1380	0.2382	1.1230	0.6394	0.5317	0.0678	2.0060	1.0200	1.4840	0.1790	1.3910	0.2936	0.6202	0.2516
glutamine	0.6133	0.0940	0.7294	0.1597	0.5699	0.4129	0.1334	0.0315	1.0700	0.5703	1.1940	0.1583	0.7474	0.1553	0.1329	0.0506
glyceric acid	0.0113	0.0024	0.0045	0.0013	0.0106	0.0073	0.0050	0.0043	0.0261	0.0077	0.0115	0.0023	0.0144	0.0007	0.0018	0.0002
glycerol	0.1836	0.0212	0.2151	0.0157	0.2184	0.0876	0.1839	0.0361	0.2069	0.0652	0.1443	0.0177	0.1635	0.0416	0.3102	0.0753
glycine	0.7297	0.1431	0.7056	0.0472	1.3940	1.7940	0.2011	0.1523	0.9278	0.3977	0.8178	0.3188	0.5738	0.1905	0.1122	0.0194
guanidine	0.0100	0.0083	0.0024	0.0029	0.0164	0.0110	0.0004	0.0002	0.0146	0.0187	0.0027	0.0027	0.0054	0.0049	0.0003	0.0004
histidine	0.0012	0.0008	0.0006	0.0004	0.0010	0.0007	0.0017	0.0012	0.0010	0.0006	0.0021	0.0012	0.0012	0.0007	0.0012	0.0010
isoleucine	0.0556	0.0097	0.0619	0.0057	0.0728	0.0260	0.0470	0.0166	0.0817	0.0175	0.0682	0.0090	0.0648	0.0091	0.0908	0.0168
lactic acid	0.0394	0.0125	0.0546	0.0348	0.0270	0.0108	0.0210	0.0080	0.0900	0.0191	0.0145	0.0090	0.0365	0.0126	0.0422	0.0194
leucine	0.0586	0.0093	0.0642	0.0076	0.0588	0.0126	0.0387	0.0118	0.0847	0.0239	0.0647	0.0076	0.0689	0.0119	0.0793	0.0083
lysine	0.0197	0.0030	0.0199	0.0027	0.0212	0.0059	0.0124	0.0046	0.0270	0.0087	0.0219	0.0008	0.0234	0.0035	0.0217	0.0015
malic acid	0.0171	0.0076	0.0191	0.0036	0.0215	0.0099	0.0292	0.0063	0.0368	0.0320	0.0261	0.0089	0.0174	0.0036	0.0202	0.0063
maltose	0.0041	0.0012	0.0033	0.0001	0.0033	0.0016	0.0026	0.0007	0.0053	0.0006	0.0050	0.0004	0.0056	0.0008	0.0014	0.0006
methionine	0.0032	0.0011	0.0036	0.0015	0.0026	0.0008	0.0020	0.0016	0.0029	0.0016	0.0035	0.0004	0.0030	0.0005	0.0029	0.0007
myo-inositol	0.4892	0.0361	0.5755	0.1683	0.3452	0.0558	0.2469	0.0312	0.6420	0.0407	0.6428	0.1642	0.5230	0.1441	0.3385	0.0680
nicotinic acid	0.0044	0.0022	0.0041	0.0016	0.0068	0.0070	0.0111	0.0084	0.0041	0.0006	0.0043	0.0014	0.0062	0.0025	0.0234	0.0060
O-acetyl-serine	0.0048	0.0012	0.0047	0.0014	0.0035	0.0012	0.0026	0.0007	0.0059	0.0010	0.0065	0.0007	0.0051	0.0011	0.0046	0.0012
ornithine	0.2149	0.0420	0.2227	0.0566	0.1883	0.1336	0.0757	0.0555	0.2595	0.0713	0.3406	0.1067	0.1982	0.0274	0.1450	0.0486
phenylalanine	0.0269	0.0031	0.0254	0.0024	0.0223	0.0075	0.0152	0.0021	0.0364	0.0033	0.0287	0.0027	0.0283	0.0046	0.0214	0.0021
phosphoric acid	0.0773	0.0558	0.1022	0.0567	0.1594	0.0985	0.1286	0.0498	0.4198	0.6168	0.1835	0.2096	0.1191	0.1227	0.1353	0.1238
proline	1.4080	0.2668	1.0730	0.5222	1.6040	0.8249	0.7368	0.1604	3.4490	2.7140	1.9060	0.1783	1.5020	0.3339	0.5944	0.1062
putrescine	0.4653	0.0139	0.4946	0.1512	0.5845	0.4263	0.3092	0.1849	0.6182	0.0331	0.6058	0.0265	0.4962	0.0245	0.5152	0.1049
pyroglutamic acid	2.8940	0.4256	2.8800	0.4901	2.6600	1.3180	1.6410	0.3322	4.8120	2.1680	4.1470	0.3343	3.2570	0.3801	1.4970	0.4669
pyruvic acid	0.0495	0.0062	0.0383	0.0068	0.0365	0.0177	0.0236	0.0024	0.0678	0.0021	0.0608	0.0155	0.0633	0.0156	0.0308	0.0049
raffinose	0.0058	0.0024	0.0062	0.0041	0.0033	0.0016	0.0011	0.0005	0.0116	0.0069	0.0077	0.0042	0.0090	0.0088	0.0022	0.0016
rhamnose	0.0136	0.0009	0.0131	0.0003	0.0141	0.0026	0.0144	0.0062	0.0155	0.0016	0.0175	0.0028	0.0137	0.0010	0.0237	0.0025
serine	7.2460	4.1320	5.5330	1.7560	6.0130	4.5080	3.0380	2.8670	6.3620	1.3820	7.4620	3.4470	8.5990	4.9320	3.8790	0.7167
succinic acid	0.0265	0.0115	0.0143	0.0004	0.0199	0.0227	0.0160	0.0150	0.0365	0.0196	0.0232	0.0089	0.0268	0.0032	0.0061	0.0023
sucrose	6.0320	0.8437	7.2450	0.9357	4.5030	2.3030	1.9630	0.6798	8.7590	0.4957	8.9180	0.6473	7.8800	0.6727	1.7940	0.4029
sugar (similar-raffinose)	0.0058	0.0024	0.0062	0.0041	0.0033	0.0016	0.0012	0.0004	0.0116	0.0069	0.0077	0.0042	0.0090	0.0088	0.0024	0.0012
sugar (similar to trehalose)	0.0031	0.0004	0.0048	0.0012	0.0035	0.0012	0.0037	0.0012	0.0047	0.0016	0.0046	0.0015	0.0033	0.0010	0.0057	0.0021
threonic acid	0.0279	0.0049	0.0277	0.0009	0.0347	0.0071	0.0306	0.0047	0.0405	0.0142	0.0371	0.0096	0.0298	0.0014	0.0328	0.0093
threonine	0.4286	0.0569	0.5107	0.0743	0.5589	0.1378	0.5994	0.3212	0.5731	0.0163	0.7312	0.1022	0.6519	0.1212	1.0310	0.1563
trehalose	0.0115	0.0022	0.0089	0.0018	0.0113	0.0034	0.0077	0.0031	0.0124	0.0022	0.0087	0.0024	0.0091	0.0011	0.0154	0.0040
tryptophan	0.0006	0.0001	0.0018	0.0018	0.0004	0.0003	0.0014	0.0015	0.0009	0.0005	0.0012	0.0010	0.0011	0.0005	0.0013	0.0005
tyrosine	0.0104	0.0010	0.0087	0.0018	0.0093	0.0014	0.0053	0.0026	0.0145	0.0025	0.0112	0.0015	0.0089	0.0038	0.0122	0.0019
urea	0.0693	0.0052	0.0480	0.0174	0.0768	0.0602	0.0236	0.0081	0.1559	0.1335	0.0280	0.0102	0.0584	0.0452	0.0353	0.0054
valine	0.3981	0.0648	0.4450	0.0670	0.3538	0.0670	0.2667	0.0388	0.5014	0.0392	0.4986	0.0052	0.4613	0.0380	0.4427	0.0528

GC-MS Data (Primary Metabolism)	HL								LL							
All arbitrary units	WT		trxf		trxm		ntrc		WT		trxf		trxm		ntrc	
N	N: 5		N: 5		N: 5		N: 5		N: 5		N: 5		N: 5		N: 5	
	Mean	SD	Mean	SD	Mean	SD	Mean	SD	Mean	SD	Mean	SD	Mean	SD	Mean	SD
2-oxo-glutaric acid	0.0032	0.0009	0.0025	0.0016	0.0021	0.0000	0.0007	0.0002	0.0028	0.0006	0.0010	0.0001	0.0026	0.0010	0.0005	0.0004
4-hydroxy-proline	0.0096	0.0008	0.0104	0.0024	0.0070	0.0022	0.0031	0.0005	0.0037	0.0001	0.0040	0.0008	0.0038	0.0008	0.0032	0.0007
adenine	0.0038	0.0012	0.0038	0.0002	0.0035	0.0021	0.0016	0.0006	0.0024	0.0017	0.0023	0.0009	0.0021	0.0002	0.0016	0.0001
alanine	4.6640	0.8425	3.9410	0.4852	4.1420	1.3420	7.8710	0.7302	3.2750	0.2709	3.1020	0.3860	1.2240	0.6649	2.0670	0.2956
arginine	0.0452	0.0263	0.0402	0.0052	0.0339	0.0159	0.0078	0.0019	0.0136	0.0027	0.0138	0.0037	0.0289	0.0158	0.0051	0.0011
ascorbic acid	0.0051	0.0009	0.0048	0.0008	0.0042	0.0018	0.0054	0.0004	0.0025	0.0011	0.0026	0.0009	0.0017	0.0016	0.0023	0.0006
asparagine	0.3808	0.1646	0.4321	0.0527	0.2315	0.0792	0.0841	0.0198	0.1527	0.0428	0.1289	0.0343	0.1356	0.0305	0.0774	0.0295
aspartic acid	0.1205	0.0041	0.0983	0.0143	0.1076	0.0107	0.1469	0.0200	0.1610	0.0477	0.1443	0.0234	0.0874	0.0410	0.1437	0.0447
benzoic acid	0.0276	0.0047	0.0253	0.0068	0.0268	0.0070	0.0382	0.0091	0.0235	0.0067	0.0229	0.0037	0.0174	0.0028	0.0284	0.0025
beta-alanine	0.0352	0.0141	0.0514	0.0028	0.0359	0.0101	0.0210	0.0025	0.0139	0.0048	0.0137	0.0033	0.0143	0.0032	0.0179	0.0042
citric acid	0.0295	0.0137	0.0355	0.0036	0.0298	0.0040	0.0075	0.0013	0.0058	0.0021	0.0040	0.0009	0.0026	0.0019	0.0036	0.0016
dehydroascorbic acid	0.5640	0.1378	0.7792	0.0662	0.3835	0.0513	0.1523	0.0045	0.0704	0.0067	0.0629	0.0058	0.0520	0.0127	0.0448	0.0067
dehydroascorbic acid dimer	0.2195	0.0519	0.3028	0.0265	0.1627	0.0221	0.0844	0.0040	0.0483	0.0071	0.0438	0.0033	0.0323	0.0079	0.0418	0.0075
fructose	8.5140	2.0200	10.9600	1.4950	5.7170	2.3240	1.0100	0.0175	0.6951	0.2778	0.6817	0.1351	0.3836	0.0582	0.1235	0.0243
fucose	0.0868	0.0146	0.0898	0.0075	0.0698	0.0025	0.0396	0.0038	0.0560	0.0039	0.0560	0.0043	0.0554	0.0010	0.0352	0.0050
fumaric acid	2.5870	0.7459	2.5370	0.1134	1.6400	1.3610	5.2620	2.7730	1.5990	0.5058	1.5680	0.0995	0.2535	0.1643	1.0450	0.0724
gaba	0.0094	0.0019	0.0109	0.0009	0.0084	0.0017	0.0014	0.0007	0.0016	0.0001	0.0023	0.0008	0.0035	0.0013	0.0015	0.0009
galactinol	0.4111	0.0206	0.4471	0.0230	0.3090	0.0133	0.1901	0.0059	0.3290	0.0317	0.3068	0.0013	0.2369	0.0022	0.2001	0.0292
galactonic acid	0.0196	0.0037	0.0217	0.0036	0.0164	0.0038	0.0106	0.0005	0.0074	0.0012	0.0072	0.0010	0.0050	0.0019	0.0041	0.0019
glucose	14.2600	2.5390	15.7600	1.5390	12.9300	0.9559	3.3820	0.1390	2.8490	0.9507	2.9710	0.7556	1.9420	0.5568	0.4279	0.0181
glucuronic acid	0.0196	0.0037	0.0217	0.0036	0.0164	0.0038	0.0106	0.0005	0.0074	0.0012	0.0072	0.0010	0.0050	0.0019	0.0041	0.0019
glutamic acid	4.0640	1.3440	5.5390	0.8445	4.4670	1.7670	1.1680	0.1940	1.1960	0.1683	0.9830	0.2028	1.4700	0.3936	0.4452	0.1512
glutamine	17.0900	8.5210	20.4500	2.8150	12.5200	5.4900	1.8840	0.6766	2.6700	0.2144	2.4900	0.7223	2.1960	0.8294	0.9217	0.1815
glyceric acid	0.0291	0.0021	0.0130	0.0036	0.0261	0.0074	0.0142	0.0010	0.0184	0.0037	0.0139	0.0028	0.0082	0.0002	0.0073	0.0018
glycerol	0.0863	0.0204	0.1201	0.0121	0.0886	0.0153	0.2003	0.0300	0.0983	0.0134	0.0828	0.0059	0.1045	0.0122	0.2544	0.0756
glycine	18.0700	0.7637	6.6730	0.2958	14.0500	5.4610	1.4690	0.4335	1.4920	0.4382	1.6090	0.4332	1.9460	0.3786	0.1849	0.0341
guanidine	0.0068	0.0029	0.0053	0.0007	0.0039	0.0017	0.0028	0.0018	0.0097	0.0083	0.0029	0.0025	0.0050	0.0051	0.0007	0.0003
histidine	0.0027	0.0016	0.0035	0.0013	0.0020	0.0009	0.0012	0.0005	0.0006	0.0002	0.0009	0.0008	0.0002	0.0001	0.0007	0.0004
isoleucine	0.1102	0.0257	0.1053	0.0233	0.0809	0.0184	0.0875	0.0150	0.0453	0.0011	0.0448	0.0058	0.0435	0.0034	0.0449	0.0062
lactic acid	0.0081	0.0018	0.0097	0.0022	0.0125	0.0044	0.0127	0.0044	0.0142	0.0065	0.0100	0.0025	0.0097	0.0025	0.0118	0.0019
leucine	0.0987	0.0319	0.0992	0.0349	0.0737	0.0008	0.0481	0.0097	0.0491	0.0037	0.0433	0.0065	0.0410	0.0035	0.0348	0.0041
lysine	0.0470	0.0156	0.0436	0.0016	0.0329	0.0044	0.0202	0.0013	0.0175	0.0001	0.0171	0.0020	0.0218	0.0010	0.0118	0.0030
malic acid	0.0425	0.0166	0.0335	0.0110	0.0192	0.0140	0.1018	0.0605	0.0320	0.0048	0.0289	0.0027	0.0129	0.0096	0.0496	0.0121
maltose	0.0123	0.0019	0.0144	0.0012	0.0122	0.0007	0.0038	0.0010	0.0049	0.0003	0.0027	0.0004	0.0033	0.0003	0.0022	0.0002
methionine	0.0360	0.0072	0.0398	0.0026	0.0305	0.0065	0.0127	0.0012	0.0138	0.0027	0.0140	0.0018	0.0120	0.0014	0.0055	0.0011
myo-inositol	1.9050	0.3383	2.5840	0.0263	1.2960	0.5112	0.4631	0.0504	0.9136	0.0087	0.9020	0.0834	0.8418	0.0585	0.2783	0.0415
nicotinic acid	0.0049	0.0024	0.0053	0.0013	0.0031	0.0003	0.0083	0.0003	0.0078	0.0023	0.0064	0.0034	0.0045	0.0017	0.0110	0.0037
O-acetyl-serine	0.0191	0.0043	0.0096	0.0003	0.0073	0.0017	0.0044	0.0005	0.0022	0.0005	0.0014	0.0005	0.0013	0.0002	0.0015	0.0003
ornithine	0.5242	0.2501	0.2511	0.0183	0.3680	0.1669	0.1115	0.0046	0.2862	0.0282	0.3377	0.1472	0.8744	0.5660	0.1266	0.0049
phenylalanine	0.1900	0.0721	0.1512	0.0332	0.1206	0.0313	0.0297	0.0020	0.0325	0.0013	0.0287	0.0013	0.0313	0.0028	0.0207	0.0035
phosphoric acid	0.0847	0.0179	0.0871	0.0226	0.0696	0.0061	0.0693	0.0253	0.0793	0.0335	0.0651	0.0225	0.0549	0.0097	0.0922	0.0268
proline	51.0900	23.3400	50.4600	0.1064	29.4700	12.5000	2.2550	0.3997	1.8740	0.4383	2.1710	0.4432	2.3450	0.8957	1.1220	0.2298
putrescine	1.1570	0.1299	1.1910	0.2105	0.9850	0.2955	0.5976	0.0384	0.7082	0.0409	0.6791	0.0847	0.6016	0.0792	0.5923	0.0961
pyroglutamic acid	25.2300	11.7500	31.5900	0.8982	20.1200	8.7770	6.4880	3.5130	7.8980	1.9460	6.0710	0.1990	5.9710	2.1440	4.4190	0.7371
pyruvic acid	0.0160	0.0036	0.0167	0.0014	0.0202	0.0075	0.0473	0.0024	0.0303	0.0041	0.0304	0.0016	0.0180	0.0066	0.0214	0.0044
raffinose	0.0154	0.0034	0.0206	0.0021	0.0171	0.0081	0.0041	0.0027	0.0133	0.0039	0.0109	0.0014	0.0142	0.0027	0.0020	0.0010
rhamnose	0.0185	0.0025	0.0208	0.0018	0.0152	0.0020	0.0150	0.0021	0.0100	0.0015	0.0105	0.0011	0.0113	0.0011	0.0113	0.0005
serine	26.7700	5.6260	29.7800	0.2595	33.6600	8.4470	2.6420	0.3908	6.3680	1.1400	4.3920	0.1107	21.1700	10.6300	1.7890	0.4137
succinic acid	0.0258	0.0077	0.0250	0.0124	0.0182	0.0075	0.0226	0.0083	0.0153	0.0041	0.0116	0.0018	0.0098	0.0050	0.0079	0.0032
sucrose	27.3000	4.0130	33.4600	1.6090	27.5900	1.2870	13.5800	1.6930	5.3740	0.4401	4.7890	0.1883	4.7790	0.2183	1.9100	0.3014
sugar (similar-raffinose)	0.0154	0.0034	0.0206	0.0021	0.0171	0.0081	0.0041	0.0027	0.0133	0.0039	0.0109	0.0014	0.0142	0.0027	0.0020	0.0010
sugar (similar to trehalose)	0.0115	0.0014	0.0135	0.0003	0.0082	0.0012	0.0043	0.0007	0.0041	0.0004	0.0038	0.0010	0.0027	0.0004	0.0050	0.0004
threonic acid	0.0360	0.0051	0.0282	0.0021	0.0250	0.0012	0.0418	0.0117	0.0189	0.0039	0.0163	0.0009	0.0131	0.0004	0.0201	0.0050
threonine	1.2790	0.3106	1.3550	0.2096	1.3330	0.1153	0.9657	0.1577	0.7882	0.0978	0.6715	0.0850	0.7997	0.0914	0.7038	0.1678
trehalose	0.0526	0.0093	0.0608	0.0047	0.0553	0.0127	0.0180	0.0013	0.0076	0.0002	0.0062	0.0005	0.0079	0.0035	0.0094	0.0032
tryptophan	0.0102	0.0038	0.0129	0.0012	0.0072	0.0032	0.0008	0.0002	0.0010	0.0009	0.0005	0.0004	0.0008	0.0002	0.0004	0.0002
tyrosine	0.0290	0.0082	0.0273	0.0047	0.0212	0.0053	0.0093	0.0018	0.0079	0.0014	0.0062	0.0013	0.0087	0.0008	0.0057	0.0003
urea	0.0588	0.0041	0.0682	0.0153	0.0594	0.0012	0.0396	0.0142	0.0295	0.0013	0.0297	0.0032	0.0330	0.0105	0.0287	0.0077
valine	0.8129	0.2252	0.9398	0.1990	0.7849	0.0880	0.4194	0.0453	0.3815	0.0578	0.3718	0.0720	0.3190	0.0525	0.2321	0.0241

Supplement Table 5.4.5. Raw data of GC-MS based metabolite profile in long-term acclimated WT, *trxf*, *trxm* and *ntrc*. 4 weeks after sowing plants were harvested in the middle of the light period. Values are given as mean ± SD from n= 3 – 5 biological replicates.

contrast (rel. to WT)	trxf	trxm	ntrc	trxf	trxm	ntrc	trxf	trxm	ntrc	trxf	trxm	ntrc	trxf	trxm	ntrc
Light		**ML**			**FL_HL**			**FL_LL**			**HL**			**LL**	
2-oxo-glutaric acid	0.546	0.219	**0.000**	0.990	0.489	0.490	0.977	0.999	**0.004**	0.405	0.071	**0.000**	**0.001**	0.990	**0.000**
4-hydroxy-proline	0.887	0.943	**0.042**	0.659	0.982	1.000	0.967	0.211	**0.038**	0.612	**0.001**	**0.000**	0.948	0.998	0.877
adenine	0.387	1.000	0.998	0.992	0.970	0.931	0.998	0.967	0.089	1.000	0.972	**0.043**	0.999	0.968	0.700
alanine	0.071	0.884	0.328	0.761	1.000	0.365	0.772	**0.038**	**0.000**	0.552	0.775	**0.000**	0.989	**0.002**	0.131
arginine	**0.002**	0.990	0.580	0.993	0.999	0.998	0.966	1.000	1.000	0.964	0.703	**0.004**	1.000	0.468	0.846
ascorbic acid	0.448	0.982	0.993	0.868	0.221	0.346	0.999	0.447	0.878	0.972	0.473	0.967	0.999	0.612	0.992
asparagine	0.178	0.992	0.791	0.998	1.000	0.944	0.992	1.000	0.949	0.466	**0.000**	**0.000**	0.905	0.962	0.149
aspartic acid	0.940	0.958	0.987	1.000	0.233	0.989	0.900	0.551	0.063	0.760	0.940	0.648	0.880	**0.009**	0.868
benzoic acid	0.968	0.139	**0.010**	0.593	0.234	0.632	1.000	0.773	0.898	0.919	0.997	**0.017**	0.999	0.310	0.504
beta-alanine	0.205	0.068	0.739	0.854	0.994	0.998	0.995	0.979	**0.023**	**0.001**	0.998	**0.006**	1.000	1.000	0.765
citric acid	0.999	1.000	0.993	0.885	0.737	**0.035**	**0.046**	0.067	**0.009**	0.898	1.000	0.065	0.997	0.983	0.994
dehydroascorbic acid	0.949	0.786	0.905	0.994	0.869	0.522	0.821	0.995	0.792	**0.000**	**0.000**	**0.000**	0.995	0.939	0.852
dehydroascorbic acid dimer	0.998	0.766	0.837	0.999	0.894	0.902	0.903	0.895	0.857	**0.000**	**0.000**	**0.000**	0.983	0.560	0.952
fructose	0.546	0.907	0.755	0.999	1.000	1.000	1.000	1.000	0.988	**0.000**	**0.000**	**0.000**	1.000	0.947	0.749
fucose	0.996	**0.019**	**0.000**	0.884	0.667	0.134	0.667	1.000	**0.038**	0.841	**0.000**	**0.000**	1.000	0.998	**0.000**
fumaric acid	0.344	0.999	0.065	1.000	1.000	0.892	1.000	0.992	0.983	1.000	0.385	**0.000**	1.000	0.114	0.785
gaba	0.647	0.443	0.963	0.862	0.968	0.098	0.730	**0.010**	**0.020**	0.545	0.823	**0.000**	0.923	0.387	1.000
galactinol	0.244	0.091	**0.005**	1.000	0.953	0.540	0.982	0.514	0.274	0.284	**0.000**	**0.000**	0.686	**0.000**	**0.000**
galactonic acid	0.996	0.950	0.942	1.000	0.992	0.993	0.985	0.517	0.495	0.325	0.062	**0.000**	0.997	0.202	**0.045**
glucose	0.483	0.347	**0.002**	0.971	0.998	0.998	1.000	0.997	0.844	0.159	0.244	**0.000**	0.998	0.577	**0.006**
glucuronic acid	0.996	0.955	0.947	0.999	0.999	0.979	0.986	0.545	0.524	0.354	0.076	**0.000**	0.998	0.228	0.056
glutamic acid	0.973	0.987	0.214	0.999	0.999	0.604	0.773	0.673	0.062	**0.005**	0.774	**0.000**	0.957	0.916	0.292
glutamine	**0.029**	1.000	0.895	1.000	1.000	0.997	1.000	0.999	0.980	0.289	0.081	**0.000**	1.000	0.994	0.789
glyceric acid	0.295	0.198	**0.000**	0.129	0.995	0.177	**0.000**	**0.002**	**0.000**	**0.000**	0.580	**0.000**	0.240	**0.000**	**0.000**
glycerol	0.998	0.971	**0.001**	0.854	0.812	1.000	0.391	0.688	0.051	0.686	1.000	**0.002**	0.957	0.997	**0.000**
glycine	0.999	**0.043**	**0.000**	1.000	0.947	0.972	1.000	0.991	0.907	**0.000**	**0.000**	**0.000**	0.999	0.963	0.508
guanidine	0.776	1.000	**0.000**	0.964	0.979	0.934	0.884	0.941	0.816	0.999	0.996	0.989	0.949	0.983	0.889
histidine	0.986	0.984	0.997	0.846	0.987	0.837	0.346	0.993	0.992	0.468	0.474	**0.017**	0.922	0.882	1.000
isoleucine	0.999	0.988	0.955	0.937	0.395	0.859	0.605	0.412	0.834	0.939	**0.005**	**0.044**	1.000	0.996	1.000
lactic acid	**0.000**	**0.000**	**0.000**	0.501	0.663	0.328	**0.000**	**0.000**	**0.000**	0.998	0.953	0.947	0.959	0.950	0.991
leucine	0.671	0.997	**0.020**	0.960	1.000	0.305	0.305	0.510	0.964	1.000	**0.030**	**0.000**	0.912	0.797	0.374
lysine	**0.033**	0.766	0.198	1.000	0.994	0.547	0.788	0.912	0.767	0.861	**0.009**	**0.000**	1.000	0.741	0.546
malic acid	0.883	0.879	0.643	0.999	0.991	0.848	0.889	0.566	0.684	0.864	0.195	**0.000**	0.993	0.358	0.431
maltose	0.993	0.915	**0.000**	0.664	0.735	0.196	0.964	0.976	**0.000**	**0.001**	1.000	**0.000**	**0.001**	**0.035**	**0.000**
methionine	0.994	0.999	1.000	0.997	0.995	0.956	0.994	1.000	1.000	0.153	**0.013**	**0.000**	1.000	0.744	**0.000**
myo-inositol	0.958	0.998	**0.002**	0.933	0.753	0.346	1.000	0.844	0.166	**0.000**	**0.000**	**0.000**	1.000	0.919	**0.000**
nicotinic acid	1.000	0.748	0.536	0.999	0.765	**0.033**	1.000	0.812	**0.000**	0.997	0.756	0.261	0.871	0.288	0.330
O-acetyl-serine	0.296	0.415	0.658	1.000	0.832	0.487	0.985	0.957	0.833	**0.000**	**0.000**	**0.000**	0.898	0.872	0.925
ornithine	**0.023**	0.374	0.216	1.000	1.000	0.942	0.987	0.994	0.966	0.482	0.844	0.143	0.993	**0.015**	0.836
phenylalanine	0.917	0.860	0.152	1.000	0.994	0.912	0.972	0.969	0.831	**0.032**	**0.000**	**0.000**	0.993	1.000	0.827
phosphoric acid	1.000	1.000	0.998	0.995	0.847	0.957	0.098	**0.020**	**0.031**	1.000	0.997	0.997	0.998	0.989	0.998
proline	0.999	1.000	0.988	1.000	1.000	0.999	0.992	0.984	0.953	0.999	**0.000**	**0.000**	1.000	0.999	0.998
putrescine	0.977	**0.001**	0.058	0.999	0.924	0.846	1.000	0.919	0.949	0.996	0.651	**0.002**	0.997	0.889	0.862
pyroglutamic acid	0.642	0.986	0.952	1.000	1.000	0.979	0.997	0.962	0.728	0.059	0.174	**0.000**	0.881	0.864	0.500
pyruvic acid	0.977	0.927	0.970	0.152	0.072	**0.000**	0.546	0.827	**0.000**	0.998	0.719	**0.000**	1.000	**0.019**	0.135
raffinose	0.701	0.654	0.499	0.999	0.843	0.428	0.578	0.830	**0.015**	0.131	0.887	**0.000**	0.739	0.983	**0.000**
rhamnose	0.669	0.452	0.763	0.992	0.990	0.949	0.610	0.690	**0.000**	0.263	0.060	**0.042**	0.978	0.737	0.719
serine	0.214	0.992	**0.003**	0.975	0.990	0.730	0.993	0.946	0.929	0.775	0.138	**0.000**	0.923	**0.000**	0.472
succinic acid	0.847	0.774	0.113	0.318	0.782	0.446	0.240	0.520	**0.000**	0.999	0.507	0.936	0.903	0.747	0.530
sucrose	**0.011**	0.341	**0.000**	0.742	0.580	**0.006**	0.999	0.883	**0.000**	**0.000**	0.989	**0.000**	0.922	0.918	**0.002**
sugar similar to trehalose	0.999	0.879	0.235	0.197	0.968	0.897	0.999	0.357	0.670	**0.022**	**0.000**	**0.000**	0.948	0.127	0.585
sugar similar to raffinose	0.700	0.653	0.498	0.999	0.843	0.440	0.577	0.829	**0.018**	0.130	0.887	**0.000**	0.738	0.983	**0.000**
threonic acid	0.768	0.074	1.000	1.000	0.475	0.941	0.894	0.115	0.373	0.149	**0.018**	0.390	0.894	0.384	0.988
threonine	0.667	0.831	0.992	0.921	0.748	0.557	0.618	0.930	**0.004**	0.874	0.949	**0.014**	0.655	0.999	0.836
trehalose	0.397	0.709	0.393	0.924	1.000	0.790	0.807	0.859	0.881	0.055	0.824	**0.000**	0.970	1.000	0.947
tryptophan	0.454	0.767	0.154	0.729	0.998	0.900	0.995	0.999	0.981	**0.023**	**0.009**	**0.000**	0.966	0.998	0.912
tyrosine	0.834	0.997	0.202	0.905	0.975	0.191	0.579	0.132	0.812	0.823	**0.001**	**0.000**	0.814	0.980	0.670
urea	0.970	0.986	0.820	0.803	0.989	0.223	**0.000**	**0.001**	**0.000**	0.955	1.000	0.721	1.000	0.998	1.000
valine	0.208	0.970	**0.001**	0.916	0.928	0.275	1.000	0.945	0.849	0.117	0.959	**0.000**	0.998	0.682	**0.047**

Supplement Table 5.4.6. List of *p* value from GC-MS based metabolites in long-term acclimated plants.
A 2-way ANOVA with *post-hoc* Tukey test was performed using the "emmeans" and "multcomp" packages from R. Values are given relative to the respective WT. Significances ($p < 0.05$) are given in bold.

Descriptive Statistics	ML				FL_HL				FL_LL				HL				LL			
LC-MS	WT	trxf	trxm	ntrc	WT	trxf	trxm	ntrc	WT	trxf	trxm	ntrc	WT	trxf	trxm	ntrc	WT	trxf	trxm	ntrc
Calvin-Benson-Cycle Intermediates	N: 5	N: 5	N: 5	N: 5	N: 3	N: 3	N: 3	N: 3	N: 3	N: 3	N: 3	N: 3	N: 5	N: 5	N: 5	N: 5	N: 5	N: 5	N: 5	N: 5
pmol/µg Protein	Mean±SD	Mean±SD	Mean±SD	Mean±SD	Mean±SD	Mean±SD	Mean±SD	Mean±SD	Mean±SD	Mean±SD	Mean±SD	Mean±SD	Mean±SD	Mean±SD	Mean±SD	Mean±SD	Mean±SD	Mean±SD	Mean±SD	Mean±SD
2PG (2 phosphoglycolate)	0.228±0.04	0.201±0.05	0.241±0.08	0.388±0.17	0.648±0.13	0.479±0.19	0.346±0.17	0.662±0.63	0.281±0.06	0.237±0.08	0.233±0.06	0.154±0.03	0.304±0.26	0.205±0.06	0.323±0.14	0.358±0.08	0.157±0.02	0.156±0.04	0.247±0.03	0.317±0.10
3PGA	NA	NA	NA	NA	10.52±5.54	8.66±2.27	12.03±7.15	9.47±2.83	33.15±3.92	18.2±6.97	23.83±3.31	8.1±2.8	NA	NA	NA	NA	NA	NA	NA	NA
aconitate	NA	NA	NA	NA	3.23±2.23	2.43±1.01	3.45±1.45	5.92±7.92	3.68±1.27	3.72±1.4	3.66±1.14	0.622±0.66	NA	NA	NA	NA	NA	NA	NA	NA
ADP	1.28±0.285	1.05±0.156	1.26±0.447	1.64±0.617	1.78±0.233	1.63±0.314	1.54±0.514	1.49±0.565	2.28±0.14	1.83±0.157	1.81±0.163	1.68±0.21	1.35±0.602	1.38±0.6	1.27±0.221	1.06±0.1	0.821±0.13	0.897±0.21	1.31±0.246	1.31±0.385
ADPG	0.202±0.04	0.146±0.02	0.206±0.06	0.178±0.11	0.046±0.03	0.043±0.01	0.057±0.05	0.057±0.02	0.205±0.01	0.122±0.01	0.128±0.00	0.079±0.01	0.22±0.083	0.193±0.08	0.229±0.04	0.185±0.06	0.077±0.01	0.067±0.00	0.114±0.02	0.156±0.12
AMP	1.4±0.651	0.832±0.12	1.13±0.317	1.19±0.581	1.45±0.245	1.31±0.556	1.21±0.28	1.05±0.317	2.04±0.27	1.76±0.325	1.77±0.456	1.09±0.255	1.47±0.604	1.61±0.953	1.37±0.294	0.69±0.036	0.631±0.14	0.741±0.31	1.06±0.569	1.08±0.729
DHAP	3.48±0.768	4.15±0.267	4.8±1.67	5.73±2.41	3.6±0.197	3.23±0.745	2.38±0.484	4.74±2.17	1.76±0.111	1.99±0.541	2±0.376	2.64±0.264	4.45±2.01	4.66±1.63	4.57±1.03	4.26±0.582	2.75±0.331	3.65±0.536	4.49±0.674	4.87±0.782
F6P	10.93±2.05	11.73±0.92	13.81±5.23	18.69±8.96	14.18±0.30	12.16±1.94	9.87±2.46	11.92±4.62	9.23±1.64	8.93±1.74	7.93±0.935	6.47±1.51	12.31±5.1	12.27±4.71	11.95±2.59	12.3±2.16	8.73±0.898	10.14±0.86	11.15±1.61	17±2.6
FBP	1.14±0.19	2.28±0.164	1.45±0.525	3.54±1.23	0.929±0.07	1.25±0.219	0.819±0.18	2.15±0.497	0.715±0.13	1.18±0.196	0.91±0.095	3.2±0.19	1.7±0.712	2.89±0.932	1.48±0.23	2.13±0.443	1.16±0.149	2.44±0.383	1.92±0.292	3.44±0.807
G1P	2.06±0.527	1.75±0.063	2.44±0.723	3.18±1.46	2.23±0.298	1.73±0.12	1.54±0.229	1.76±0.684	1.75±0.147	1.29±0.187	1.58±0.138	1.26±0.337	2.52±1.14	2.5±1.11	2.24±0.394	1.97±0.289	1.83±0.225	2±0.318	2.61±0.442	3.15±0.576
G6P	19.11±3.63	17.45±0.88	23.33±8.44	32.26±14.6	17.64±0.74	16.01±2.4	14.43±3.88	14.24±2.17	15.98±2.23	14.61±1.44	13.98±1.02	11.19±1.18	19.76±8.83	17.77±6.38	17.95±4.26	18.15±3.07	18.36±1.44	19.05±2.01	23.47±3.41	34.29±6.07
NAD	2.01±0.352	1.62±0.151	2.23±0.656	2.63±0.91	NA	NA	NA	NA	NA	NA	NA	NA	2.29±0.991	2.24±0.924	1.87±0.241	1.8±0.27	1.58±0.139	1.68±0.263	2.11±0.43	2.38±0.576
NADP	0.39±0.066	0.369±0.04	0.512±0.16	0.486±0.19	NA	NA	NA	NA	NA	NA	NA	NA	0.556±0.27	0.501±0.10	0.543±0.09	0.351±0.04	0.291±0.05	0.342±0.07	0.616±0.31	0.527±0.19
R5P	0.39±0.15	0.465±0.03	0.398±0.15	1.01±0.47	0.49±0.092	0.398±0.05	0.358±0.09	0.445±0.14	0.362±0.03	0.351±0.03	0.332±0.08	0.331±0.05	0.451±0.17	0.514±0.18	0.392±0.11	0.599±0.04	0.3±0.088	0.461±0.16	0.53±0.18	0.878±0.13
Ru5P+Xu5P	2.88±0.84	2.17±0.073	2.92±0.922	3.44±1.46	3.85±0.959	2.29±0.59	1.73±0.492	2.62±1.91	1.7±0.364	1.38±0.211	1.27±0.286	0.859±0.18	4.55±2	4.21±1.55	4.15±0.776	2.34±0.095	2.14±0.554	2.03±0.595	4.42±1.54	3.65±0.579
RuBP	3.07±0.5	1.79±0.287	3.16±1.07	2.52±0.881	2.79±0.572	1.56±0.83	1.44±0.575	2.03±1.47	1.45±0.293	0.822±0.13	1.04±0.129	0.582±0.25	4.58±3.26	3.16±0.567	4.54±1.19	2.02±0.098	2.96±1.01	2.18±0.692	6.43±1.58	3.19±1.17
S7P	5.09±0.933	5.25±0.811	5.35±1.68	8.15±3.13	7.58±0.499	5.43±1.05	4.46±1.89	5.55±3.81	4.42±0.939	3.7±0.896	3.42±0.774	2.03±0.506	5.7±2.76	5.67±2.01	5.86±1.67	6.04±0.674	2.87±0.199	3.4±0.475	3.33±0.64	7.53±1.26
SBP	1.16±0.155	1.75±1.48	1.57±0.589	6.77±2.52	1.03±0.169	1±0.284	1.42±0.212	3.35±1.34	0.501±0.12	0.458±0.11	0.616±0.07	5.53±0.099	1.4±0.643	1.3±0.427	1.53±0.215	3.79±0.986	1.03±0.179	1.5±0.42	2.04±0.485	6.95±3
shikimate	2.36±0.146	2.22±0.324	2.97±1.1	2.09±1.03	2.87±0.151	2.9±0.394	2.55±0.67	2.33±1.75	3.03±0.162	3.08±0.21	3.11±0.082	1.32±0.259	3.16±1.67	2.84±1.19	2.73±0.485	1.96±0.272	1.66±0.244	1.99±0.274	2.03±0.335	1.28±0.194
UDPG	8.71±1.62	7.75±0.47	11.45±4.04	11.51±5.08	8.2±1.1	8.53±1.56	8.05±2.12	6.21±1.3	7.53±0.682	7.73±0.271	8.25±1.28	5.06±0.591	11±4.46	10.22±4.01	9.41±1.8	7.58±0.864	7.7±0.911	8.45±1.25	10.92±1.61	9.69±1.24

Supplement Table 5.4.7. Raw data of LC-MS based metabolite profile in long-term acclimated WT, *trxf*, *trxm* and *ntrc*.

4 weeks after sowing plants were harvested in the middle of the light period. Values are given as mean ± SD from n= 3 – 5 biological replicates.

contrast (rel. to WT)	trxf	trxm	ntrc	trxf	trxm	ntrc	trxf	trxm	ntrc	trxf	trxm	ntrc	trxf	trxm	ntrc
Light	**ML**			**FL HL**			**FL LL**			**HL**			**LL**		
2PG	0.994	0.999	0.391	0.570	0.106	1.000	0.987	0.983	0.764	0.763	0.998	0.952	1.000	0.807	0.392
3PGA	NA	NA	NA	0.961	0.979	0.993	**0.007**	0.113	**0.000**	NA	NA	NA	NA	NA	NA
aconitate	NA	NA	NA	0.988	1.000	0.714	1.000	1.000	0.626	NA	NA	NA	NA	NA	NA
ADP	0.757	1.000	0.401	0.959	0.857	0.771	0.463	0.405	0.205	0.999	0.986	0.587	0.988	0.165	0.168
ADPG	0.465	1.000	0.921	1.000	0.997	0.996	0.335	0.407	0.061	0.896	0.996	0.800	0.994	0.771	0.178
AMP	0.254	0.814	0.905	0.986	0.927	0.740	0.892	0.908	0.085	0.962	0.990	0.062	0.984	0.497	0.459
DHAP	0.800	0.287	**0.017**	0.979	0.578	0.633	0.995	0.994	0.790	0.992	0.999	0.994	0.617	0.098	**0.028**
F6P	0.984	0.581	**0.006**	0.899	0.454	0.864	1.000	0.970	0.779	1.000	0.998	1.000	0.925	0.707	**0.003**
FBP	**0.007**	0.804	**0.000**	0.879	0.994	**0.033**	0.717	0.970	**0.000**	**0.005**	0.919	0.579	**0.002**	0.130	**0.000**
G1P	0.884	0.795	**0.040**	0.786	0.568	0.816	0.824	0.988	0.795	1.000	0.910	0.556	0.976	0.242	**0.011**
G6P	0.967	0.646	**0.003**	0.985	0.900	0.884	0.991	0.973	0.732	0.945	0.958	0.970	0.997	0.491	**0.000**
NADP	0.997	0.635	0.785	NA	NA	NA	NA	NA	NA	0.950	0.999	0.203	0.959	**0.014**	0.114
NAD	0.707	0.933	0.326	NA	NA	NA	NA	NA	NA	0.999	0.654	0.527	0.993	0.478	0.141
R5P	0.895	1.000	**0.000**	0.912	0.779	0.988	1.000	0.996	0.996	0.937	0.945	0.520	0.443	0.152	**0.000**
Ru5P+Xu5P	0.697	1.000	0.821	0.254	0.065	0.464	0.981	0.957	0.748	0.952	0.922	**0.006**	0.998	**0.004**	0.101
RuBP	0.318	0.999	0.876	0.575	0.494	0.857	0.911	0.972	0.798	0.227	1.000	**0.005**	0.723	**0.000**	0.989
S7P	0.999	0.994	**0.021**	0.378	0.099	0.428	0.948	0.872	0.282	1.000	0.999	0.988	0.956	0.970	**0.000**
SBP	0.846	0.942	**0.000**	1.000	0.976	0.073	1.000	0.999	**0.000**	0.999	0.997	**0.008**	0.915	0.510	**0.000**
shikimate	0.990	0.583	0.939	1.000	0.956	0.818	1.000	0.999	**0.036**	0.910	0.805	0.066	0.903	0.864	0.860
UDPG	0.928	0.304	0.284	0.998	1.000	0.758	1.000	0.984	0.614	0.959	0.738	0.137	0.963	0.176	0.584

Supplement Table 5.4.8. List of *p* value from LC-MS based metabolites in long-term acclimated plants.
A 2-way ANOVA with *post-hoc* Tukey test was performed using the "emmeans" and "multcomp" packages from R. Values are given relative to the respective WT. Significances ($p < 0.05$) are given in bold.

Contrast	Light	2PG	3PGA	DHAP	F6P	FBP	S7P	SBP	R5P	RuBP	shikimate	Ru5P+Xu5P
trxm-trxf	FL LL	1.000	0.472	1.000	0.845	0.244	0.970	0.308	0.973	0.627	0.998	0.964
ntrc-trxf	FL LL	0.431	0.099	0.199	0.258	**0.000**	0.122	**0.000**	0.968	0.546	**0.000**	0.165
WT-trxf	FL LL	0.837	**0.016**	0.851	0.994	**0.030**	0.693	0.956	0.995	**0.028**	0.988	0.507
ntrc-trxm	FL LL	0.474	**0.012**	0.203	0.643	**0.000**	0.223	**0.000**	1.000	0.116	**0.000**	0.306
WT-trxm	FL LL	0.795	0.133	0.844	0.718	0.480	0.454	0.547	0.911	0.156	0.957	0.294
WT-ntrc	FL LL	0.148	**0.001**	0.065	0.185	**0.000**	**0.026**	**0.000**	0.901	**0.005**	**0.000**	**0.022**
trxm-trxf	FL HL	0.964	0.831	0.816	0.750	0.322	0.947	0.882	0.961	0.998	0.970	0.930
ntrc-trxf	FL HL	0.915	0.997	0.441	1.000	**0.022**	1.000	**0.014**	0.941	0.925	0.886	0.983
WT-trxf	FL HL	0.931	0.964	0.978	0.813	0.545	0.648	1.000	0.701	0.428	1.000	0.392
ntrc-trxm	FL HL	0.694	0.915	0.143	0.805	**0.002**	0.928	**0.039**	0.730	0.863	0.991	0.777
WT-trxm	FL HL	0.720	0.980	0.604	0.304	0.965	0.370	0.902	0.440	0.354	0.976	0.182
WT-ntrc	FL HL	1.000	0.993	0.652	0.759	**0.004**	0.685	**0.015**	0.948	0.759	0.899	0.575

Supplement Table 5.4.9. List of *p* values from LC-MS based CBC metabolites in long-term acclimated plants under FL.
A 1-way ANOVA with *post-hoc* Tukey test was performed using R ("aov", "TukeyHSD"). Significances ($p < 0.05$) are given in bold.

5.5 Light sources

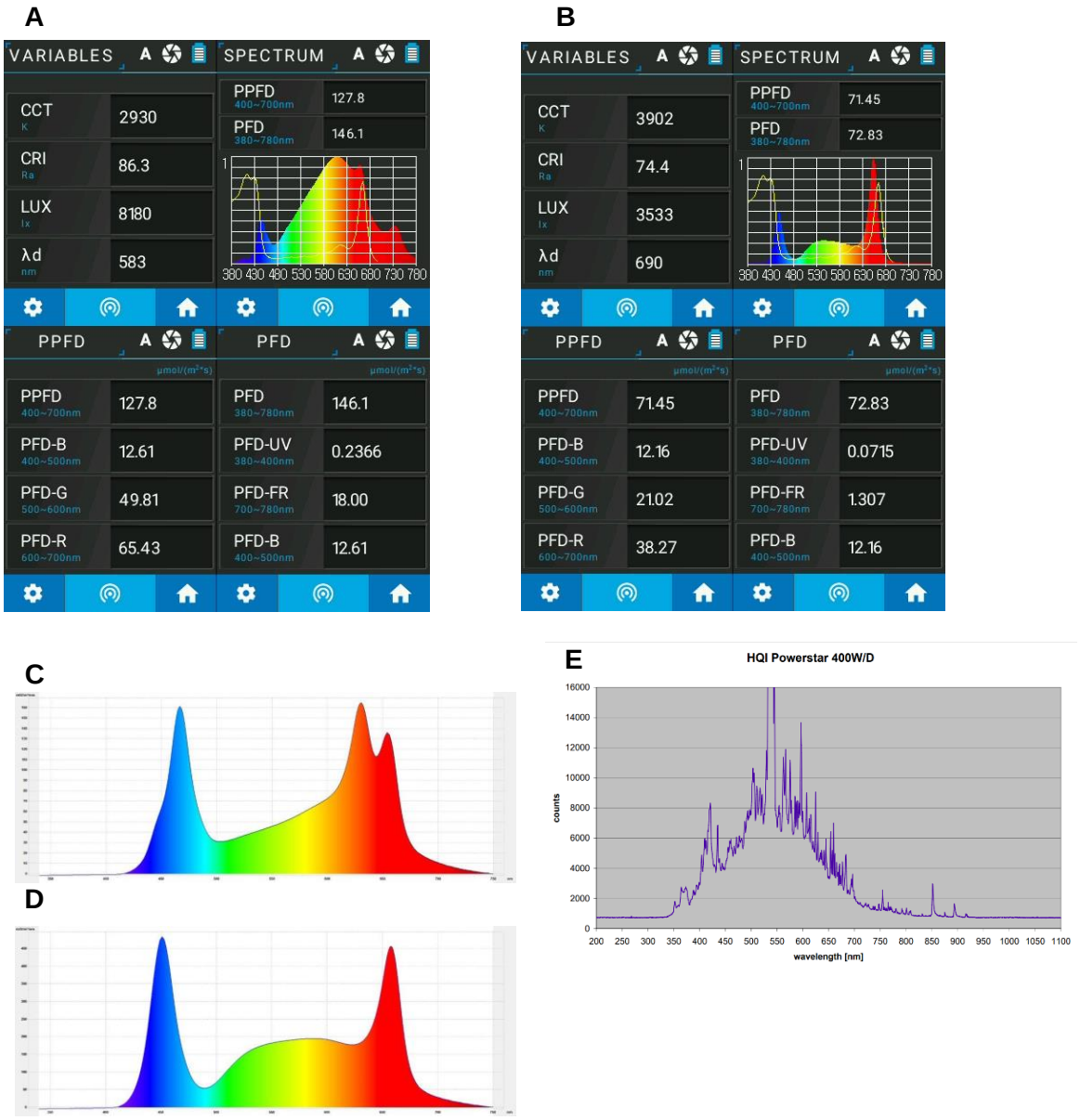

Supplement Figure 5.5.1. Spectra of LED lights.
(A) Medium light (München); (B) Fluctuating light (München); (C) Medium Light (Golm); (D) Fluctuating light (Golm); (E) mercury lamp for High Light (München). PPFD, photosynthetic photo flux density in µmol photons m^{-2} s^{-1}.

6 Literature

Abdi, H., & Williams, L. J. (2010). Principal component analysis. *Wiley Interdisciplinary Reviews: Computational Statistics*, *2*(4), 433–459. https://doi.org/10.1002/wics.101

Akula, R., Sarvajeet Singh, G., Kumar, V., Khare, T., Shaikh, S., & Wani, S. H. (2019). Compatible Solutes and Abiotic Stress Tolerance in Plants. *Metabolic Adaptations in Plants During Abiotic Stress*, *September*, 213–220. https://doi.org/10.1201/b22206-18

Alter, P., Dreissen, A., Luo, F. L., & Matsubara, S. (2012). Acclimatory responses of Arabidopsis to fluctuating light environment: Comparison of different sunfleck regimes and accessions. *Photosynthesis Research*, *113*(1–3), 221–237. https://doi.org/10.1007/s11120-012-9757-2

Ancín, M., Millan, A. F. S., Larraya, L., Morales, F., Veramendi, J., Aranjuelo, I., & Farran, I. (2019). Overexpression of thioredoxin m in tobacco chloroplasts inhibits the protein kinase STN7 and alters photosynthetic performance. *Journal of Experimental Botany*, *70*(3), 731–733. https://doi.org/10.1093/jxb/ery415

Apel, K., & Hirt, H. (2004). Reactive oxygen species: Metabolism, oxidative stress, and signal transduction. *Annual Review of Plant Biology*, *55*, 373–399. https://doi.org/10.1146/annurev.arplant.55.031903.141701

Armbruster, U., Leonelli, L., Galvis, V. C., Strand, D., Quinn, E. H., Jonikas, M. C., & Niyogi, K. K. (2016). Regulation and levels of the thylakoid K+/H+ antiporter KEA3 shape the dynamic response of photosynthesis in fluctuating light. *Plant and Cell Physiology*, *57*(7), 1557–1567. https://doi.org/10.1093/pcp/pcw085

Armbruster, U., Pesaresi, P., Pribil, M., Hertle, A., & Leister, D. (2011). Update on chloroplast research: New tools, new topics, and new trends. *Molecular Plant*, *4*(1), 1–16. https://doi.org/10.1093/mp/ssq060

Arnold, J. B. (2021). *ggthemes: Extra Themes, Scales and Geoms for "ggplot2."* https://cran.r-project.org/package=ggthemes

Arrivault, S., Guenther, M., Fry, S. C., Fuenfgeld, M. M. F. F., Veyel, D., Mettler-Altmann, T., Stitt, M., & Lunn, J. E. (2015). Synthesis and Use of Stable-Isotope-Labeled Internal Standards for Quantification of Phosphorylated Metabolites by LC-MS/MS. *Analytical Chemistry*, *87*(13), 6896–6904. https://doi.org/10.1021/acs.analchem.5b01387

Arrivault, S., Guenther, M., Ivakov, A., Feil, R., Vosloh, D., Van Dongen, J. T., Sulpice, R., & Stitt, M. (2009). Use of reverse-phase liquid chromatography, linked to tandem mass spectrometry, to profile the Calvin cycle and other metabolic intermediates in Arabidopsis rosettes at different carbon dioxide concentrations. *Plant Journal*, *59*(5), 826–839. https://doi.org/10.1111/j.1365-313X.2009.03902.x

Asada, K. (1999). The water-water cycle in chloroplasts: Scavenging of active oxygens and dissipation of excess photons. *Annual Review of Plant Biology*, *50*, 601–639. https://doi.org/10.1146/annurev.arplant.50.1.601

Attali, D., & Baker, C. (2019). *ggExtra: Add Marginal Histograms to "ggplot2", and More "ggplot2" Enhancements*. https://cran.r-project.org/package=ggExtra

Bache, S. M., & Wickham, H. (2022). *magrittr: A Forward-Pipe Operator for R*. https://cran.r-project.org/package=magrittr

Bailey, S., Horton, P., & Walters, R. G. (2004). Acclimation of Arabidopsis thaliana to the light environment: The relationship between photosynthetic function and chloroplast composition. *Planta*, *218*(5), 793–802. https://doi.org/10.1007/s00425-003-1158-5

Baker, N. R. (2008). Chlorophyll Fluorescence: A Probe of Photosynthesis In Vivo. *Annual Review of Plant Biology*, *59*(1), 89–113. https://doi.org/10.1146/annurev.arplant.59.032607.092759

Baslam, M., Baroja-Fernaândez, E., Ricarte-Bermejo, A., Sánchez-López, Á. M., Aranjuelo, I., Bahaji, A., Muñoz, F. J., Almagro, G., Pujol, P., Galarza, R., Teixidor, P., & Pozueta-Romero, J. (2017). Genetic and isotope ratio mass spectrometric evidence for the occurrence of starch degradation and cycling in illuminated Arabidopsis leaves. *PLoS ONE*, *12*(2). https://doi.org/10.1371/journal.pone.0171245

Bassham, J. A., Benson A. A., & Calvin, M. (1954). The path of carbon in photosynthesis. *Journal of the American Chemical Society*, *76*(7), 1760–1770. https://doi.org/10.1038/scientificamerican0662-88

Belin, C., Bashandy, T., Cela, J., Delorme-Hinoux, V., Riondet, C., & Reichheld, J. P. (2015). A comprehensive study of thiol reduction gene expression under stress conditions in Arabidopsis thaliana. *Plant, Cell and Environment*, *38*(2), 299–314. https://doi.org/10.1111/pce.12276

Bellafiore, S., Barneche, F., Peltler, G., & Rochalx, J. D. (2005). State transitions and light adaptation require chloroplast thylakoid protein kinase STN7. *Nature*, *433*(7028), 892–895. https://doi.org/10.1038/nature03286

Benjamini, Y., & Hochberg, Y. (1995). Controlling the False Discovery Rate: A Practical and Powerful Approach to Multiple Testing. In *Biometrika* (Vol. 61, Issue 1, pp. 1–15).

Bernal-Bayard, P., Hervaś, M., Cejudo, F. J., & Navarro, J. A. (2012). Electron transfer pathways and dynamics of chloroplast NADPH-dependent thioredoxin reductase C (NTRC). *Journal of Biological Chemistry*, *287*(40), 33865–33872. https://doi.org/10.1074/jbc.M112.388991

Bonardi, V., Pesaresi, P., Becker, T., Schleiff, E., Wagner, R., Pfannschmidt, T., Jahns, P., & Leister, D. (2005). Photosystem II core phosphorylation and photosynthetic acclimation require two different protein kinases. *Nature*, *437*(7062), 1179–1182. https://doi.org/10.1038/nature04016

Bradford, M. M. (1976). A Rapid and Sensitive Method for the Quantitation Microgram Quantities of Protein Utilizing the Principle of Protein-Dye Binding. *Analytical Biochemistry*. https://doi.org/10.1016/j.cj.2017.04.003

Bräutigam, K., Dietzel, L., Kleine, T., Ströher, E., Wormuth, D., Dietz, K. J., Radke, D., Wirtz, M., Hell, R., Dörmann, P., Nunes-Nesi, A., Schauer, N., Fernie, A. R., Oliver, S. N., Geigenberger, P., Leister, D., & Pfannschmidt, T. (2009). Dynamic plastid redox signals integrate gene expression and metabolism to induce distinct metabolic states in photosynthetic acclimation in Arabidopsis. *Plant Cell*, *21*(9), 2715–2732. https://doi.org/10.1105/tpc.108.062018

Bräutigam, K., Dietzel, L., & Pfannschmidt, T. (2010). Hypothesis: A binary redox control mode as universal regulator of photosynthetic light acclimation. *Plant Signaling and Behavior*, *5*(1), 81–85. https://doi.org/10.4161/psb.5.1.10294

Buchanan, B. B., Schürmann, P., & Kalberer, P. P. (1971). Ferredoxin-activated fructose diphosphatase of spinach chloroplasts. Resolution of the system, properties of the alkaline fructose diphosphatase component, and physiological significance of the ferredoxin-linked activation. *Journal of Biological Chemistry*, *246*(19), 5952–5959. https://doi.org/10.1016/S0021-9258(18)61819-8

Buchanan, Bob B. (2016). The Path to Thioredoxin and Redox Regulation in Chloroplasts. *Annual Review of Plant Biology*, *67*(1), 1–24. https://doi.org/10.1146/annurev-arplant-043015-111949

Buchanan, Bob B., Kalberer, P. P., & Arnon, D. I. (1967). Ferredoxin-activated fructose diphosphatase in isolated chloroplasts. *Biochemical and Biophysical Research Communications*, *29*(1), 74–79. https://doi.org/10.1016/0006-291X(67)90543-8

Buchanan, Bob B., & Luan, S. (2005). Redox regulation in the chloroplast thylakoid lumen: A new frontier in photosynthesis research. *Journal of Experimental Botany*, *56*(416), 1439–1447. https://doi.org/10.1093/jxb/eri158

Butler, W. L. (1978). Energy Distribution in the Photochemical Apparatus of Photosynthesis. *Ann. Rev. Plant PhysioL*, *29*, 345–378.

Carrera, D., Oddsson, S., Grossmann, J., Trachsel, C., & Streb, S. (2018). Comparative Proteomic Analysis of Plant Acclimation to Six Different Long-Term Environmental Changes. *Plant and Cell Physiology*, *59*(3), 510–526. https://doi.org/10.1093/pcp/pcx206

Carrera, F. P., Noceda, C., Maridueña-Zavala, M. G., & Cevallos-Cevallos, J. M. (2021). Metabolomics, a powerful tool for understanding plant abiotic stress. *Agronomy*, *11*(5), 1–28. https://doi.org/10.3390/agronomy11050824

Carrillo, L. R., Froehlich, J. E., Cruz, J. A., Savage, L. J., & Kramer, D. M. (2016). Multi-level regulation of the chloroplast ATP synthase: the chloroplast NADPH thioredoxin reductase C (NTRC) is required for redox modulation specifically under low irradiance. *The Plant Journal : For Cell and Molecular Biology*, *87*(6), 654–663. https://doi.org/10.1111/tpj.13226

Chae, H. B., Moon, J. C., Shin, M. R., Chi, Y. H., Jung, Y. J., Lee, S. Y., Nawkar, G. M., Jung, H. S., Hyun, J. K., Kim, W. Y., Kang, C. H., Yun, D. J., Lee, K. O., & Lee, S. Y. (2013). Thioredoxin reductase type C (NTRC) orchestrates enhanced thermotolerance to arabidopsis by its redox-dependent holdase chaperone function. *Molecular Plant*, *6*(2), 323–336. https://doi.org/10.1093/mp/sss105

Chia, D. W., Yoder, T. J., Reiter, W. D., & Gibson, S. I. (2000). Fumaric acid: An overlooked form of fixed carbon in Arabidopsis and other plant species. *Planta*, *211*(5), 743–751. https://doi.org/10.1007/s004250000345

Chong, J., Wishart, D. S., & Xia, J. (2019). Using MetaboAnalyst 4.0 for Comprehensive and Integrative Metabolomics Data Analysis. *Current Protocols in Bioinformatics*, *68*(1), 1–128. https://doi.org/10.1002/cpbi.86

Collin, V., Issakidis-Bourguet, E., Marchand, C., Hirasawa, M., Lancelin, J. M., Knaff, D. B., & Miginiac-Maslow, M. (2003). The Arabidopsis plastidial thioredoxins. New functions and new insights into specificity. *Journal of Biological Chemistry*, *278*(26), 23747–23752. https://doi.org/10.1074/jbc.M302077200

Courteille, A., Vesa, S., Sanz-Barrio, R., Cazalé, A. C., Becuwe-Linka, N., Farran, I., Havaux, M., Rey, P., & Rumeau, D. (2013). Thioredoxin m4 controls photosynthetic alternative electron pathways in Arabidopsis. *Plant Physiology*, *161*(1), 508–520. https://doi.org/10.1104/pp.112.207019

Cox, J., & Mann, M. (2008). MaxQuant enables high peptide identification rates, individualized p.p.b.-range mass accuracies and proteome-wide protein quantification. *Nature Biotechnology*, *26*(12), 1367–1372. https://doi.org/10.1038/nbt.1511

Deshmukh, R., Sonah, H., Patil, G., Chen, W., Prince, S., Mutava, R., Vuong, T., Valliyodan, B., & Nguyen, H. T. (2014). Integrating omic approaches for abiotic stress tolerance in soybean. *Frontiers in Plant Science*, *5*(JUN), 1–12. https://doi.org/10.3389/fpls.2014.00244

Dietz, K. J. (2015). Efficient high light acclimation involves rapid processes at multiple mechanistic levels. *Journal of Experimental Botany*, *66*(9), 2401–2414. https://doi.org/10.1093/jxb/eru505

Dietzel, L., Bräutigam, K., & Pfannschmidt, T. (2008). Photosynthetic acclimation: State transitions and adjustment of photosystem stoichiometry - Functional relationships between short-term and long-term light quality acclimation in plants. *FEBS Journal*, *275*(6), 1080–1088. https://doi.org/10.1111/j.1742-4658.2008.06264.x

Dietzel, L., & Pfannschmidt, T. (2008). Photosynthetic acclimation to light gradients in plant stands comes out of shade. *Plant Signaling and Behavior*, *3*(12), 1116–1118. https://doi.org/10.4161/psb.3.12.7038

Domon, B., & Aebersold, R. (2010). Options and considerations when selecting a quantitative proteomics strategy. *Nature Biotechnology*, *28*(7), 710–721. https://doi.org/10.1038/nbt.1661

Eberhard, S., Finazzi, G., & Wollman, F. A. (2008). The dynamics of photosynthesis. *Annual Review of Genetics*, *42*, 463–515. https://doi.org/10.1146/annurev.genet.42.110807.091452

Fernández-Trijueque, J., Serrato, A. J., & Sahrawy, M. (2019). Proteomic analyses of thioredoxins f and m arabidopsis thaliana mutants indicate specific functions for these proteins in plants. *Antioxidants*, *8*(3). https://doi.org/10.3390/antiox8030054

Flügge, U. I., Westhoff, P., & Leister, D. (2016). Recent advances in understanding photosynthesis. *F1000Research*, *5*(0), 1–10. https://doi.org/10.12688/f1000research.9744.1

Fox, J. (2022). *RcmdrMisc: R Commander Miscellaneous Functions*. https://cran.r-project.org/package=RcmdrMisc

Garcia-Molina, A., Kleine, T., Schneider, K., Mühlhaus, T., Lehmann, M., & Leister, D. (2020). Translational Components Contribute to Acclimation Responses to High Light, Heat, and Cold in Arabidopsis. *IScience*, *23*(7). https://doi.org/10.1016/j.isci.2020.101331

Geigenberger, P. (2011). Regulation of starch biosynthesis in response to a fluctuating environment. *Plant Physiology*, *155*(4), 1566–1577. https://doi.org/10.1104/pp.110.170399

Geigenberger, P., & Fernie, A. R. (2014). Metabolic control of redox and redox control of metabolism in plants. *Antioxidants & Redox Signaling*, *21*(9), 1389–1421. https://doi.org/10.1089/ars.2014.6018

Geigenberger, P., Kolbe, A., & Tiessen, A. (2005). Redox regulation of carbon storage and partitioning in response to light and sugars. *Journal of Experimental Botany*, *56*(416), 1469–1479. https://doi.org/10.1093/jxb/eri178

Geigenberger, P., Thormählen, I., Daloso, D. M., & Fernie, A. R. (2017). The Unprecedented Versatility of the Plant Thioredoxin System. *Trends in Plant Science*, *22*(3), 249–262. https://doi.org/10.1016/j.tplants.2016.12.008

Gibon, Y., Blaesing, O. E., Hannemann, J., Carillo, P., Höhne, M., Hendriks, J. H. M., Palacios, N., Cross, J., Selbig, J., & Stitt, M. (2004). A robot-based platform to measure multiple enzyme activities in Arabidopsis using a set of cycling assays: Comparison of changes of enzyme activities and transcript levels during diurnal cycles and in prolonged darkness. *Plant Cell*, *16*(12), 3304–3325. https://doi.org/10.1105/tpc.104.025973

Gibon, Y., Usadel, B., Blaesing, O. E., Kamlage, B., Hoehne, M., Trethewey, R., & Stitt, M. (2006). Integration of metabolite with transcript and enzyme activity profiling during diurnal cycles in Arabidopsis rosettes. *Genome Biology*, *7*(8). https://doi.org/10.1186/gb-2006-7-8-r76

Gillis, J., & Pavlidis, P. (2012). "Guilt by association" is the exception rather than the rule in gene networks. *PLoS Computational Biology*, *8*(3). https://doi.org/10.1371/journal.pcbi.1002444

Glinski, M., & Weckwerth, W. (2006). The role of mass spectrometry in plant systems biology. *Mass Spectrometry Reviews*, *25*(2), 173–214. https://doi.org/10.1002/mas.20063

González, M., Delgado-Requerey, V., Ferrández, J., Serna, A., Cejudo, F. J., & Noctor, G. (2019). Insights into the function of NADPH thioredoxin reductase C (NTRC) based on identification of NTRC-interacting proteins in vivo. *Journal of Experimental Botany*, *70*(20), 5787–5798. https://doi.org/10.1093/jxb/erz326

Graffelman, J., & van Eeuwijk, F. (2005). Calibration of multivariate scatter plots for exploratory analysis of relations within and between sets of variables in genomic research. *Biometrical Journal*, *47*(6), 863–879.

Grieco, M., Tikkanen, M., Paakkarinen, V., Kangasjärvi, S., & Aro, E. M. (2012). Steady-state phosphorylation of light-harvesting complex II proteins preserves photosystem I under fluctuating white light. *Plant Physiology*, *160*(4), 1896–1910. https://doi.org/10.1104/pp.112.206466

Gu, Z., Eils, R., & Schlesner, M. (2016). Complex heatmaps reveal patterns and correlations in multidimensional genomic data. *Bioinformatics*.

Gu, Z., Gu, L., Eils, R., Schlesner, M., & Brors, B. (2014). circlize implements and enhances circular visualization in R. *Bioinformatics*, *30*(19), 2811–2812.

Guadagno, C. R., Ewers, B. E., & Weinig, C. (2018). Circadian rhythms and redox state in plants: Till stress do us part. *Frontiers in Plant Science*, *9*(March), 1–9. https://doi.org/10.3389/fpls.2018.00247

Guinea Diaz, M., Nikkanen, L., Himanen, K., Toivola, J., & Rintamäki, E. (2020). Two chloroplast thioredoxin systems differentially modulate photosynthesis in Arabidopsis depending on light intensity and leaf age. *Plant Journal*, *104*(3), 718–734. https://doi.org/10.1111/tpj.14959

Hall, M., Mata-Cabana, A., Åkerlund, H. E., Florencio, F. J., Schröder, W. P., Lindahl, M., & Kieselbach, T. (2010). Thioredoxin targets of the plant chloroplast lumen and their implications for plastid function. *Proteomics*, *10*(5), 987–1001. https://doi.org/10.1002/pmic.200900654

Hammel, A., Sommer, F., Zimmer, D., Stitt, M., Mühlhaus, T., & Schroda, M. (2020). Overexpression of Sedoheptulose-1,7-Bisphosphatase Enhances Photosynthesis in Chlamydomonas reinhardtii and Has No Effect on the Abundance of Other Calvin-Benson Cycle Enzymes. *Frontiers in Plant Science*, *11*(June), 1–12. https://doi.org/10.3389/fpls.2020.00868

Han, M., Zhang, C., Suglo, P., Sun, S., Wang, M., & Su, T. (2021). L-aspartate: An essential metabolite for plant growth and stress acclimation. *Molecules*, *26*(7), 1–17. https://doi.org/10.3390/molecules26071887

Harrell Jr, F. E. (2021). *Hmisc: Harrell Miscellaneous*. https://cran.r-project.org/package=Hmisc

Harrison, E. P., Willingham, N. M., Lloyd, J. C., & Raines, C. A. (1997). Reduced sedoheptulose-1,7-bisphosphatase levels in transgenic tobacco lead to decreased photosynthetic capacity and altered carbohydrate accumulation. *Planta*, *204*(1), 27–36. https://doi.org/10.1007/s004250050226

Hendriks, J. H. M., Kolbe, A., Gibon, Y., Stitt, M., & Geigenberger, P. (2003). ADP-Glucose Pyrophosphorylase Is Activated by Posttranslational Redox-Modification in Response to Light and to Sugars in Leaves of Arabidopsis and Other Plant Species. *Plant Physiology*, *133*(2), 838–849. https://doi.org/10.1104/pp.103.024513

Hertle, A. P., Blunder, T., Wunder, T., Pesaresi, P., Pribil, M., Armbruster, U., & Leister, D. (2013). PGRL1 Is the Elusive Ferredoxin-Plastoquinone Reductase in Photosynthetic Cyclic Electron Flow. *Molecular Cell*, *49*(3), 511–523. https://doi.org/10.1016/j.molcel.2012.11.030

Heyneke, E., & Fernie, A. R. (2018). Metabolic regulation of photosynthesis. *Biochemical Society Transactions*, *46*(2), 321–328. https://doi.org/10.1042/BST20170296

Hildebrandt, T. M., Nunes Nesi, A., Araújo, W. L., & Braun, H. P. (2015). Amino Acid Catabolism in Plants. *Molecular Plant*, *8*(11), 1563–1579. https://doi.org/10.1016/j.molp.2015.09.005

Hollywood, K., Brison, D. R., & Goodacre, R. (2006). Metabolomics: Current technologies and future trends. *Proteomics*, *6*(17), 4716–4723. https://doi.org/10.1002/pmic.200600106

Holt, N. E., Fleming, G. R., & Niyogi, K. K. (2004). Toward an understanding of the mechanism of nonphotochemical quenching in green plants. *Biochemistry*, *43*(26), 8281–8289. https://doi.org/10.1021/bi0494020

Hooper, C. M., Castleden, I. R., Tanz, S. K., Aryamanesh, N., & Millar, A. H. (2017). SUBA4: The interactive data analysis centre for Arabidopsis subcellular protein locations. *Nucleic Acids Research*, *45*(D1), D1064–D1074. https://doi.org/10.1093/nar/gkw1041

Hothorn, T., Bretz, F., & Westfall, P. (2008). Simultaneous Inference in General Parametric Models. *Biometrical Journal*, *50*(3), 346–363.

Hou, L. Y., Ehrlich, M., Thormählen, I., Lehmann, M., Krahnert, I., Obata, T., Cejudo, F. J., Fernie, A. R., & Geigenberger, P. (2019). NTRC plays a crucial role in starch metabolism, redox balance, and tomato fruit growth. *Plant Physiology*, *181*(3), 976–992. https://doi.org/10.1104/pp.19.00911

Igamberdiev, A. U., & Kleczkowski, L. A. (2018). The glycerate and phosphorylated pathways of serine synthesis in plants: The branches of plant glycolysis linking carbon and nitrogen metabolism. *Frontiers in Plant Science*, *9*(March), 1–12. https://doi.org/10.3389/fpls.2018.00318

Ikegami, A., Yoshimura, N., Motohashi, K., Takahashi, S., Romano, P. G. N., Hisabori, T., Takamiya, K. I., & Masuda, T. (2007). The CHLI1 subunit of Arabidopsis thaliana magnesium chelatase is a target protein of the chloroplast thioredoxin. *Journal of Biological Chemistry*, *282*(27), 19282–19291. https://doi.org/10.1074/jbc.M703324200

Jahns, P., Latowski, D., & Strzalka, K. (2009). Mechanism and regulation of the violaxanthin cycle: The role of antenna proteins and membrane lipids. *Biochimica et Biophysica Acta - Bioenergetics*, *1787*(1), 3–14. https://doi.org/10.1016/j.bbabio.2008.09.013

Jedelská, T., Luhová, L., & Petřivalský, M. (2020). Thioredoxins: Emerging players in the regulation of protein s-nitrosation in plants. *Plants*, *9*(11), 1–16. https://doi.org/10.3390/plants9111426

Jeffery, C. J. (2003). Moonlighting proteins: Old proteins learning new tricks. *Trends in Genetics*, *19*(8), 415–417. https://doi.org/10.1016/S0168-9525(03)00167-7

Joshi, V., Joung, J. G., Fei, Z., & Jander, G. (2010). Interdependence of threonine, methionine and isoleucine metabolism in plants: Accumulation and transcriptional regulation under abiotic stress. *Amino Acids*, *39*(4), 933–947. https://doi.org/10.1007/s00726-010-0505-7

Kadereit, J. W., Nick, P., & Sonnewald, U. (2020). *Strasburger – Lehrbuch der Pflanzen-* (38th ed.). Springer Spektrum.

Kaiser, E., Morales, A., & Harbinson, J. (2018). Fluctuating light takes crop photosynthesis on a rollercoaster ride. *Plant Physiology*, *176*(2), 977–989. https://doi.org/10.1104/pp.17.01250

Kaiser, E., Zhou, D., Heuvelink, E., Harbinson, J., Morales, A., & Marcelis, L. F. M. (2017). Elevated CO2 increases photosynthesis in fluctuating irradiance regardless of photosynthetic induction state. *Journal of Experimental Botany*, *68*(20), 5629–5640. https://doi.org/10.1093/jxb/erx357

Karamoko, M., Gabilly, S. T., & Hamel, P. P. (2013). Operation of trans-thylakoid thiol-metabolizing pathways in photosynthesis. *Frontiers in Plant Science*, *4*(NOV), 1–6. https://doi.org/10.3389/fpls.2013.00476

Kassambara, A., & Mundt, F. (2020). *factoextra: Extract and Visualize the Results of Multivariate Data Analyses*. https://cran.r-project.org/package=factoextra

Kinoshita, E., & Kinoshita-Kikuta, E. (2011). Improved Phos-tag SDS-PAGE under neutral pH conditions for advanced protein phosphorylation profiling. *Proteomics*, *11*(2), 319–323. https://doi.org/10.1002/pmic.201000472

Kinoshita, E., Kinoshita-Kikuta, E., & Koike, T. (2009). Separation and detection of large phosphoproteins using phos-tag sds-page. *Nature Protocols*, *4*(10), 1513–1521. https://doi.org/10.1038/nprot.2009.154

Kleine, T., Nägele, T., Neuhaus, H. E., Schmitz-Linneweber, C., Fernie, A. R., Geigenberger, P., Grimm, B., Kaufmann, K., Klipp, E., Meurer, J., Möhlmann, T., Mühlhaus, T., Naranjo, B., Nickelsen, J., Richter, A., Ruwe, H., Schroda, M., Schwenkert, S., Trentmann, O., … Leister, D. (2021). Acclimation in plants – the Green Hub consortium. In *Plant Journal* (Vol. 106, Issue 1). https://doi.org/10.1111/tpj.15144

Klie, S., & Nikoloski, Z. (2012). The choice between MapMan and Gene ontology for automated gene function prediction in plant science. *Frontiers in Genetics*, *3*(JUN), 1–14. https://doi.org/10.3389/fgene.2012.00115

Knuesting, J., & Scheibe, R. (2018). Small Molecules Govern Thiol Redox Switches. *Trends in Plant Science*, *23*(9), 769–782. https://doi.org/10.1016/j.tplants.2018.06.007

Köhler, I. H., Ruiz-Vera, U. M., VanLoocke, A., Thomey, M. L., Clemente, T., Long, S. P., Ort, D. R., & Bernacchi, C. J. (2017). Expression of cyanobacterial FBP/SBPase in soybean prevents yield depression under future climate conditions. *Journal of Experimental Botany*, *68*(3), 715–726. https://doi.org/10.1093/jxb/erw435

Kolbe, A., Oliver, S. N., Fernie, A. R., Stitt, M., Dongen, J. T. Van, & Geigenberger, P. (2006). Combined Transcript and Metabolite Profiling of Arabidopsis Leaves Reveals Fundamental Effects of the. *Plant Physiology*, *141*(June), 412–422. https://doi.org/10.1104/pp.106.081208.412

Kromdijk, J., & Long, S. P. (2016). Improving photosynthesis and crop productivity by accelerating recovery from photoprotection. *Science*, *354*(6314), 857–862.

Kuhn, M., Jackson, S., & Cimentada, J. (2020). *corrr: Correlations in R*. https://cran.r-project.org/package=corrr

Laurent, T. C., Moore, E. C., & Reichard, P. (1964). Synthesis of Deoxyribonucleotides. *The Journal of Biological Chemistry*, *239*(10), 3436–3444. https://doi.org/10.1016/S0021-9258(18)97742-2

Lê, S., Josse, J., & Husson, F. (2008). FactoMineR: A Package for Multivariate Analysis. *Journal of Statistical Software*, *25*(1), 1–18. https://doi.org/10.18637/jss.v025.i01

Leister, D. (2019). Genetic engineering, synthetic biology and the light reactions of photosynthesis. *Plant Physiology*, *179*(3), 778–793. https://doi.org/10.1104/pp.18.00360

Lemaire, S. D., Michelet, L., Zaffagnini, M., Massot, V., & Issakidis-Bourguet, E. (2007). Thioredoxins in chloroplasts. *Current Genetics*, *51*(6), 343–365. https://doi.org/10.1007/s00294-007-0128-z

Lemeille, S., Willig, A., Depège-Fargeix, N., Delessert, C., Bassi, R., & Rochaix, J. D. (2009). Analysis of the Chloroplast Protein Kinase Stt7 during State Transitions. *PLoS Biology*, *7*(3). https://doi.org/10.1371/journal.pbio.1000045

Lenth, R. V. (2022). *emmeans: Estimated Marginal Means, aka Least-Squares Means*. https://cran.r-project.org/package=emmeans

Lepistö, A., Kangasjärvi, S., Luomala, E. M., Brader, G., Sipari, N., Keränen, M., Keinänen, M., & Rintamäki, E. (2009). Chloroplast nadph-thioredoxin reductase interacts with photoperiodic development in arabidopsis. *Plant Physiology*, *149*(3), 1261–1276. https://doi.org/10.1104/pp.108.133777

Li, L., Dou, N., Zhang, H., & Wu, C. (2021). The versatile GABA in plants. *Plant Signaling and Behavior*, *16*(3). https://doi.org/10.1080/15592324.2020.1862565

Lindahl, M., Mata-Cabana, A., & Kieselbach, T. (2011). The disulfide proteome and other reactive cysteine proteomes: Analysis and functional significance. *Antioxidants and Redox Signaling*, *14*(12), 2581–2642. https://doi.org/10.1089/ars.2010.3551

Lisec, J., Schauer, N., Kopka, J., Willmitzer, L., & Fernie, A. R. (2006). Gas chromatography mass spectrometry-based metabolite profiling in plants. *Nature Protocols*, *1*(1), 387–396. https://doi.org/10.1038/nprot.2006.59

LNBio. (2014). *Tutorial for proteome data analysis using the Perseus software platform* (Issue January, pp. 1–22). Laboratory of Mass Spectrometry, LNBio, CNPEM.

Loewus, F. A., & Murthy, P. P. N. (2000). myo-Inositol metabolism in plants. *Plant Science*, *150*(1), 1–19. https://doi.org/10.1016/S0168-9452(99)00150-8

Longoni, P., Douchi, D., Cariti, F., Fucile, G., & Goldschmidt-Clermont, M. (2015). Phosphorylation of the light-harvesting complex II isoform Lhcb2 is central to state transitions. *Plant Physiology*, *169*(4), 2874–2883. https://doi.org/10.1104/pp.15.01498

Luo, W., Pant, G., Bhavnasi, Y. K., Blanchard, S. G., & Brouwer, C. (2017). Pathview Web: User friendly pathway visualization and data integration. *Nucleic Acids Research*, *45*(W1), W501–W508. https://doi.org/10.1093/nar/gkx372

Maechler, M., Rousseeuw, P., Struyf, A., Hubert, M., & Hornik, K. (2021). *cluster: Cluster Analysis Basics and Extensions*. https://cran.r-project.org/package=cluster

Marri, L., Thieulin-Pardo, G., Lebrun, R., Puppo, R., Zaffagnini, M., Trost, P., Gontero, B., & Sparla, F. (2014). CP12-mediated protection of Calvin-Benson cycle enzymes from oxidative stress. *Biochimie*, *97*(1), 228–237. https://doi.org/10.1016/j.biochi.2013.10.018

Marri, L., Zaffagnini, M., Collin, V., Issakidis-Bourguet, E., Lemaire, S. D., Pupillo, P., Sparla, F., Miginiac-Maslow, M., & Trost, P. (2009). Prompt and easy activation by specific thioredoxins of calvin cycle enzymes of arabidopsis thaliana associated in the GAPDH/CP12/PRK supramolecular complex. *Molecular Plant*, *2*(2), 259–269. https://doi.org/10.1093/mp/ssn061

Maxwell, K., & Johnson, G. N. (2000). Chlorophyll fluorescence - A practical guide. *Journal of Experimental Botany*, *51*(345), 659–668. https://doi.org/10.1093/jxb/51.345.659

Mettler, T., Mühlhaus, T., Hemme, D., Schöttler, M. A., Rupprecht, J., Idoine, A., Veyel, D., Pal, S. K., Yaneva-Roder, L., Winck, F. V., Sommer, F., Vosloh, D., Seiwert, B., Erban, A., Burgos, A., Arvidsson, S., Schönfelder, S., Arnold, A., Günther, M., … Stitt, M. (2014). Systems analysis of the response of photosynthesis, metabolism, and growth to an increase in irradiance in the photosynthetic model organism Chlamydomonas reinhardtii. *Plant Cell*, *26*(6), 2310–2350. https://doi.org/10.1105/tpc.114.124537

Michalska, J., Zauber, H., Buchanan, B. B., Cejudo, F. J., & Geigenberger, P. (2009). NTRC links built-in thioredoxin to light and sucrose in regulating starch synthesis in chloroplasts and amyloplasts. *Proceedings of the National Academy of Sciences of the United States of America*, *106*(24), 9908–9913. https://doi.org/10.1073/pnas.0903559106

Michelet, L., Zaffagnini, M., Morisse, S., Sparla, F., Pérez-Pérez, M. E., Francia, F., Danon, A., Marchand, C. H., Fermani, S., Trost, P., & Lemaire, S. D. (2013). Redox regulation of the Calvin-Benson cycle: Something old, something new. *Frontiers in Plant Science*, *4*(NOV), 1–21. https://doi.org/10.3389/fpls.2013.00470

Mikkelsen, R., Mutenda, K. E., Mant, A., Schürmann, P., & Blennow, A. (2005). α-Glucan, water dikinase (GWD): A plastidic enzyme with redox-regulated and coordinated catalytic activity and binding affinity. *Proceedings of the National Academy of Sciences of the United States of America*, *102*(5), 1785–1790. https://doi.org/10.1073/pnas.0406674102

Mills, Mitchell, S. (1980). Modulation of coupling factor ATPase Activity in intact Chloroplasts. *FEBS Letters*, *2*, 173–177. https://doi.org/10.1016/0014-5793(80)80173-6

Montrichard, F., Alkhalfioui, F., Yano, H., Vensel, W. H., Hurkman, W. J., & Buchanan, B. B. (2009). Thioredoxin targets in plants: The first 30 years. *Journal of Proteomics*, *72*(3), 452–474. https://doi.org/10.1016/j.jprot.2008.12.002

Morales, A., & Kaiser, E. (2020). Photosynthetic Acclimation to Fluctuating Irradiance in Plants. *Frontiers in Plant Science*, *11*(March), 1–12. https://doi.org/10.3389/fpls.2020.00268

Motohashi, K., & Hisabori, T. (2006). HCF164 receives reducing equivalents from stromal thioredoxin across the thylakoid membrane and mediates reduction of target proteins in the thylakoid lumen. *Journal of Biological Chemistry*, *281*(46), 35039–35047. https://doi.org/10.1074/jbc.M605938200

Motohashi, K., & Hisabori, T. (2010). CcdA is a thylakoid membrane protein required for the transfer of reducing equivalents from stroma to thylakoid lumen in the higher plant chloroplast. *Antioxidants and Redox Signaling*, *13*(8), 1169–1176. https://doi.org/10.1089/ars.2010.3138

Mugford, S. T., Fernandez, O., Brinton, J., Flis, A., Krohn, N., Encke, B., Feil, R., Sulpice, R., Lunn, J. E., Stitt, M., & Smith, A. M. (2014). Regulatory properties of ADP glucose pyrophosphorylase are required for adjustment of leaf starch synthesis in different photoperiods. *Plant Physiology*, *166*(4), 1733–1747. https://doi.org/10.1104/pp.114.247759

Murchie, E. H., & Lawson, T. (2013). Chlorophyll fluorescence analysis: A guide to good practice and understanding some new applications. *Journal of Experimental Botany*, *64*(13), 3983–3998. https://doi.org/10.1093/jxb/ert208

Nägele, T. (2014). Linking metabolomics data to underlying metabolic regulation. *Frontiers in Molecular Biosciences*, *1*(NOV), 1–6. https://doi.org/10.3389/fmolb.2014.00022

Naranjo, B., Diaz-Espejo, A., Lindahl, M., & Cejudo, F. J. (2016). Type-f thioredoxins have a role in the short-term activation of carbon metabolism and their loss affects growth under short-day conditions in Arabidopsis thaliana. *Journal of Experimental Botany*, *67*(6), 1951–1964. https://doi.org/10.1093/jxb/erw017

Naranjo, B., Mignée, C., Krieger-Liszkay, A., Hornero-Méndez, D., Gallardo-Guerrero, L., Cejudo, F. J., & Lindahl, M. (2016). The chloroplast NADPH thioredoxin reductase C, NTRC, controls non-photochemical quenching of light energy and photosynthetic electron transport in Arabidopsis. *Plant Cell and Environment*, *39*(4), 804–822. https://doi.org/10.1111/pce.12652

Navrot, N., Finnie, C., Svensson, B., & Hägglund, P. (2011). Plant redox proteomics. *Journal of Proteomics*, *74*(8), 1450–1462. https://doi.org/10.1016/j.jprot.2011.03.008

Neuhaus, H. E., & Stitt, M. (1990). Control analysis of photosynthate partitioning. *Planta*, *182*(3), 445–454.

Neuwirth, E. (2014). *RColorBrewer: ColorBrewer Palettes*. https://cran.r-project.org/package=RColorBrewer

Nikkanen, L., & Rintamäki, E. (2019). Chloroplast thioredoxin systems dynamically regulate photosynthesis in plants. *Biochemical Journal*, *476*(7), 1159–1172. https://doi.org/10.1042/BCJ20180707

Nikkanen, L., Toivola, J., & Rintamäki, E. (2016). Crosstalk between chloroplast thioredoxin systems in regulation of photosynthesis. *Plant Cell and Environment*, *39*(8), 1691–1705. https://doi.org/10.1111/pce.12718

O'Malley, R. C., & Ecker, J. R. (2010). Linking genotype to phenotype using the Arabidopsis unimutant collection. *Plant Journal*, *61*(6), 928–940. https://doi.org/10.1111/j.1365-313X.2010.04119.x

Obata, T., & Fernie, A. R. (2012). The use of metabolomics to dissect plant responses to abiotic stresses. *Cellular and Molecular Life Sciences*, *69*(19), 3225–3243. https://doi.org/10.1007/s00018-012-1091-5

Ojeda, V., Pérez-Ruiz, J. M., & Cejudo, F. J. (2018). 2-Cys Peroxiredoxins Participate in the Oxidation of Chloroplast Enzymes in the Dark. *Molecular Plant*, *11*(11), 1377–1388. https://doi.org/10.1016/j.molp.2018.09.005

Ojeda, V., Pérez-Ruiz, J. M., González, M., Nájera, V. A., Sahrawy, M., Serrato, A. J., Geigenberger, P., & Cejudo, F. J. (2017). NADPH thioredoxin reductase C and thioredoxins act concertedly in seedling development. *Plant Physiology*, *174*(3), 1436–1448. https://doi.org/10.1104/pp.17.00481

Okegawa, Y., & Motohashi, K. (2015). Chloroplastic thioredoxin m functions as a major regulator of Calvin cycle enzymes during photosynthesis in vivo. *Plant Journal*, *84*(5), 900–913. https://doi.org/10.1111/tpj.13049

Pang, Z., Chong, J., Zhou, G., De Lima Morais, D. A., Chang, L., Barrette, M., Gauthier, C., Jacques, P. É., Li, S., & Xia, J. (2021). MetaboAnalyst 5.0: Narrowing the gap between raw spectra and functional insights. *Nucleic Acids Research*, *49*(W1), W388–W396. https://doi.org/10.1093/nar/gkab382

Parthasarathy, A., Savka, M. A., & Hudson, A. O. (2019). The synthesis and role of ß-alanine in plants. *Frontiers in Plant Science*, *10*(July). https://doi.org/10.3389/fpls.2019.00921

Pérez-Ruiz, J. M., Spínola, M. C., Kirchsteiger, K., Moreno, J., Sahrawy, M., & Cejudo, F. J. (2006). Rice NTRC is a high-efficiency redox system for chloroplast protection against oxidative damage. *Plant Cell*, *18*(9), 2356–2368. https://doi.org/10.1105/tpc.106.041541

Pesaresi, P., Schneider, A., Kleine, T., & Leister, D. (2007). Interorganellar communication. *Current Opinion in Plant Biology*, *10*(6), 600–606. https://doi.org/10.1016/j.pbi.2007.07.007

Pfalz, J., Liebers, M., Hirth, M., Grübler, B., Holtzegel, U., Schröter, Y., Dietzel, L., & Pfannschmidt, T. (2012). Environmental control of plant nuclear gene expression by chloroplast redox signals. *Frontiers in Plant Science*, *3*(NOV), 1–9. https://doi.org/10.3389/fpls.2012.00257

Pfannschmidt, T. (2003). Chloroplast redox signals: How photosynthesis controls its own genes. *Trends in Plant Science*, *8*(1), 33–41. https://doi.org/10.1016/S1360-1385(02)00005-5

Pfannschmidt, T., Allen, J. F., & Oelmüller, R. (2001). Principles of redox control in photosynthesis gene expression. *Physiologia Plantarum*, *112*(1), 1–9. https://doi.org/10.1034/j.1399-3054.2001.1120101.x

Phillips, N. (2017). *yarrr: A Companion to the e-Book "YaRrr!: The Pirate's Guide to R."* https://cran.r-project.org/package=yarrr

Pollak, N., Dölle, C., & Ziegler, M. (2007). The power to reduce: Pyridine nucleotides - Small molecules with a multitude of functions. *Biochemical Journal*, *402*(2), 205–218. https://doi.org/10.1042/BJ20061638

Puthiyaveetil, S. (2011). A mechanism for regulation of chloroplast LHC II kinase by plastoquinol and thioredoxin. *FEBS Letters*, *585*(12), 1717–1721. https://doi.org/10.1016/j.febslet.2011.04.076

Puthiyaveetil, S., Ibrahim, I. M., & Allen, J. F. (2012). Oxidation-reduction signalling components in regulatory pathways of state transitions and photosystem stoichiometry adjustment in chloroplasts. *Plant, Cell and Environment*, *35*(2), 347–359. https://doi.org/10.1111/j.1365-3040.2011.02349.x

Queval, G., & Foyer, C. H. (2012). Redox regulation of photosynthetic gene expression. *Philosophical Transactions of the Royal Society B: Biological Sciences*, *367*(1608), 3475–3485. https://doi.org/10.1098/rstb.2012.0068

Raines, C. A. (2003). The Calvin cycle revisited. *Photosynthesis Research*, *75*(1), 1–10. https://doi.org/10.1023/A:1022421515027

Raines, C. A., Lloyd, J. C., & Dyer, T. A. (1999). New insighits into the structure and function of sedoheptulose-1,7-bisphosphatase; an important but neglected Calvin cycle enzyme. *Journal of Experimental Botany*, *50*(330), 1–8. https://doi.org/10.1093/jxb/50.330.1

Richter, A. S., Peter, E., Rothbart, M., Schlicke, H., Toivola, J., Rintamäki, E., & Grimm, B. (2013). Posttranslational influence of NADPH-dependent thioredoxin reductase C on enzymes in tetrapyrrole synthesis. *Plant Physiology*, *162*(1), 63–73. https://doi.org/10.1104/pp.113.217141

Rinalducci, S., Murgiano, L., & Zolla, L. (2008). Redox proteomics: Basic principles and future perspectives for the detection of protein oxidation in plants. *Journal of Experimental Botany*, *59*(14), 3781–3801. https://doi.org/10.1093/jxb/ern252

Rintamäki, E., Martinsuo, P., Pursiheimo, S., & Aro, E. M. (2000). Cooperative regulation of light-harvesting complex II phosphorylation via the plastoquinol and ferredoxin-thioredoxin system in chloroplasts. *Proceedings of the National Academy of Sciences of the United States of America*, *97*(21), 11644–11649. https://doi.org/10.1073/pnas.180054297

Rochaix, J. D. (2013). Redox regulation of thylakoid protein kinases and photosynthetic gene expression. *Antioxidants and Redox Signaling*, *18*(16), 2184–2201. https://doi.org/10.1089/ars.2012.5110

Rühle, T., & Leister, D. (2016). Photosystem II assembly from scratch. *Frontiers in Plant Science*, *6*(JAN2016), 1–5. https://doi.org/10.3389/fpls.2015.01234

Sanchez, G. (2013). *colortools: Tools for colors in a Hue-Saturation-Value (HSV) color model*. https://cran.r-project.org/package=colortools

Schneider, T., Bolger, A., Zeier, J., Preiskowski, S., Benes, V., Trenkamp, S., Usadel, B., Farré, E. M., & Matsubara, S. (2019). Fluctuating light interacts with time of day and leaf development stage to reprogram gene expression. *Plant Physiology*, *179*(4), 1632–1657. https://doi.org/10.1104/pp.18.01443

Schopfer, P., & Brennicke, A. (2010). *Pflanzenphysiologie* (7th ed.). Spektrum Akademischer Verlag.

Schöttler, M. A., & Tóth, S. Z. (2014). Photosynthetic complex stoichiometry dynamics in higher plants: Environmental acclimation and photosynthetic flux control. *Frontiers in Plant Science*, *5*(MAY), 1–15. https://doi.org/10.3389/fpls.2014.00188

Schreiber, U. (1986). Detection of rapid induction kinetics with a new type of high-frequency modulated chlorophyll fluorometer. *Photosynthesis Research*, *9*(1–2), 261–272. https://doi.org/10.1007/BF00029749

Schwarz, O., Schürmann, P., & Strotmann, H. (1997). Kinetics and thioredoxin specificity of thiol modulation of the chloroplast H+-ATPase. *Journal of Biological Chemistry*, *272*(27), 16924–16927. https://doi.org/10.1074/jbc.272.27.16924

Seaton, D. D., Graf, A., Baerenfaller, K., Stitt, M., Millar, A. J., & Gruissem, W. (2018). Photoperiodic control of the Arabidopsis proteome reveals a translational coincidence mechanism . *Molecular Systems Biology*, *14*(3), 1–19. https://doi.org/10.15252/msb.20177962

Serrato, A. J., Pérez-Ruiz, J. M., Spínola, M. C., & Cejudo, F. J. (2004). A novel NADPH thioredoxin reductase, localised in the chloroplast, which deficiency causes hypersensitivity to abiotic stress in Arabidopsis thaliana. *Journal of Biological Chemistry*, *279*(42), 43821–43827. https://doi.org/10.1074/jbc.M404696200

Shapiguzov, A., Chai, X., Fucile, G., Longoni, P., Zhang, L., & Rochaix, J. D. (2016). Activation of the Stt7/STN7 Kinase through dynamic interactions with the cytochrome b6 f complex. *Plant Physiology*, *171*(1), 82–92. https://doi.org/10.1104/pp.15.01893

Sharkey, T. D. (2019). Discovery of the canonical Calvin–Benson cycle. *Photosynthesis Research*, *140*(2), 235–252. https://doi.org/10.1007/s11120-018-0600-2

Slattery, R. A., Walker, B. J., Weber, A. P. M., & Ort, D. R. (2018). The impacts of fluctuating light on crop performance. *Plant Physiology*, *176*(2), 990–1003. https://doi.org/10.1104/pp.17.01234

Sparla, F., Costa, A., Lo Schiavo, F., Pupillo, P., & Trost, P. (2006). Redox regulation of a novel plastid-targeted ß-amylase of arabidopsis. *Plant Physiology*, *141*(3), 840–850. https://doi.org/10.1104/pp.106.079186

Stitt, M., & Fernie, A. R. (2003). From measurements of metabolites to metabolomics: An "on the fly" perspective illustrated by recent studies of carbon-nitrogen interactions. *Current Opinion in Biotechnology*, *14*(2), 136–144. https://doi.org/10.1016/S0958-1669(03)00023-5

Stitt, M., & Gibon, Y. (2014). Why measure enzyme activities in the era of systems biology? *Trends in Plant Science*, *19*(4), 256–265. https://doi.org/10.1016/j.tplants.2013.11.003

Streb, S., & Zeeman, S. C. (2012). Starch Metabolism in Arabidopsis. *The Arabidopsis Book*, *10*, e0160. https://doi.org/10.1199/tab.0160

Sulpice, R., Flis, A., Ivakov, A. A., Apelt, F., Krohn, N., Encke, B., Abel, C., Feil, R., Lunn, J. E., & Stitt, M. (2014). Arabidopsis coordinates the diurnal regulation of carbon allocation and growth across a wide range of Photoperiods. *Molecular Plant*, *7*(1), 137–155. https://doi.org/10.1093/mp/sst127

Sulpice, R., Pyl, E. T., Ishihara, H., Trenkamp, S., Steinfath, M., Witucka-Wall, H., Gibon, Y., Usadel, B., Poree, F., Piques, M. C., Von Korff, M., Steinhauser, M. C., Keurentjes, J. J. B., Guenther, M., Hoehne, M., Selbig, J., Fernie, A. R., Altmann, T., & Stitt, M. (2009). Starch as a major integrator in the regulation of plant growth. *Proceedings of the National Academy of Sciences of the United States of America*, *106*(25), 10348–10353. https://doi.org/10.1073/pnas.0903478106

Supek, F., Bošnjak, M., Škunca, N., & Šmuc, T. (2011). Revigo summarizes and visualizes long lists of gene ontology terms. *PLoS ONE*, *6*(7). https://doi.org/10.1371/journal.pone.0021800

Szklarczyk, D., Gable, A. L., Lyon, D., Junge, A., Wyder, S., Huerta-Cepas, J., Simonovic, M., Doncheva, N. T., Morris, J. H., Bork, P., Jensen, L. J., & Von Mering, C. (2019). STRING v11: Protein-protein association networks with increased coverage, supporting functional discovery in genome-wide experimental datasets. *Nucleic Acids Research*, *47*(D1), D607–D613. https://doi.org/10.1093/nar/gky1131

Szklarczyk, D., Gable, A. L., Nastou, K. C., Lyon, D., Kirsch, R., Pyysalo, S., Doncheva, N. T., Legeay, M., Fang, T., Bork, P., Jensen, L. J., & von Mering, C. (2021). The STRING database in 2021: Customizable protein-protein networks, and functional characterization of user-uploaded gene/measurement sets. *Nucleic Acids Research*, *49*(D1), D605–D612. https://doi.org/10.1093/nar/gkaa1074

Thormählen, I., Meitzel, T., Groysman, J., Öchsner, A. B., Von Roepenack-Lahaye, E., Naranjo, B., Cejudo, F. J., & Geigenberger, P. (2015). Thioredoxin f1 and NADPH-dependent thioredoxin reductase C have overlapping functions in regulating photosynthetic metabolism and plant growth in response to varying light conditions. *Plant Physiology*, *169*(3), 1766–1786. https://doi.org/10.1104/pp.15.01122

Thormählen, I., Ruber, J., Von Roepenack-Lahaye, E., Ehrlich, S. M., Massot, V., Hümmer, C., Tezycka, J., Issakidis-Bourguet, E., & Geigenberger, P. (2013). Inactivation of thioredoxin f1 leads to decreased light activation of ADP-glucose pyrophosphorylase and altered diurnal starch turnover in leaves of Arabidopsis plants. *Plant, Cell and Environment*, *36*(1), 16–29. https://doi.org/10.1111/j.1365-3040.2012.02549.x

Thormählen, I., Zupok, A., Rescher, J., Leger, J., Weissenberger, S., Groysman, J., Orwat, A., Chatel-Innocenti, G., Issakidis-Bourguet, E., Armbruster, U., & Geigenberger, P. (2017). Thioredoxins Play a Crucial Role in Dynamic Acclimation of Photosynthesis in Fluctuating Light. *Molecular Plant*, *10*(1), 168–182. https://doi.org/10.1016/j.molp.2016.11.012

Tian, T., Liu, Y., Yan, H., You, Q., Yi, X., Du, Z., Xu, W., & Su, Z. (2017). AgriGO v2.0: A GO analysis toolkit for the agricultural community, 2017 update. *Nucleic Acids Research*, *45*(W1), W122–W129. https://doi.org/10.1093/nar/gkx382

Tierney, N. (2017). visdat: Visualising Whole Data Frames. *JOSS*, *2*(16), 355. https://doi.org/10.21105/joss.00355

Tierney, N., Cook, D., McBain, M., & Fay, C. (2021). *naniar: Data Structures, Summaries, and Visualisations for Missing Data*. https://cran.r-project.org/package=naniar

Toivola, J., Nikkanen, L., Dahlström, K. M., Salminen, T. A., Lepistö, A., Vignols, F., & Rintamäki, E. (2013). Overexpression of chloroplast NADPH-dependent thioredoxin reductase in Arabidopsis enhances leaf growth and elucidates in vivo function of reductase and thioredoxin domains. *Frontiers in Plant Science*, *4*(OCT), 1–18. https://doi.org/10.3389/fpls.2013.00389

Trösch, R., Barahimipour, R., Gao, Y., Badillo-Corona, J. A., Gotsmann, V. L., Zimmer, D., Mühlhaus, T., Zoschke, R., & Willmund, F. (2018). Commonalities and differences of chloroplast translation in a green alga and land plants. *Nat. Plants*, *4*(8), 564–575.

Tyanova, S., & Cox, J. (2018). Perseus: A bioinformatics platform for integrative analysis of proteomics data in cancer research. *Methods in Molecular Biology*, *1711*, 133–148. https://doi.org/10.1007/978-1-4939-7493-1_7

Usadel, B., Poree, F., Nagel, A., Lohse, M., Czedik-Eysenberg, A., & Stitt, M. (2009). A guide to using MapMan to visualize and compare Omics data in plants: A case study in the crop species, Maize. *Plant, Cell and Environment*, *32*(9), 1211–1229. https://doi.org/10.1111/j.1365-3040.2009.01978.x

Vandereyken, K., Van Leene, J., De Coninck, B., & Cammue, B. P. A. (2018). Hub protein controversy: Taking a closer look at plant stress response hubs. *Frontiers in Plant Science*, *9*(June), 1–24. https://doi.org/10.3389/fpls.2018.00694

Verslues, P. E., & Sharma, S. (2010). Proline Metabolism and Its Implications for Plant- Environment Interaction Authors. *Arabidopsis Book*, 8:e0140. https://doi.org/10.1199/tab.0140

Wagner, R., Dietzel, L., Bräutigam, K., Fischer, W., & Pfannschmidt, T. (2008). The long-term response to fluctuating light quality is an important and distinct light acclimation mechanism that supports survival of Arabidopsis thaliana under low light conditions. *Planta*, *228*(4), 573–587. https://doi.org/10.1007/s00425-008-0760-y

Walters, R. G. (2005). Towards an understanding of photosynthetic acclimation. *Journal of Experimental Botany*, *56*(411), 435–447. https://doi.org/10.1093/jxb/eri060

Walters, R. G., & Horton, P. (1994). Acclimation of Arabidopsis thaliana to the light environment: Changes in composition of the photosynthetic apparatus. *Planta*, *195*(2), 248–256. https://doi.org/10.1007/BF00199685

Wang, P., Liu, J., Liu, B., Feng, D., Da, Q., Wang, P., Shu, S., Su, J., Zhang, Y., Wang, J., & Wang, H. Bin. (2013). Evidence for a role of chloroplastic m-type thioredoxins in the biogenesis of photosystem II in arabidopsis. *Plant Physiology*, *163*(4), 1710–1728. https://doi.org/10.1104/pp.113.228353

Wanichthanarak, K., Fahrmann, J. F., & Grapov, D. (2015). Genomic, proteomic, and metabolomic data integration strategies. *Biomarker Insights*, *10*(Table 1), 1–6. https://doi.org/10.4137/BMI.S29511

Warnes, G. R., Bolker, B., Bonebakker, L., Gentleman, R., Liaw, W. H. A., Lumley, T., Maechler, M., Magnusson, A., Moeller, S., Schwartz, M., & Venables, B. (2016). Package "gplots": Various R programming tools for plotting data. *R Package Version 2.17.0.*, *1*, 1–68. https://doi.org/10.1111/j.0022-3646.1997.00569.x

Wegener, K. M., Singh, A. K., Jacobs, J. M., Elvitigala, T., Welsh, E. A., Keren, N., Gritsenko, M. A., Ghosh, B. K., Camp, D. G., Smith, R. D., & Pakrasi, H. B. (2010). Global proteomics reveal an atypical strategy for carbon/nitrogen assimilation by a cyanobacterium under diverse environmental perturbations. *Molecular and Cellular Proteomics*, *9*(12), 2678–2689. https://doi.org/10.1074/mcp.M110.000109

Wei, T., & Simko, V. (2021). *R package "corrplot": Visualization of a Correlation Matrix*. https://github.com/taiyun/corrplot

Weiszmann, J., Fürtauer, L., Weckwerth, W., & Nägele, T. (2018). Vacuolar sucrose cleavage prevents limitation of cytosolic carbohydrate metabolism and stabilizes photosynthesis under abiotic stress. *FEBS Journal*, *285*(21), 4082–4098. https://doi.org/10.1111/febs.14656

Wickham, H. (2016). *ggplot2: Elegant Graphics for Data Analysis*. Springer-Verlag New York. https://ggplot2.tidyverse.org

Wickham, H., Averick, M., Bryan, J., Chang, W., McGowan, L. D., François, R., Grolemund, G., Hayes, A., Henry, L., Hester, J., Kuhn, M., Pedersen, T. L., Miller, E., Bache, S. M., Müller, K., Ooms, J., Robinson, D., Seidel, D. P., Spinu, V., … Yutani, H. (2019). Welcome to the tidyverse. *Journal of Open Source Software*, *4*(43), 1686. https://doi.org/10.21105/joss.01686

Wickham, H., Hester, J., Chang, W., & Bryan, J. (2021). *devtools: Tools to Make Developing R Packages Easier*. https://cran.r-project.org/package=devtools

Wickham, H., & Seidel, D. (2020). *scales: Scale Functions for Visualization*. https://cran.r-project.org/package=scales

Wiedemann, C., Kumar, A., Lang, A., & Ohlenschläger, O. (2020). Cysteines and Disulfide Bonds as Structure-Forming Units: Insights From Different Domains of Life and the Potential for Characterization by NMR. *Frontiers in Chemistry*, *8*(April), 1–8. https://doi.org/10.3389/fchem.2020.00280

Wienkoop, S., Morgenthal, K., Wolschin, F., Scholz, M., Selbig, J., & Weckwerth, W. (2008). Integration of metabolomic and proteomic phenoptypes. *Molecular and Cellular Proteomics*, *7*(9), 1725–1736. https://doi.org/10.1074/mcp.M700273-MCP200

Winter, D., Vinegar, B., Nahal, H., Ammar, R., Wilson, G. V., & Provart, N. J. (2007). An "electronic fluorescent pictograph" Browser for exploring and analyzing large-scale biological data sets. *PLoS ONE*, *2*(8), 1–12. https://doi.org/10.1371/journal.pone.0000718

Wojdyla, K., & Rogowska-Wrzesinska, A. (2015). Differential alkylation-based redox proteomics - Lessons learnt. *Redox Biology*, *6*, 240–252. https://doi.org/10.1016/j.redox.2015.08.005

Wunder, T., Liu, Q., Aseeva, E., Bonardi, V., Leister, D., & Pribil, M. (2013). Control of STN7 transcript abundance and transient STN7 dimerisation are involved in the regulation of STN7 activity. *Planta*, *237*(2), 541–558. https://doi.org/10.1007/s00425-012-1775-y

Wunder, T., Xu, W., Liu, Q., Wanner, G., Leister, D., & Pribil, M. (2013). The Major thylakoid protein kinases STN7 and STN8 revisited: Effects of altered STN8 levels and regulatory specificities of the STN kinases. *Frontiers in Plant Science*, *4*(OCT), 1–15. https://doi.org/10.3389/fpls.2013.00417

Yamori, W. (2016). Photosynthetic response to fluctuating environments and photoprotective strategies under abiotic stress. *Journal of Plant Research*, *129*(3), 379–395. https://doi.org/10.1007/s10265-016-0816-1

Yang, J., Carroll, K. S., & Liebler, D. C. (2016). The expanding landscape of the thiol redox proteome. *Molecular and Cellular Proteomics*, *15*(1), 1–11. https://doi.org/10.1074/mcp.O115.056051

Yoo, K. S., Ok, S. H., Jeong, B. C., Jung, K. W., Cui, M. H., Hyoung, S., Lee, M. R., Song, H. K., & Shin, J. S. (2011). Single cystathionine ß-synthase domain-containing proteins modulate development by regulating the thioredoxin system in Arabidopsis. *Plant Cell*, *23*(10), 3577–3594. https://doi.org/10.1105/tpc.111.089847

Yoshida, K., Hara, S., & Hisabori, T. (2015). Thioredoxin selectivity for thiol-based redox regulation of target Proteins in Chloroplasts. *Journal of Biological Chemistry*, *290*(23), 14278–14288. https://doi.org/10.1074/jbc.M115.647545

Yoshida, K., & Hisabori, T. (2018). Determining the rate-limiting step for light-responsive redox regulation in chloroplasts. *Antioxidants*, *7*(11). https://doi.org/10.3390/antiox7110153

Zaffagnini, M., Fermani, S., Marchand, C. H., Costa, A., Sparla, F., Rouhier, N., Geigenberger, P., Lemaire, S. D., & Trost, P. (2019). Redox Homeostasis in Photosynthetic Organisms: Novel and Established Thiol-Based Molecular Mechanisms. *Antioxidants and Redox Signaling*, *31*(3), 155–210. https://doi.org/10.1089/ars.2018.7617

Zeeman, S. C., Kossmann, J., & Smith, A. M. (2010). Starch: Its Metabolism, Evolution, and Biotechnological Modification in Plants. *Annual Review of Plant Biology*, *61*(1), 209–234. https://doi.org/10.1146/annurev-arplant-042809-112301

Other sources

LNBio. (2014). *Tutorial for proteome data analysis using the Perseus software platform* (Issue January, pp. 1–22). Laboratory of Mass Spectrometry, LNBio, CNPEM.

ACKNOWLEDGEMENT

An erster Stelle möchte ich mich besonders bei Herrn Prof. Dr. Peter Geigenberger bedanken, der es mir ermöglichte, in seiner Arbeitsgruppe zu promovieren. Danke dir Peter für die offenherzige Unterstützung in jeglicher Hinsicht.
Dem anschließend möchte ich mich bei Dr. Tatjana Kleine, Prof. Dr. Alisdair Fernie und besonders bei Dr. Ute Armbruster für das Mentoring bedanken, die mir sehr viel mit auf den Weg gegeben hat. Außerordentlich danken möchte ich ebenfalls Prof. Dr. Thomas Nägele für die stete Betreuung, vor allem gegen Ende meiner Arbeit. Mein Dank gilt ebenfalls Prof. Dr. Wolfgang Frank, Dr. Tatjana Kleine, Prof. Dr. Herwig Stibor, Prof. Dr. Heinrich Jung und Prof. Dr. Laura Busse für die Begutachtung meiner Arbeit. Herzlichst möchte ich mich auch bei Dr. Reimo Zoschke für die Messung des RNA Output, bei Dr. Saleh Alseekh für die Messung der GC-MS und Dr. Stephanie Arrivault für die Messung der LC-MS bedanken. Ferner gilt mein Dank Dr. Alex Graf und Dr. Beata Siemiątkowska für die Erstellung der Proteomics. Ebenfalls danken möchte ich Dr. Martin Lehman für die freundliche Zusammenarbeit und Dr. Giada Marino, die mich bei der Auswertung der Proteomics unterstützt hat.
Als Nächstes bedanke ich mich natürlich bei den Kollegen der AG Geigenberger, für die großartige Zeit innerhalb und außerhalb des Labors, für gegenseitige Unterstützung, für gute, aber auch für schlechte Tage, die einem gleichwohl halfen, zu wachsen: Ina, Anne, Benji, Martin, Mel, Verena, Luke und Martina. Daneben grüße ich noch die anderen Kollegen aus dem 1. Stock: Thilo, Toni, Belen und vor allem Bennet und Marcel, für das ein oder andere Schwätzchen. Ohne euch wär's nur halb so lustig gewesen! Nicht zu vergessen sind die fleißigen Studis: allen voran Louis für die Messung der Stärke, Luca für die Messung der LHC Phosphorylierung, ferner Sarina, Anne und Christopher für die lustige Zeit. Ihr habt es alle drauf! Ich war ja aber auch ein guter Betreuer. Mein Dank gilt auch allen zuverlässigen Kräften rund um das Institut, der IT, der Werkstatt und des Gewächshauses. Zuletzt ein großes, liebes Dankeschön an meine geliebte Frau Mama, die mich immer bekräftigt hat, meinen eigenen Weg zu gehen.

Eidesstattliche Erklärung

Ich versichere hiermit an Eides statt, dass meine Dissertation selbständig und ohne unerlaubte Hilfsmittel angefertigt worden ist. Die vorliegende Dissertation wurde weder ganz noch teilweise bei einer anderen Prüfungskommission vorgelegt. Ich habe noch zu keinem früheren Zeitpunkt versucht, eine Dissertation einzureichen oder an einer Doktorprüfung teilzunehmen.

München, den 30.5.2022 Dejan Dziubek